ABSTRACT

YUZUAK, SEYIT. Utilizing Metabolomics and Model Systems to Gain Insight into Precursors and Polymerization of Proanthocyanidins in Plants (Under the direction of Dr. De-Yu Xie).

Proanthocyanidins (PAs) are oligomers or polymers of flavan-3-ols. In plants, PAs have multiple protective functions against biotic and abiotic stresses. PAs are also important nutraceuticals existing in common beverages and food products to benefit human health. To date, although the biosynthesis of PAs has been intensively studieed and fundamental progress has been made in over the past decades, many questions remain unanswered. For example, its direct precursors of extension units are unknown and their monomer structure diversity are also unclear. These questions about proanthocyanidins result from not having of model systems and effective technologies. Our laboratory has made significant progress in enhancing the understanding of these unknown and unclear points regarding proanthocyanidins. In my dissertation research reported here, I focus on two areas: testing muscadine as a crop system to develop metabolomics for studying precursor diversity and isolating enzymes from a red cell tobacco system to understand the precursors of the extension units of PA.

First, I developed a metabolomics protocol to analyze anthocyanidins and anthocyanins in muscadine grape. This study demonstrated that muscadine berries can produce at least six anthocyanidins, revealing the diversity of pathway precursors for PAs. The Journal of Agriculture and Food Chemistry is reviewing this work.

Second, I developed a metabolomics protocol of HPLC-qTOF-MS/MS to analyze flavan-3-ols and dimeric PAs in muscadine grape. This study also demonstrated the high structure diversity of flavan-3-ols, particularly methylated flavan-3-ols. In addition, this protocol allowed the annotation of multiple dimeric PAs, revealing the structural diversity of PAs in muscadine

berries. This study shows that muscadine is an appropriate crop model system because of demonstrating high diversities for flavan-3-ol and PAs. This work is being prepared for submission to Molecules.

Third, our laboratory has succeeded in engineering transgenic red tobacco cells as a model system to study PA biosynthesis. Our laboratory's previous experiments have shown that red cells expressing enzymes (polyphenol oxidases, PPO) are likely involved in polymerization of flavan-3-ols (unpublished). Based on previous biochemical and proteomic work, I developed an effective protocol to extract pigment-free PPO and other proteins. This work is under the second revision by Plant Methods journal. The reviewers suggested to study more native proteins extracted by our new protocol from plant tissues. I further developed a purification protocol to isolate putative condensing synthase(s) with PPO activity. Although I am unable to finish biochemical characterization of candidate condensing synthase`s involvement in PA formation, my preliminary study has shown that purified condensing synthase with PPO activity catalyzes flavan-3-ols to form dimeric PA-like compounds. These preliminary experiments will be useful for our next step to characterize functionally putative condensing synthase(s) and mechanisms of PA polymerization in plants.

Utilizing Metabolomics and Model Systems to Gain Insight into Precursors and Polymerization of Proanthocyanidins in Plants

by
Seyit Yuzuak

A dissertation submitted to the Graduate Faculty of
North Carolina State University
in partial fulfillment of the
requirements for the degree of
Doctor of Philosophy

Plant Biology

Raleigh, North Carolina

2018

APPROVED BY:

_____	_____
Dr. De-Yu Xie Committee Chair	Dr. Amy Grunden
_____	_____
Dr. Marcela Rojas-Pierce	Dr. Vincent Chiang
_____	
Dr. Ralph Dewey	

DEDICATION

To my parents, Mr. Ali Yuzuak and Mrs. Guldane Yuzuak, whose patience, guidance, pray and love give me the strength, motivation and hope to make this dream come true. To those who got a special place in my thought and heart, and loved me by truth.

BIOGRAPHY

Seyit Yuzuak was born in Mersin, Turkey in 1982. He was third child, out of five, of Ali and Guldane Yuzuak. He got his bachelor`s degree in Biology in Adnan Menderes University in Aydin, Turkey. During his undergraduate study, he had some laboratory and fieldwork experiences in plant tissue culture and plant biotechnology area. After graduate, he worked as administrator for three years in Turkish government. He also did his obligatory military service in military hospitals for six months in Istanbul, Turkey. After getting a full scholarship from Turkish government, he moved to United States for his master and doctorate degree. After completing one year of English Language Program in University of Alabama at Tuscaloosa, AL, he pursued his academic career in Mississippi State University (MSU), Starkville, MS. He got his Master of Science degree in Biological Sciences under the direction of Dr David Chevalier. His master thesis entitled as "Characterization the structure and function of *Dawdle* gene (*DDL*) in Arabidopsis". In 2013, he decided to work on plant metabolites for his PhD degree and future work, and then moved to Raleigh, North Carolina to join to Dr De-Yu Xie Laboratory in Plant Biology, North Carolina State University. He worked on profiling of anthocyanin and proanthocyanidins in muscadine grapes and polymerization mechanism of proanthocyanidins in plants under the direction of Dr. De-Yu Xie.

ACKNOWLEDGMENTS

My dissertation research has been conducted under the supervision of Dr. De-Yu Xie. I especially thank Dr. Xie not only for supporting me in the accomplishment of this doctoral program but also for showing me his kind empathy and sensibility to understand my goals and needs. I am also grateful to Dr. Xie for teaching me how to be and to do the best. I sincerely thank him for his insightful mentoring that has helped me go through every single challenge of my dissertation research. I am thankful to his friendship, caring, support, and all encouragements.

I am deeply grateful to my advisory committee, Dr. Vincent Chiang, Dr. Ralph Dewey, Dr. Amy Grunden, and Dr. Marcela Pierce, for their kindest and great advices, suggestions and guidance during my PhD study and research.

I want to thank Dr. Xianzhi He for his generous assistance, deep friendship, and advices that help me to conduct my dissertation research.

I am so grateful to members of Dr. Xie's Laboratory for their kind help and advices in the past five years. When I experienced challenging in my experiments, they shared their experiences with me and gave me good technical suggestions. Their help and friendship played important roles to motivate me to complete all experiments included in my dissertation.

My special thanks go to my family for their unselfish love and support. My special gratitude and thanks also go to Dr. Lakshmi Narayanan, Dr. Gui Li, Miss Abir Abdelmoujib, Dr. Begum Matik, Dr. Oğuz Turkozan, Dr. Ayse Gul Mutlu, Dr. Yusuf Kurt, Dr Adnan Erdag, Dr Bengi Erdag, Dr Mesut Kirmaci, Dr. Ali Ozmen, Dr. Alev Karagozler, Dr. Yelda Emek, Miss Wu Yan and to my elementary school teacher, Miss Hadice Sadi, for their contribution, continuous support, advices and suggestions, and sincere friendships.

I would like to give my special thanks to all of friends of mine in the department pf Plant Biology for their sincere friendship and helps.

I am grateful to the Turkish Government for financially supporting me a five-year's scholarship to pursue my PhD study in the United States and to the Department of Plant and Microbial Biology for extending my GSSP and providing me a teaching assistantship during the last year of my PhD study. Finally yet importantly, I am thankful to all faculty and staffs of the Department of Plant and Microbial Biology for being part of my PhD education experience and for contribution to my personal and professional development.

TABLE OF CONTENTS

LIST OF TABLES

LIST OF FIGURES

CHAPTER 1:

CHAPTER 2:

CHAPTER 3:

CHAPTER 4:

CHAPTER 5:

CHAPTER 1

Literature Review

ANTHOCYANINS

Anthocyanins

Anthocyanins are a class of plant flavonoids belonging to the group of polyphenolics. Anthocyanins are water-soluble pigments that give pink/red/purple/blue color to plant tissues. All anthocyanins are derived from a specific chromophore core, namely 2-phenyl-benzopyrylium or flavylium, which consists of two aromatic rings (A and B) that are bound together by three carbon atoms that form an oxygenated heterocyclic pyran ring (C) (Figure 1). The core of the anthocyanidin has the typical C6-C3-C6 flavonoid skeleton consisting of seven positions that are subjected to modification of any organic group like a methoxyl group or sugar (Harborne and Williams 2000; Kong, Chia et al. 2003). To date, most anthocyanins are predominantly found in nature as glycosides of 2-phenyl-benzopyrylium or flavylium salts in plant tissues, such as flowers, fruits, seed coats, leaves, stems and, others. Furthermore, their hue features in plants depend on the vacuolar pH values, which can reversibly modify the core chromophore structure.

Structure and stability of anthocyanins

To date, more than 600 anthocyanins have been found in plants. All anthocyanins are derivatives of anthocyanidins. In the cation form, anthocyanidins have two double bonds in the C ring and therefore carry a positive charge. 19 anthocyanidins have been found in plants (Table 1). Of these, pelargonidin (orange to red hues), cyaniding (red to magenta hues), delphinidin (magenta to purple hues), peonidin (purple to red hues), petunidin (dark-red to purple hues) and malvidin (red to blue hues) are the most common ones produced in plant tissues (Delgado-

Vargas, Jimenez et al. 2000; Iwashina 2000; Welch, Wu et al. 2008). Generally, anthocyanidin-glucosides are the common derivatives, which are composed of one anthocyanidin aglycone with one or more sugar(s) attached at C3, C5, or C7 of the core chromophore. The sugar molecules attached to anthocyanidins in natural anthocyanins include glucose, xylose, arabinose, rhamnose, fructose, thamnose, and galactose. In addition to glycosylation, other common modification at these positions include acylation and acetylation, and malonylation. Common acylation observed in nature includes the addition of a coumaric, caffeic, ferulic, p-hydroxy benzoic, synaptic, malonic, acetic, succinic, oxalic, or malic acid (Delgado-Vargas, Jimenez et al. 2000; Wrolstad 2004). Furthermore, secondary, ternary, and more complicated metrifications on sugars or acrylate groups diversify anthocyanin structures. Most of those modifications result from enzymatic reactions catalyzed by glycosyltransferases, methyltransferases, acyltransferases, malonyltransferases, and others (Winefield 2002; Kong, Chia et al. 2003). These modifications are associated with anthocyanin transportation and physiological functions described below. Since anthocyanins lead to pigmentation in a diversity of fruits, vegetables, crops and other plants, color intensity, hue and color stability of anthocyanins are very significant properties. These properties are highly effected by pH, structure, temperature, light, oxygen, copigmentation, hydration and a number of other factors (Andersen 2008; Czibulya, Horvath et al. 2015).

Anthocyanins undergo structural transformations as a result of pH changes. Studies showed the dramatic effect of pH range on the color and stability of anthocyanins. At a pH 3 or lower, the anthocyanin exists as the flavylium cation in orange or red color. When pH increases, the hydration reaction of the flavylium cation and the proton transfer reactions of the acidic hydroxyl groups of the flavylium cation occur. As the first reaction gives a colorless carbinol

pseudo-base, which may undergo ring opening to a yellow chalcone, the second reaction leads to quinonoidal base. At a pH of 6-7, further deprotonation of the quinonoidal base forms purplish blue resonance-stabilized quinonoid anions (Torskangerpoll and Andersen 2005; Ananga, Georgiev et al. 2013).

The structure of anthocyanin such as hydroxyl and methoxyl moieties can also influence their color. The hydroxyl group at C-3 is frequently glycosylated leading to the color shift of anthocyanins from yellow-orange to red (Ahmed, Shivhare et al. 2004). Anthocyanidins with just one free hydroxyl group on the B ring, including pelargonidin, peonidin, and malvidin, were found to give more blue colors and be more stable than anthocyanidins, including petunidin and delphinidin at above pH 8 (Cabrita, Fossen et al. 2000). Glucosidic subtitutions, such as the C3-glucoside and C5-glucosides of anthocyanins, can also show bluer color in alkaline solutions but lower the color stability. It is suggested that introduction of a sugar moiety would result in color loss because of the electron-withdrawing from the flavylium cation, which enhances electrophilicity of the flavylium cation (Borkowski, Szymusiak et al. 2005). Anthocyanins can also differ in acylating groups of the sugar moieties. Acylated anthocyanins indicate low sensitivity to pH changes, and possess higher color stability in neutral and alkaline solutions, producing a bluer hue compared to non-acylated anthocyanins. This increased color stability results from the fact that the flavylium ion of acylated anthocyanins are more resistant to hydration leading to an equilibrium towards to more quinonoidal base forms. In summary, while acylation increases the bluer pigmentation, which is already enhanced by glucosidic moieties, it decreases the stability of the color which was already increased by sugar attachment (Torskangerpoll and Andersen 2005).

Since anthocyanins are highly reactive and easily degraded, both light and temperature breakdown their structure. It is better to keep anthocyanins at temperatures around 2-4 °C and in dark environments because sunlight and high temperatures effectively cause the loss of pigmentation (Reyes and Cisneros-Zevallos 2007; Andersen 2008). Anthocyanins can be also degraded by oxidative mechanisms in which plant polyphenol oxidase (PPO) is involved. However, PPOs need the presence of another substrate such as caffeic acid, chlorogenic acid, or gallic acid to be able to degrade anthocyanins. All these substrates mentioned are o-diphenolic compounds found in many fruits and play a role in the first step of polyphenolic oxidation. These acids are oxidized to their o-quinone, and then oxidize the anthocyanins to form brown colored polymeric compounds. Thus, reduction of the quinone or inhibiting PPO activity would effectively inhibit the oxidative degradation of anthocyanins. Addition of ascorbic acid converts the quinone back to its acid form by acting as the hydrogen donor, so the presence of ascorbic acid can protect anthocyanins from being degraded by PPO (Kader, Haluk et al. 1998; Kader, Nicolas et al. 1999; Kader, Irmouli et al. 2001; Salamon, Farkas et al. 2017).

Copigmentation is another property of color and intensity of anthocyanins. A copigment is a typically colorless compound such as catechin, epicatechin, procyanidin B2, caffeic acid, p-coumaric acid, chlorogenic acid, pyruvic acid, myricetin, quercetin, metal ions, or other organic acids. They produce weak chemical bonds with anthocyanins, but increase their physical and chemical properties. When they are added to anthocyanins, they greatly enhance the color of the anthocyanin solutions.

Anthocyanins are exposed to the nucleophilic attack of water preferentially at the C4 position of the original anthocyanin structure. This attack converts the flavylium cation into colorless carbinol pseudo-base form. However, copigment-anthocyanin interaction stabilizes the

flavylium cation and prevents its hydration. Eventually, more flavylium cations lead to intense and more stable red color in the solution, even at increasing pH values (Cai, Lilley et al. 1990; WilskaJeszka and Korzuchowska 1996; Figueiredo, George et al. 1999; Boulton 2001; Olson, Kittelson et al. 2002; Gris, Ferreira et al. 2007; Escribano-Bailon and Santos-Buelga 2012; Zou, Ma et al. 2018).

In the early steps of the general flavonoid biosynthesis pathway, a relatively non-reactive hydrophobic compound, naringenin chalcone, goes through chemical alterations by a series of structural enzymes. Enzymatic modifications such as adding amino acids, sugar and glutathione (GSH) serve different purposes such as reducing of hydrophobicity of end-products and tagging for recognition by transporter proteins that transports the modified product out of the cytoplasm. Therefore, such modifications are necessary for anthocyanins to be transported and to fulfill its cellular functions in the correct tissue and time, as well. Modifications of the basic structure of anthocyanin could differ among plant species. For example, anthocyanins are glycosylated and malonylated, which results in being negatively charged in maize. However, they are not malonylated in Arabidopsis. In addition, it has been observed that transgenic plants overexpressing regulatory genes involved in anthocyanin biosynthesis accumulate acylated anthocyanin. Thus, this is a long-standing question regarding what is the role and contribution of anthocyanin modifications in distribution, transport and storage of anthocyanins (Martinoia, Maeshima et al. 2007; Zhao 2015).

Natural occurring and physiological functions of anthocyanins

Anthocyanins are found in the majority of higher plant species except for plant species in the Caryophyllales. Moreover, anthocyanins have also been found in some lower plants such

as mosses and ferns (Fossen, Slimstad et al. 2002). Certainly, anthocyanins are important agronomical traits in many crops, particularly those crops for flowers and fruits (Fabroni, Ballistreri et al. 2016). In plant cells, anthocyanins are mainly stored in the vacuoles, [such as epidermal cells in the peel of fruits and flower petals], (Passeri, Koes et al. 2016).

Anthocyanins play important physiological functions associated with plant reproduction and defense. First of all, anthocyanins act as visual signals to attract pollinators for pollination of flowers and dispersers to spread seeds or fruits (Kong, Chia et al. 2003). Second, anthocyanins can provide a warning signal to repulse birds and insects for protection of plant tissues from being consumed (Furuta 1986). Third, they serve as filters to absorb UV-B light and visible light irradiation for protecting molecules in plant tissues from being degraded (Page and Towers 2002). The accumulation of anthocyanins protect leaves from radiation-caused damage of photosynthesis by absorbing extra light (Ferreyra, Rius et al. 2012). Fourth, many anthocyanin-rich structures defend plants against diseases infected by various pathogens and damages caused by abiotic stresses including cold shock, drought, osmotic and wounding, and biotic stresses (Harborne and Williams 2000; Winkel-Shirley 2001; Sun, Li et al. 2012). Finally, anthocyanidins are essential precursors of proanthocyanidins, which are powerful anti-oxidative, anti-pathogen, and anti-pest flavonoids in most plant species (Xie and Dixon 2005).

Health benefits

Anthocyanins are of growing interest for their beneficial effects on human and animal health given their anti-oxidant, anti-bacterial and anti-cancer activity in vitro (Poracova, Tkacikova et al. 2011). Anthocyanins are powerful free radical scavengers that can remove reactive oxygen species in human cells. The free radical scavenging properties result from the

structural electron deficiency feature, which increases specificity toward radical oxygen (Galvano, La Fauci et al. 2004; Welch, Wu et al. 2008). It has been demonstrated that the same doses of anthocyanins have higher anti-oxidative activity than those of ascorbic acid, β-carotene and vitamin E (Kowalczyk, Krzesinski et al. 2003). More studies have showed that the antioxidative activity of anthocyanins helps to improve visual acuity by accelerating the activation of the G-protein-coupled receptors in the retina (Matsumoto, Nakamura et al. 2003), protect from heart attack via their anti-inflammation activity, enhance capillary strength and permeability, and inhibit platelet formation (Folts 1998; Keevil, Osman et al. 1998). Other beneficial facts include the prevention of obesity and diabetes by inhibiting both body weight and adipose tissue increase (Tsuda, Horio et al. 2003; Xie, Su et al. 2018). These health benefits of anthocyanins are correlated to the number of hydroxyl groups on the core structure (Hou, Fujii et al. 2004). All these health-promoting benefits can be obtained from the consumption of high levels of dietary anthocyanin-rich food. Therefore, many engineering efforts have been invested to improve and increase anthocyanins in food and dietary products (Francisco, Regalado et al. 2013).

Biosynthesis of anthocyanins

The biosynthetic pathway of anthocyanins starting from phenylalanine was elucidated in plants in numerous studies. The anthocyanin biosynthesis in four model plant species has particularly gained intensive studies, including Arabidopsis (*Arabidopsis thaliana*), snapdragon (*Antirrhinum majus*), maize (*Zea mays*), and petunia (*Petunia hybrid*) (Holton and Cornish 1995; Springob, Nakajima et al. 2003; Azuma 2018). Characterization of Arabidopsis *transparent testa* (*tt*) mutants showing reduced or lack of proanthocyanidins in vacuoles of the endothelial cell

layer of the seed coat has greatly revealed several genes encoding biosynthetic enzymes and transcription factors (Lepiniec, Debeaujon et al. 2006). To date, every gene step has been cloned from plants and the corresponding enzymes have been biochemically and genetically characterized from different plant species. All steps have also been demonstrated to occur in the cytosol or at the cytosolic surface of the endoplasmic reticulum (ER).

The anthocyanin biosynthetic pathway includes the beginning, early, and late steps (Figure 2) (Shi and Xie 2014). The beginning steps consist of three enzymatic reactions. The first biosynthetic step begins with the conversion of phenylalanine into cinnamic acid by phenylalanine ammonia lyase (PAL). Cinnamic acid then undergoes to a conversion to P-coumaric acid by cinnamate-4-hydroxylase (C4H). P-Coumaric acid is subsequently modified to p-coumaryl-CoA under the control of 4-coumarate: coenzyme A ligase (4CL). The early steps include four catalytic reactions. Chalcone synthase (CHS) catalyzes sequential condensations of p-coumaryl-CoA with three malonyl-CoA to yield naringenin chalcone. The open ring structure of the naringenin chalcone immediately cyclizes by the action of chalcone isomerase (CHI) to form chalcone, which represents a basic skeleton structure of flavonoids. Chalcone, a flavanone, is then converted to dihydroflavonols (dihydrokaempferol, dihydroquercetin and dihydromyricetin) by P450 monooxygenase enzymes. Chalcone is, first, converted to a dihydrokaempferol, which will give the pelargonidin pigment, by flavanone-3-hydroxylase (F3H), which adds a hydroxyl group to the carbon atom at position (3) on the A-ring of the chalcone. From this point, the dihydrokaempferol can undergo further conversion into dihydroquercetin and then to a dihydromyricetin, the reactions which are catalyzed by flavanoid-3`-hydroxylase (F3`H) and flavanoid-3`5`-hydroxylase (F3`5`H), respectively (Winkel-Shirley 2001; Welch, Wu et al. 2008; Petrussa, Braidot et al. 2013). These three are collectively termed

dihydroflavonols essentially relating to pink (pelargonidin), red (cyanidin), and blue (delphinidin) pigments. The late steps include three reactions. Dihydroflavonol 4-reductase (DFR) converts dihydrofalavonols to leucoanthocyanidins (leucopelargonidin, leucocyanidin, and leucodephinidin), which are catalyzed by anthocyanidin synthase (ANS, also known as leucoanthocyanidin dioxygenase; LDOX) to anthocyanidins. Finally, anthocyanidin aglycones are modified by glycosylated glucosyltransferase (GT) or methylation, and/or acylation, which results in diversity of anthocyanin structures. Methylation of the reactive hydroxyl groups and acylation of the sugar moieties lead to higher structure stability and protecting the sugar moieties against degradation by glucosidases, respectively. In addition, acylation can also increase water solubility of anthocyanins, producing a bluer color than non-acylated anthocyanins. Most of anthocyanins are transported into the central vacuoles of plant cells for storage. In the plant vacuoles, anthocyanins are stored within the colored flavylium ion form due to the acidic conditions of the vacuoles (Winefield 2002; Welch, Wu et al. 2008; Cheynier, Comte et al. 2013).

Studies involving the regulation mechanism of the anthocyanin biosynthetic pathway in both model and crop plants has increased genetic and biochemical understanding of the pathway. Transcription factors belonging to three different protein families including MYB (myeloblastosis) family, basic helix-loop-helix (bHLH) family, and tryptophan-aspartic acid (W-D) dipeptide repeat (WD40 R) family of transcription factors have been identified to essentially control the activation of the anthocyanin biosynthetic pathway. MYB members and bHLH members interact with a WD40 proteins to form a ternary MBW complex, also called the metabolon. MYB75 (PAP1) and MYB90 (PAP2) are two members from Arabidopsis. TT8 (Transparent Testa 8) and GL3 (Glabra 3) are two members of bHLH from Arabidopsis, too (Shi

and Xie 2014). MYB75, TT8, GL3, and WD40 (TTG1) have been demonstrated to form such a metabolon. This metabolon has been demonstrated to tightly and coordinately regulate most of the genes involved in the anthocyanin biosynthesis, modification and sequestration at transcriptional level (Koes, Verweij et al. 2005; Hichri, Barrieu et al. 2011; Xu, Dubos et al. 2015).

Transport of anthocyanins

Because subcellular distribution and the accumulation of anthocyanins are essential to show their brilliant color and proper function, their transport from the cytosol to the central vacuole is a required process. In the last decade, although the structural and regulatory components of the biosynthetic pathway of anthocyanins have been well studied, the mechanism and steps involved in their transport from the biosynthetic site into the final destination, the central vacuole, is still poorly understood (Mathews, Clendennen et al. 2003).

Up to now, three different but potentially non-exclusive models have been suggested and proposed for anthocyanin transport from the cytosol to within the central vacuole; vesicle trafficking-mediated, membrane transporter-mediated, and glutathione S-transferase mediated models (Mueller and Walbot 2001; Zhao and Dixon 2010; Zhao 2015). These proposed models are supported by two types of research. Firstly, vacuolar uptake of flavonoids was recently uncovered by functional characterization of new flavonoid transporters with novel biochemical properties. These studies partly address the involvement of the multidrug resistance (MR) transport proteins and glutathione S-transferase (GSTs) in flavonoid transport. Secondly, the identification and characterization of green fluorescent seed 9 (GFS9), which involves in vesicle membrane trafficking, further suggested a new hypothesis that proposes the collaborative and

integrated transport of flavonoids by GST-MR transporters-vesicle trafficking-mediated mechanism (Zhao 2015). The collaborative and integrated model proposes that the transport of anthocyanins and other flavonoids is completed by "GSTs-Membrane Transporters-Vesicle Trafficking-Mediated Transport". A comprehensive scenario for the collaboration of GST-MATE transporters-Vesicle trafficking for vacuolar sequestration of flavonoids has been recently suggested based on growing evidence about committing steps in anthocyanin transport. The first two investigations on collaboration of GST and MATE transporters in grapevine and Arabidopsis supported this scenario. GST examples are *Vv*GST from grape and TT19 from Arabidopsis. MATE examples are AM1 and AM3 from grape and TT12 from Arabidopsis. The grapevine *Vv*GST-knockdown hairy roots showed anthocyanin accumulation only in small vesicles but not in the central vacuole, while the AM1 and AM3 (MATE transporters) knockdown grapevine hairy roots did not exhibit small vesicle filled with anthocyanin. These observations proposed that AM1 and AM3 transport anthocyanins from the cytosol to small vesicles before *Vv*GST-guided transport from the small vesicles to the central vacuole by vesicle trafficking (Gomez, Conejero et al. 2011; Zhao 2015). A similar observation has been obtained from the study of proanthocyanidin (PA) transportation in Arabidopsis. TT19 and TT12 are homologs of *Vv*GST AM1 and AM3, respectively. The tt19-1 mutant seeds were found to accumulate PAs only inside small vacuolar-like structures (vesicles) while the *tt-12* mutant seeds were found to sequester PAs at peripheral regions of small vacuoles. Furthermore, seeds of *tt-19-1 tt12* double mutants accumulate PAs at peripheral regions of small vacuoles, indicating that the different localization of PAs in *tt12* and *tt19-1 tt12* double mutant illustrate a function of TT19 in transportation of PAs into the central vacuole by small vesicles (Kitamura, Matsuda et al. 2010; Zhao 2015). It is known that prevacuolar-like vesicles (compartments) tend to fuse and form the

central vacuole (Rojas-Pierce 2013). Studies on *tt19* mutant seeds have also showed an accumulation of prevacuolar-like vesicles instead of the central vacuole. In addition to *tt19*, a mutant, namely, gfs9-4, was obtained from GFS9 encoding a peripheral membrane protein localized at the Golgi apparatus, which has been demonstrated to be specifically involved in vesicle trafficking. The gfs9-4 mutant is also characterized by prevacuolar-like vesicles. Based on these data, TT19 is proposed to be involved in vesicle-trafficking and directing the transportation and fusion of ER-derived anthocyanin containing vesicles to the central vacuole by collaboration with GFS9 (Ichino, Fuji et al. 2014; Zhao 2015). To demonstrate this hypothesis, further evidence is necessary to demonstrate the interaction between TT19 and GSF9 in flavonoid transport.

A general mechanism is that once flavonoids are loaded to vesicles, those vesicles with cargos are transported to targeted destination membrane in tonoplast. This has been demonstrated by the GSF9 function. GFS9 has been shown to perform membrane-trafficking to drive to fuse the membrane vesicles with anthocyanins to the vacuole. In addition to fusion, GFS9-mediated membrane trafficking functions in vacuolar protein transport from ER to the central vacuole. An assumption is that anthocyanin transport by vesicle trafficking associated with GFS9 might be connected or directed by other vesicle-trafficking proteins such as MATE transporters because localization of different MATE transporters from different plant species on both small vesicle membranes and tonoplast supports co-migration of transporters with membrane vesicles (Ichino, Fuji et al. 2014). Accordingly, it is hypothesized that flavonoid membrane transporters (MATE type) might load anthocyanins into the vesicles, then co-migrate with loaded vesicles toward to the central vacuole thorough the vesicle trafficking (Zhao 2015).

In summary, those previous data support the hypothesis that GST-mediated-, membrane transporter-, and vesicle trafficking-mediated flavonoid transport are most likely collaborative to complete transport of anthocyanins from the synthesis site to the central vacuole (Zhao 2015). To further demonstrate this hypothesis, more data are necessary; how do GSTs interact with anthocyanins and membrane vesicles and facilitate their transport? How does GSF9 interact with GSTs or membrane transporters? Evidence for real-time transport of anthocyanins crossing membranes of vesicles and tonoplast in vitro and in vivo (under different conditions) is necessary.

PROANTHOCYANIDINS

Proanthocyanidins

Proanthocyanidins (PAs), also referred to as condensed tannins, are the oligomeric or polymeric plant flavonoids. They are widely produced in the plant kingdom from ferns to angiosperm (Zhao, Pang et al. 2010). Different tissues such as fruits, leaves, roots, flowers, or seeds can produce PAs. Wood, or bark parts from many woody plants, such as pine, also produce PAs. In particular, many berry fruits such as blue berries are rich in PAs. To plants, PAs play important protective roles against herbivores and pathogens. Many experiments have demonstrated that PAs have strong anti-bacterium, anti-fungus, and anti-virus activities (Xie and Dixon 2005).

Benefits for human health and livestock

Numerous nutritional and pharmaceutical studies have shown that PAs and its monomers (flavan-3-ols, such as catechin and epicatechin) are important pharmaceuticals with multiple benefit to human health. They are powerful antioxidants to form effective free radical scavenger. The uptake of PAs from food has been shown to effectively remove oxygen free radical species in the human body (Xie and Dixon 2005). Other activities include immunomodulatory, anti-inflammatory, anti-cancer, anti-allergic, anti-microbial, cardiovascular-protective, and antithrombotic functions (Nile and Park 2014; Sieniawska 2015). In addition, certain types of polymerization of PAs has been reported to enhance these activities, such as anti-cancer (Sun, Leandro et al. 1998; Zhang, Li et al. 2017). People can obtain these health benefits via uptake of PAs from regular food products, given that PAs and flavan-3-ols are widely existing in berry fruits such as blueberry and non-alcoholic beverages such as green tea. Actually, flavan-3-ols such as epicatechin are the most commonly consumed nutrients because (-)-epicatechin is rich in many food products and green tea. Because of the high nutritional values of (-)-epicatechin and other flavan-3-ols, food rich in flavan-3-ols (monomeric or condensed) are called “superfoods” (Scalbert and Williamson 2000).

PAs are important nutrients for ruminant animals. Forage crops such as alfalfa and white clover are highly rich in proteins and favorable food of milk cow and goat. Unfortunately, the two nutritional forage crops can easily cause pasture bloat leading to the loss of animals. Adding appropriate dose of PAs in animal feedstock significantly reduce the pasture bloat disease via the binding of proteins in the stomach to slow down protein digestion and increase bypass of proteins into the small intestine (Lees 1992; Dixon and Sumner 2003). As a result, the animals gain weight and produce more and higher quality milk (Xie and Dixon 2005).

Structure of proanthocyanidins

PAs are oligomers or polymers of flavan-3-ols (monomers) such as (+/-)- catechin and (+/-)-epicatechin. The commonest monomeric units are (+)-catechin, (-)-epicatechin, (+)-gallocatechin, (-)-epigallocatechin, (+)-afzelechin, and (-)-epiafzelechin. Based on the interlinkage numbers and types, PAs are categorized into two types, A and B. The majority of PAs identified from plants are of B type. The B type has only one type of linkage between monomeric units, interflavan bond via C4-8 or C4-6. A type has two types of linkages between monomeric units, one interflavan bond via C4-8 or C4-6 and the other ether linkage C2-O-C7. In two types of PAs, the bottom unit is termed as starter unit, while the upper units are called as extension units (Figure 1).

Based on the structures of flavan-3-ols, there are four main types of PAs, procyanidin, propelargonidin, prodelphinidin, and miscellaneous types. Procyanidins are composed of (-)-epicatechin, (+)-catechin, (+)-epicatechin, and (-)-catechin, which are four isomers and structurally characterized by two hydroxyl groups in the B-ring. This group of PAs is widely produced in the plant kingdom. Prodelphinidins are built from (-)-epigallocatechin, (+)-epigallocatechin, (+)-gallocatechin, and (-)-epigallocatechin, which are four isomers and structurally characterized by three hydroxyl groups in the B-ring. Propelargonidins are polymerized from (-)-epiafzelechin, (+)-epiafzelechin, (+)-afzelechin, and (-)-afzelechin, which are also isomers and structurally featured with one hydroxyl group in the B-ring. Miscellaneous PAs are polymerized from different types of flavan-3-ol monomers. In addition, methylation, acylation, glycosylation, galloylation of the monomeric units can diversify structures of PAs (Hemingway 1996; de Jesus, Falcao et al. 2012; Glavnik, Vovk et al. 2017; Smeriglio, Barreca et al. 2017). These structural diversities have been found to be associated with plant defenses of

biotic and abiotic stresses (Dixon, Xie et al. 2005). In particular, many structures are potent pharmaceuticals that can benefit human health. For example, procyanidin A1 and A2 can strongly prevent women's urination tract infection caused by bacterium (Xie and Dixon 2005).

The PA biosynthetic pathway

In the last decade, great progress in understanding the biosynthetic pathway of PAs have been made by the cloning and identification of key structural genes involved in the flavonoid pathway. Particularly, multiple yellowish or pale transparent testa (tt) mutant seeds of Arabidopsis have expedited the demonstration of key steps toward both PA and anthocyanin bisoynthesis (Dixon, Xie et al. 2005; Xie and Dixon 2005; Shi and Xie 2014).

To date, it has been demonstrated that the biosynthetic pathway of PAs shares the same beginning, early, and late steps starting with phenylalanine and ending at anthocyanidins or flavan-3,4-diols (Xie, Sharma et al. 2003; Dixon, Xie et al. 2005; Xie and Dixon 2005). As stated above in the section of the anthocyanin biosynthesis, all genes and their corresponding enzymes have been functionally characterized from Arabidopsis and other plants. These enzymes include PAL, C4H, 4CL, CHS, CHI, F3H, F3'H, F3'5H, DFR, and ANS (Figure 2). All of these steps are carried in the cytosol or membranes and both anthocyanidins and their precursors are then mainly transported to the central vacuole (He, Mu et al. 2010; Zhao, Pang et al. 2010).

The last step toward flavan-3-ols was unknown until two genes were identified one decade ago (Xie and Dixon 2005). One gene is ANR encoding an anthocyanidin reductase and the other is *LAR* encoding the leucoanthocyanidin reductase (Figure 2). ANR is a novel flavonoid reductase with a dual function that converts each anthocyanidin to three or four types of flavan-3-ols. For example, ANR can convert cyanidin to (-)-epicatechin, (+)-epicatechin, (+)-catechin, and/or (-)-

catechin (Zhao, Pang et al. 2010). The significance of the ANR discovery is that this knowledge corrects the dogma of plant flavonoids, in which anthocyanidins were defined as the "END" products of the plant flavonoid pathway and proanthocyanidins are the precursors of anthocyanidins. Compared with ANR, LAR was proposed in 1970s. Its gene was not identified until 2003 when a cDNA was cloned from Desmodium uninatum, a PA-rich legume plant (Tanner, Francki et al. 2003). Its recombinant protein was demonstrated to convert leucoanthocyanidins to only one type of flavan-3-ols, such (+)-catechin.

To date, these two enzymes are demonstrated to form two pathways toward flavan-3-ols in plants, ANR and LAR pathways. These two pathways have been found to co-exist in many plant species. In comparison to LAR pathway, the ANR pathway is more widely existing in plants. For example, Arabidopsis has been demonstrated to contain the ANR pathway only. More importantly, metabolic engineering using the ANR pathway has succeeded in model and crop plants for production of PAs. Unfortunately, metabolic engineering of the LAR pathway for PAs has been challenging. To understand the LAR activity, more studies have been performed recently. An unexpected and fundamental result was recently reported and showed that LAR plays a new catalytic function to condense flavan-3-ol-cysteine to PAs localized in the plant cell wall (Wang, Zhang et al. 2018). This new function raises many additional interesting questions about the LAR pathway role in plants. For example, how do PAs are formed in plants, such as Arabidopsis, which do not have LAR? The last step of PA formation is polymerization. Until now, the catalytic mechanism of this step is unclear. Two hypotheses are proposed and discussed below.

Regulation of the PA biosynthesis

The biosynthetic pathway of PAs is essentially regulated by several families of transcription factors. As introduced above in the section of anthocyanins, the biosynthetic pathway of PAs is mainly regulated by WD40, bHLB, and MYB transcription factors. TT2 in Arabidopsis is a homolog of PAP1. TT2 plays an essential role in activating the biosynthetic pathway of PAs. GL3 and TT8 described above also control the biosynthetic pathway. To date, the complex formed by WD40-TT8/GL3-TT8 (WBM) has been demonstrated to form the main regulatory complex to control the PA formation in Arabidopsis. Mutation of any members in the complex can result in the loss or the reduction of PAs in the seed coat of Arabidopsis (Dixon, Xie et al. 2005). More importantly, homologs of the WBM complex have been found in investigated plants. In addition, other transcription factors, such as WD40-like [Tryptophan-Aspartic acid (W-D) dipeptide], WRKY (WRKY domain proteins, zinc finger-like proteins), Homedomain (Hox) and bMADs (Mads box proteins), Myc (basic helix-loop-helix proteins) and WIP (transcription factor IIIA-like protein) have been shown to be associated with the regulation of the PA biosynthesis (Dixon, Xie et al. 2005).

The most direct metabolon of the TTG1-TT8/GL3-TT2 consists of DFR, ANS ANR (BAN) (Xie, Sharma et al. 2003; Xie 2017). In addition, the TTG1-TT8/GL3-PAP2 (another WBM complex described above) activates the anthocyanin pathway to provide substrates, although this complex does not directly activate the PA formation (Gonzalez, Zhao et al. 2008). In addition to these positive regulatory complexes, members of MYB4 have been shown to interact with a member of Myc protein family to repress the transcription of the beginning pathway genes of the PA biosynthesis (Zimmermann, Heim et al. 2004). In summary, although regulation mechanisms of PA formation by the WBM complexes have been elucidated, other

regulation mechanisms are hypothesized to exist in the plant cells and thus remain open for investigations in the future.

Current hypotheses of polymerization mechanism

The last step of PA formation is polymerization. This step has been studied for more than 60 years. Although the polymerization mechanism is unknown, two hypotheses have been proposed. The long-term hypothesis is that the polymerization of PAs is the result of a spontaneous non-enzymatic condensation in the rich oxygen rich *in vitro* conditions. The direct evidence is that in the presence of catalysts, catechin and leucocyanidin have been condensed to dimeric PAs. The second hypothesis is that a condensing synthase is required for the polymerization.

Herein, I focus on discussion of the second hypothesis in two areas, building blocks of polymerization and a putative condensing synthase. What types of precursors are the building units to form extension unites in PAs? As introduced above, PAs are oligomers or polymers of flavan-3-ols, in which the bottom one is termed as starter unit and all upper ones are termed as extension units. Although it has been elucidated that any flavan-3-ols can form the starter unit, which types of molecules are precursors of extension units remains unknown. The long-term hypothesis is that leucoanthocyanidins are the precursors of the extension units (Xie and Dixon 2005) . This hypothesis proposes that 2R,3S,4S-leucoanthocyanidins (flavan-3, 4-diols) are firstly converted to 2R,3S-quinone methides, which can be used as 2R,3S- extension units directly in polymerization, by auto-oxidation. Meanwhile, these 2R,3S-quinone methides can be also converted to 2R,3R-quinone methides by the flavan-3-en-3-ol intermediates, which could be condensed as 2R,3R- extension units directly to produce PAs. Furthermore, these trans- or cis-

quinone methides are further converted to their corresponding carbocations that would be condensed with (+)-catechins or (-)-epicatechins directly to form PAs (Hemingway and Laks 1985). The direct evidence to support this hypothesis was the chemical synthesis of dimeric PAs using catechin and leucocyanidin substrates. However, this model neglects the fact that predominant extension units found in PAs isolated from different plants are (-)-epicatechin monomers. In addition, what type of condensing synthase could catalyze this step is unknown. This long-term hypothesis was not challenged until a decade ago when the ANR pathway was discovered and precursor molecules were proposed to form extension units (Xie and Dixon 2005).

New potential precursors include flavan-3-ols and anthocyanidins. In this new model, flavan-3-ol such as (+)-catechins and (-)-epicatechins and anthocyanidins are converted to their corresponding o-quinone and quinone methides by an enzymatic reaction. Three groups of enzymes, polyphenol oxidase (PPO), laccase and peroxidase are proposed to be condensing synthases that catalyze polymerization. After this enzymatic reaction, the o-quinone and quinone methides can be further converted to their corresponding carbocations by flavan-3-en-3-ol intermediates or reduced to carbocations thorough auto-oxidation. Later, these carbocations can be condensed as direct extension units (Dixon, Xie et al. 2005).

Although direct evidence for this new hypothesis is lacking, chemical synthesis has demonstrated that flavan-3-ols can be used as extension unit precursors to form dimeric PAs (Ohmori, Ushimaru et al. 2004). Anthocyanins and anthocyanidins have also been shown to condense with flavan-3-ols to form oligomeric PAs (Vidal, Cartalade et al. 2002). This new hypothesis is globally accepted to understand PA formation. To demonstrate this new model,

both appropriate model and crop systems are necessary to provide phytochemical, biochemistry, and genetic evidence.

MUSCADINE GRAPE

Muscadine grape and health benefits

The Vitis (grapevines) genus in the Vitaceae family is divided into two subgenera, Euvitis Planch. (Bunch grapes) and Muscadinia Planch (muscadine grapes). Many species in this genus are important economic crops forming the main source of wine, fresh fruits, non-alcoholic beverages, and other products. The Muscadinia subgenera (muscadine grapes) consists of three species *V. rotundifolia, V. munsonianam*, and *V. popenoei*. *V. rotundifolia* is the common muscadine grape native to southeastern area of United States. *V. munsonianam* is a semitropical species native to Florida. *V. popenoei* is a tropical species native to Mexico. Each species has 40 chromosomes (38 in *V.vinifera*). They are morphologically characterized by loose and smaller clusters of up to 40 grapes (not in bunches), unbranched tendrils, small roundish leaves, thick-skinned berries (1-1.5 inch in diameter) with a unique fruity aroma, a few hard and oblong seeds, and berries abscessed individually and ripen very unevenly at maturity (Olien 1990; Qu, Lu et al. 1996; Greenspan, Bauer et al. 2005; Huang, Wang et al. 2009; Sandhu and Gu 2010; Ananga, Georgiev et al. 2013; Conner and MacLean 2013).

Since decades ago, *V. rotundifolia* (*Muscadiniana rotundifolia*) has been cropped for wine and other products in southeastern regions of the United States (Olien 1990; Qu, Lu et al. 1996). This species and its cultivars are appropriately adapted to heat, UV radiation and humid environment in southeastern states such as North Carolina, Florida and Georgia. They are also

highly resistant to fungi, grape pests and Pierce`s disease caused by a bacteria, *Xylella fastidiosa*, that severely reduces the fruit production of grapevine species in the southeastern United States. Therefore, this muscadine grape is one of the main small fruit crops in southeastern states (Bouquet 1980; Louime, Lu et al. 2011; Xu, Yagiz et al. 2014; Yu, Jiao et al. 2016; Wei, Luo et al. 2017). Muscadines grow better on fertile sandy loams and alluvial soil types than on wet and heavy soil types in the hot and humid regions. Muscadines are not tolerant of extremely cold winter temperatures and cannot grow in regions with temperatures lower than -12 °C in winter (Conner 2009). Adult vines take approximately 100 days to produce fully ripe fruits.

In addition to its economic values, many previous studies have shown nutritional significance of fresh muscadine fruits, wine, and non-alcoholic beverages. Given that muscadine berries produce numerous metabolites described below, a regular intake of muscadine grapes and related products can prevent from having cancer, cardiovascular disease, type-2 diabetes, and inflammations (Manach, Williamson et al. 2005; Banini, Boyd et al. 2006; He, Mu et al. 2010; Zhang, Chang et al. 2017).

Genetic breeding of muscadine grapes

Muscadine has many agronomic shortages in cropping. Fruits have multiple seeds, and show quick fruit softening, uneven ripening, short harvest season, and high perishability during postharvest storage and processing. To overcome these problems, since 400 years ago, both private and public muscadine breeding programs have been continuously breeding elite cultivars (Barchenger, Clark et al. 2015). In 1800s, six cultivars including Hopkins (1845), Flowers (1800), James (1866), Memory (1868), and Mish (1846) were developed to produce better fruits (Olien 1990). From 1900s to 1970s, the U. S. Department of Agriculture developed genetic

breeding programs in North Carolina (1907), Mississippi (1941), Georgia (1909), Texas (1909) and Florida (1971). These states started to use *V. vinifera* and *V. rotundifolia* to develop hybrids to improve fruit quality, disease resistance, and environmental adaptation. Another major goal of those early breeding programs was to develop perfect-flowered and self-fertile cultivars. Later on, those breeding programs focused on developing seedless hybrids (Olien 1990). As a productive result, more than 100 new varieties were introduced to the muscadine industry. Many of them show improved fruit quality for the fresh market and beverage industries. Popular cultivars include Tarheel, Nesbitt, Flowers, Olmo, Noble, FLH13-11, FLH17-66, Alachua, Fry, Granny Val and Carlos. A few muscadine varieties such as Noble, Ison and Carlos are particularly welcomed due to their increased quality of taste and flavor by both fresh fruit market and wine, jam, and jelly industries in different states, such as North Carolina, Florida and Georgia (Wei, Luo et al. 2017). Moreover, different colored varieties were created for both fresh market and wine industries. For example, the bronze cultivar, Scuppernong, also named as the Big White Grape, was developed for high quality fresh fruit. This bronze cultivar was later found to produce acylated mono and diglucoside anthocyanin pigments, which are good for high quality for wine color (Figure 1) (Ballinger, Maness et al. 1974).

Anthocyanin biosynthesis in muscadine

Investigation of structural and regulatory enzymes involved in the flavonoid biosynthesis pathway in muscadine grape is essential because flavonoid biosynthetic pathway plays an important role in not only berry development and ripening but also the concentration and content of phenolic compounds, particularly anthocyanins in muscadine berries (Oglesby, Ananga et al. 2016). Anthocyanins accumulated in grape berry skin is an important

determination of berry quality, cultivar differentiation for consumers, and health benefits (Keller and Hrazdina 1998). Several studies have shown that anthocyanin biosynthesis in grapes might be induced in coordinating during the developmental process of grape berries by light, particularly UV radiation, biotic and abiotic stress conditions, and enzymes (Takos, Jaffe et al. 2006; Castellarin, Pfeiffer et al. 2007; Berli, Moreno et al. 2010; Di Martino, Guzzi et al. 2015). It is also suggested that the expression of the genes encoding the biosynthetic enzymes in anthocyanin biosynthesis in grape is regulated by transcriptional factors (TF) (Deluc, Barrieu et al. 2006; Deluc, Bogs et al. 2008). Among TFs, MYB (myeloblastosis) family of transcription factor genes have been studied and determined to be involved in anthocyanin biosynthesis in grapes. A few studies have demonstrated that many of the white grape cultivars were derived from multi-allelic mutations of the myeloblastosis 1 (MYB1) and myeloblastosis 2 (MYB2) genes that regulate the last steps of anthocyanin biosynthesis (Lijavetzky, Ruiz-Garcia et al. 2006; Walker, Lee et al. 2006; Walker, Lee et al. 2007). Later on, it was shown that upregulation of *Vr*MybA1 and *Vr*MYBCS1 play an essential role in accumulation of anthocyanin and regulation of anthocyanin biosynthesis at the transcriptional level in muscadine grapes (Oglesby, Ananga et al. 2016).

Muscadine anthocyanins

Anthocyanins are important to muscadine grape quality. Anthocyanins are water-soluble pigments, which are composed of an anthocyanidin aglycone and different side moieties, such as glucose, xylose and other organic compounds. To date, the main anthocyanidins identified in muscadine fruits include Cyanidin (Cy), Delphinidin (Del), Petunidin (Pt), Peonidin (Pn), and Malvidin (Mv) (Huang, Wang et al. 2009). In addition, Pelargonidin (Pg) is found in

some muscadine cultivars. The main anthocyanins in muscadine grapes have been determined to be non-acylated 3,5-O-diglucosides of delphinidin, cyaniding, petunidin, peonidin, and malvidin in their skins of berries (Lamikanra 1989; Talcott and Lee 2002; Garcia-Beneytez, Cabello et al. 2003; Sandhu and Gu 2010; Wang, Tong et al. 2010; Conner and MacLean 2013). Pelargonidin 3, 5-diglucoside has also been identified in some cultivars. This anthocyanin profile is different to that of *V. vinifera*, which mainly produce 3-O-monoglucosides of anthocyanidins that are either acyalated or non-acylated (Janvary, Hoffmann et al. 2009).

The diglucosides of anthocyanidins are the pigments that control the color of all muscadine products, such as juice and pomace (Greenspan, Bauer et al. 2005; Plundrich, Grace et al. 2013; Wei, Luo et al. 2017). The number of hydroxyl groups in the B ring is closely associated with color. For example, blue color intensity can be increased with higher amount of free hydroxyl groups, while reddish intensity can be enhanced by increasing of the methylation of the hydroxyl groups. The five main muscadine anthocyanidins described above were found in most of muscadine cultivars (He, Mu et al. 2010; Conner and MacLean 2013). Of them, malvidin, a methylated delphinidin, is the reddest one (Nesbitt, Maness et al. 1974; He, Mu et al. 2010; Conner and MacLean 2013).

Previous studies have shown that unlike monoglucosides of anthocyanidins, these diglucosides are more prone to oxidation and browning (Sims and Morris 1986; Talcott, Brenes et al. 2003). This is because the 5-O-sugar moiety reduces the capacity of pigment polymerization that can stabilize color. In all muscadine 3,5-diglucosides of anthocyanidins, delphinidin and cyanidin 3, 5-O-diglucosides have the poorest stability, while malvidin 3,5-O-diglucoside has the highest stability. Also, many studies have showed that methylated anthocyanidins, such as peonidin and petunidin, have better color stability than their

corresponding non-methylated ones. This increase of color stability results from the methylation-related reduction of oxidation of the ortho-phenols of the B ring to ortho-quinones (Jain and Srivastava 1970). Other anthocyanin studies have found that other side moiety structures such as aromatic or aliphatic acids (p-coumaric acid and caffeic or ferrulic acids) can stabilize color (Lamikanra 1989; He, Mu et al. 2010). In addition, the proanthocyanidins described below can stabilize anthocyanin color, as well. Recently, a few the 3-monoglucosides of anthocyanidins that are produced in *V. vinifera* were found in some hybrids (Conner and MacLean 2013). This discovery shows a potential to create novel muscadine varieties for improvement of muscadine color stability in the future.

Furthermore, it has been reported that condensation reactions between anthocyanins and flavonols or procyanidins by acetaldehyde and cycloaddition reactions produce pyranoanthocyanins. This interaction not only contributes to the degradation of flavonoids in wine but also generates more stable oligomeric pigments which are less vulnerable to pH (Dufour and Bayonove 1999; Monagas, Bartolome et al. 2005). Although anthocyanin content of muscadine varieties has been widely studied, the MS/MS analysis of anthocyanins in muscadine grapes has not received adequate attention so far. The color stability of muscadine grapes and muscadine products is not only related to the total anthocyanin content, but is also related to the type of anthocyanins. Therefore, analysis of individual anthocyanins is important for the elucidation of pigment stability of muscadine grapes for different purposes (Huang, Wang et al. 2009).

Early studies on anthocyanin profiling of muscadine grapes was limited due to the resolution of the techniques used, and lack of available standard reference compounds. Today, most modern techniques have being used to study the pigment profile of muscadine grapes.

Polyphenol compounds including anthocyanins have been identified based on total ion chromatogram, elution order, retention time, exact molecular weight, spectroscopic characteristics and time of flight mass/mass spectrometer (TOF MS/MS) fragmentation patterns.

Muscadine proanthocyanidins

Proanthocyanidins (PAs) are powerful nutrients widely existing in the grapes, particularly in skin and seed of grape berries. In *V. vinifera*, PAs have gained intensive studies in both structures and biosynthesis in berries for high quality wines. The grape seed is the most abundant source of PAs compared to grape skin and stem (Ricardo-Da-Silva, Rigaud et al. 1991; Zhang, Li et al. 2017), thus grape seeds are the main natural source for PA extraction supplements. Moreover, PAs in wines play vital roles to stabilize red color. In comparison, structures and biosynthesis of PAs in muscadine remains open for future study. To date, a few flavan-3-ol monomers and proanthocyanidin dimers have been reported. Monomers include (+)-catechin, (-)-epicatechin and (-)-epicatechin-3-O-gallate (Spranger, Sun et al. 2008). Dimers include procyanidin B1 and B2 (Zhang, Li et al. 2017). These data show limitation of current understanding of PAs in muscadine. The lack of this knowledge actually limits the development of muscadine products. Accordingly, these types of studies are essential for muscadine breeding to create novel varieties with better agronomic traits, for example protection of berries from pests and plant diseases, color stabilization, and value-added nutrition (Treutter 2006).

Other phenolics in muscadine

In addition to anthocyanins and PAs, muscadine berries produce numerous other phenolic compounds, which are either stored in the vacuole or bound to the cell walls (Xu, Yagiz

et al. 2014). The phenolics in muscadine berries not only contribute to the bitterness and astringency of fruits, but also affect color stability. These phenolic compounds are mainly distributed in grapes seeds (65%), skin (30%) and pulp (5%). The main phenolic compounds in muscadine are gallic acid, ellagic acids, and their derivatives (Pastrana-Bonilla, Akoh et al. 2003; Yilmaz and Toledo 2004). Ellagic acids are metabolite markers for muscadine, given that they are not produced in other Vitis species. Ellagitannins are the main derivatives of ellagic acid in skin and seeds and form the main nutrients in wine and non-beverage products (Talcott and Lee 2002; Wei, Luo et al. 2017). Other phenolics include flavonol aglycone and, glucosides. The primary flavanol aglycones identified in muscadine are myrecetin, quercetin, laricitin, syringetin and kaempferol. Myrecetin and its derivatives are another metabolite marker that is produced in muscadine but not *V. vinifera* (Meepagala, Magee et al. 2002; Pastrana-Bonilla, Akoh et al. 2003; Wei, Luo et al. 2017).

Effects of cultivation on muscadine metabolites

The production of all metabolites described above are highly affected by field conditions and grow seasons. Multiple reports showed that the content of total and individual metabolites of these compounds greatly vary in different environments (Pastrana-Bonilla, Akoh et al. 2003; Lee, Johnson et al. 2005; Sandhu and Gu 2010; Wei, Luo et al. 2017). The contents of total phenolic compounds are also highly affected by different genotypic cultivars (Zhao, Yagiz et al. 2017). Studies have shown that the dark-skinned cultivars have higher total phenolic compounds than the bronze counterparts (Sandhu and Gu 2010; Wei, Luo et al. 2017). Climatic factors such as temperature, solar radiation, sunshine duration, and rainfall have been found to change phenolic composition and content. It was reported that grape polyphenol

compounds greatly varied in different vineyards. Growing seasons were also found to affect contents of metabolites (Downey, Dokoozlian et al. 2006; Xu, Zhang et al. 2011). However, only a few studies have reported the effects of these climatic parameters on total phenolic composition and concentrations in muscadine grapes (Wei, Luo et al. 2017). Herein, we also report a significant effect of growing season on anthocyanins. To understand effects of different factors on total phenolics, different elicitors and stimulating agents were directly applied to plants during fruiting period (Garcia-Estevez, Andres-Garcia et al. 2015; da Silva, Cazarin et al. 2016; Wei, Luo et al. 2017). For example, exogenous application of abscisic acid (ABA) enhances the antioxidant capacity, anthocyanins and phenolic content of muscadine grapes (Sandhu, Gray et al. 2011). Fruit development and ripening, and agricultural practices (planting, harvesting and management) also affected anthcoyanins, PAs and other phenolics in both contents and compositions (Noratto, Angel et al. 2009; Sandhu and Gu 2010; Quideau, Deffieux et al. 2011). All these data indicate that the quality of fresh muscadine fruits and other products depend on genotypes, cultivation, and growing seasons.

Problems and perspectives related to muscadine and muscadine-based products

Although muscadine has been cropped for more than 400 years, numerous major problems remain unsolved. The first problem is the poor color stability of wine and non-alcoholic beverages. Because the main anthocyanins are 3,5-diglucosides of anthocyanidins, producing monoglucosides of anthocyanidins appears to be a direct solution. Accordingly, interspecific crossing between different species have been carried out by different muscadine breeding programs. Although certain improvements have been made, all results of these breeding programs are hardly meeting the requirement of industries. The second main problem is diseases.

To date, although genetic breeding has created varieties with improved desease resistance, berry quality and production of muscadine are still another challenging. The third problem is that the basic studies such molecular biology, omics, and biochemistry in muscadine are still at an infant stage. The knowledge gap limits all efforts to create elite varieties for value-added muscadine. Actually, muscadine is an appropriate crop to study complexity of anthocyanins and PAs. Compared with *V. vinifera*, muscadine produces more diverse anthocyanin, flavan-3-ol, and PA structures, such as delphinidin and gallocatechin, which are not produced by *V. vinifera*. More importantly, muscadine is an excellent model crop to study methylated flavan-3-ols and PAs. Many model plants such as Arabidopsis and *Medicago truncatula* do not produce these compounds. Many crops such as *V. vinifera* do not produce these either. Study of the formation of these metabolites will not only provide new knowledge in plant anthocyanins and PAs, but also enhance breeding efforts to create new varieties with much improved color stability and pathogen resistance.

In my dissertation, I developed a LC-MS based metabolomics approach to study anthocyanins, flavan-3-ols, and PAs in berries of two new interspecific muscadine varieties. I developed a protocol to annotate anthocyanins, flavan-3-ols, and PAs. These protocols will be useful to study these three groups of metabolites. In addition, I used a red suspension cell culture to isolate potential enzymes involved in the formation of PAs. Despite that characterization of the enzymes remains for future studies, I developed an effective novel protocol to isolate proteins from anthocyanin and other pigment-rich plant tissues. This protocol will be useful to study enzymes from all other plants.

CHROMATOGRAPHY, MS and HPLC-MS ANALYSIS of ANTHOCYANINS

Chromatographic separation methods (coupled with identification methods)

Multiple methods have been developed to analyze and elucidate anthocyanins from plants. A general protocol includes three main steps, extraction from plant tissues, isolation and purification from crude plant extracts, and structure elucidation. Although it seems simple, elucidation of every single new anthocyanin is highly challenging. In this section, four chromatographic separation approaches to achieve isolation of anthocyanins are summarized. These include paper chromatography (PC), thin-layer chromatography (TLC), capillary electrophoresis (CE), and high performance liquid chromatography (HPLC). Furthermore, identification methods of anthocyanins summarized here include UV/Vis spectrometry, mass spectrometry (MS), and nuclear magnetic resonance (NMR) (de Rijke, Out et al. 2006; Gonzalez-Paramas, Santos-Buelga et al. 2011).

Paper chromatography (PC) and thin layer chromatography (TLC)

Paper and thin layer chromatography are two simple techniques used for separation of anthocyanins. PC was one of the first methods. It depends on specific samples, different mobile phases, and papers used. This technique is very quick but has limitations for the large quantities of anthocyanins and poor separation capacity for anthocyanins with similar polarity and molecular features. TLC uses silicon or cellulose gel or both. The separation capacity depends on silicone and cellulose size as well as developing solvents. In comparison, TLC can overcome poor separation problems occurred in PC. To date, these two methods are used in common for anthocyanin research because they are simple, fast and cost efficient (de Rijke, Out et al. 2006; Welch, Wu et al. 2008).

Capillary electrophoresis (CE)

Capillary electrophoresis (CE) is a separation method based on electrophoretic motility of metabolites. This technique has an excellent mass sensitivity, high resolution, low sample requirement, and decreased solvent waste. In this method, a sample is introduced into the capillary tube at the anode and the basic or acidic mobile phase will migrate some components of the sample towards the cathode while others are stuck at the anode. Because anthocyanins are not stable in basic solvents, acidic solvents must be used to maintain protonated flavylium in the cation form. Accordingly, the separation of anthocyanins by CE is performed in acidic solvent and the system is configured from cathode to anode. Based on its charge-to-size ratio, particular anthocyanins or other compounds are migrated in the CE system. The migration time of compounds with higher charge-to-size ratio is larger. Detection of compounds is achieved by the UV/Vis spectrophotometry coupled to CE, which collects the spectrum from 200 to 599 nm for each peak (da Costa, Horton et al. 2000; Saenz-Lopez, Fernandez-Zurbano et al. 2003; Calvo, Saenz-Lopez et al. 2004). Presently, mass spectrophotometry (MS) is coupled with CE to identify molecular weights of metabolites described below.

High performance liquid chromatography (HPLC) coupled with UV/vis detector

High performance liquid chromatography (HPLC) has been widely used for the qualitative and quantitative analysis of anthocyanins. Two major types of silicon columns, analytical and preparative, are used for separation of anthocyanins and other compounds. The preparative column allows preparation of samples on the gram scale. The analytical-size column in the microgram scale is used to analyze small-scale extractions. For identification and detection of individual compounds, HPLC is coupled with UV/vis spectrophotometry detection (HPLC-

UV), with mass spectrometry (HPLC-MS), or with nuclear magnetic resonance detection (HPLC-NMR) (Welch, Wu et al. 2008; de Villiers, Venter et al. 2016) described below. Three chemical characteristics are used to separate compounds by HPLC, such as polarity, electrical charge, and molecular size. For the polarity, there are two separation systems, which are normal-phase mode and reverse-phase mode. Normal phase systems consist of the non-polar mobile phase and polar stationary phase. Reverse-phase systems use polar mobile phase and non-polar stationary phase. Normal-phase systems are not effective for the separation of anthocyanins because of polarity of these compounds. By contrast, reverse-phase chromatography is effective for separation of anthocyanins. Normally, compounds with higher polarity elutes earlier. For anthocyanins in an optimized gradient solvent system such as acetonitrile-water or methanol-water solutions supplemented with 0.1%-1% acetic acid or formic acid, diglycosylated or more glycosylated anthocyanins are eluted earlier in the column, followed by monoglycosylated anthocyanins, aglycones, and lastly the acylated anthocyanins. In addition, because hydroxyl groups on the flavylium ion increase water solubility and polarity, aglycones (anthocyanidins) elute in an order of delphinidin, cyaniding, petunidin, pelargonidin, peonidin, and malvidin (Markham and Kohen 2006; de Villiers, Venter et al. 2016).

Chosing a detector to couple with HPLC is dependent on metabolites. For anthocyanins, regular detectors including UV detector, diode-array detection (DAD), and photodiode-array detection (PDA) are useful. These detector systems allowed a limited spectrophotometric scan on each peak as it elutes and provided a unique chromatogram for each anthocyanin that is used to compare with others for identification aims (Mazza, Cacace et al. 2004; Welch, Wu et al. 2008). In an acidic condition, the flavylium cation specifically keeps its red color and gives an absorption at maximum between 510 and 545 nm (depending on the

number of oxygenated carbon atom on the B-ring). Because of these unique and maximum absorptions, anthocyanins can be apart from other flavonoids in the same plant extracts and can be accurately identified and quantified (da Costa, Horton et al. 2000; Welch, Wu et al. 2008).

The HPLC method has limitations because the retention times and resolution obtained from HPLC is very dependent on the instrument and conditions used. Also, modificaitons in mobile-phase composition may results in drastic changes in separation and even in the elution order of the pigments. Further, HPLC methods using organic acids such as formic acid as acid modifier might cause the formation of analytical artifacts, as well. The use of a photodiode array (PDA) detector partially help to reduce these limitations by providing spectral characteristics that give information about acylation and glycosylation patterns (Bakker and Timberlake 1985; Hong and Wrolstad 1990; Giusti, Rodriguez-Saona et al. 1999; Garcia-Beneytez, Cabello et al. 2003). However, these methodologies are sometimes not enough to positively discriminate hundreds of anthocyanins with similar retention times if they have very similar spectral characteristics and their isomeric forms (Strack, Akavia et al. 1980; Hong and Wrolstad 1990; Gao and Mazza 1994; Giusti, Rodriguez-Saona et al. 1999). Therefore, mass spectrometry (MS) has been applied as a supporting technique in the characterization of individual anthocyanin structures (Baldi, Romani et al. 1995; Wang and Sporns 1999).

Electrospray ionization mass spectrometry (ESI-MS) and tandem mass spectrometry (MS/MS)

Ion spray mass spectrometry and electron impact ionization MS have been described and used for structure analyses of all types of water-soluble flavonoids including anthocyanins (Aramendia, Garcia et al. 1995; Sagesser and Deinzer 1996; Giusti, Rodriguez-Saona et al. 1999;

Favretto and Flamini 2000). Electrospray ionization (ESI) is an appropriate method to generate ions. To date, ESI-mass spectrometry (ESI-MS) is a powerful technology to identify molecular weights of anthocyanins. In addition, ESI-MS is a powerful versatile ionization for thermally labile, volatile, nonvolatile, and polar compounds because this soft ionization technique can produce intact ions from large and complex compounds. The only prerequisite that ESI ionization needs is that the sample of interest should be soluble in some solvents (Fenn, Mann et al. 1989; Hutton and Major 1995; Dugo, Mondello et al. 2001; Garcia-Beneytez, Cabello et al. 2003). For anthocyanin identification, ESI-MS delivers the anthocyanin sample in a liquid phase and sprays it into a chamber where a dry gas flows opposite to the sample spray (mist) and a low voltage applied disintegrate the sample drops into charged droplets which get smaller as the solvent vaporizes (Giusti, Rodriguez-Saona et al. 1999).

Tandem mass spectrometry is highly beneficial to characterize individual compounds and identify the structure of compounds by separate ionization and fragmentation steps. Tandem MS (MS/MS) or MSn capabilities are necessary for structural elucidation purposes especially in combination with HPLC-ESI-MS where limited fragmentation information and isomeric compounds may be obtained. Tandem mass allows for the formation of the fragments of each individual molecule by collision-induced dissociation (CID). Individual compounds are detected by the first quadrupole mass detector and then fragmented in the collision cell via a suitable gas, usually argon or nitrogen, and their fragments are detected by the second quadrupole mass analyzer (Giusti, Rodriguez-Saona et al. 1999).

HPLC coupled with ESI-MS and ESI-quantitative-Time-of-Flight MS/MS (ESI-qTOF-MS/MS)

Although HPLC-UV-DAD system is good to choose for detection and identification of anthocyanins, Mass Detector coupled HPLC (HPLC-MS) offer better and more sensitive molecular analysis of anthocyanins due to the separation by mass. Because of some possible drawbacks, which were mentioned in CE chromatography, in this system, the analysis of specific types of individual compounds by HPLC-MS requires an appropriate ionization interface between physical coupling of LC and MS. The most suitable ionization techniques for the chemical structure of anthocyanins are continuous-flow fast-atom bombardment (CF-FAB), matrix –assisted laser desorption ionization (MALDI), atmospheric pressure chemical ionization (APCI), and electrospray ionization (EIS). Today, ESI, as a soft ionization, is the most common interface between LC-MS because it avoids many problems seen with other LC-MS ionization interfaces. Furthermore, ESI is a quite convenient for anthocyanins due to producing gaseous ions from highly charged evaporating liquid droplets.

Regardless of the large number of ionization techniques being used for mass spectrophotometry, electrospray ionization (ESI) is used as the principal interface for CE/MS. CS-ESI-MS effectively combines liquid phase separation of CE and gas phase-based MS. However, there is a drawback of this combination because ESI, as a soft ionization, produces gaseous ions from highly charged evaporating liquid droplets, and most of buffers used in CE are non-volatile solvents. Thus, the solvent system of CE-ESI-MS analysis has to be considered when it is applied for anthocyanin analysis. So, it has been demonstrated that acidic media consisting of methanol, acetic acid and acetonitrile is more acceptable for anthocyanin analysis

under certain conditions (Bednar, Papouskova et al. 2005; Simo, Barbas et al. 2005; Smyth 2005; Ignat, Volf et al. 2011).

For LC-MS interfaces, there are different types of mass analyzers available such as magnetic sectors, time-of-flight (TOF) analyzers, quadrupole mass filters, quadrupole ion traps, and ion cyclotron resonance. Mass analyzers can broadly be divided into two main groups including high and low resolution analyzers depending on their ability to distinguish ions with small mass-to-charge (m/z) differences. The best suited mass analyzer can be determined depending on the analysis being performed, such as targeted (quantitative) or untargeted (screening or qualitative) compound analysis. Mass accuracy of mass analyzers can be figured out by the relative difference between measured and theoretical m/z values, reported in parts per million (ppm) units (de Villiers, Venter et al. 2016).

Time-of-flight mass analyzers work on the principle that lighter ions travel faster than heavier ions following an initial acceleration by an electric field. All ions acquire the same kinetic energy during this initial acceleration period, and are separated in the field-free flight tube according to their different velocities. The physical property that is measured is flight time, which is directly related to the mass-to-charge ratio of the ion. Due to this mode of operation, TOF instruments offer very high mass ranges, very high acquisition rates relatively high resolving power and good sensitivity (Welch, Wu et al. 2008; Ignat, Volf et al. 2011; de Villiers, Venter et al. 2016).

Ion trap analyzers enable the true MS^n operation by allowing selective trapping and fragmentation of parent and/or daughter ions as a function of time. In general, while ion trap analyzers are for qualitative analysis, quadrupole or triple quadrupole ion traps are for quantitation purposes. For the structure elucidation of an individual compound, triple quadrupole

ion trap is the most appropriate mass analyzer for HPLC-ESI-MS due to specifically and sensitively filtering the ion of choice. Within the triple quadrupoles, the first quadrupole (Q1) and the third quadrupole (Q3) function as mass filters to isolate parent ions (precursor-ion) and to monitor selected daughter ions (fragment or product-ion), respectively. The second quadrupole (Q2) serves as a collision cell, where parent ions are fragmented by the ionization. Eventually, the structure of the original parent ion can be elucidated. However, since ESI is a soft ionization, it does not produce many fragments for MS-MS. Because sufficient fragmentation is a key point to deduce parent ion, HPLC-MS-MS uses two ionization methods including ESI and collision-induced dissociation (CID). Within the combination of both ionization, ESI introduces a parent ion into the Q1 mass spectrometer and then CID enhances the fragmentation of parent ion inside Q2 (Figure 1). Several hybrid TOF instruments available provides the option of tandem MS operation with high resolving power acquisition. The most common hybrid preferred is the quadrupole-TOF (Q-TOF) due to allowing collimation of the ion beam as well as the option of mass selections of parent and fragment ions in Q1 and Q3, respectively (Flamini 2003; Welch, Wu et al. 2008; Huang, Wang et al. 2009; de Villiers, Venter et al. 2016; Ganzera and Sturm 2018). The combination of both tandem mass (MS/MS) and high resolving power (Q-TOF) is ideal, and this explains why the Q-TOF MS-MS systems are better to choose for the non-targeted analysis of compounds, especially flavonoids including anthocyanins (de Villiers, Venter et al. 2016).

Analysis of anthocyanins in grapes

Several previous studies have quantified the total anthocyanin content in muscadine grapes, however; the structure analysis of individual anthocyanins is still not completed

(Pastrana-Bonilla, Akoh et al. 2003). Because anthocyanins are essential for the quality and health benefits of muscadine grape and muscadine products, it is critical to elucidate the types of individual anthocyanins in muscadine grapes. But, identification of anthocyanin is challenging due to their complex structure and the lack of reference compounds (Huang, Wang et al. 2009).

Earlier studies on analyzing of individual anthocyanins used thin layer chromatography or HPLC coupled with photo-diode array detector (PDA) or diode array detection (DAD). Anthocyanin identification via these techniques are based on the UV-visible spectrum or retention time and using reference compounds. However; these techniques are limited because UV-Vis detector cannot differentiate the co-eluted compounds. Later on, HPLC assisted by mass spectrometer (HPLC-MS) has been used since the last decades for chemical separation and identification of anthocyanins in grape extracts because a characteristic mass spectrum exist for each compound (Ruberto, Renda et al. 2007; Pati, Liberatore et al. 2009; Ivanova, Stefova et al. 2011). The mass spectrometer can be operated in both positive and negative ionization modes in the HPLC. Since anthocyanins have inherent positive charge, they have maximum sensitivity in the positive mode of the mass spectrometer. However, the highest sensitivity can be obtained in the negative modes for most other flavonoids (Beecher 2003). Also, since anthocyanins are found as conjugates in nature, fragmentation data from MS and previous literature data can be used to identify a sugar or other moieties attached to the anthocyanidins (Lee, Johnson et al. 2005; Sandhu and Gu 2010). Afterwards, HPLC coupled with a diode array detector and a mass spectrometry (HPLC-DAD-MS) was used to analyze and identify anthocyanins in crude plant extracts because it provides useful structural information when standard references are unavailable, and peaks have similar retention time and UV spectra (Seeram, Lee et al. 2006; Sandhu and Gu 2010).

More recently, HPLC coupled with electrospray ionization mass spectrometer (ESI-MS), or tandem mass spectrometer has been introduced for the qualitative and quantitative analyses of anthocyanins because the analytical advantage of these techniques are capable of providing mass spectrum of certain molecular and fragment ions, relevant retention times, and the spectrum of UV absorption for chemical and structural characterization (Charrouf, Hilali et al. 2007; Oh, Lee et al. 2008; You, Chen et al. 2012). Thus, HPLC-ESI-MS/MS would be the best method for analysis of anthocyanins in muscadine grapes (Morais, Ramos et al. 2002; Huang, Wang et al. 2009).

Since the heterocycle of anthocyanidins is pyrilium cation (+), anthocyanidins do not naturally present as free aglycones in the vacuoles of coloured plant tissues. Therefore, for anthocyanin analysis, it is a good strategy to initial analysis of anthocyanidins first because it yields information of the chemical structure of the aglycones (Wang, Tong et al. 2010).

Overall objectives of my dissertation research

My dissertation research focuses on phytochemistry, metabolomics, and biochemistry of PA formation in model and crop systems. Before I joined our lab, our previous members had established an appropriate red cell model system to understand precursors and polymerization of PAs. The red cells were cloned from transgenic red tobacco plants, which have been programed to produce high production of anthocyanins by overexpression of PAP1. Based on our lab's previous research (Zhou, Zeng et al. 2008), our hypothesis is that red cells express a condensing synthase that might be involved in polymerization of flavan-3-ols. My research on protein purification and enzymatic assay described in the chapter 5 provide strong preliminary data that flavan-3-ols are precursors of extension units and a peroxidase-like protein with PPO activity or

a PPO is a potential condensing synthase candidate to be involved in the polymerization. In addition, our lab has selected muscadine grape as an appropriate crop model to understand PA formation and structural diversification. Muscadine has a few advantages. One advantage is that its berries producs a much more diverse array of anthocyanidins than other crops and model plants. For example, it produces methylated anthocyanidins leading to diversification of flavan-3-ols and PAs. The other advantage is that muscadine provides an appropriate material to understand the mechanism of methylated PAs. Additional advantage includes its economic value, being native to North Carolina, and having high nutritional valuea. I developed phytochemistry, HPLC, and LC-MS approaches to characterize anthocyanidins, anthocyanin, and PAs in berries of muscadine, which are included in chapters 2 and 3. All data provides valuable knowledge to understand the biosynthesis of PAs in plants.

REFERENCES

Ahmed, J., U. S. Shivhare, et al. (2004). "Thermal degradation kinetics of anthocyanin and visual colour of plum puree." European Food Research and Technology 218(6): 525-528.

Ananga, A., V. Georgiev, et al. (2013). "Production of Anthocyanins in Grape Cell Cultures: A Potential Source of Raw Material for Pharmaceutical, Food, and Cosmetic Industries." Mediterranean Genetic Code - Grapevine and Olive: 247-287.

Andersen, O. M. (2008). "Recent Advances in the Field of Anthocyanins - Main Focus on Structures." Recent Advances in Polyphenol Research, Vol 1 1: 167-201.

Aramendia, M. A., I. Garcia, et al. (1995). "Determination of Isoflavones Using Capillary Electrophoresis in Combination with Electrospray Mass-Spectrometry." Journal of Chromatography A 707(2): 327-333.

Azuma, A. (2018). "Genetic and Environmental Impacts on the Biosynthesis of Anthocyanins in Grapes." Horticulture Journal 87(1): 1-17.

Bakker, J. and C. F. Timberlake (1985). "The Distribution of Anthocyanins in Grape Skin Extracts of Port Wine Cultivars as Determined by High-Performance Liquid-Chromatography." Journal of the Science of Food and Agriculture 36(12): 1315-1324.

Baldi, A., A. Romani, et al. (1995). "Hplc/Ms Application to Anthocyanins of Vitis-Vinifera L." Journal of Agricultural and Food Chemistry 43(8): 2104-2109.

Ballinger, W. E., E. P. Maness, et al. (1974). "Comparison of Anthocyanins and Wine Color Quality in Black Grapes of 39 Clones of Vitis-Rotundifolia Michx." Journal of the American Society for Horticultural Science 99(4): 338-341.

Banini, A. E., L. C. Boyd, et al. (2006). "Muscadine grape products intake, diet and blood constituents of nondiabetic and type 2 diabetic subjects." Nutrition 22(11-12): 1137-1145.

Barchenger, D. W., J. R. Clark, et al. (2015). "Evaluation of Physicochemical and Storability Attributes of Muscadine Grapes. (Vitis rotundifolia Michx.)." Hortscience 50(1): 104-111.

Bednar, P., B. Papouskova, et al. (2005). "Utilization of capillary electrophoresis/mass spectrometry (CE/MSn) for the study of anthocyanin dyes." J Sep Sci 28(12): 1291-1299.

Beecher, G. R. (2003). "Overview of dietary flavonoids: Nomenclature, occurrence and intake." Journal of Nutrition 133(10): 3248s-3254s.

Berli, F. J., D. Moreno, et al. (2010). "Abscisic acid is involved in the response of grape (Vitis vinifera L.) cv. Malbec leaf tissues to ultraviolet-B radiation by enhancing ultraviolet-absorbing compounds, antioxidant enzymes and membrane sterols." Plant Cell and Environment 33(1): 1-10.

Borkowski, T., H. Szymusiak, et al. (2005). "The effect of 3-O-beta-glucosylation on structural transformations of anthocyanidins." Food Research International 38(8-9): 1031-1037.

Boulton, R. (2001). "The copigmentation of anthocyanins and its role in the color of red wine: A critical review." American Journal of Enology and Viticulture 52(2): 67-87.

Bouquet, A. (1980). "Vitis X Muscadinia Hybridization as Method of Introgression of Resistance Characteristics of Cultivated Vine and Resulting Cytogenic and Taxonomic Problems." Annales De L Amelioration Des Plantes 30(2): 213-214.

Cabrita, L., T. Fossen, et al. (2000). "Colour and stability of the six common anthocyanidin 3-glucosides in aqueous solutions." Food Chem 68(1): 101-107.

Cai, Y., T. H. Lilley, et al. (1990). "Polyphenol Anthocyanin Copigmentation." Journal of the Chemical Society-Chemical Communications(5): 380-383.

Calvo, D., R. Saenz-Lopez, et al. (2004). "Migration order of wine anthocyanins in capillary zone electrophoresis." Analytica Chimica Acta 524(1-2): 207-213.

Castellarin, S. D., A. Pfeiffer, et al. (2007). "Transcriptional regulation of anthocyanin biosynthesis in ripening fruits of grapevine under seasonal water deficit." Plant Cell and Environment 30(11): 1381-1399.

Charrouf, Z., M. Hilali, et al. (2007). "Separation and characterization of phenolic compounds in argan fruit pulp using liquid chromatography-negative electrospray ionization tandem mass spectroscopy." Food Chem 100(4): 1398-1401.

Cheynier, V., G. Comte, et al. (2013). "Plant phenolics: Recent advances on their biosynthesis, genetics, and ecophysiology." Plant Physiology and Biochemistry 72: 1-20.

Conner, P. J. (2009). "Performance of Muscadine Grape Cultivars in Southern Georgia." Journal of the American Pomological Society 63(3): 101-107.

Conner, P. J. and D. MacLean (2013). "Fruit Anthocyanin Profile and Berry Color of Muscadine Grape Cultivars and Muscadinia Germplasm." Hortscience 48(10): 1235-1240.

Czibulya, Z., I. Horvath, et al. (2015). "The effect of temperature, pH, and ionic strength on color stability of red wine." Tetrahedron 71(20): 3027-3031.

da Costa, C. T., D. Horton, et al. (2000). "Analysis of anthocyanins in foods by liquid chromatography, liquid chromatography-mass spectrometry and capillary electrophoresis." Journal of Chromatography A 881(1-2): 403-410.

da Silva, J. K., C. B. B. Cazarin, et al. (2016). "Bioactive compounds of juices from two Brazilian grape cultivars." Journal of the Science of Food and Agriculture 96(6): 1990-1996.

de Jesus, N. Z. T., H. D. Falcao, et al. (2012). "Tannins, Peptic Ulcers and Related Mechanisms." Int J Mol Sci 13(3): 3203-3228.

de Rijke, E., P. Out, et al. (2006). "Analytical separation and detection methods for flavonoids." Journal of Chromatography A 1112(1-2): 31-63.

de Villiers, A., P. Venter, et al. (2016). "Recent advances and trends in the liquid-chromatography-mass spectrometry analysis of flavonoids." Journal of Chromatography A 1430: 16-78.

Delgado-Vargas, F., A. R. Jimenez, et al. (2000). "Natural pigments: Carotenoids, anthocyanins, and betalains - Characteristics, biosynthesis, processing, and stability." Critical Reviews in Food Science and Nutrition 40(3): 173-289.

Deluc, L., F. Barrieu, et al. (2006). "Characterization of a grapevine R2R3-MYB transcription factor that regulates the phenylpropanoid pathway." Plant Physiology 140(2): 499-511.

Deluc, L., J. Bogs, et al. (2008). "The transcription factor VvMYB5b contributes to the regulation of anthocyanin and proanthocyanidin biosynthesis in developing grape berries." Plant Physiology 147(4): 2041-2053.

Di Martino, M. T., P. H. Guzzi, et al. (2015). "Integrated analysis of microRNAs, transcription factors and target genes expression discloses a specific molecular architecture of hyperdiploid multiple myeloma." Oncotarget 6(22): 19132-19147.

Dixon, R. A. and L. W. Sumner (2003). "Legume natural products: Understanding and manipulating complex pathways for human and animal health." Plant Physiology 131(3): 878-885.

Dixon, R. A., D. Y. Xie, et al. (2005). "Proanthocyanidins - a final frontier in flavonoid research?" New Phytologist 165(1): 9-28.

Downey, M. O., N. K. Dokoozlian, et al. (2006). "Cultural practice and environmental impacts on the flavonoid composition of grapes and wine: A review of recent research." American Journal of Enology and Viticulture 57(3): 257-268.

Dufour, C. and C. L. Bayonove (1999). "Interactions between wine polyphenols and aroma substances. An insight at the molecular level." Journal of Agricultural and Food Chemistry 47(2): 678-684.

Dugo, P., L. Mondello, et al. (2001). "Identification of anthocyanins in berries by narrow-bore high-performance liquid chromatography with electrospray ionization detection." Journal of Agricultural and Food Chemistry 49(8): 3987-3992.

Escribano-Bailon, M. T. and C. Santos-Buelga (2012). "Anthocyanin Copigmentation - Evaluation, Mechanisms and Implications for the Colour of Red Wines." Current Organic Chemistry 16(6): 715-723.

Fabroni, S., G. Ballistreri, et al. (2016). "Screening of the anthocyanin profile and in vitro pancreatic lipase inhibition by anthocyanin-containing extracts of fruits, vegetables, legumes and cereals." Journal of the Science of Food and Agriculture 96(14): 4713-4723.

Favretto, D. and R. Flamini (2000). "Application of electrospray ionization mass spectrometry to the study of grape anthocyanins." American Journal of Enology and Viticulture 51(1): 55-64.

Fenn, J. B., M. Mann, et al. (1989). "Electrospray Ionization for Mass-Spectrometry of Large Biomolecules." Science 246(4926): 64-71.

Ferreyra, M. L. F., S. P. Rius, et al. (2012). "Flavonoids: biosynthesis, biological functions, and biotechnological applications." Front Plant Sci 3.

Figueiredo, P., F. George, et al. (1999). "New features of intramolecular copigmentation by acylated anthocyanins." Phytochemistry 51(1): 125-132.

Flamini, R. (2003). "Mass spectrometry in grape and wine chemistry. Part I: Polyphenols." Mass Spectrometry Reviews 22(4): 218-250.

Folts, J. D. (1998). "Antithrombotic potential of grape juice and red wine for preventing heart attacks." Pharm Biol 36: 21-27.

Fossen, T., R. Slimstad, et al. (2002). "Anthocyanins of grasses." Biochemical Systematics and Ecology 30(9): 855-864.

Francisco, R. M., A. Regalado, et al. (2013). "ABCC1, an ATP Binding Cassette Protein from Grape Berry, Transports Anthocyanidin 3-O-Glucosides." Plant Cell 25(5): 1840-1854.

Furuta, K. (1986). "Host Preference and Population-Dynamics in an Autumnal Population of the Maple Aphid, Periphyllus-Californiensis Shinji (Homoptera, Aphididae)." Journal of Applied Entomology-Zeitschrift Fur Angewandte Entomologie 102(1): 93-100.

Galvano, F., L. La Fauci, et al. (2004). "Cyanidins: metabolism and biological properties." Journal of Nutritional Biochemistry 15(1): 2-11.

Ganzera, M. and S. Sturm (2018). "Recent advances on HPLC/MS in medicinal plant analysis-An update covering 2011-2016." J Pharm Biomed Anal 147: 211-233.

Gao, L. and G. Mazza (1994). "Rapid Method for Complete Chemical Characterization of Simple and Acylated Anthocyanins by High-Performance Liquid-Chromatography and Capillary Gas-Liquid-Chromatography." Journal of Agricultural and Food Chemistry 42(1): 118-125.

Garcia-Beneytez, E., F. Cabello, et al. (2003). "Analysis of grape and wine anthocyanins by HPLC-MS." Journal of Agricultural and Food Chemistry 51(19): 5622-5629.

Garcia-Estevez, I., P. Andres-Garcia, et al. (2015). "Relationship between Agronomic Parameters, Phenolic Composition of Grape Skin, and Texture Properties of Vitis vinifera L. cv. Tempranillo." Journal of Agricultural and Food Chemistry 63(35): 7663-7669.

Giusti, M. M., L. E. Rodriguez-Saona, et al. (1999). "Electrospray and tandem mass spectroscopy as tools for anthocyanin characterization." Journal of Agricultural and Food Chemistry 47(11): 4657-4664.

Glavnik, V., I. Vovk, et al. (2017). "High performance thin-layer chromatography-mass spectrometry of Japanese knotweed flavan-3-ols and proanthocyanidins on silica gel plates." Journal of Chromatography A 1482: 97-108.

Gomez, C., G. Conejero, et al. (2011). "In vivo grapevine anthocyanin transport involves vesicle-mediated trafficking and the contribution of anthoMATE transporters and GST." Plant Journal 67(6): 960-970.

Gonzalez-Paramas, A. M., C. Santos-Buelga, et al. (2011). "Analysis of Flavonoids in Foods and Biological Samples." Mini-Reviews in Medicinal Chemistry 11(14): 1239-1255.

Gonzalez, A., M. Zhao, et al. (2008). "Regulation of the anthocyanin biosynthetic pathway by the TTG1/bHLH/Myb transcriptional complex in Arabidopsis seedlings." Plant Journal 53(5): 814-827.

Greenspan, P., J. D. Bauer, et al. (2005). "Antiinflammatory properties of the muscadine grape (Vitis rotundifolia)." Journal of Agricultural and Food Chemistry 53(22): 8481-8484.

Gris, E. F., E. A. Ferreira, et al. (2007). "Caffeic acid copigmentation of anthocyanins from Cabernet Sauvignon grape extracts in model systems." Food Chem 100(3): 1289-1296.

Harborne, J. B. and C. A. Williams (2000). "Advances in flavonoid research since 1992." Phytochemistry 55(6): 481-504.

He, F., L. Mu, et al. (2010). "Biosynthesis of Anthocyanins and Their Regulation in Colored Grapes." Molecules 15(12): 9057-9091.

Hemingway, R. W. (1996). "An introduction to the chemistry and significance of condensed tannins." Antec '96: Plastics - Racing into the Future, Vols I-Iii 42: 1382-1386.

Hemingway, R. W. and P. E. Laks (1985). "Condensed Tannins - a Proposed Route to 2r,3r-(2,3-Cis)-Proanthocyanidins." Journal of the Chemical Society-Chemical Communications(11): 746-747.

Hichri, I., F. Barrieu, et al. (2011). "Recent advances in the transcriptional regulation of the flavonoid biosynthetic pathway." Journal of Experimental Botany 62(8): 2465-2483.

Holton, T. A. and E. C. Cornish (1995). "Genetics and Biochemistry of Anthocyanin Biosynthesis." Plant Cell 7(7): 1071-1083.

Hong, V. and R. E. Wrolstad (1990). "Use of Hplc Separation Photodiode Array Detection for Characterization of Anthocyanins." Journal of Agricultural and Food Chemistry 38(3): 708-715.

Hou, D. X., M. Fujii, et al. (2004). "Molecular mechanisms behind the chemopreventive effects of anthocyanidins." Journal of Biomedicine and Biotechnology(5): 321-325.

Huang, Z. L., B. W. Wang, et al. (2009). "Identification of anthocyanins in muscadine grapes with HPLC-ESI-MS." Lwt-Food Science and Technology 42(4): 819-824.

Hutton, T. and H. J. Major (1995). "Characterizing biomolecules by electrospray ionization mass spectrometry coupled to liquid chromatography and capillary electrophoresis." Biochemical Society Transactions 23(4): 924-927.

Ichino, T., K. Fuji, et al. (2014). "GFS9/TT9 contributes to intracellular membrane trafficking and flavonoid accumulation in Arabidopsis thaliana." Plant Journal 80(3): 410-423.
Ignat, I., I. Volf, et al. (2011). "A critical review of methods for characterisation of polyphenolic compounds in fruits and vegetables." Food Chem 126(4): 1821-1835.
Ivanova, V., M. Stefova, et al. (2011). "Identification of polyphenolic compounds in red and white grape varieties grown in R. Macedonia and changes of their content during ripening." Food Research International 44(9): 2851-2860.
Iwashina, T. (2000). "The structure and distribution of the flavonoids in plants." Journal of Plant Research 113(1111): 287-299.
Jain, S. P. and S. N. Srivastava (1970). "Studies on the effect of some anionic detergents on the stability of emulsions stabilised by partially flocculated sols." Bulletin of the Chemical Society of Japan 43(12): 3644-3650.
Janvary, L., T. Hoffmann, et al. (2009). "A Double Mutation in the Anthocyanin 5-O-Glucosyltransferase Gene Disrupts Enzymatic Activity in Vitis vinifera L." Journal of Agricultural and Food Chemistry 57(9): 3512-3518.
Kader, F., J. P. Haluk, et al. (1998). "Degradation of cyanidin 3-glucoside by blueberry polyphenol oxidase: Kinetic studies and mechanisms." Journal of Agricultural and Food Chemistry 46(8): 3060-3065.
Kader, F., M. Irmouli, et al. (2001). "Proposed mechanism for the degradation of pelargonidin 3-glucoside by caffeic acid o-quinone." Food Chem 75(2): 139-144.
Kader, F., J. P. Nicolas, et al. (1999). "Degradation of pelargonidin 3-glucoside in the presence of chlorogenic acid and blueberry polyphenol oxidase." Journal of the Science of Food and Agriculture 79(4): 517-522.
Keevil, J. G., H. Osman, et al. (1998). "Grape juice inhibits human ex vivo platelet aggregation while orange and grapefruit juices do not." Journal of the American College of Cardiology 31(2): 172a-172a.
Keller, M. and G. Hrazdina (1998). "Interaction of nitrogen availability during bloom and light intensity during veraison. II. Effects on anthocyanin and phenolic development during grape ripening." American Journal of Enology and Viticulture 49(3): 341-349.
Kitamura, S., F. Matsuda, et al. (2010). "Metabolic profiling and cytological analysis of proanthocyanidins in immature seeds of Arabidopsis thaliana flavonoid accumulation mutants." Plant Journal 62(4): 549-559.
Koes, R., W. Verweij, et al. (2005). "Flavonoids: a colorful model for the regulation and evolution of biochemical pathways." Trends in Plant Science 10(5): 236-242.
Kong, J. M., L. S. Chia, et al. (2003). "Analysis and biological activities of anthocyanins." Phytochemistry 64(5): 923-933.
Kowalczyk, E., P. Krzesinski, et al. (2003). "Anthocyanins in medicine." Polish Journal of Pharmacology 55(5): 699-702.
Lamikanra, O. (1989). "Anthocyanins of Vitis-Rotundifolia Hybrid Grapes." Food Chem 33(3): 225-237.
Lee, J. H., J. V. Johnson, et al. (2005). "Identification of ellagic acid conjugates and other polyphenolics in muscadine grapes by HPLC-ESI-MS." Journal of Agricultural and Food Chemistry 53(15): 6003-6010.
Lees, G. L. (1992). "Condensed Tannins in Some Forage Legumes - Their Role in the Prevention of Ruminant Pasture Bloat." Plant Polyphenols : Synthesis, Properties, Significance 59: 915-934.

Lepiniec, L., I. Debeaujon, et al. (2006). "Genetics and biochemistry of seed flavonoids." Annual Review of Plant Biology 57: 405-430.

Lijavetzky, D., L. Ruiz-Garcia, et al. (2006). "Molecular genetics of berry colour variation in table grape." Molecular Genetics and Genomics 276(5): 427-435.

Louime, C., J. Lu, et al. (2011). "Resistance to Elsinoe Ampelina and Expression of Related Resistant Genes in Vitis Rotundifolia Michx. Grapes." Int J Mol Sci 12(6): 3473-3488.

Manach, C., G. Williamson, et al. (2005). "Bioavailability and bioefficacy of polyphenols in humans. I. Review of 97 bioavailability studies." American Journal of Clinical Nutrition 81(1): 230s-242s.

Markham, K. A. and A. Kohen (2006). "Analytical procedures for the preparation, isolation, analysis and preservation of reduced nicotinamides." Current Analytical Chemistry 2(4): 379-388.

Martinoia, E., M. Maeshima, et al. (2007). "Vacuolar transporters and their essential role in plant metabolism." Journal of Experimental Botany 58(1): 83-102.

Mathews, H., S. K. Clendennen, et al. (2003). "Activation tagging in tomato identifies a transcriptional regulator of anthocyanin biosynthesis, modification, and transport." Plant Cell 15(8): 1689-1703.

Matsumoto, H., Y. Nakamura, et al. (2003). "Stimulatory effect of cyanidin 3-glycosides on the regeneration of rhodopsin." Journal of Agricultural and Food Chemistry 51(12): 3560-3563.

Mazza, G., J. E. Cacace, et al. (2004). "Methods of analysis for anthocyanins in plants and biological fluids." Journal of Aoac International 87(1): 129-145.

Meepagala, K. M., J. B. Magee, et al. (2002). "Phenolic constituents from muscadine grape (Vitis rotundifolia) cultivar polyanna seeds." Abstracts of Papers of the American Chemical Society 223: U37-U37.

Monagas, M., B. Bartolome, et al. (2005). "Updated knowledge about the presence of phenolic compounds in wine." Critical Reviews in Food Science and Nutrition 45(2): 85-118.

Morais, H., C. Ramos, et al. (2002). "Influence of storage conditions on the stability of monomeric anthocyanins studied by reversed-phase high-performance liquid chromatography." Journal of Chromatography B-Analytical Technologies in the Biomedical and Life Sciences 770(1-2): 297-301.

Mueller, L. A. and V. Walbot (2001). "Models for vacuolar sequestration of anthocyanins." Regulation of Phytochemicals by Molecular Techniques 35: 297-312.

Nesbitt, W. B., E. P. Maness, et al. (1974). "Relationship of Anthocyanins of Black Muscadine Grapes (Vitis-Rotundifolia Michx) to Wine Color." American Journal of Enology and Viticulture 25(1): 30-32.

Nile, S. H. and S. W. Park (2014). "Edible berries: Bioactive components and their effect on human health." Nutrition 30(2): 134-144.

Noratto, G. D., G. Angel, et al. (2009). "Effects of Polyphenolics from Grape (Vitis rotundifolia) and acai (Euterpe oleracea Mart.) on the expresion of microRNAs relevant to inflammation in vascular diseases." Faseb Journal 23.

Oglesby, L., A. Ananga, et al. (2016). "Anthocyanin Accumulation in Muscadine Berry Skins Is Influenced by the Expression of the MYB Transcription Factors, MybA1, and MYBCS1." Antioxidants 5(4).

Oh, Y. S., J. H. Lee, et al. (2008). "Characterization and quantification of anthocyanins in grape juices obtained from the grapes cultivated in Korea by HPLC/DAD, HPLC/MS, and HPLC/MS/MS." J Food Sci 73(5): C378-C389.

Ohmori, K., N. Ushimaru, et al. (2004). "Oligomeric catechins: An enabling synthetic strategy by orthogonal activation and C(8) protection." Proceedings of the National Academy of Sciences of the United States of America 101(33): 12002-12007.

Olien, W. C. (1990). "The Muscadine Grape - Botany, Viticulture, History, and Current Industry." Hortscience 25(7): 732-739.

Olson, D. K., S. Kittelson, et al. (2002). "Study of the copigmentation effect between anthocyanins and organic acids." Abstracts of Papers of the American Chemical Society 223: U306-U306.

Page, J. E. and G. H. N. Towers (2002). "Anthocyanins protect light-sensitive thiarubrine phototoxins." Planta 215(3): 478-484.

Passeri, V., R. Koes, et al. (2016). "New Challenges for the Design of High Value Plant Products: Stabilization of Anthocyanins in Plant Vacuoles." Front Plant Sci 7.

Pastrana-Bonilla, E., C. C. Akoh, et al. (2003). "Phenolic content and antioxidant capacity of muscadine grapes." Journal of Agricultural and Food Chemistry 51(18): 5497-5503.

Pati, S., M. T. Liberatore, et al. (2009). "Rapid screening for anthocyanins and anthocyanin dimers in crude grape extracts by high performance liquid chromatography coupled with diode array detection and tandem mass spectrometry." Journal of Chromatography A 1216(18): 3864-3868.

Petrussa, E., E. Braidot, et al. (2013). "Plant Flavonoids-Biosynthesis, Transport and Involvement in Stress Responses." Int J Mol Sci 14(7): 14950-14973.

Plundrich, N., M. H. Grace, et al. (2013). "Bioactive polyphenols from muscadine grape and blackcurrant stably concentrated onto protein-rich matrices for topical applications." International Journal of Cosmetic Science 35(4): 394-401.

Poracova, J., L. Tkacikova, et al. (2011). "The Importance of Anthocyanins for Human and Animal Health." Planta Medica 77(12): 1447-1447.

Qu, X. P., J. Lu, et al. (1996). "Genetic diversity in muscadine and American bunch grapes based on randomly amplified polymorphic DNA (RAPD) analysis." Journal of the American Society for Horticultural Science 121(6): 1020-1023.

Quideau, S., D. Deffieux, et al. (2011). "Plant Polyphenols: Chemical Properties, Biological Activities, and Synthesis." Angewandte Chemie-International Edition 50(3): 586-621.

Reyes, L. F. and L. Cisneros-Zevallos (2007). "Degradation kinetics and colour of anthocyanins in aqueous extracts of purple- and red-flesh potatoes (Solanum tuberosum L.)." Food Chem 100(3): 885-894.

Ricardo-Da-Silva, J. M., J. Rigaud, et al. (1991). "Procyanidin Dimers and Trimers from Grape Seeds." Phytochemistry 30(4): 1259-1264.

Rojas-Pierce, M. (2013). "Targeting of tonoplast proteins to the vacuole." Plant Science 211: 132-136.

Ruberto, G., A. Renda, et al. (2007). "Polyphenol constituents and antioxidant activity of grape pomace extracts from five Sicilian red grape cultivars." Food Chem 100(1): 203-210.

Saenz-Lopez, R., P. Fernandez-Zurbano, et al. (2003). "Development and validation of a capillary zone electrophoresis method for the quantitative determination of anthocyanins in wine." Journal of Chromatography A 990(1-2): 247-258.

Sagesser, M. and M. Deinzer (1996). "HPLC-ion spray tandem mass spectrometry of flavonol glycosides in hops." Journal of the American Society of Brewing Chemists 54(3): 129-134.

Salamon, B., V. Farkas, et al. (2017). "Effect of added sugar and ascorbic acid on the anthocyanin content of high pressure processed strawberry juices during storage." Joint Airapt-25th & Ehprg-53rd International Conference on High Pressure Science and Technology, 2015 950.

Sandhu, A. K., D. J. Gray, et al. (2011). "Effects of exogenous abscisic acid on antioxidant capacities, anthocyanins, and flavonol contents of muscadine grape (*Vitis rotundifolia*) skins." Food Chem 126(3): 982-988.

Sandhu, A. K. and L. W. Gu (2010). "Antioxidant Capacity, Phenolic Content, and Profiling of Phenolic Compounds in the Seeds, Skin, and Pulp of Vitis rotundifolia (Muscadine Grapes) As Determined by HPLC-DAD-ESI-MSn." Journal of Agricultural and Food Chemistry 58(8): 4681-4692.

Scalbert, A. and G. Williamson (2000). "Dietary intake and bioavailability of polyphenols." Journal of Nutrition 130(8): 2073s-2085s.

Seeram, N. P., R. Lee, et al. (2006). "Identification of phenolic compounds in strawberries by liquid chromatography electrospray ionization mass spectroscopy." Food Chem 97(1): 1-11.

Shi, M. Z. and D. Y. Xie (2014). "Biosynthesis and metabolic engineering of anthocyanins in Arabidopsis thaliana." Recent Pat Biotechnol 8(1): 47-60.

Sieniawska, E. (2015). "Activities of Tannins - From In Vitro Studies to Clinical Trials." Nat Prod Commun 10(11): 1877-1884.

Simo, C., C. Barbas, et al. (2005). "Capillary electrophoresis-mass spectrometry in food analysis." Electrophoresis 26(7-8): 1306-1318.

Sims, C. A. and J. R. Morris (1986). "Effects of Acetaldehyde and Tannins on the Color and Chemical Age of Red Muscadine (Vitis-Rotundifolia) Wine." American Journal of Enology and Viticulture 37(2): 163-165.

Smeriglio, A., D. Barreca, et al. (2017). "Proanthocyanidins and hydrolysable tannins: occurrence, dietary intake and pharmacological effects." British Journal of Pharmacology 174(11): 1244-1262.

Smyth, W. F. (2005). "Recent applications of capillary electrophoresis-electrospray ionisation-mass spectrometry in drug analysis." Electrophoresis 26(7-8): 1334-1357.

Spranger, I., B. Sun, et al. (2008). "Chemical characterization and antioxidant activities of oligomeric and polymeric procyanidin fractions from grape seeds." Food Chem 108(2): 519-532.

Springob, K., J. Nakajima, et al. (2003). "Recent advances in the biosynthesis and accumulation of anthocyanins." Natural Product Reports 20(3): 288-303.

Strack, D., N. Akavia, et al. (1980). "High-Performance Liquid-Chromatographic Identification of Anthocyanins." Zeitschrift Fur Naturforschung C-a Journal of Biosciences 35(7-8): 533-538.

Sun, B. S., C. Leandro, et al. (1998). "Separation of grape and wine proanthocyanidins according to their degree of polymerization." Journal of Agricultural and Food Chemistry 46(4): 1390-1396.

Sun, Y., H. Li, et al. (2012). "Arabidopsis TT19 Functions as a Carrier to Transport Anthocyanin from the Cytosol to Tonoplasts." Molecular Plant 5(2): 387-400.

Takos, A. M., F. W. Jaffe, et al. (2006). "Light-induced expression of a MYB gene regulates anthocyanin biosynthesis in red apples." Plant Physiology 142(3): 1216-1232.

Talcott, S. T., C. H. Brenes, et al. (2003). "Phytochemical stability and color retention of copigmented and processed muscadine grape juice." Journal of Agricultural and Food Chemistry 51(4): 957-963.

Talcott, S. T. and J. H. Lee (2002). "Ellagic acid and flavonoid antioxidant content of muscadine wine and juice." Journal of Agricultural and Food Chemistry 50(11): 3186-3192.

Tanner, G. J., K. T. Francki, et al. (2003). "Proanthocyanidin biosynthesis in plants - Purification of legume leucoanthocyanidin reductase and molecular cloning of its cDNA." Journal of Biological Chemistry 278(34): 31647-31656.

Torskangerpoll, K. and O. M. Andersen (2005). "Colour stability of anthocyanins in aqueous solutions at various pH values." Food Chem 89(3): 427-440.

Treutter, D. (2006). "Significance of flavonoids in plant resistance: a review." Environmental Chemistry Letters 4(3): 147-157.

Tsuda, T., F. Horio, et al. (2003). "Dietary cyanidin 3-O-beta-D-glucoside-rich purple corn color prevents obesity and ameliorates hyperglycemia in mice." Journal of Nutrition 133(7): 2125-2130.

Vidal, S., D. Cartalade, et al. (2002). "Changes in proanthocyanidin chain length in winelike model solutions." Journal of Agricultural and Food Chemistry 50(8): 2261-2266.

Walker, A. R., E. Lee, et al. (2007). "White grapes arose through the mutation of two similar and adjacent regulatory genes." Plant Journal 49(5): 772-785.

Walker, A. R., E. Lee, et al. (2006). "Two new grape cultivars, bud sports of Cabernet Sauvignon bearing pale-coloured berries, are the result of deletion of two regulatory genes of the berry colour locus." Plant Molecular Biology 62(4-5): 623-635.

Wang, J. and P. Sporns (1999). "Analysis of anthocyanins in red wine and fruit juice using MALDI-MS." Journal of Agricultural and Food Chemistry 47(5): 2009-2015.

Wang, P. Q., L. J. Zhang, et al. (2018). "Evolutionary and functional characterization of leucoanthocyanidin reductases from Camellia sinensis." Planta 247(1): 139-154.

Wang, X., H. R. Tong, et al. (2010). "Chemical characterization and antioxidant evaluation of muscadine grape pomace extract." Food Chem 123(4): 1156-1162.

Wei, Z., J. M. Luo, et al. (2017). "Profile of Polyphenol Compounds of Five Muscadine Grapes Cultivated in the United States and in Newly Adapted Locations in China." Int J Mol Sci 18(3).

Welch, C. R., Q. L. Wu, et al. (2008). "Recent advances in anthocyanin analysis and characterization." Current Analytical Chemistry 4(2): 75-101.

WilskaJeszka, J. and A. Korzuchowska (1996). "Anthocyanins and chlorogenic acid copigmentation - Influence on the colour of strawberry and chokeberry juices." Zeitschrift Fur Lebensmittel-Untersuchung Und-Forschung 203(1): 38-42.

Winefield, C. (2002). The final steps in anthocyanin formation: A story of modification and sequestration. Advances in Botanical Research, Vol 37. 37: 55-74.

Winkel-Shirley, B. (2001). "Flavonoid biosynthesis. A colorful model for genetics, biochemistry, cell biology, and biotechnology." Plant Physiology 126(2): 485-493.

Wrolstad, R. E. (2004). "Symposium 12: Interaction of natural colors with other ingredients - Anthocyanin pigments - Bioactivity and coloring properties." J Food Sci 69(5): C419-C421.

Xie, D. Y. (2017). "Regulation of Anthocyanin Biosynthesis in the WD40-bHLH-MYB Complex-Programmed Arabidopsis Cells." In Vitro Cellular & Developmental Biology-Animal 53: S13-S13.

Xie, D. Y. and R. A. Dixon (2005). "Proanthocyanidin biosynthesis - still more questions than answers?" Phytochemistry 66(18): 2127-2144.

Xie, D. Y., S. B. Sharma, et al. (2003). "Role of anthocyanidin reductase, encoded by BANYULS in plant flavonoid biosynthesis." Science 299(5605): 396-399.

Xie, L. H., H. M. Su, et al. (2018). "Recent advances in understanding the anti-obesity activity of anthocyanins and their biosynthesis in microorganisms." Trends in Food Science & Technology 72: 13-24.

Xu, C. M., Y. Yagiz, et al. (2014). "Enzyme release of phenolics from muscadine grape (Vitis rotundifolia Michx.) skins and seeds." Food Chem 157: 20-29.

Xu, C. M., Y. L. Zhang, et al. (2011). "Influence of Growing Season on Phenolic Compounds and Antioxidant Properties of Grape Berries from Vines Grown in Subtropical Climate." Journal of Agricultural and Food Chemistry 59(4): 1078-1086.

Xu, W. J., C. Dubos, et al. (2015). "Transcriptional control of flavonoid biosynthesis by MYB-bHLH-WDR complexes." Trends in Plant Science 20(3): 176-185.

Yilmaz, Y. and R. T. Toledo (2004). "Major flavonoids in grape seeds and skins: Antioxidant capacity of catechin, epicatechin, and gallic acid." Journal of Agricultural and Food Chemistry 52(2): 255-260.

You, Q., F. Chen, et al. (2012). "Analysis of phenolic composition of Noble muscadine (*Vitis rotundifolia*) by HPLC-MS and the relationship to its antioxidant capacity." J Food Sci 77(10): C1115-C1123.

Yu, Y., L. Jiao, et al. (2016). "Callose Synthase Family Genes Involved in the Grapevine Defense Response to Downy Mildew Disease." Phytopathology 106(1): 56-64.

Zhang, S. T., L. X. Li, et al. (2017). "Preparative high-speed counter-current chromatography separation of grape seed proanthocyanidins according to degree of polymerization." Food Chem 219: 399-407.

Zhang, Y., S. K. C. Chang, et al. (2017). "Characterization of titratable acids, phenolic compounds, and antioxidant activities of wines made from eight mississippi-grown muscadine varieties during fermentation." Lwt-Food Science and Technology 86: 302-311.

Zhao, J. (2015). "Flavonoid transport mechanisms: how to go, and with whom." Trends in Plant Science 20(9): 576-585.

Zhao, J. and R. A. Dixon (2010). "The 'ins' and 'outs' of flavonoid transport." Trends in Plant Science 15(2): 72-80.

Zhao, J., Y. Z. Pang, et al. (2010). "The Mysteries of Proanthocyanidin Transport and Polymerization." Plant Physiology 153(2): 437-443.

Zhao, L., Y. Yagiz, et al. (2017). "Identification and characterization of vitamin E isomers, phenolic compounds, fatty acid composition, and antioxidant activity in seed oils from different muscadine grape cultivars." Journal of Food Biochemistry 41(4).

Zhou, L. L., H. N. Zeng, et al. (2008). "Development of tobacco callus cultures over expressing Arabidopsis PAP1/MYB75 transcription factor and characterization of anthocyanin biosynthesis." Planta 229(1): 37-51.

Zimmermann, I. M., M. A. Heim, et al. (2004). "Comprehensive identification of Arabidopsis thaliana MYB transcription factors interacting with R/B-like BHLH proteins." Plant Journal 40(1): 22-34.

Zou, H., Y. Ma, et al. (2018). "Isolation of strawberry anthocyanins using high-speed counter-current chromatography and the copigmentation with catechin or epicatechin by high pressure processing." Food Chem 247: 81-88.

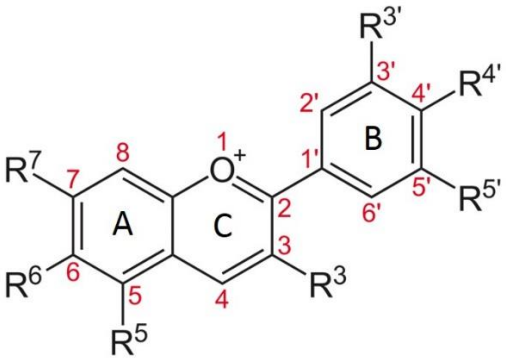

Figure 1.1: The core chemical structure of anthocyanidins. A; Aromatic ring, B; Phenyl ring, C; Benzopyran ring. R; Substitutes.

Table 1.1: A basic chemical structure of selected anthocyanidins and their substitutions.
Modified from (Welch, Wu et al. 2008).

Anthocyanidins	Substitutions						
	R^3	R^5	R^6	R^7	$R^{3'}$	$R^{4'}$	$R^{5'}$
Cyanidin	OH	OH	H	OH	OH	OH	H
Delphinidin	OH	OH	H	OH	OH	OH	OH
Pelargonidin	OH	OH	H	OH	H	OH	H
Peonidin	OH	OH	H	OH	OMe	OH	H
Petunidin	OH	OH	H	OH	OMe	OH	OH
Malvidin	OH	OH	H	OH	OMe	OH	OMe
Apigenidin	H	OH	H	OH	H	OH	H
Aurantinidin	OH	OH	OH	OH	H	OH	H
Capensinidin	OH	OMe	H	OH	OMe	OH	OMe
Europinidin	OH	OMe	H	OH	OMe	OH	OH
Hirsutidin	OH	OH	H	OMe	OMe	OH	OMe
6-Hydroxycyanidin	OH	OH	OH	OH	OH	OH	H
6-Hydroxydelphinidin	OH	OH	OH	OH	OH	OH	OH
Luteolinidin	H	OH	H	OH	OH	OH	H
5-Methylcyanidin	OH	OMe	H	OH	OH	OH	H
Pulchellidin	OH	OMe	H	OH	OH	OH	OH
Riccionidin A	H	H	OH	OH	H	OH	H
Rosinidin	OH	OH	H	OMe	OMe	OH	H
Tricetinidin	H	OH	H	OH	OH	OH	OH

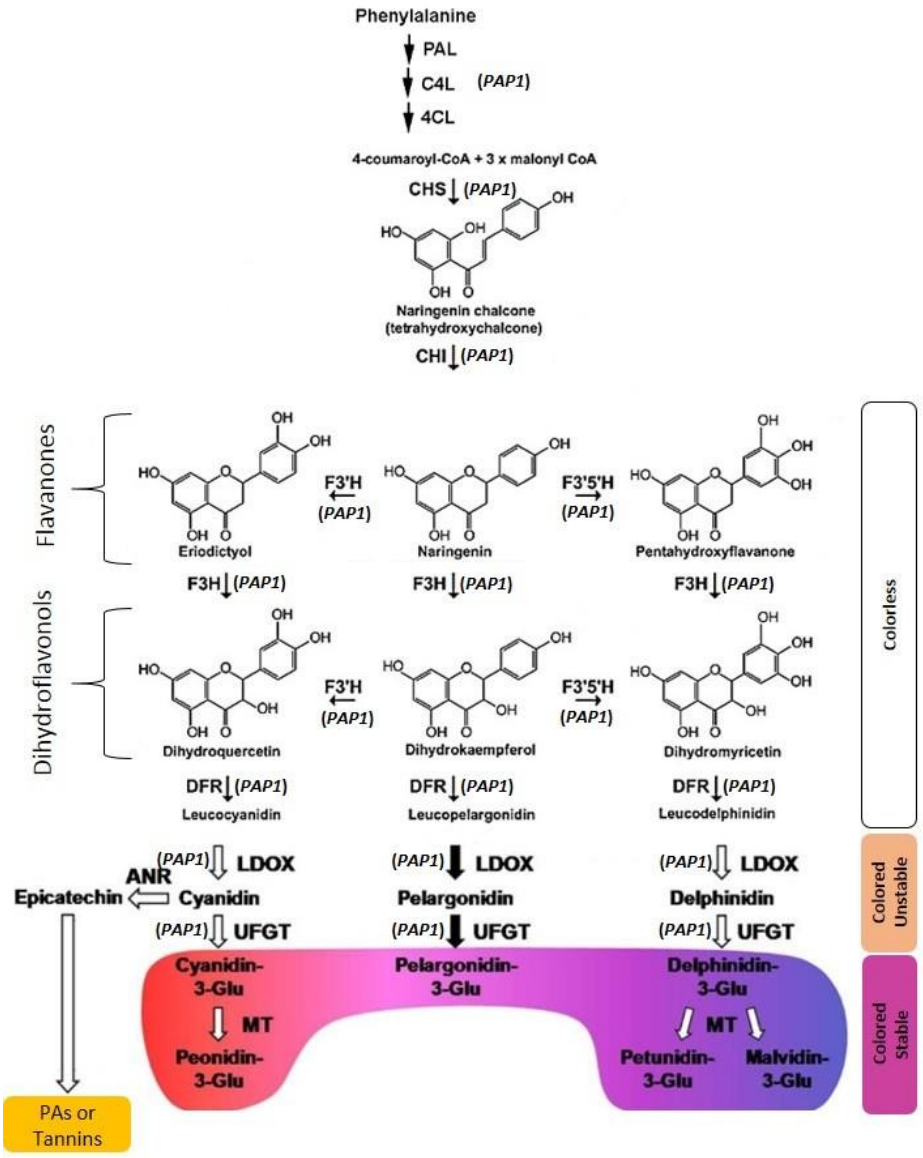

Figure 1.2: Biosynthesis of anthocyanidins: cyanidin, pelargonidin and delphinidin. The simplified scheme of the general flavonoid biosynthetic pathway in plant cells demonstrates the anthocyanidin branch end products. Anthocyanins are synthesized by a multienzyme complex including CHS, chalcone synthase; CHI, chalcone isomerase; F3H, flavonoid-3-hydroxylase; F3′H, flavonoid-3′-hydroxylase; F3′5′H, flavonoid 3′,5′-hydroxylase; DFR, dihydroflavonol 4-reductase; ANS, anthocyanidin synthase (or LDOX, leucoanthocyanidin oxidase); UFGT, UDP-glucose flavonoid 3-O-glucosyl transferase; MT, methyltransferase; PAP1, production of anthocyanin pigment 1. Modified from (Ferreyra, Rius et al. 2012; Petrussa, Braidot et al. 2013).

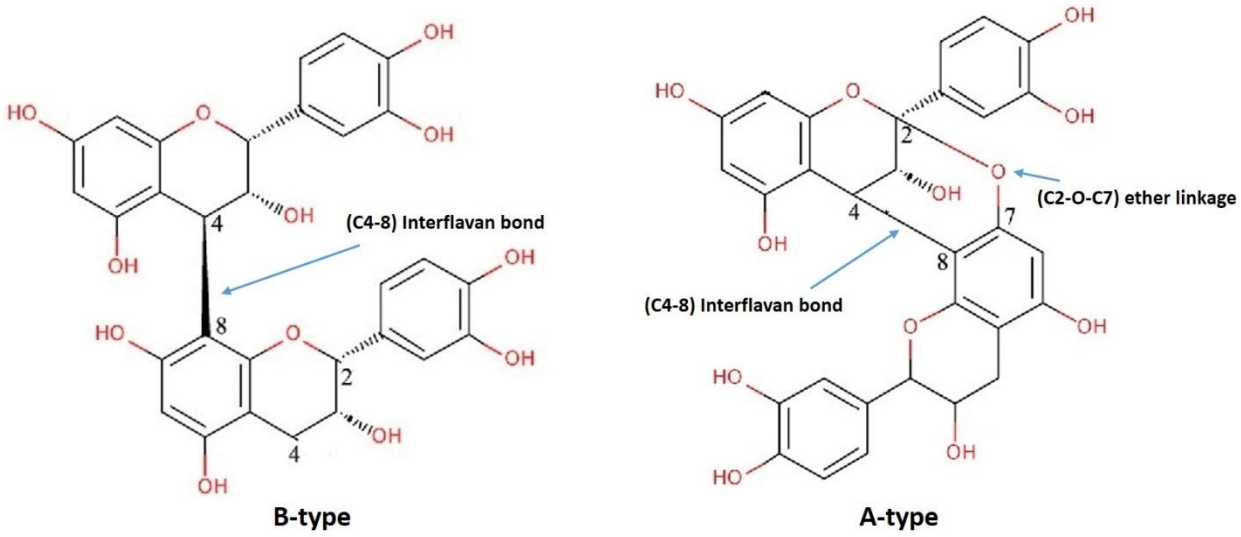

Figure 1.3: Structure of A and B-type dimeric proanthocyanidins

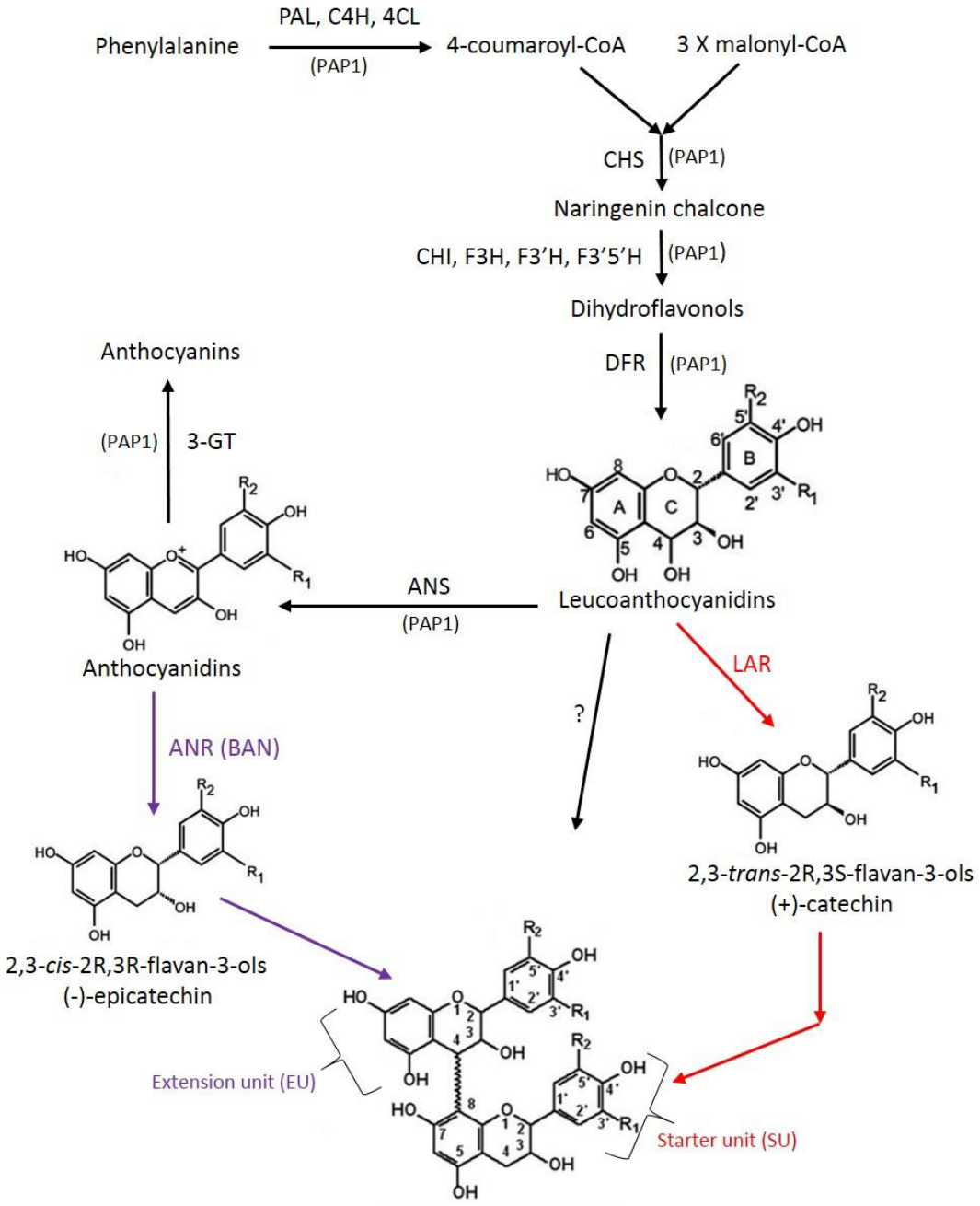

Figure 1.4: Biosynthetic pathway for formation of proanthocyanidins. LAR; leucoanthocyanidin reductase, ANR; anthocyanidin reductase.

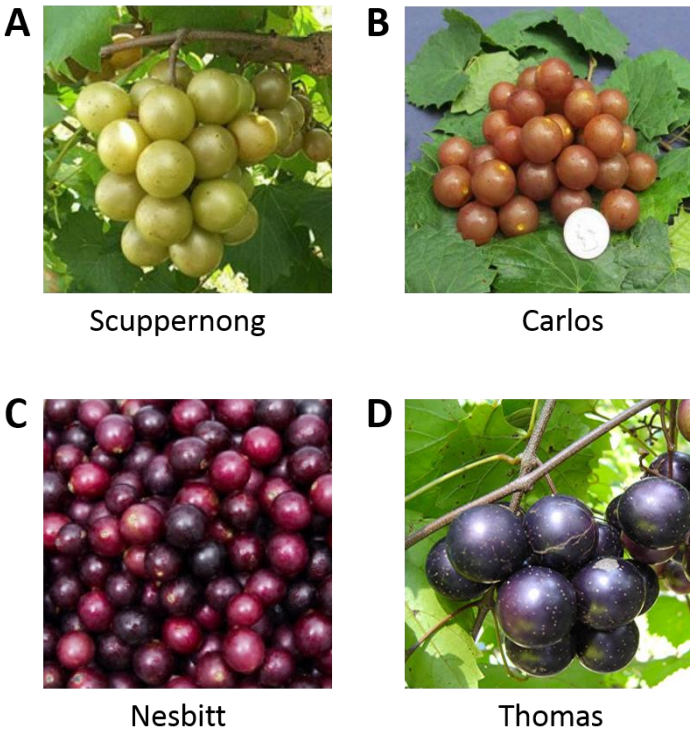

Figure 1.5: Bronze and black colored berries of commercially important muscadine cultivars. A-B; bronze cultivars, C-D; black cultivars

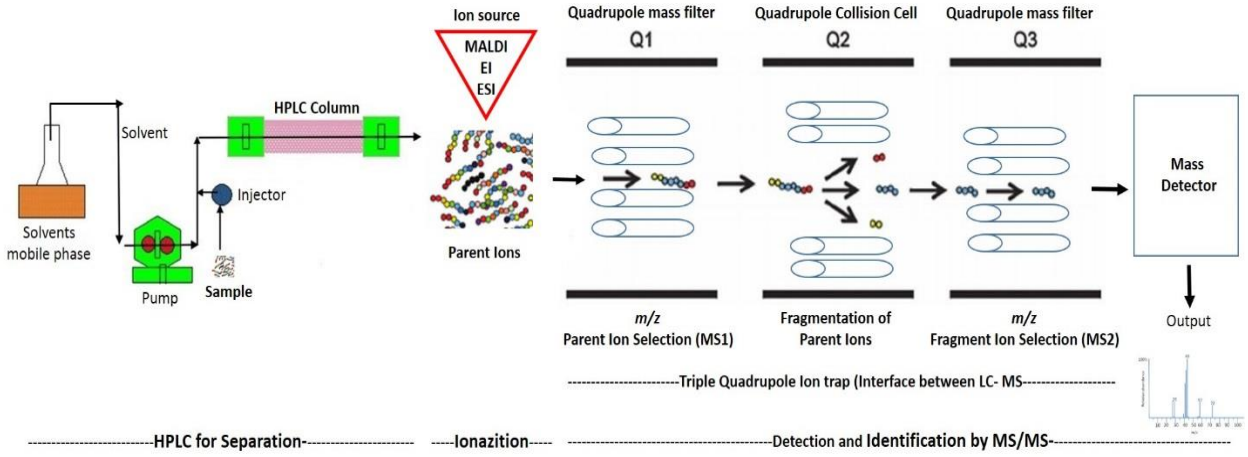

Figure 1.6: Diagram of an LC-ESI-q(TOF)-MS/MS chromatography

CHAPTER 2

HPLC-qTOF-MS/MS based profiling of anthocyanins in berries of two hybrid muscadine varieties FLH 13-11 and FLH 17-66 in two continuous cropping seasons

Seyit Yuzuak[1], James Ballington[2], and De-Yu Xie[1*]

1 Department of Plant and Microbial Biology, North Carolina State University

2 Department of Horticultural Sciences, North Carolina State University

*: corresponding author, dxie@ncsu.edu

Abstract

FLH 13-11 and FLH 17-66 are two F_1 interspecific hybrid muscadine grape genotypes developed to produce new anthocyanins for pigment color stability. The two hybrids resulted from crossing 'Marsh' (*Vitis munsoniana*) and 'Magoon' (*V. rotundifolia*). This report characterizes anthocyanins produced in fully ripe berries of the two hybrid cultivars in two continuous cropping seasons (years). The total anthocyanin contents were significantly different in the two years. High performance liquid chromatography-photodiode array detector (HPLC-DAD) and HPLC-quadrupole time-of-flight tandem mass spectrometer (HPLC-qTOF-MS/MS) were performed to profile and to annotate anthocyanins and anthocyanidins. The resulting data showed that twelve anthocyanins were detected from berries. Hydrolysis of anthocyanins released six known anthocyanidins (pelargonidin, cyanidin, peonidin, delphinidin, petunidin, and malvidin) and three unidentified ones from anthocyanin extracts of two varieties. The negative mode was used to ionize anthocyanins to generate primary mass spectrum (MS1), and collision

induced dissociation was performed to generate detail features of MS/MS fragments (secondary mass spectrum, MS2). Based on anthocyanidin structure, MS1, and MS2, six anthocyanin peaks were annotated to be diglucosides of anthocyanidins, delphinidin 3,5-diglucoside (Del-3,5-dG), cyanidin 3,5-diglucoside (Cy-3,5-dG), petunidin 3,5-diglucoside (Pt-3,5-dG), malvidin 3,5-diglucoside (Mal-3,5-dG), peonidin 3,5-diglucoside (Pn-3,5-dG), and pelargonidin 3,5-diglucoside (Pel-3,5-dG). Furthermore, two anthocyanin peaks were annotated to be monoglucosides, Pn-3-G and Del 3-G. Four additional anthocyanin peaks were shown to be cyanidin, pelargonidin, or peonidin-derived anthocyanins. These data show that both FLH 13-11 and FLH 17-66 can produce anthocyanidin-diglucosides and -monoglucosides, indicating their potential commercial value for stable color of muscadine products.

Key words: Anthocyanidins, anthocyanidin-3,5-diglucoside, anthocyanidin-3-O-monoglucoside, anthocyanins, HPLC-quadrupole time-of-flight tandem mass spectrometer, *Vitis rotundifolia*, metabolic profiling,

Introduction

Muscadine (*Vitis rotundifolia* Michx) is a grape crop native to the south-eastern and south-central regions of the United State (Brown 1940). To date, this crop is being commercially produced in Florida, Georgia, Alabama, Louisiana, South Carolina, and North Carolina (Olien 2001). Many years of breeding efforts have created multiple superior cultivars for fresh market, wine, and unfermented juice industries (Mortensen 2001).

Anthocyanins are the main active nutraceuticals in muscadine berries, which provide antioxidative and other health benefits (Striegler, Carter et al. 2005; Wang, Tong et al. 2010; You, Chen et al. 2011; Gourineni, Shay et al. 2012). To date, multiple studies have intensively analyzed total anthocyanins in a particular muscadine cultivars. The first anthocyanin molecule isolated from muscadine berries of the Hunt cultivar was named muscadinin (3, 5-diglycosidyl-3'-O-methyldelphinidin, namely petunidin 3, 5-diglucoside) by W.L. Brown in 1940 (Brown 1940). The main anthocyanins were then identified from berries and other tissues (Nesbitt, Maness et al. 1974; Goldy, Ballinger et al. 1987; Cardona, Lee et al. 2009; You, Chen et al. 2012; Conner and MacLean 2013; Barchenger, Clark et al. 2015). The most common muscadine anthocyanidins are delphinidin, malvidin, petunidin, cyanidin, and peonidin (Fig. 1). The most common anthocyanins are non-acylated 3,5 diglucosides of delphinidin, malvidin, petunidin, cyanidin, and peonidin (Fig. 1), which have been elucidated from fresh fruits of Noble, Tarheel, and other cultivars (Nesbitt, Maness et al. 1974; You, Chen et al. 2012; You, Chen et al. 2012; Conner and MacLean 2013). The contents of these six anthocyanins in muscadine berries varies widely among cultivars. More importantly, the ratio of each of five anthocyanins has been demonstrated to control wine and juice color. For example, high quality wine color was found to be caused by high amounts and percentages of malvidin 3,5-diglucoside but low amounts and

percentages of delphinidin 3,5-diglucoside and cyanidin 3,5-diglucoside (Nesbitt, Maness et al. 1974). Wine production research has showed that muscadine varieties with high amounts of cyanidin 3,5-diglucoside produce the poorest wine color and color stability (Nesbitt, Maness et al. 1974). Given that malvidin 3,5-diglucoside is structurally featured with two methyl groups in the B-ring, there is a general assumption that the degree of methylation of each aglycone is associated with pigment stability of muscadine wine (Nesbitt, Maness et al. 1974). However, maintaining pigment stability remains a challenging problem with muscadine wine and juice product (Goldy, Maness et al. 1989; Conner and MacLean 2013). To address this problem, both intraspecific and interspecific muscadine hybrids have been generated and clonally propagated to attempt to produce new genotypes with more color stable anthocyanin pigment ratios (Ballinger, Maness et al. 1973; Goldy, Ballinger et al. 1986; Lamikanra 1989; Conner and MacLean 2013). These studies have achieved progress in not only improving anthocyanin ratios of methylated to non-methylated ones, but also producing additional muscadine anthocyanins. For example, 25 anthocyanins including five common anthocyanidin-3,5-diglucosides (Fig. 1) and new anthocyanins were identified in 14 black muscadine hybrids (Lamikanra 1989). Although pelargonidin and its monoglucoside and diglucoside (Fig. 1) have not been reported from common commercial varieties such as Noble and Nesbitt, these metabolites were observed in hybrids. These results demonstrated that conventional breeding methods can produce genotypes with improved anthocyanin ratios and new anthocyanins for color quality improvement of wine and juice products.

FLH 13-11 and FLH 17-66 are two independent progeny of an interspecific muscadine F_1 hybrid that resulted from the cross of ‘Marsh’ x ‘Magoon’ accomplished by the grape breeding program of the University of Florida, located at Leesburg, Florida. ‘Marsh’ is a wild

selection of *Vitis munsoniana* and ‘Magoon’ is a *V. rotundifolia* cultivar that resulted from the cross ‘Thomas’ x ‘Burgaw’. These two varieties were chosen in our study because they show potential to have increased anthocyanin content and to produce new anthocyanins due to their dark colored fruit skins. These two variety are being cropped at the Castle Hayne research station in Wilmington, North Carolina. In this study, our goal was to use HPLC-qTOF-MS/MS technology to determine the anthocyanin profile and structure in berries of these two hybrid muscadine genotypes.

MATERIALS AND METHODS

Chemical agents

Peonidin 3-O-glucoside (≥97%, HPLC grade, cat# 42008), Cyanidin 3,5-diglucoside ((≥90%, HPLC grade, cat# 74397), pelargonidin chloride (HPLC grade, cat# P1659), and cyanidin chloride (≥95%, HPLC grade, cat# 79457) were purchased from Sigma-Aldrich® (St Louis, MO, USA). Delphinidin chloride (≥95%, HPLC grade, cat# 43725) was purchased from Fluka™ Chemical (Ronkonkoma, NY, USA). Hydrochloric acid (36.5–38%) was purchased from BDH (cat#: BHH3028-2.5L, West Chester, PA, 19380, USA). Acetonitrile (LC-MS grade, cat#: 9829-03), glacial acetic acid (HPLC grade, cat#: 9515-03) and methanol (LC-MS grade, cat#: 9830-03) were purchased from Avantor® (Center Valley, PA 18034, USA). Ethyl alcohol, 200 proof (cat#: EX0276-1) was purchased from EMD (Burlington, MA 01803, USA).

Plant material

FLH 13-11 and FLH 17-66 vines were grown at Castle Hayne research station in Wilmington, North Carolina (Elevation: 33 feet, 34.27 °N, 77.9 °W). Berries were fully ripened in the first two weeks of September each year. FLH 13-11 berries were collected on Sept. 6 in 2011 and Sept. 10 in 2012. FLH 17-66 berries were collected on Sept. 6 in both 2011 and 2012. Fruits were harvested and immediately placed on ice in a cooler and transported to the laboratory. All fresh berries were frozen in liquid nitrogen and then stored in -80°C freezers. Frozen berries were ground to fine powder in liquid nitrogen using a steel blender. Powdered samples were completely dried via lyophilization from -40°C to -20°C for 72 hours. Dried powder samples were stored in -80°C until extraction of anthocyanins described below.

Extraction and measurement of anthocyanins

One hundred milligrams of freeze-dried berry powder were suspended in 1.0 ml extraction buffer, which was composed of 0.5% HCl in methanol: dH_2O (50:50, v/v) in a 2 ml Eppendorf tube at room temperature. The tube was vigorously vortexed 45 sec, sonicated 10 min, and then centrifuged at 10,000 rpm for 10 min. The supernatant was transferred into a new 1.5 ml tube. This step was repeated using 0.5 ml extraction buffer. The two extractions were pooled together in the 1.5 ml tube. To remove chlorophyll and non-polar lipids in the extraction, the 1.5 ml ethanol: water extraction was mixed with 0.5 ml chloroform in a 2 ml tube. The mixture was vortexed vigorously 45 sec and centrifuged at the speed of 10,000 rpm for 5 min. The resulting upper ethanol: water-phase (about 750 µl) containing red pigment was pipetted into a new 1.5 ml tube. The bottom chloroform phase containing chlorophyll and non-polar lipids was disposed of into a waste container. This step was repeated once. The resulting upper red phase

was stored at -20°C for anthocyanin analysis described below. Three sample and experimental replications were included in this experiment.

The absorbance (ABS) of ethanol-water phase extracts was recorded at the wavelength of 530 nm on a HEλIOSγ UV-Visible spectrophotometer. The extraction buffer was used as a blank control. Ten µl of extract were added to 990 µl extraction buffer to dilute anthocyanin concentrations, and measure ABS value. Authentic standard peonidin 3-O-glucoside was used to establish a standard curve. Total anthocyanin content in berries was estimated as peonidin 3-O-glucoside equivalent (µg/g) according to the standard curve.

After measurement of total anthocyanin contents for each sample, 720 µl ethanol-water anthocyanin extract was dried for 2 hrs using a SpeedVac Concentrator connected to Refrigerated Condensation Trap. The remaining pellet was dissolved in 720 µl of 0.1% HCl-methanol (v/v) in a 1.5 ml tube. The tube was centrifuged 10 min at 10,000 rpm. The resulting clear supernatant was transferred to a new 1.5 ml tube and then stored at -20°C for anthocyanin analysis. Two hundred µl of HCl-methanol extract for each sample were transferred to a glass insert, which was placed in a 1.5 ml glass vial for HPLC and HPLC-qTOF-MS/MS analysis described below. Fifty µl of HCl-methanol extract was used for hydrolysis.

Hydrolysis of anthocyanins

Hydrolysis of anthocyanins followed our protocol reported previously (Shi and Xie 2010). In brief, fifty µl of anthocyanin extraction was added into 450 µl of *n*-butanol: HCl (95:5, v/v) solvent contained in a 1.5 ml tube. This mixture was boiled 1 hr. After the sample was cooled down to room temperature, it was dried off with flow nitrogen gas. The remaining residue was suspended in 200 µl of 0.1% HCl-methanol. The sample was centrifuged 10 min at 12,000

rpm. The supernatant was transferred to a new 1.5 ml tube and stored at -20°C for anthocyanidin analysis. Two hundred µl HCl-methanol extract for each sample was transferred to a glass insert, which was placed in a 1.5 ml glass vial for HPLC and LC-MS/MS analysis described below.

High performance liquid chromatography- photodiode array detectors analysis

Anthocyanins profiling was carried out using high performance liquid chromatography-photodiode array detector (HPLC-DAD) on 2,010 eV LC instrument (Shimadzu, Japan) as reported previously(Zhou, Zeng et al. 2008; Shi and Xie 2010). Both anthocyanidins and anthocyanins were separated on an analytical column of Eclipse XDB-C18 (250 mm x 4.6 mm, 5 µm, Agilent) as reported previously(Zhou, Zeng et al. 2008). The mobile phase solvents were composed of 1% acetic acid in water (solvent A: 1% HPLC grade acetic acid in LC-MS grade water) and 100% acetonitrile (solvent B) (LC-MS grade). The column was equilibrated for 30 min using solvent A: B (80:20). Then a gradient solvent system was developed to separate metabolites. It was composed of ratios of solvent A to B: 80:20 (0-5 min), 80:20 to 70:30 (5-10 min), 70:30 to 65:35 (10-20 min), 65:35 to 60:40 (20-30 min), 60:40 to 55:45 (30-40 min), 55:45 to 50:50 (40-45 min), 50:50 to 48:52 (45-50 min), 48:52 to 45:55 (50-55 min), 45:55 to 40:60 (55-58 min), 40:60 to 10:90 (58-58.5 min), 10:90 to 80:20 (58.5-60 min). After these gradient steps, the column was equilibrated and washed 10 min with solvent A: B (80:20). The flow rate was 0.4 ml/min and the injection volume was 20 µl. The UV spectrum was recorded from 190 to 800 nm. Pelargonidin chloride, cyanidin chloride, delphinidin chloride, and peonidin 3-glucoside were used as authentic standard controls.

HPLC- quadrupole time-of-flight-tandem mass spectrometer (HPLC-qTOF-MS/MS) Analysis

HPLC-TOF-MS/MS analysis was performed on an Agilent Technologies (Santa Clara, CA, USA) 6210 time-of-flight LC-MS/MS as reported recently(He, Li et al. 2017). The mobile phase solvents were composed of 1% acetic acid in water (solvent A: 1% HPLC grade acetic acid in LC-MS grade water) and 100% acetonitrile (solvent B) (LC-MS grade), which formed another gradient solvent system to separate anthocyanins and anthocyanidins for LC/MS/MS assay. A gradient solvent system was composed of gradient ratios of solvent A to B: 85:15 (0-10 min), 85:15 to 80:20 (10-20 min), 80:20 to 75:25 (20-30 min), 75:25 to 65:35 (30-35 min), 65:35 to 60:40 (35-40 min), 60:40 to 50:50 (40-55 min), 50:50 to 10:90 (55-60 min), 10:90 to 90:10 (60-70 min). After the last gradient step, the column was equilibrated and washed 10 min with solvents A: B (85:15). The flow rate was 0.4 ml/min. The injection volume of samples was 5.0 µl. The drying gas flow was set to 12 l/min, and the nebulizer pressure was set to 50 psi. As our recent report using an optimized protocol for anthocyanin ionization (He, Li et al. 2017), the negative mode was used for ionization. Mass spectrum was scanned from 100 to 3000 m/z. The acquisition rate was three spectra per second. Other parameters include fragmentor: 150 v, skimmer: 65 v, OCT 1 RF Vpp: 750 v, and collision energy: 30. In addition, the UV spectrum was recorded from 190 to 600 nm. Pelargonidin chloride, cyanidin chloride, delphinidin chloride, peonidin 3-O-glucoside, and cyanidin 3, 5-O-diglucoside were used as authentic standard controls.

Structure annotation

Anthocyanidin and anthocyanin structure annotation was performed using Agilent MassHunter Software for 6200 Series TOF and 6500 Series G-TOF version B.05.00. To identify anthocyanidins released from hydrolysis of anthocyanin extracts, retention time, extracted ion chromatogram (EIC), and mass to charge (m/z) ratio for each peak was analyzed to compare with available standards. For those peaks without standards, their EICs and m/z ratios were used for annotation. For each anthocyanin peak detected at 530 nm by HPLC-DAD in two different instruments, their EIC, m/z ratio, finger fragments from CID, and maximum UV spectrum were integrated for structure annotation. The peonidin 3-O-glucoside and cyanidin 3, 5-O-diglucoside standards were used to generate primary mass spectra and secondary mass spectrum fragments (MS2) resulted from collision induced dissociation, which were used to develop structure annotation protocols. Anthocyanin structures reported in the literature (Fig. 1) were utilized as our references for annotation. If anthocyanin peaks couldn't match a reported structure, their EIC, m/z, CID fragments, and UV spectrum were provided to show molecular features.

Statistical analysis

Student`s *t* test was used to statistically compare contents of total anthocyanins. Standard deviation was calculated to reflect variation of contents between biological replicates.

RESULTS AND DISCUSSION

Total anthocyanin contents in berries

Anthocyanins were measured to compare effects of two cropping seasons on the total content in berries from the field. According to the climate summary of National Weather Service (https://www.weather.gov/ilm/ClimateSummaryfor2012) for Wilmington / NC, July 2012 was reported as the hottest single month recorded since temperature records started in 1874. In addition, although overall 2011 was reported as another year with very large temperature extremes from winter to summer, persistently above normal temperatures was also recorded from January through August in 2012. The average of annual temperature were recorded as 63.4 and 65.7 °F between September 2010-September 2011, and September 2011- September 2012, respectively. Annual average of precipitation was also reported as 43.96 and 50.46 inches in 2011 and 2012, respectively. The resulting data revealed that the contents of anthocyanin in berries of two varieties in 2012 were approximately 2.5 fold higher than those in 2011 (Fig. 2). This result revealed that two different growth seasons significantly controlled the production of total anthocyanins. This result is a common phenomenon, given that the biosynthesis of anthocyanins is highly regulated by different environmental conditions. Light conditions and temperatures are two main environmental factors that have been demonstrated to tightly control anthocyanin biosynthesis in plant tissues (Cominelli, Gusmaroli et al. 2008; Albert, Lewis et al. 2009; Matus, Loyola et al. 2009; Rowan, Cao et al. 2009; Shi and Xie 2010).

Anthocyanin profiles

Anthocyanin profiles were analyzed by HPLC-DAD based profiling. Chromatographic peaks were recorded at 530 nm to compare anthocyanin profiles in berries between two growth seasons. At least three sample and extraction replicates for each variety were performed. The resulting peak profiles were used to compare anthocyanin profiles in two varieties from two years, 2011 and 2012 (Fig. 3 A-F). In the extracts of two years' both FLH 13-11 and FLH-17-66 berries, 12 anthocyanin peaks were detected. Based on retention times, these peaks were labelled as F-AN1 to F-AN12, meaning FLH-anthocyanins (Fig. 3 A-B and D-E), among which two peaks, F-AN2 and 3, overlapped with each other. F-AN5 through AN12 were relatively small in berries from both varieties from two seasons. Detailed analysis of peaks revealed that anthocyanin profiles were similar in berries of two varieties and the levels of all these peaks were affected by growing seasons.

Anthocyanidin profiles

The different chromophores of anthocyanidins are the structural bases of anthocyanin hues. Butanol: HCl based boiling was performed to completely hydrolyze anthocyanin extracts to release all anthocyanidins. HPLC-DAD based profiling and HPLC-qTOF-MS/MS were performed to analyze anthocyanidins. The resulting data showed that anthocyanidin profiles were the same from the extracts of the two varieties' berries (Fig. 4 A-B). These data showed that berries from two varieties biosynthesized the same anthocyanidins. Based on four authentic standards, delphinidin, cyanidin, pelargonidin, and peonidin, which were co-eluted as positive controls, hydrolysis of anthocyanins produced four main peaks with the same retention time as these three core anthocyanidins (Fig. 4 A-B and D-E). HPLC-qTOF-MS/MS analysis using the

negative mode of ionization further showed that the primary mass-to-charge ratio values of pelargonidin ($C_{15}H_{11}O_5^+$, molecular weight, MW, 271.24), cyanidin ($C_{15}H_{12}O_6^+$, MW, 287.24), delphinidin ($C_{15}H_{13}O_7^+$, MW, 303.24), and peonidin ($C_{16}H_{13}O_6^+$, MW, 301.24) standards, 269.265, 285.223, 301.213 [M-2H], and 299. 213 respectively. Two ions were reduced from these standards in the negative mode. This ionization feature with the negative mode was likely associated the flavylium cation form of anthocyanidins (Fig. 1) in the acidic condition. In addition, a second main m/z ratio value for each standard was created by ESI. The m/z second value for each standard was added 18, which resulted from $[NH_3]^+$. Therefore, the 2nd m/z values for pelargonidin, cyanidin, delphinidin, and peonidin were 287.265, 303.223, 319.213, and 317.213 $[M+18-2H]^-$, respectively. In our annotation of anthocyanins, we also found that all anthocyanins described below had the second m/z value with an addition of 18 from $[NH3]^+$. Based on these MS features, it was concluded that the berries produced all these four anthocyanidins.

In addition, five additional peaks were detected from hydrolysis (Fig. 4 A-B). One peak was co-eluted with cyanidin. HPLC-qTOF-MS analysis revealed that the m/z values of this peak were 315.1347 [M-2H] and 333.1347 [M+18-2H]. It is annotated to be petunidin (MW, 317). Four other peaks were eluted after pelargonidin and labelled as P1, 2, 3, and 4 (Fig. 4 A and B). The primary m/z ratios of P1, P2 and P3 were 343.1336 and 337.0486, and 357.0544, respectively. The molecular weight of the acetyl group is 43.05. Thus, these three peaks are likely acetyl-delphinidin, -cyanidin, and petunidin [M-2H]. The m/z values for P4 were 329.1465 [M-2H] and 345.0.195 [M+18-2H]. This peak was annotated to be malvidin.

HPLC-qTOF-MS/MS features of peonidin 3-O- glycoside and cyanidin 3,5-O-diglucoside standards

Peonidin 3-glycoside (Pn-3-G) standard was used to develop HPLC-qTOF-MS/MS protocols to annotate anthocyanins detected in the extracts of berries (Fig. 3). Pn3-G was ionized using the negative mode. The resulting ions (primary ions) were separated by mass-to-charge ratio in the first stage of mass spectrometry (MS1). Each particular mass-to-charge ratio was selected to create fragment ions by collision induced dissociation (CID). The resulting fragment ions (secondary ions) were separated and detected in a second stage of mass spectrometry (MS2). Both MS1 and MS2 were analyzed to standardize fragmentation features of Pn-3-G. The molecular weight (MW) of PN-3-G is 463.415. After ESI, its EIC was searched from total ion chromatographs (TIC). The resulting EIC and enhanced charge capacity (ECC) ion products showed that two primary m/z ratio values were 479.2307 and 461.1927 [M-2H] (Fig. 5 A-C). The m/z ratio of 479.1927 was derived from 463.415+18-2H [M+18-2H], in which the ion 18 resulted from $[NH_3]^+$, a common ion addition detected in ESI. Therefore, these two m/z ratios represented two main MS1 values of Pn-3-G. CID was performed to demonstrate the core structure in 479.1927 and 461.1927 $[m/z]^-$. CID analysis revealed that two typical fragments 299.1927 and 163.0682 (Fig. 5 D and E) were generated from 479.2307 and 461.1927 $[m/z]^-$. These ion fragments resulted from the homolytic dissociation of peonidin (299.1927) and the glucose group (163.0682) in both 461.1927 and 479.1927 $[m/z]^-$. In addition, fragments relating to peonidin observed from CID included 300.1927 and 301.1927. Fragments relating to glucose observed from CID consisted of 161. 06 through 163.0682 and 165.0841 to 168.1036 (Fig. 5 E). These CID fragmentation profiles resulted from a heterolytic fragmentation that has been commonly observed in MS/MS analysis (Bloor and Abrahams 2002; Es-Safi, Kerhoas et al.

2005; Geng, Sun et al. 2009; Ilboudo, Tapsoba et al. 2012; Yang, Ye et al. 2012). All these data showed that in addition to an expected m/z ratio and homolytic fragmentations from CID of Pn-3-G, other m/z ratios and heterolytic dissociation fragmentation were generated from this anthocyanin molecule. Therefore, the MS2 values of Pn-3-G included homolytic and heterolytic fragments generated from CID.

LC-QTOF-MS/MS analysis revealed MS1 and MS2 features of cyanidin 3,5-O-diglucoside (Cy-3,5-dG. It is molecular weight is 611. 529. In the condition of the negative mode, its mass-to-charge ratio in MS1 were 609.1347 [M-2H] and 627.1435 [M+18-2H] $[m/z]^-$ (S-Fig. 1). Its MS2 profile from CID consisted of four groups, including 447.0722, 448.0523, and 449.0633 [m/z], group two including 355.0467, 329.065, and 303.0321, group three including 284.0118, 285.0203, 286.0244, and 287.0309, and group 4 including 161.0071, 163.9959, 165.0011, 167.015, and 168.0201. Homolytic and heterolytic dissociations also occurred in CID. Based on these observations, analysis protocols from both MS1 and MS2 features of Pn-3-G and Cy3,5-dG were used to annotate anthocyanin peaks from berries in the following descriptions.

HPLC-qTOF-MS/MS based characterization of anthocyanins from FLH 13-11 and FLH17-66 berries

As described above, HPLC-qTOF-MS/MS was performed to annotate anthocyanins detected in the extracts of berries. MS1 and MS2 features (Table 1) for 12 peaks were used to annotate and characterize known and unknown anthocyanins detected in the extracts of berries (Fig. 3).

In our samples, the F-AN1 peak detected by HPLC-DAD was annotated to be delphinidin 3,5- diglucoside (Del-3,5-dG), which is a common anthocyanin molecule in berries of muscadine. The MW of Del-3,5-dG is 627.5280. MS search from TIC obtained two primary m/z values for this peak, 643.2822 [M+18-2H] and 625.2822 [M-2H], which were further demonstrated by its extracted EIC and EIC-ECC ion products (Fig. 6 A, B, and C). CID of 625.2822 and 643.2822 generated five groups of secondary ion fragments (Table 1), group 1: 481.2083 [463.1951+18] and group 2: 463.1951 (Fig. 5 D), group 3: 301.0886 and 303.1268 and group 4: 317.1254 and 319.1353 (Fig. 5 E), and group 5: 163.0963, 165.0832, 166.0824, 167.0988, and 168.1047 (Fig. 5 F). Based on these ion fragment features, the group 2 that resulted from the dissociation of the first glucose group (163.0686) from 625.2822 was relating to Del-3-glucoside. The group 3 that resulted from dissociation of the second glucose group from 463.1951 was relating to delphinidin aglycone. The group 5 that resulted from the dissociation of 625.2822 and 464.2128-467.2174 was relating to glucose. Fragments 463.1951, 301.0886, and 163.0686 are exactly relating to Del-3-G, delphinidin aglycone, and glucose.

The F-AN2 peak was identified to be cyanidin 3,5- diglucoside (Cy-3, 5-dG), which is another common anthocyanin molecule produced in berries of different muscadine cultivars. After ESI, two primary m/z values of this peak were 609.529 $[M-2H]^-$ and 627.529 $[M+18-2H]^-$ $[m/z]^-$ (Fig. 7 A-C). CID of 609.529 and 627.529 generated fragments (Fig. 7 D-F), which were characterized by five groups of secondary m/z values (Table 1). Fragments 447.1979, 285.1244 and 163.0677 were exactly relating to Cy-3-G, cyanidin aglycone, and glucose. These MS1 and MS2 features were highly identical to the Cy-3, 5-dG standards (S-Fig. 1).

The F-AN3 peak is overlapped with the peak F-AN2. Both MS1 and MS2 analyses annotated this peak to be petunidin 3, 5-O-diglucoside (Pt-3,5-dG). Its MS1 from ESI and MS2 features from CID are summarized in Fig. 8 and Table 1.

The F-AN4, F-AN5, F-AN6, and F-AN7 peaks were annotated to be delphinidin 3-O-glycoside (Del-3-G), pelargonidin 3, 5-diglucoside (Pel-3,5-dG), peonidin 3,5-O-diglucoside (Pn-3,5-dG), and malvidin 3,5-O-diglucoside (Mv-3,5-dG), respectively. The MS1 and MS2 features for Pn-3,5-dG are shown in Figure 9. The MS1 and MS2 features for Del-3-G, Pel-3,5-dG, and Mv-3,5-dG are shown in S-Figs. 2, 3, and 4, respectively. The fragments of these four anthocyanins are summarized in Table 1.

The F-AN8 was identified to be Pn-3-G, which is one of the monoglucosides important to color stability of muscadine beverage products. The annotation of Pn-3-G was mainly based on the comparison of its retention time, UV-spectrum, and MS1 and MS2 features (Fig. 10 and Table 1) with those from the authentic standard (Fig. 5). The resulting data showed that its m/z values and EIC were the same as those of the Pn-3-G standard (Fig. 5 A, B, and C). Its CID fragment profiles were also highly identical to those of the Pn-3-G standard (Fig. 5 E and E). The resulting data identified the F-AN8 peak to be Pn-3-G.

MS/MS analysis provided useful MS1 and MS2 features to characterize the F-AN9, 10, 11, and 12 (S-Figs. 5-8 and Table 1). Based on anthocyanidins released from hydrolysis of extracts (Fig. 4), their MS2 features, and anthocyanin molecules reported in the muscadine literature (Ballinger, Maness et al. 1973; Nesbitt, Maness et al. 1974; Lamikanra 1989; You, Chen et al. 2012; You, Chen et al. 2012) , these four peaks are cyanidin, pelargonidin, or peonidin-related anthocyanins (Table 1).

In conclusion

The production of anthocyanins in berries of FLH 13-11 and FLH 17-16 are fundamentally impacted by cropping years, and also these two varieties basically produce similar types of anthocyanins as other muscadine grapes. In addition to 3,5-diglucosides of anthocyanidins, berries of these two varieties produce monoglucoside of anthocyanins.

Acknowledgement

This research was funded by North Carolina State University for Plant Breeding Programs.

REFERENCES

Albert, N. W., D. H. Lewis, et al. (2009). "Light-induced vegetative anthocyanin pigmentation in Petunia." J. Exp. Bot. 60(7): 2191-2202.

Ballinger, W. E., E. P. Maness, et al. (1973). "Anthocyanins of black grapes of 10 clones of *Vitis rotundifolia*, MICHX." J Food Sci 38(5): 909-910.

Barchenger, D. W., J. R. Clark, et al. (2015). "Evaluation of physicochemical and storability attributes of muscadine grapes (*Vitis rotundifolia* Michx.)." Hortscience 50(1): 104-111.

Bloor, S. J. and S. Abrahams (2002). "The structure of the major anthocyanin in Arabidopsis thaliana." Phytochemistry 59(3): 343-346.

Brown, W. L. (1940). "The anthocyanin pigment of the hunt muscadine grape." J Am Chem Soc 62: 2808-2810.

Cardona, J. A., J. H. Lee, et al. (2009). "Color and polyphenolic stability in extracts produced from muscadine grape (*Vitis rotundifolia*) pomace." J Agric Food Chem 57(18): 8421-8425.

Cominelli, E., G. Gusmaroli, et al. (2008). "Expression analysis of anthocyanin regulatory genes in response to different light qualities in *Arabidopsis thaliana*." J Plant Physiol 165: 886-894.

Conner, P. J. and D. MacLean (2013). "Fruit Anthocyanin Profile and Berry Color of Muscadine Grape Cultivars and Muscadinia Germplasm." Hortscience 48(10): 1235-1240.

Es-Safi, N. E., L. Kerhoas, et al. (2005). "Application of positive and negative electrospray ionization, collision-induced dissociation and tandem mass spectrometry to a study of the fragmentation of 6-hydroxyluteolin 7-O-glucoside and 7-O-glucosyl-(l -> 3)-glucoside." Rapid Commun Mass Spectrom. 19(19): 2734-2742.

Geng, P., J. H. Sun, et al. (2009). "An investigation of the fragmentation differences of isomeric flavonol-O-glycosides under different collision-induced dissociation based mass spectrometry." Rapid Commun Mass Spectrom 23(10): 1519-1524.

Goldy, R. G., W. E. Ballinger, et al. (1986). "Fruit anthocyanin content of some Euvitis x *Vitis rotundifolia* hybrids." J Am Soc Hortic Sci 111(6): 955-960.

Goldy, R. G., W. E. Ballinger, et al. (1987). "Anthocyanin content of fruit, stem, tendril, leaf, and leaf petioles in muscadine grape." J Am Soc Hortic Sci 112(5): 880-882.

Goldy, R. G., E. P. Maness, et al. (1989). "Pigment quantity and quality characteristics of some native *Vitis rotundifolia* Michx." Am J Enol Vitic 40(4): 253-258.

Gourineni, V., N. F. Shay, et al. (2012). "Muscadine grape (*Vitis rotundifolia*) and wine phytochemicals prevented obesity-associated metabolic complications in C57BL/6J Mice." J Agric Food Chem 60(31): 7674-7681.

He, X., Y. Li, et al. (2017). "Metabolic engineering of anthocyanins in dark tobacco varieties" Physiol Plant 159: 2-12.

Ilboudo, O., I. Tapsoba, et al. (2012). "Targeting structural motifs of flavonoid diglycosides using collision-induced dissociation experiments on flavonoid/Pb2+ complexes." Eur J Mass Spectrom 18(5): 465-473.

Lamikanra, O. (1989). "Anthocyanins of *Vitis rotundifolia* hybrid grapes." Food Chem 33(3): 225-237.

Matus, J. T., R. Loyola, et al. (2009). "Post-veraison sunlight exposure induces MYB-mediated transcriptional regulation of anthocyanin and flavonol synthesis in berry skins of *Vitis vinifera*." J Exp Bot 60(3): 853-867.

Mortensen, J. A. (2001). Cultivars. Muscadine Grapes. F. M. Basiounny and D. G. Himelrick. Alexandria VA, ASHS Press: 91-105.

Nesbitt, W. B., E. P. Maness, et al. (1974). "Relationship of Anthocyanins of Black Muscadine Grapes (Vitis-Rotundifolia Michx) to Wine Color." American Journal of Enology and Viticulture 25(1): 30-32.

Nesbitt, W. B., E. P. Maness, et al. (1974). "Relationship of anthocyanins of black muscadine grapes (*Vitis rotundifolia* Michx) to wine color." Am J Enol Vitic 25(1): 30-32.

Olien, W. C. (2001). Introduction to the Muscadines. Muacadine Grapes. F. M. Basiouny and D. G. Himelrick. Alexandria, VA, ASHA Press: 1-13.

Rowan, D. D., M. Cao, et al. (2009). "Environmental regulation of leaf colour in red 35S:PAP1 *Arabidopsis thaliana*." New Phytol 182(1): 102-115.

Shi, M.-Z. and D.-Y. Xie (2010). "Features of anthocyanin biosynthesis in *pap1-D* and wild-type *Arabidopsis* thaliana plants grown in different light intensity and culture media conditions." Planta 231: 1385-1400.

Striegler, R. K., P. M. Carter, et al. (2005). "Yield, quality, and nutraceutical potential of selected muscadine cultivars grown in southwestern Arkansas." Horttechnology 15(2): 276-284.

Wang, X., H. R. Tong, et al. (2010). "Chemical characterization and antioxidant evaluation of muscadine grape pomace extract." Food Chem 123(4): 1156-1162.

Yang, W. Z., M. Ye, et al. (2012). "Collision-induced dissociation of 40 flavonoid aglycones and differentiation of the common flavonoid subtypes using electrospray ionization ion-trap tandem mass spectrometry and quadrupole time-of-flight mass spectrometry." Eur J Mass Spectrom 18(6): 493-503.

You, Q., F. Chen, et al. (2012). "High-performance liquid chromatography-mass spectrometry and evaporative light-scattering detector to compare phenolic profiles of muscadine grapes." J Chromatogr A 1240: 96-103.

You, Q., F. Chen, et al. (2011). "Inhibitory effects of muscadine anthocyanins on alpha-glucosidase and pancreatic lipase activities." J Agric Food Chem 59(17): 9506-9511.

You, Q., F. Chen, et al. (2012). "Analysis of phenolic composition of Noble muscadine (*Vitis rotundifolia*) by HPLC-MS and the relationship to its antioxidant capacity." J Food Sci 77(10): C1115-C1123.

Zhou, L.-L., H.-N. Zeng, et al. (2008). "Development of tobacco callus cultures over expressing *Arabidopsis* PAP1/MYB75 transcription factor and characterization of anthocyanin biosynthesis" Planta 229: 37-51.

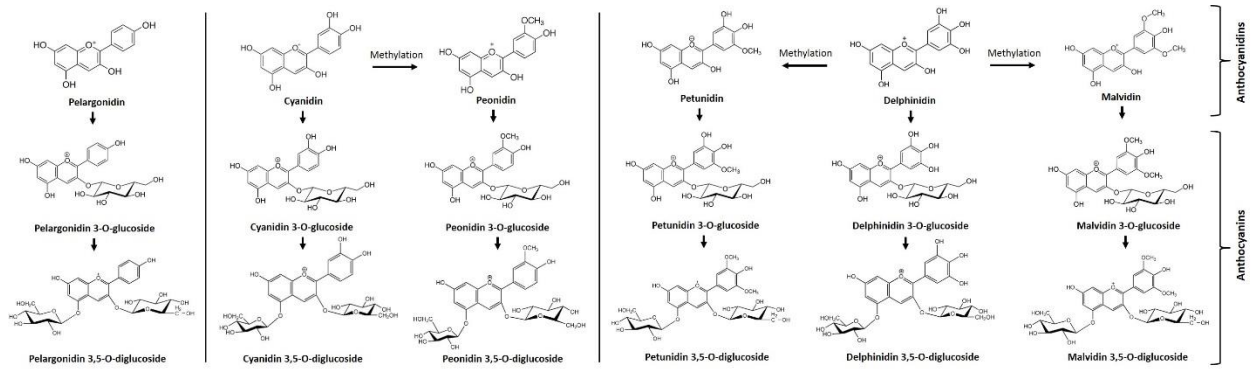

Figure 2.1: Overview of main types of anthocyanidins and anthocyanins identified in berries of different muscadine varieties. Six anthocyanidins include pelargonidin, cyanidin, delphinidin, peonidin, petunidin, and malvidin. Anthocyanins include six monoglucosides of anthocyanidins and six diglucosides of anthocyanidins

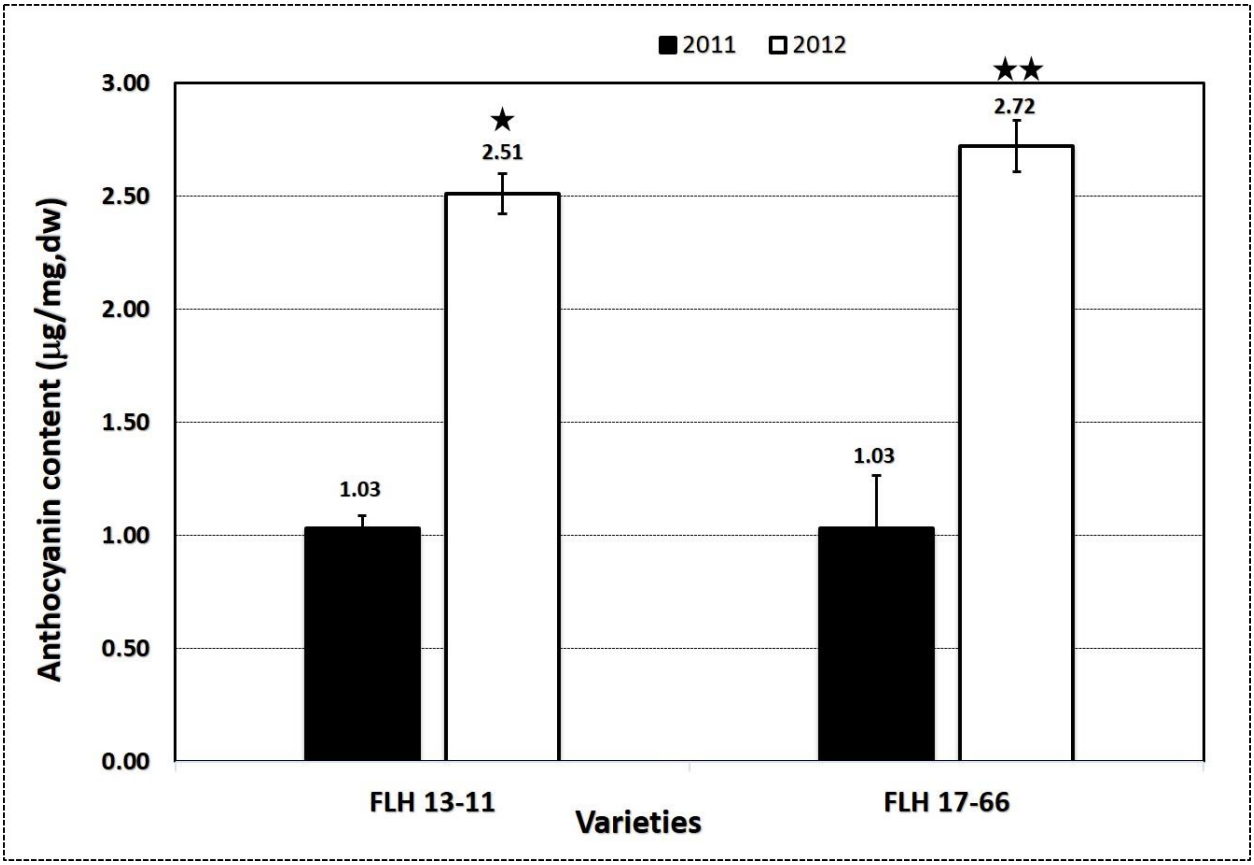

Figure 2.2: Contents of total anthocyanin extract from berries collected in 2011 and 2012. Three biological and experimental replicates were used to generate averaged total anthocyanin content of each cultivars, FLH13-11 and FLH17-66, in the two growing seasons, 2011 and 2012 Two bars labeled "*" and "**" mean significant difference. (p-value ≤0.05, t-value: 4.3)

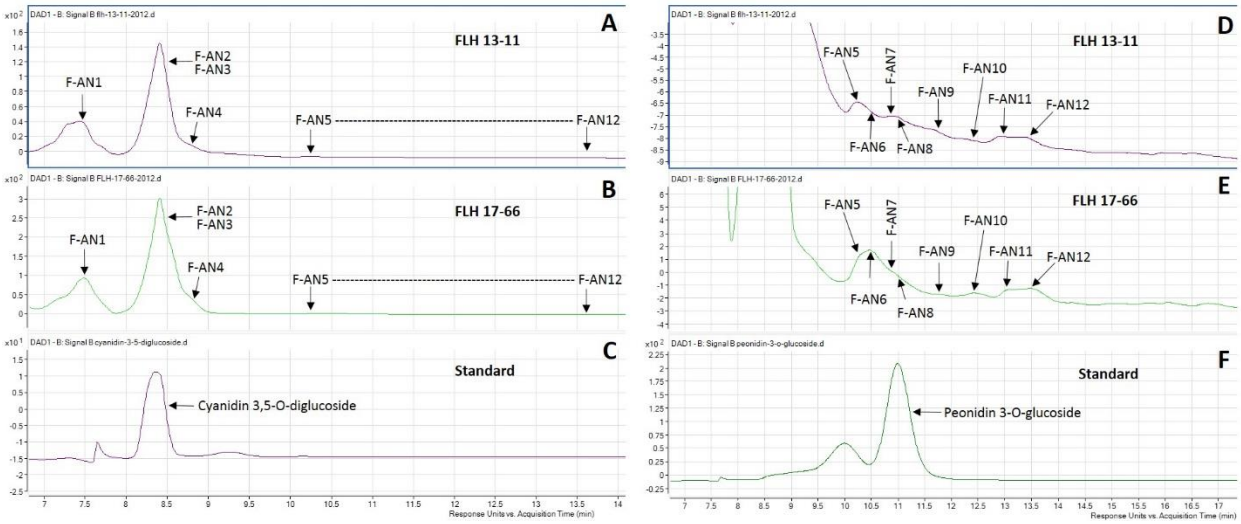

Figure 2.3: Comparison of anthocyanin profiles in berries from FLH 13-11 and FLH 17-66 harvested in the 2011 and 2012 cropping seasons. A-C, an overview comparison of anthocyanin profiles in berries FLH 13-11 (A) and FLH 17-66 (B) as well as the cyanidin 3,5-O-diglucoside standard (C); D-F: A snapshot showing anthocyanin peak profiles in FLH 13-11 (D) and FLH 17-66 (E) berries as well as the peonidin 3-glucoside standard (F) after 10 min of retention time. Each peak is designed a number, the order of which is assigned from the early to late retention time.

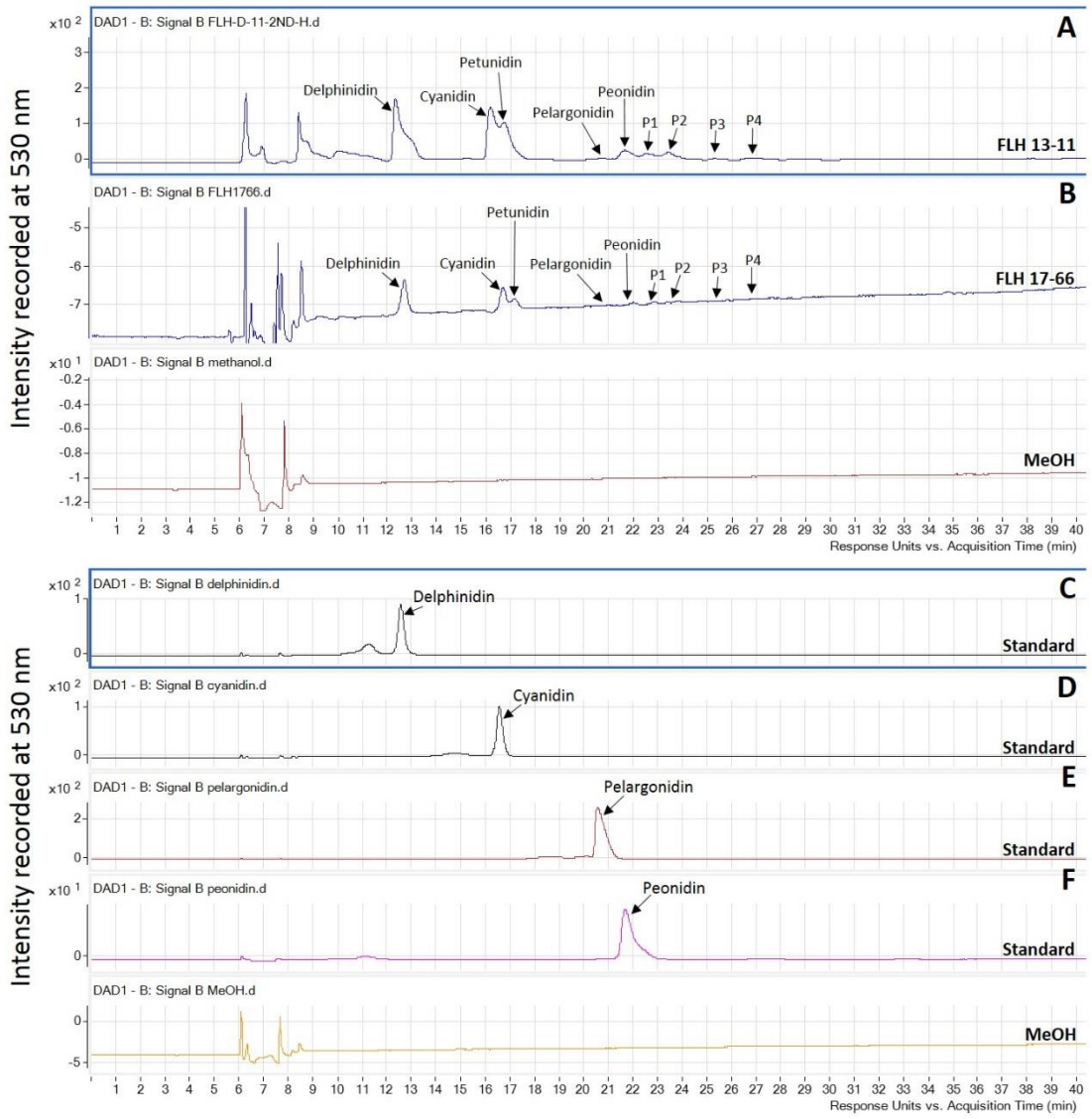

Figure 2.4: Comparison of anthocyanidin profiles from hydrolysis of anthocyanin extracts from berries of FLH 13-11 and FLH 17-66 harvested in the 2011 and 2012 cropping seasons. A-B, anthocyanidin profiles released from the hydrolysis of anthocyanins of FLH 13-11 (A) and FLH 17-66 (B). The chromatogram of methanol solvent is used as a negative control. C-F, standards, delphinidin (C), cyanidin (D), pelargonidin (E), and peonidin (F).

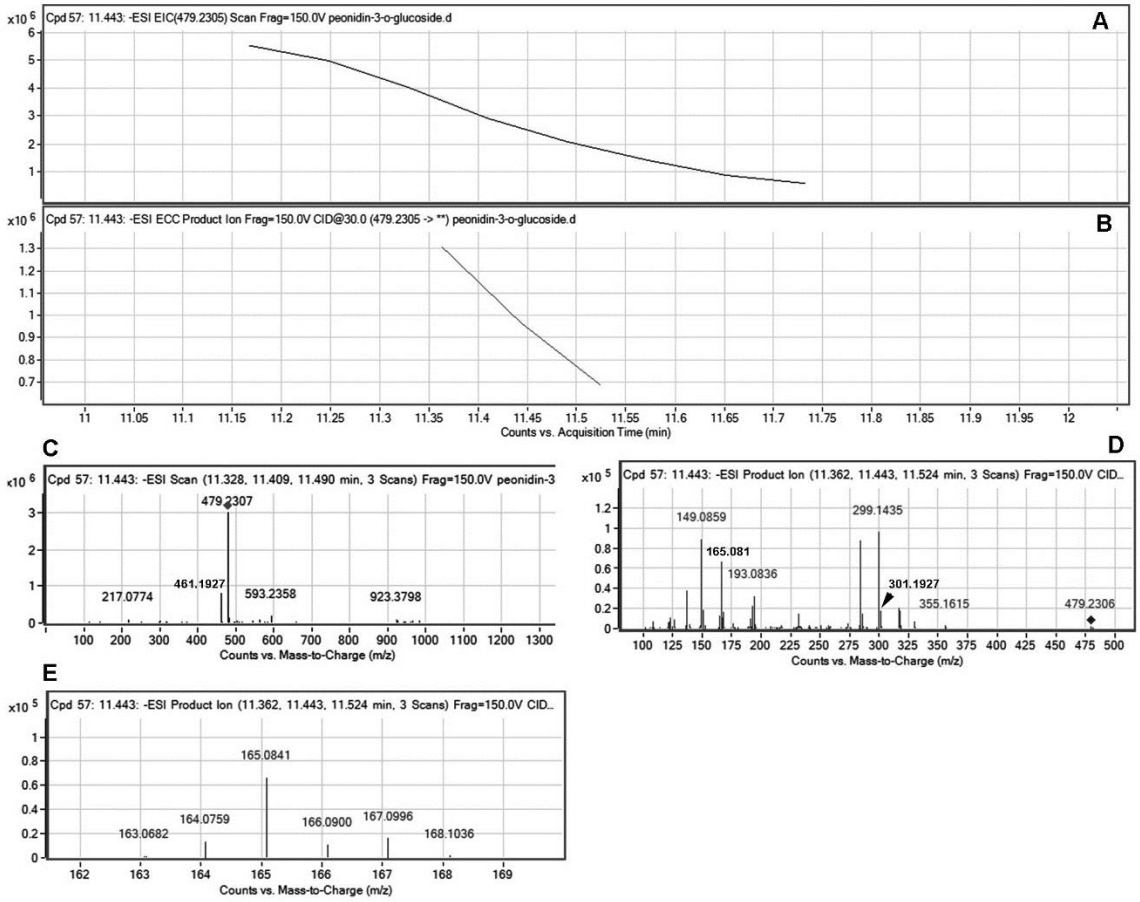

Figure 2.5: Extracted ion chromatogram (EIC) of primary mass spectrum (MS1) and m/z features of secondary ion fragments (MS2) derived from LC-MC/MS of the peonidin 3-gluoside (Pn-3-G, molecular weight: 463.415) standard. A: EIC of primary ion 479.2305 $[M+18-2H]^-$, in which 18 is from $[NH3]^+$, B: enhanced charge capacity (ECC) ion product for 479.2305, C: a MS profile showing two extracted m/z values, 461.1927 $[M-2H]^-$ and 479.2307 $[M+18-2H]^-$, D-E: fragments from CID of 479.2307 and 461.1927 showing 299.1435 $[m/z]^-$ and 301.1927 $[m/z]^-$ relating to peonidin aglycone (D) and 161.0858-165.082, 166.0858 relating to glucose (E).

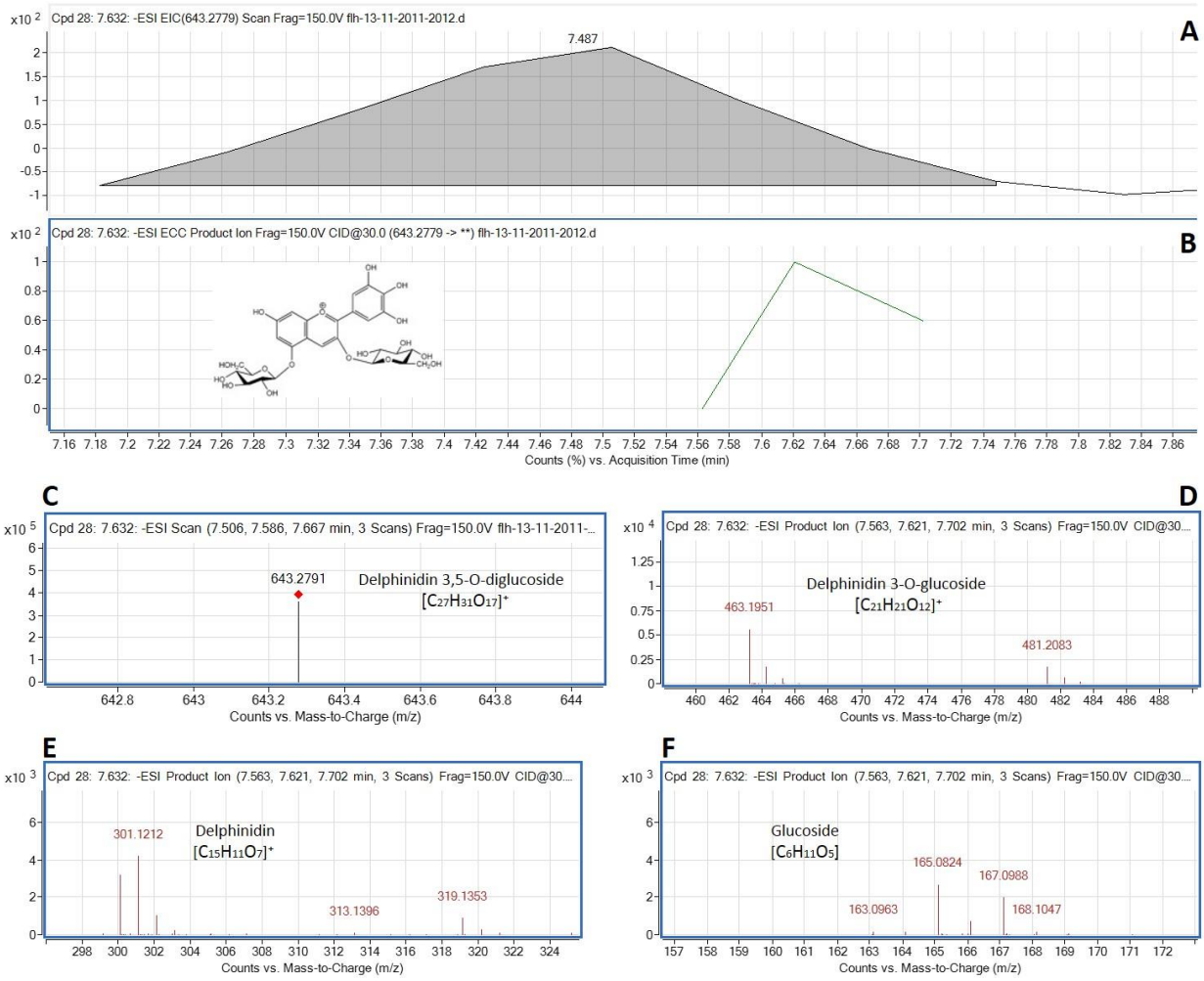

Figure 2.6: Extracted ion chromatogram (EIC) of primary mass spectrum and m/z features of secondary ion fragments derived from LC-MC/MS of peak F-AN1. These data annotate this peak to be delphinidin 3, 5-digluoside (Del-3,5-dG, molecular weight: 427.528). A: EIC of primary ion 643.2791 $[m/z]^-$, [M+18-2H], B: enhanced charge capacity (ECC) ion product for 643.2791 $[m/z]^-$, C: a MS profile showing an extracted m/z value, 643.2791 $[m/z]^-$, [M+18-2H], D-F: fragments from CID of 643.2791 showing 463.1951 and 464.1953 $[m/z]^-$ relating to Del-3-G (D), 300.111, 301.1212 and 302.1213 $[m/z]^-$ relating to delphinidin aglycone (E), and 163.0963-168.1047 relating to glucose (F).

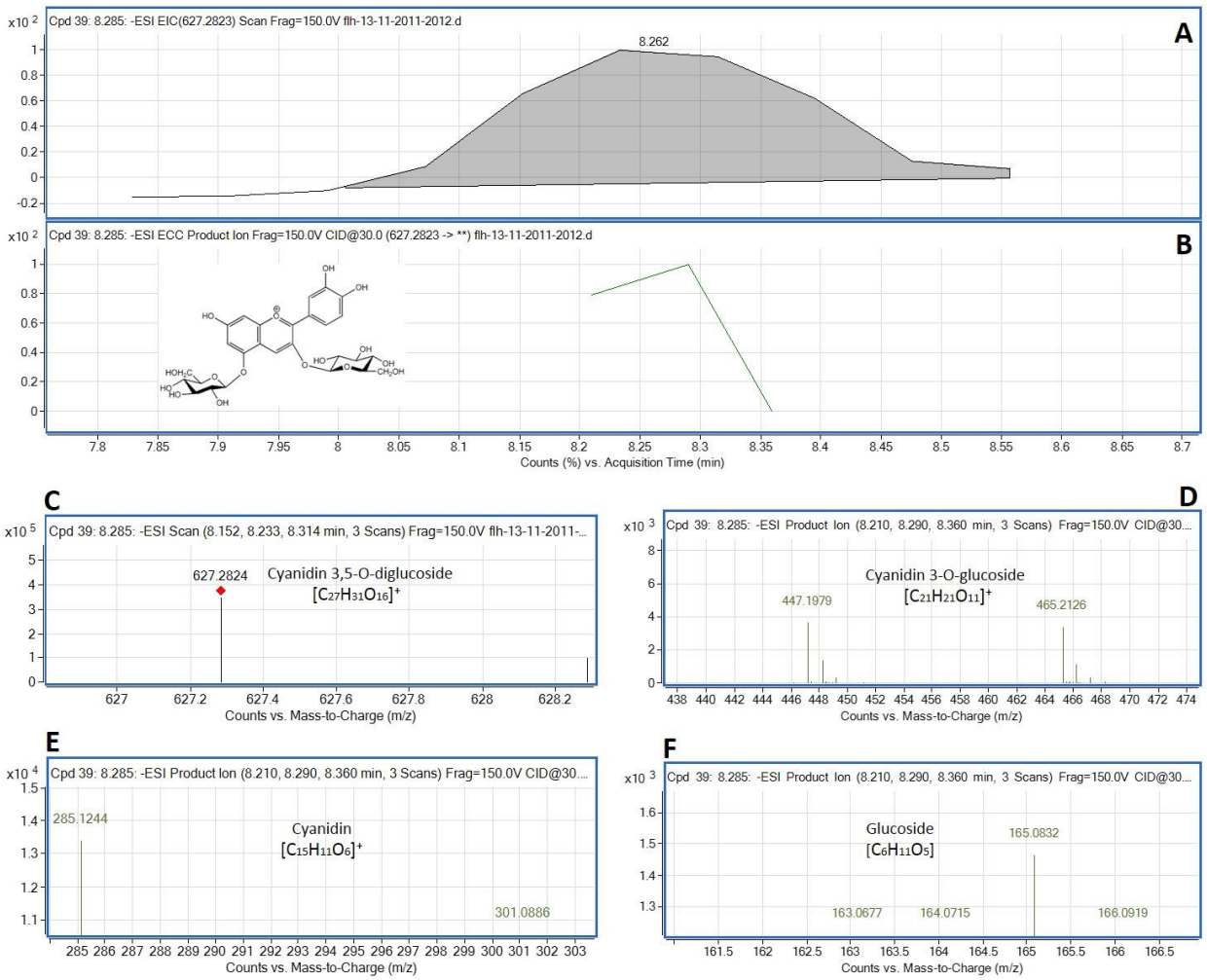

Figure 2.7: Extracted ion chromatogram (EIC) of primary mass spectrum and m/z features of secondary ion fragments derived from LC-MC/MS of peak F-AN2. These data and the comparison with standard identify this peak to be cyanidin 3, 5-digluosides (Cy-3,5-dG, molecular weight: 611.529). A: EIC of primary ion 627.2824 $[m/z]^{-}$, [M+18-2H], B: enhanced charge capacity (ECC) ion product for 627.2824 $[m/z]^{-}$, C: a MS profile showing an extracted m/z value, 627.2824 $[m/z]^{-}$, [M+18-2H], D-F: fragments from CID of 627.2824 showing 447.1979 and 448.1953 $[m/z]^{-}$ relating to Cy-3-G (D), 285.1244 $[m/z]^{-}$ relating to cyanidin aglycone (E), and 163.0677-166.0919 relating to glucose (F).

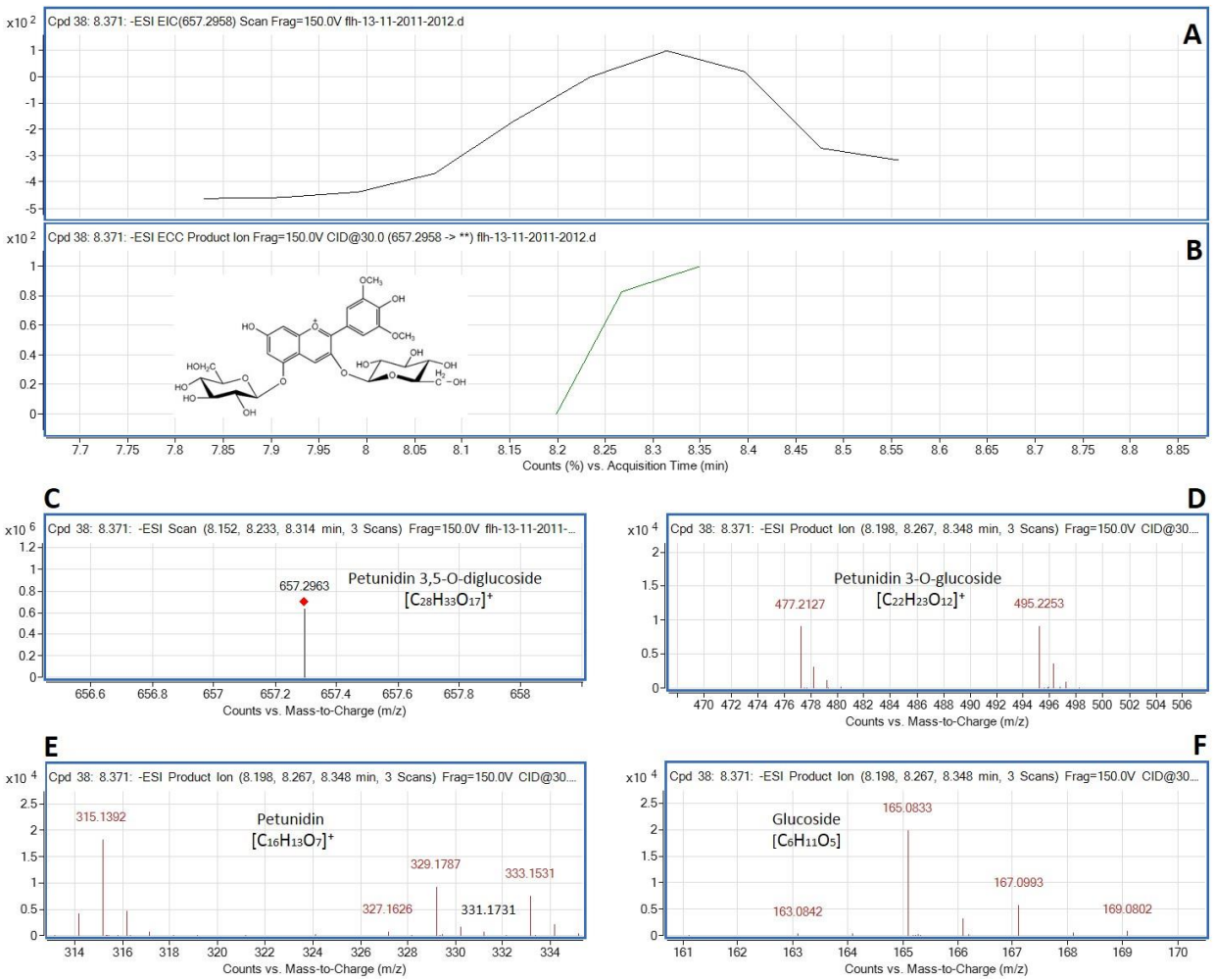

Figure 2.8: Extracted ion chromatogram (EIC) of primary mass spectrum and m/z features of secondary ion fragments derived from LC-MC/MS of peak F-AN3. These data annotate this peak to be petunidin 3, 5-digluosides (Pt-3,5-dG, molecular weight: 641.282). A: EIC of primary ion 657.2963 $[m/z]^{-}$, [M+18-2H], B: enhanced charge capacity (ECC) ion product for 657.2963 $[m/z]^{-}$, C: a MS profile showing an extracted m/z value, 657.2963 $[m/z]^{-}$, [M+18-2H], D-F: fragments from CID of 657.2963 showing 477.2a MS profile27 and 478.2127 $[m/z]^{-}$ relating to Pt-3-G (D), 314.1391, 315.1392, and 316.1389 $[m/z]^{-}$ relating to petunidin aglycone (E), and 163.0842-169.0802 relating to glucose (F).

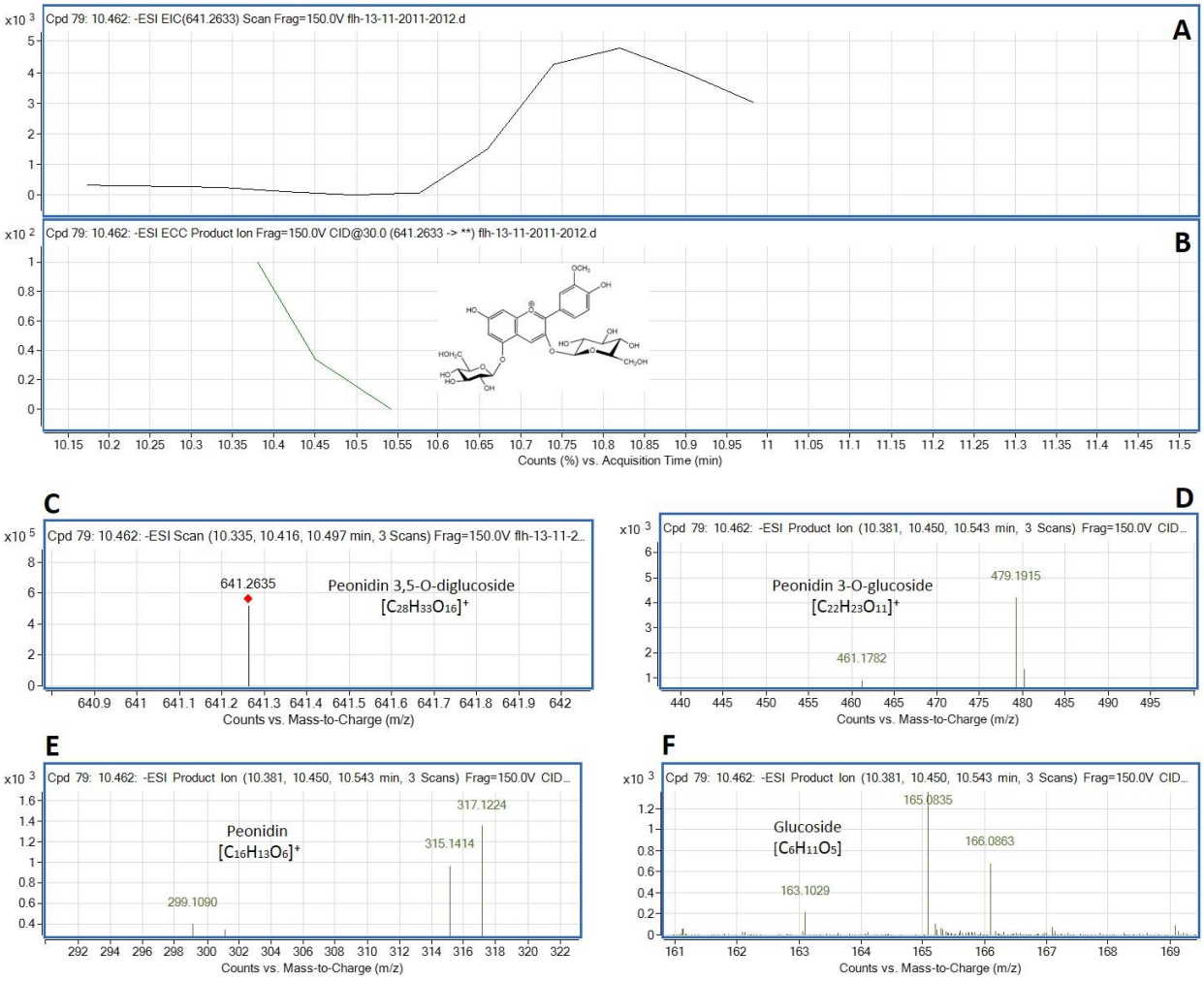

Figure 2.9: Extracted ion chromatogram (EIC) of primary mass spectrum and m/z features of secondary ion fragments derived from LC-MC/MS of peak F-AN6. These data annotate this peak to be peonidin 3, 5-digluosides (Pn-3,5-dG, molecular weight: 625.556). A: EIC of primary ion 641.2635 $[m/z]^{-}$, [M+18-2H], B: enhanced charge capacity (ECC) ion product for 641.2635 $[m/z]^{-}$, C: a MS profile showing an extracted m/z value, 641.2635 $[m/z]^{-}$, [M+18-2H], D-F: fragments from CID of 641.2635 showing 461.1782 and 479.1915 $[m/z]^{-}$ relating to Pn-3-G (D), 299.1090 and 301.1093 $[m/z]^{-}$ relating to petunidin aglycone (E), and 163.1029-166.0863 relating to glucose (F).

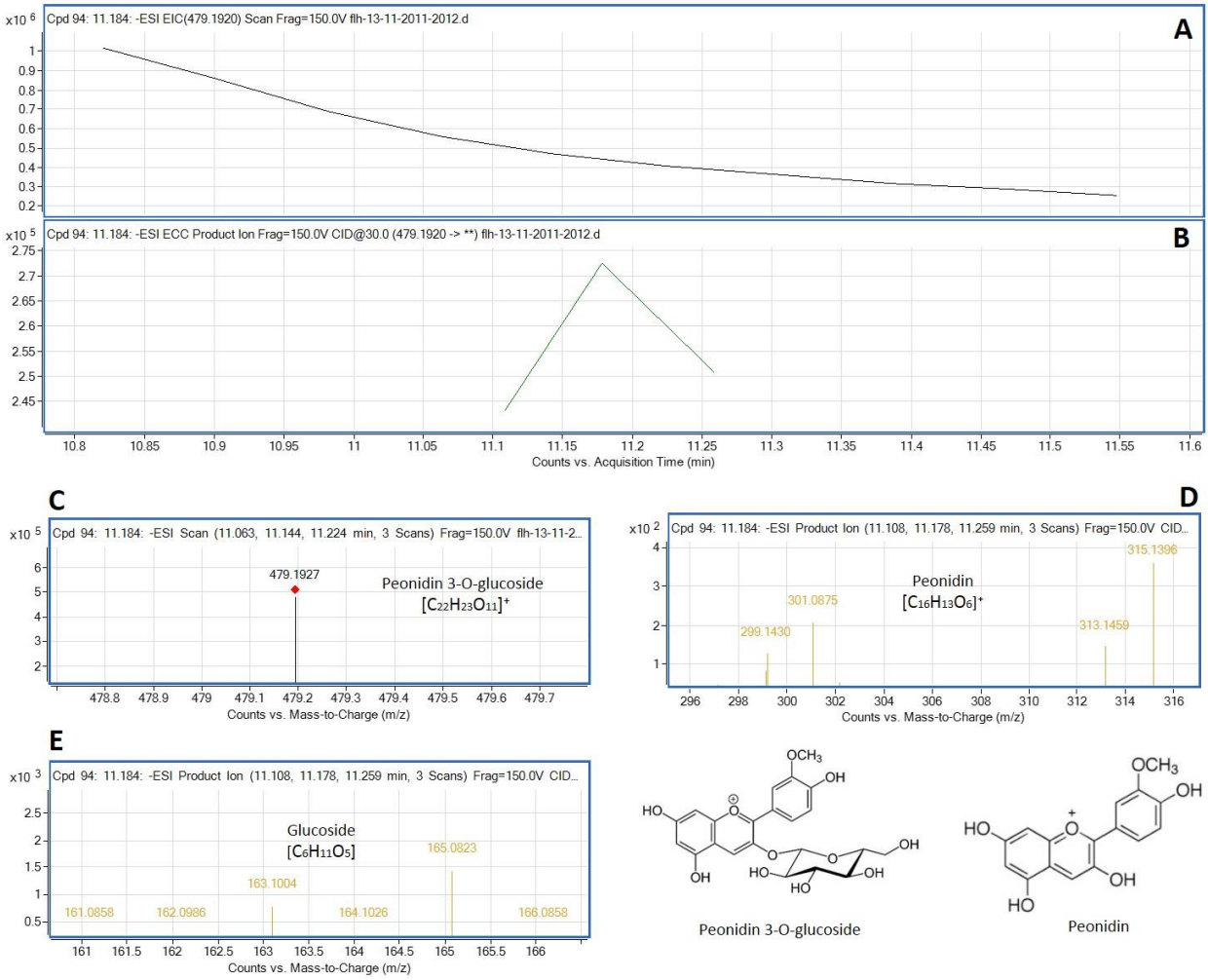

Figure 2.10: Extracted ion chromatogram (EIC) of primary mass spectrum and m/z features of secondary ion fragments derived from LC-MC/MS of peak F-AN8. These data show this peak being peonidin 3-glucoside. A: EIC of primary ion 479.2305 $[m/z]^{-}$, [M+18-2H], B: enhanced charge capacity (ECC) ion product for 479.2305, C: a MS profile showing one extracted m/z value, 479.2307 $[m/z]^{-}$, D-E: fragments from CID of 479.2307 showing 299.1435 [m/z] and 301.1927 [m/z] relating to peonidin aglycone (D), and 161.0858-165.0823, 166.0858 [m/z] relating to glucose (E), F: structures of peonidin 3-glucoside and peonidin.

Table 2.1: **Mass spectrum characterization and annotation of 12 anthocyanin peaks by HPLC-qTOF-MS/MS analysis.**

Peak #	λ (nm) Rt (min)	MW and MS1 [m/z]$^-$	MS2 [m/z] fragments from CID	Anthocyanin annotation	Figures (#)
F-AN1	**λ:** 523 Rt: 7.632	MW: 627.5280 MS1:643.2791	**1.** 481.2083; **2.** **463.1951**; **3.** **301.0886**; 303.1268; **4.** 317.1254,**319.1353**; **5.** **163.0963**, 165.0832, 166.0824, 167.0988,168.1047	Delphinidin 3,5-O-diglucoside	Fig.#6
F-AN2	**λ:** 517 Rt: 8.285	MW: 611.5290 MS1:627.2824	**1.** 465.2126; 466.2126; **2.** **447.1979**, 448.1979; **3.** **285.1244**; 287.1318; **4.** 301.0886, 303.1381; **5.** **163.0677**, 164.0716, 165.0832, 166.0919	Cyanidin 3,5-O-diglucoside	Fig. #7
F-AN3	**λ:** 520 Rt: 8.371	MW: 641.2820 MS1: 657.2963	**1.** 495.2253, 496.2263; **2.** **477.2127**, 478.2127; **3.** 327.1626, 329.1787, 331.1731, 333.1531; **4.** 314. 1392, **315.1392**, 317.1399; **5.** **163.0843**, 165.0822, 167.0933, 169.0802	Petunidin 3,5-O-diglucoside	Fig. #8
F-AN4	**λ:** 520 Rt: 8.995	MW:465.3870 MS1:481.2044	**1.** **463.1575**, 465.1416 **2.** **301.0864**, 303.0889 **3.** **165.0829, 169.0785**	Delphinidin 3-O-glucoside like	S-Fig. #2
F-AN5	**λ:** 512 Rt:10.219	MW:595.398 MS1:593.2516	**1.** **433.1761** **4.** **271.1066, 272.1158** **5.** 161.0855, **163.0656**, 164.0722, **165.0840**	Pelargonidin-3, 5-diglucoside like	S-Fig. #3
F-AN6	**λ:** 523 Rt: 10.462	MW: 625.5560 MS1:641.2635	**1.** **461.1782,** 479.1915; **2.** 315.1414, 317.1224; **3.** **299.1090**, 301.1226; **4.** **163.1029**, 165.0835, 166.0863	Peonidin 3,5-O-diglucoside	Fig. #9
F-AN7	**λ:** 524 Rt: 11.039	MW: 655.587 MS1: 673.2911	**1.** **493.2083**, 494.2080, 495.2101; **2.** 330.1328, **331.1448**, 332.1328; **3.** **161.1010**, 163.0708,165.0829, 166.0869	Malvidin 3,5-O-diglucoside	S-Fig. #4
F-AN8	**λ:** 529 Rt: 11.184	MW: 463.4150 MS1:479.1927	**1.** 313.1459, 315.1396 **2.** **299.1430,** 301.0875; **3.** 161.0858, **163.0709**, 165.082, 166.0858	Peonidin 3-O-glucoside	Fig. #10
F-AN9	**λ:** 519 Rt: 11.928	MW: 449.3880 MS1:465.2110	**1.** 303.1385, 301.0894 **2.** 285.1243**, 287.1198** **3.** 165.0802, **163.0684**	Cyanidin monosaccahraide related	S-Fig. #5
F-AN10	**λ:** 523 Rt: 12.852	MW: MS1:785.2247	**1.** 461.1418, **463.1591**, 465.1770 **2.** 299.0717, **301.0856**, 302.0881 **3.** 153.0825, **169.0775**, 193.0790	Peonidin monosugar related	S-Fig. #6
F-AN11	**λ:** 518 Rt: 13.210	MW: MS1:687.3091	**1.** **449.2154**, 450.2188, 451.2083 **2.** 285.1255, **287.1405**, 288.1456 **3.** 161.0889, **163.0685**, 165.0868	Cyanidin monosaccharide related	S-Fig. #7
F-AN12	**λ:** 524 Rt: 13.499	MW: MS1:665.1924	**1.** 431.1254, **433.1501**, 449.1460 **2.** **271.0723**, 287.0710 **3.** **163.0991**, 165.0911, 167.0659	Pelargonidin monosaccharide related	S-Fig. #8

Supplementary Figure 2.1: Extracted ion chromatogram (EIC) of primary mass spectrum (MS1) and m/z features of secondary ion fragments (MS2) derived from LC-MC/MS of the cyanidin 3,5-diglucoside (Cy-3,5-dG) standard. A: EIC of primary ion 609.1319 [M-2H] and 627.0958 [M+18-2H] $[m/z]^-$, B: enhanced charge capacity (ECC) ion product for 627.0958 $[m/z]^-$, C: a MS profile showing an extracted m/z value, 627.0958 $[m/z]^-$, and D-F: fragments from CID of 627.0958 showing 447.0722 and 448.0636 $[m/z]^-$ relating to cyanidin-3-G structure (D), 285.0203 and 286.0304 $[m/z]^-$ relating to cyanidin aglycone (E), and 163.9959-168.0202 relating to glucose (F).

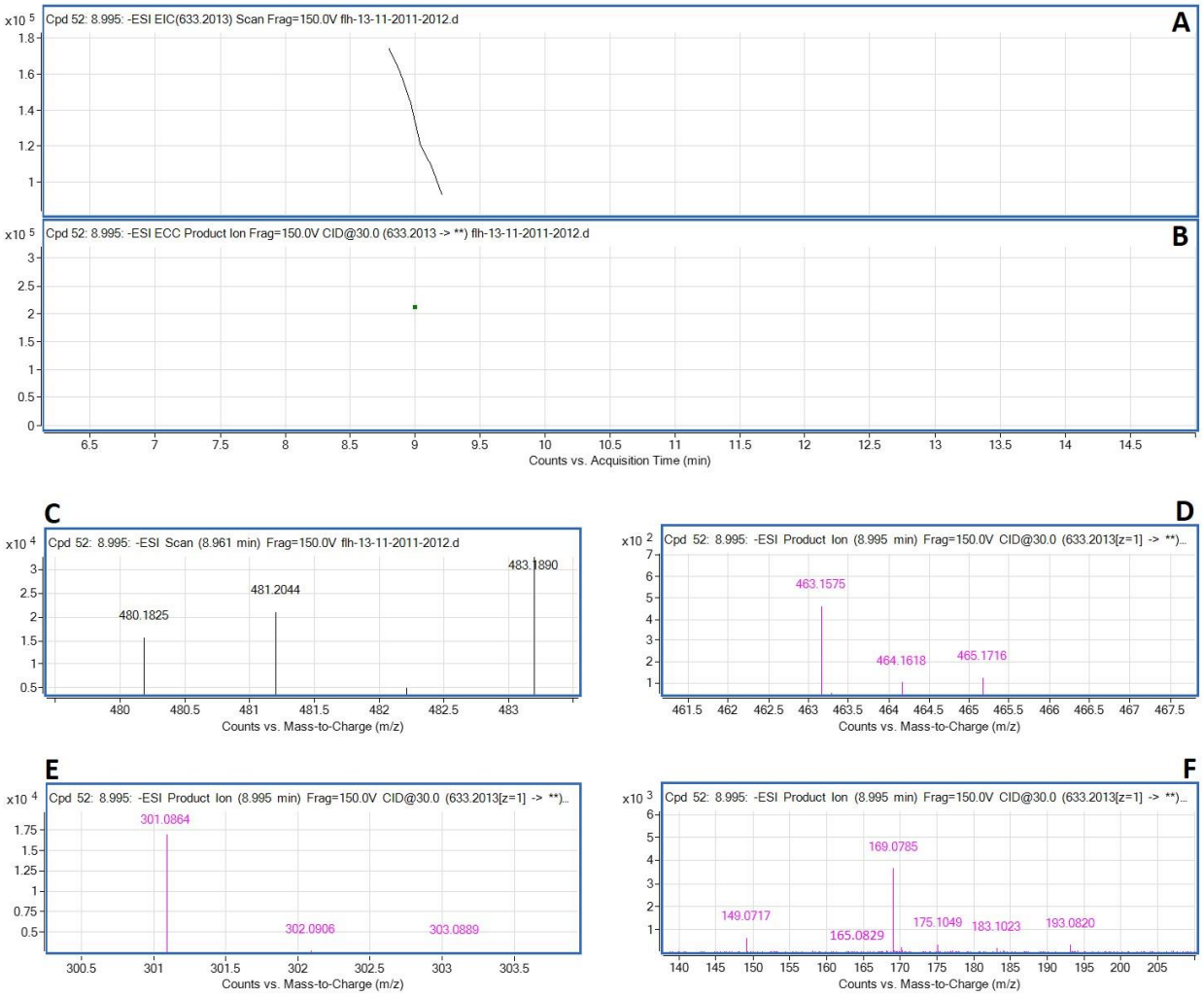

Supplementary Figure 2.2: Extracted ion chromatogram (EIC) of primary mass spectrum (MS1) and m/z features of secondary ion fragments (MS2) derived from LC-MC/MS of peak F-AN4. These data annotate this peak to be delphinidin 3-O-glucoside (Del-3-G) (MW: 465.387). A: EIC of primary ion 481.2044 [equals 465.387+18-2H] $[m/z]^-$, B: enhanced charge capacity (ECC) ion product for 481.2044 $[m/z]^-$, C: a MS profile showing an extracted m/z value, 481.2044 $[m/z]^-$, and D-F: fragments from CID of 481.2044showing 463.1575 $[m/z]^-$ relating to Del-3-G structure (D), 301.0864, 302.0906, and 303.0889$[m/z]^-$ relating to delphinidin aglycone (E), and 165.0829 and 169.0785 relating to glucose (F) (Table 1).

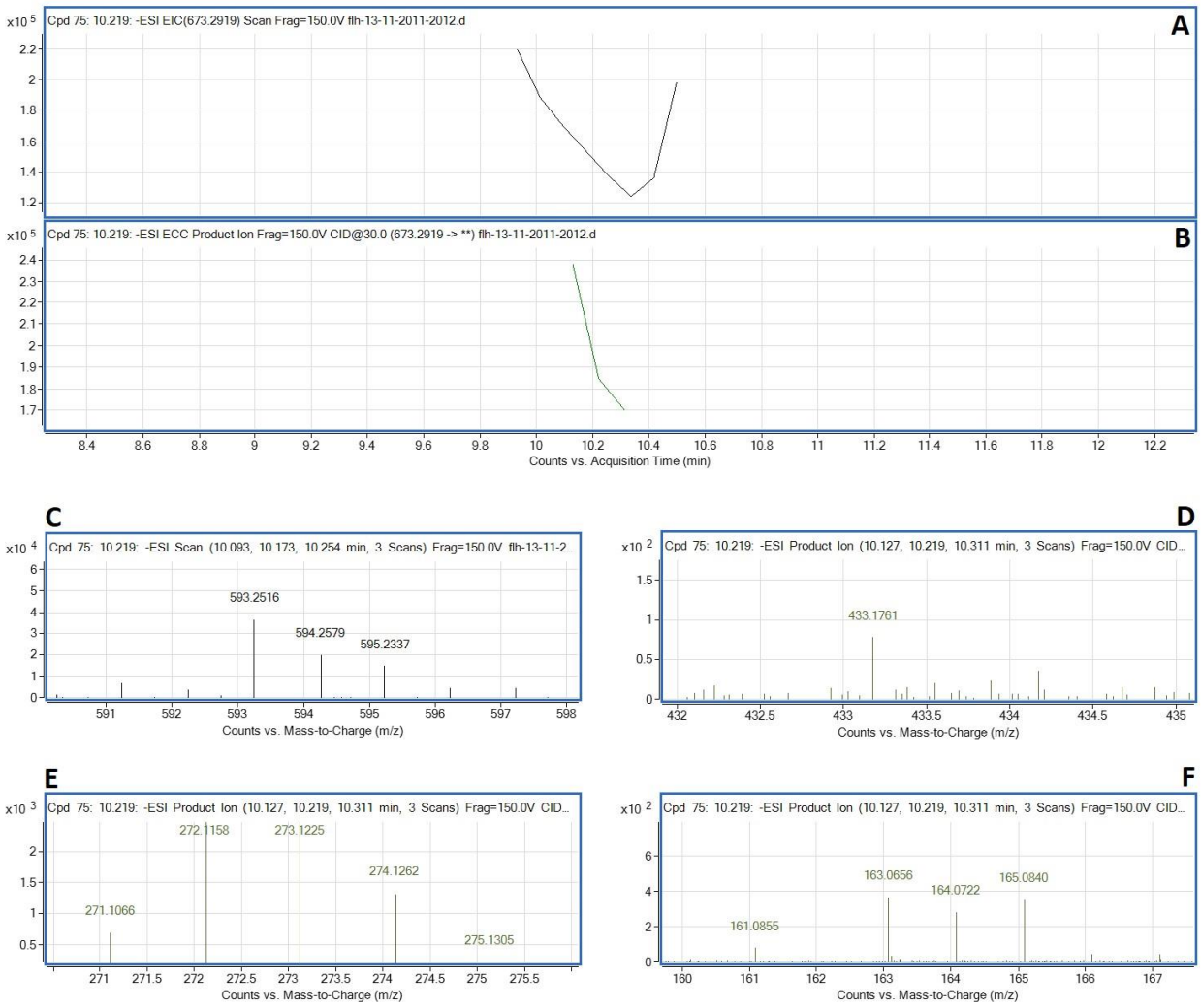

Supplementary Figure 2.3: Extracted ion chromatogram (EIC) of primary mass spectrum (MS1) and m/z features of secondary ion fragments (MS2) derived from LC-MC/MS of peak F-AN5. These data annotate this peak to be a pelargonidin 3, 5-O-diglucoside (Pel-3,5-dG, MW: 595.398). A: EIC of primary ion 593.2516 [M-2H] $[m/z]^{-}$, B: enhanced charge capacity (ECC) ion product for 593.2516 $[m/z]^{-}$, C: a MS profile showing an extracted m/z value, 593.2516 $[m/z]^{-}$, and D-F: fragments from CID of 593.2516 607 showing 433.1761$[m/z]^{-}$ relating to Pel-3-G like structure, 271.1066 and 272.1158-275.1350 $[m/z]^{-}$ relating to pelargonidin aglycone (E), and 161.0855, 163.0656, 164.0722, and 165.0640 relating to glucose (F) (Table 1).

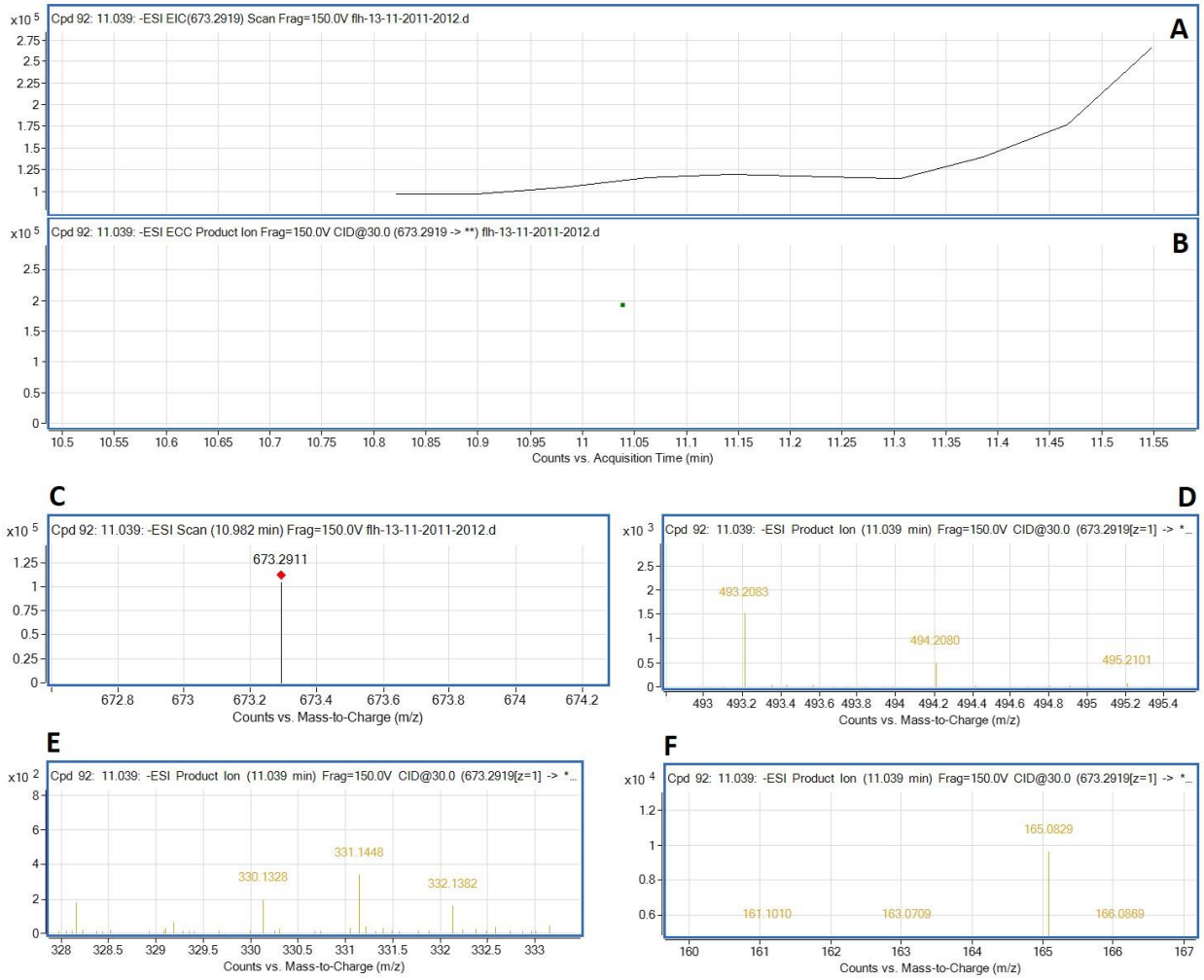

Supplementary Figure 2.4: Extracted ion chromatogram (EIC) of primary mass spectrum (MS1) and m/z features of secondary ion fragments (MS2) derived from LC-MC/MS of peak F-AN7. These data annotate this peak to be malvidin 3, 5-O-diglucoside (MW, 655.587). A: EIC of primary ion 673.2911[M+18-2H] $[m/z]^-$, B: enhanced charge capacity (ECC) ion product for 673.2911 $[m/z]^-$, C: a MS profile showing an extracted m/z value, 673.2911 $[m/z]^-$, and D-F: fragments from CID of 673.2911showing 493.2083 $[m/z]^-$ relating to malvidin 3-glucoside structure (D), 330.1328, 331.1448, and 332.1382 $[m/z]^-$ relating to malvidin aglycone (E), and 161.1010, 163.0709, 165.0829, and 166.0809 relating to glucose (F) (Table 1).

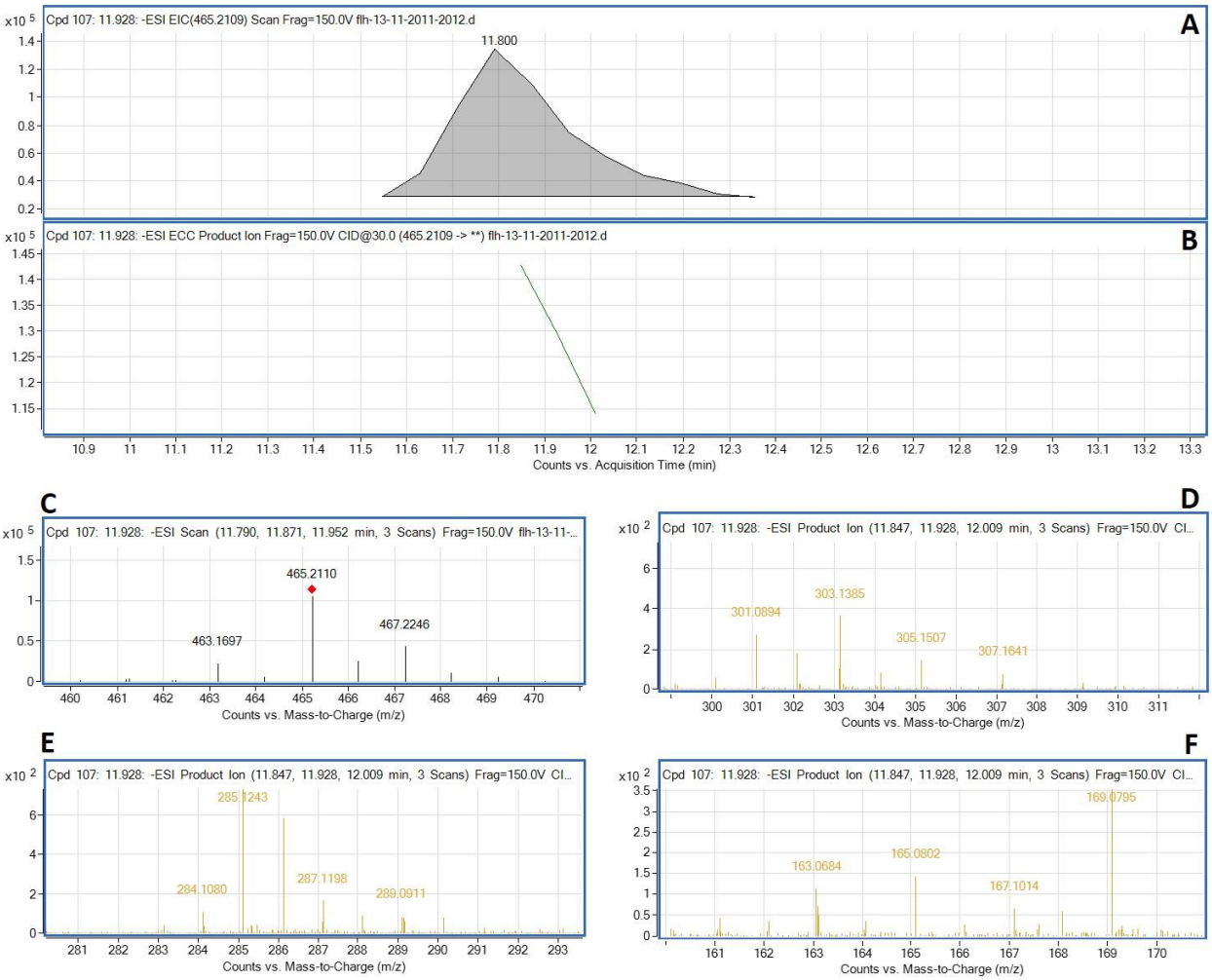

Supplementary Figure 2.5: Extracted ion chromatogram (EIC) of primary mass spectrum (MS1) and m/z features of secondary ion fragments (MS2) derived from LC-MC/MS of peak F-AN9. These data annotate this peak to be a cyanidin-related anthocyanin. A: EIC of primary ion 465.2110 $[m/z]^-$, B: enhanced charge capacity (ECC) ion product for 465.2110 $[m/z]^-$, C: a MS profile showing an extracted m/z value, 465.2110 $[m/z]^-$, and D-F: fragments from CID of 465.2110 showing 301.0894-307.1641 $[m/z]^-$ relating to a methylated-cyanidin structure (E), and 163.0684-169.0795 (F) (Table 1).

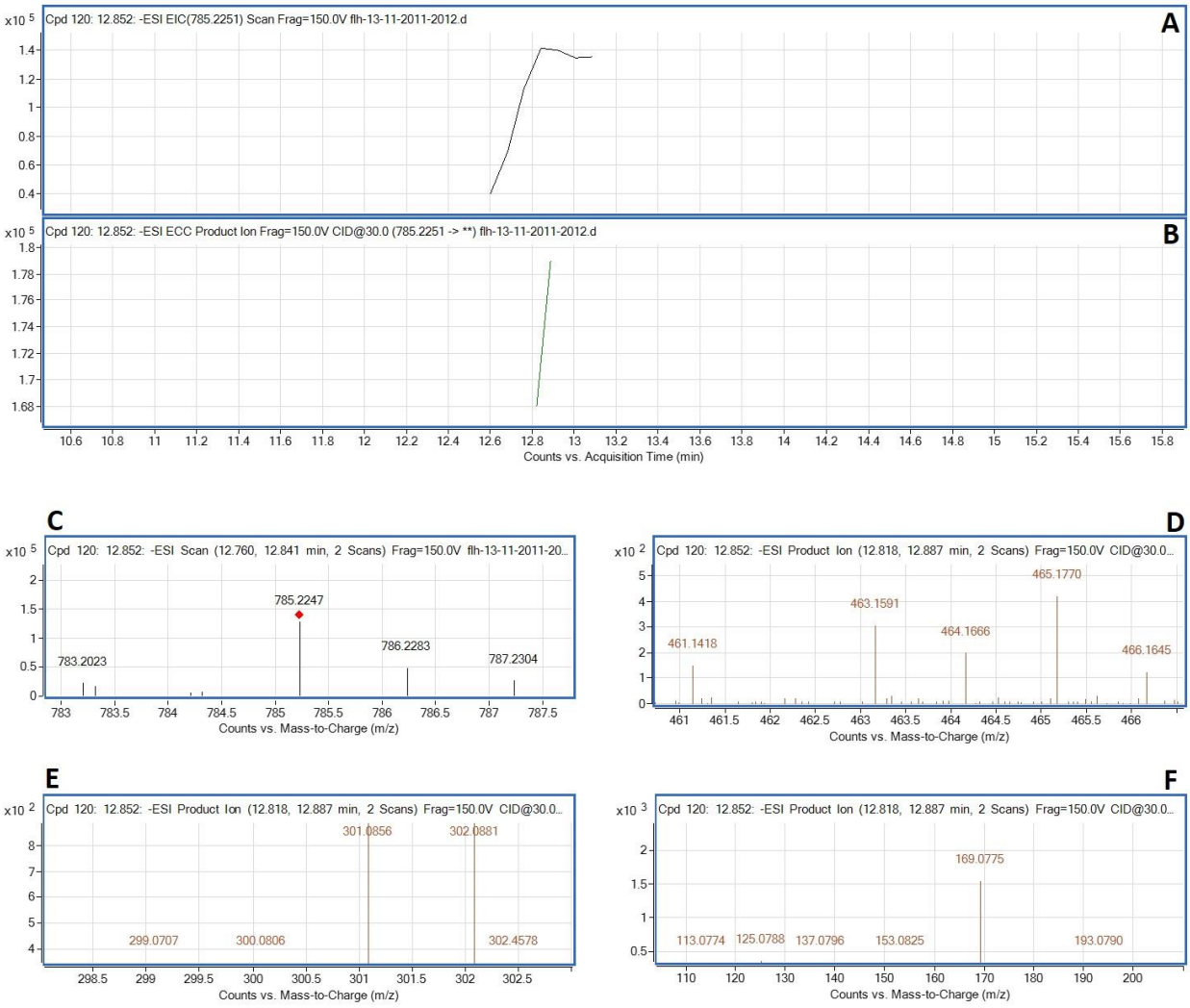

Supplementary Figure 2.6: Extracted ion chromatogram (EIC) of primary mass spectrum (MS1) and m/z features of secondary ion fragments (MS2) derived from LC-MC/MS of peak F-AN10. These data annotate this peak to be a peonidin-related anthocyanin. A: EIC of primary ion 785.2247 $[m/z]^{-}$, B: enhanced charge capacity (ECC) ion product for 785.2247 $[m/z]^{-}$, C: a MS profile showing an extracted m/z value, 785.2247 $[m/z]^{-}$, and D: fragments from CID of 785.2247showing 301.0856 $[m/z]^{-}$ relating to peonidin (Table 1).

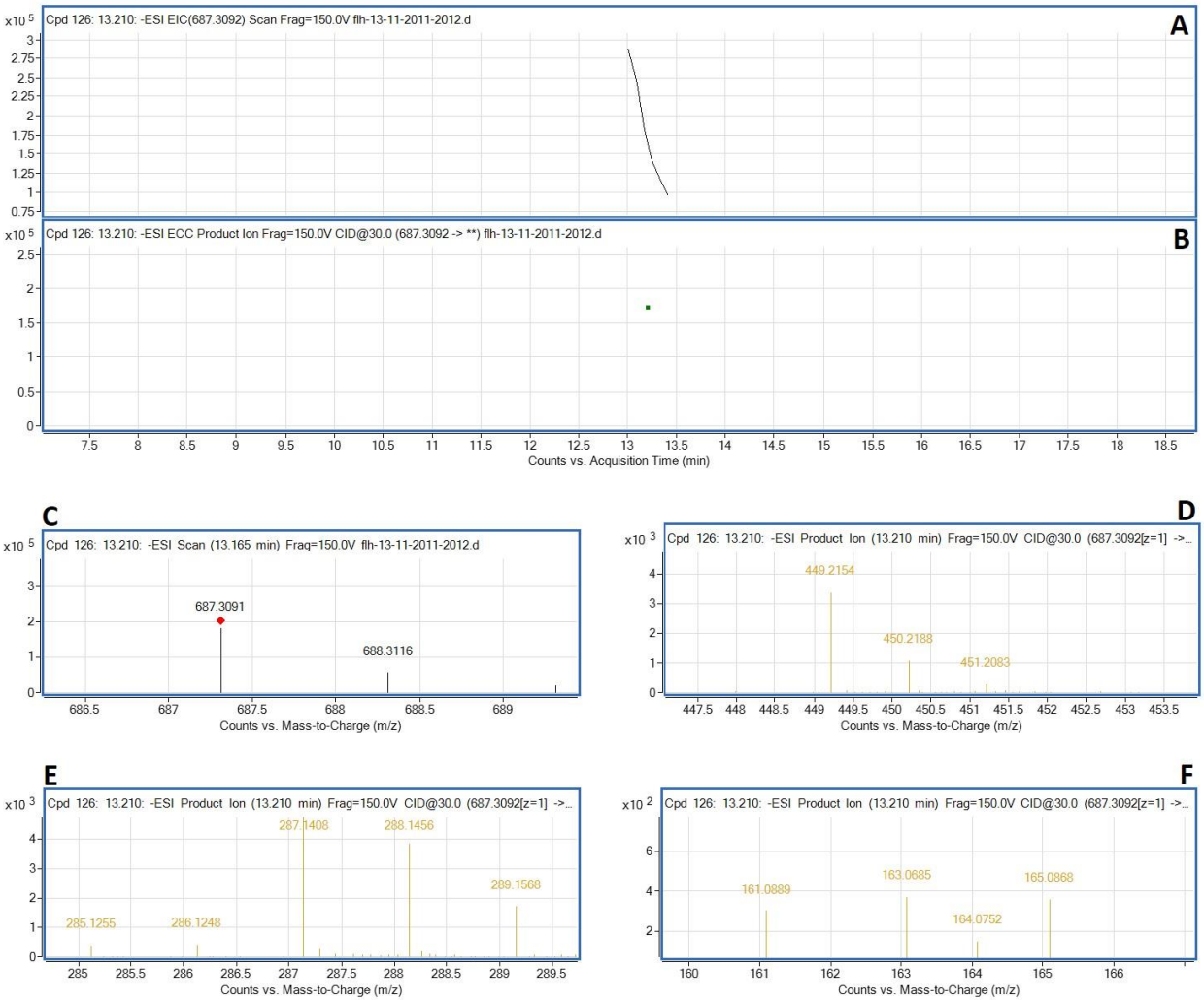

Supplementary Figure 2.7: Extracted ion chromatogram (EIC) of primary mass spectrum (MS1) and m/z features of secondary ion fragments (MS2) derived from LC-MC/MS of peak F-AN11. These data annotate this peak to be a cyanidin-related anthocyanin. A: EIC of primary ion 687.3091 $[m/z]^{-}$, B: enhanced charge capacity (ECC) ion product for 687.3091 $[m/z]^{-}$, C: a MS profile showing an extracted m/z value, 687.3091 $[m/z]^{-}$, D: and fragments from CID of 687.3091 showing 287.1408 $[m/z]^{-}$ relating to cyanidin (Table 1).

Supplementary Figure 2.8: Extracted ion chromatogram (EIC) of primary mass spectrum (MS1) and m/z features of secondary ion fragments (MS2) derived from LC-MC/MS of peak F-AN12. These data annotate this peak to be a cyanidin or pelargonidin-related anthocyanin. A: EIC of primary ion 665.1924 $[m/z]^-$, B: enhanced charge capacity (ECC) ion product for 665.1924 $[m/z]^-$, C: a MS profile showing an extracted m/z value, 665.1924 $[m/z]^-$, and D-F: fragments from CID of 665.1924 showing 423.1567-451.1542 $[m/z]^-$ relating to a cyanidin or pelargonidin-related fragment (D), 271.0723 through 285.1154 to 295.1303 (E), and 163.0991-169.0782 relating to a monosaccharide (F) (Table 1).

CHAPTER 3

HPLC-qTOF-MS/MS based profiling for characterizeing flavan-3-ol and dimeric proanthocyanidin profiles in berries of two interspecific muscadine hybrids FLH 13-11 and FLH 17-66 in two continuous cropping seasons

Seyit Yuzuak[1], James Ballington[2], and De-Yu Xie[1]

1 Department of Plant and Microbial Biology, North Carolina State University

2 Department of Horticultural Sciences, North Carolina State University

Abstract

Muscadine FLH 13-11 FL and FLH 17-66 FL are two interspecific hybrid varieties developed to produce new flavonoids for color stability and organoleptic properties. The compositions of flavan-3-ols and proanthocyanidins (PAs) in berries remain uncharacterized. Herein, we report the use high performance liquid chromatography-quadrupole time-of-flight tandem mass spectrometer (HPLC-qTOF-MS/MS) to characterize flavan-3-ols and dimeric PAs in berries. Ripe berries were collected from consecutive cropping years and extracted to obtain flavan-3-ols and PAs. Metabolites were ionized using the negative mode, and collision induced dissociation was performed to fragment molecules to obtain feature fragment profiles. Nine standards were used to establish finger printing features. Based on standards and features of MS and MS/MS, thirty metabolites were annotated to four flavan-3-ol aglycones, eighteen gallated or glycosylated conjugates, and eight dimeric procyanidins (A1, B1, B2, B4, B5, B6, B7, and B8). In particular, six new methylated flavan-3-ol conjugates were detected in berries. Absence and presence analysis of these metabolites revealed that both cultivars and cropping seasons altered

the composition of these metabolites in berries. These data will be informative to enhance the application of these two cultivars for grape and wine industry. The resulting data showed that the profile of flavan 3-ols and proanthocyanidins were slightly altered in two years for each variety but significantly different between varieties, indicating that genotypes and the two growth years had a crucial effect on flavan-3-ols and proanthocyanidin.

Introduction

Muscadine (*Vitis rotundifolia* Michx) is an indigenous grape crop in the southeastern region of the United States (Brown 1940). This grape crop is widely cultivated in several states, such as Florida, Georgia, Alabama, Louisiana, South Carolina, and North Carolina. Because of its resistance to fungal pathogens and tolerance of local growing conditions, it has been shown that it is a more favorable for cropping than bunch grapes in the southeastern US. (Olien 2001). The past many years of breeding efforts have created over one hundred superior cultivars, such as FLH 11-13 FL and FLH 17-66 FL, for both wine and juice industries (Mortensen 2001). Berries from multiple cultivars have been traditionally used for the production of wine, juice, jam, jelly, and fresh-market fruit. Multiple nutritional studies have shown that muscadine berries and different products are rich in phenolic compounds, such as flavan-3-ols and oligomeric proanthocyanidins with high health benefits. To date, the consumption demand for fresh berries and products has been dramatically increasing (Barchenger, Clark et al. 2015). Furthermore, muscadine is one of main small berry crops in the southeastern region of the US.

Proanthocyanidins (PAs), also known as condensed tannins, are oligomeric or polymeric flavan-3-ols, such as (+)- catechin, (-)- epicatechin, synthesized in many crops such as grapes. Flavan-3-ols are linked by an interflavan bond between C4 of the extension unit (the

top unit) and C6 or C8 of the starter unit (the lower unit). Two types of PAs occur in plants, A- and B-type. In B-type, only interflavan bond forms the linkage between the starter and the immediate extension unit and between extension units. In A-type, in addition to an interflavan bond, an additional ether linkage is formed between C7 or C5 of the starter unit and the C2 of the extension unit (Fig. 1) (Zhang, Li et al. 2017). PAs occur in different plant tissues, such as fruit skin and seed coats (Zhang, Li et al. 2017). For instance, grape seed is rich natural resource of PAs (Spranger, Sun et al. 2008). Numerous previous studies have revealed that PAs defend plants against herbivores and pathogens and protect plants from irradiation-caused damages. Moreover, PAs are important nutrients to protect ruminant animals, such as milk cows, from pasture bloat, a disease caused by high protein contents in forage crops, such as alfalfa. Furthermore, PAs provide multiple health benefits for humans, such as antioxidative activity against free radicals-mediated diseases (Blade, Aragones et al. 2016; Jonker and Yu 2017). The presence of PAs also contributes the astringent and bitter tastes and maintain color stability of juices and wine (Gourineni, Shay et al. 2012).

To date, several studies have reported flavan-3-ols and PAs in muscadine grapes. Phytochemical characterization and profiling have been undertaken to understand flavan-3-ols, PAs, anthocyanins, and other phenolics in a few different muscadine cultivars (Sandhu and Gu 2010; You, Chen et al. 2012; You, Chen et al. 2012). A metabolic profiling study using high-performance liquid chromatography coupled with a diode array detector and electrospray ionization mass spectrometry (HPLC-DAD-ESI-MS) has characterized that, in Florida-grown muscadine grapes bronze cultivars including Doreen, Fry, Carlos, Triumph, black cultivars; Southland, Magoon, Alachua, and Noble produced epicatechin, epicatechin gallate, gallocatechin, epicatechin digallate, and dimeric procyanidins. This study further characterized

that the majority of flavan-3-ols monomers were found in skin and pulp of berries, while the majority of PAs were present in seeds (Sandhu and Gu 2010). These characterizations were further supported by three other profiling methods, studies of HPLC coupled with ultraviolet and a mass spectrometer (HPLC-UV-MS), HPLC coupled with an evaporative light scattering detection (HPLC-ELSD), and HPLC-UV-ESI-MS, which were applied to two black and bronze cultivars, Noble and Carlos, respectively (You, Chen et al. 2012). Results from these three metabolic profiling methods showed that differences of flavan-3-ols and PAs as well as other phenolic compositions were mainly associated with seed and skin of berries, but were only slightly associated with the two varieties. These data indicate that the biosynthetic similarity of flavan-3-ols and PAs in these two cultivars. A recent comparative study revealed that flavan-3-ols and PAs profiles were biogeographically regulated by field growth in China and USA (Wei, Luo et al. 2017). All these studies enhance characterization of phenolic compositions in the muscadine berries investigated. To date, more than 100 cultivars have been developed to seek new grapes for high quality wines and other products. However, understanding of phenolics in these cultivars is limited. Comprehensive characterization phenolics profiles particularly flavan-3-ols and PAs in these cultivars will enhance commercialization of new cultivars. (Quideau, Deffieux et al. 2011; Wei, Luo et al. 2017).

FLH 13-11 and FLH 17-66 are two interspecific muscadine hybrids. They were progeny created from the cross of Marsh x Magoon. Marsh is a *M. munsoniana* and Magoon is a *M. rotundifolia* resulting from a cross between Thomas x Burgaw. Two cultivars have been planted in a research station for field growing tests for commercial purposes in North Carolina. To date, profiles of flavan-3-ols and PAs in these two cultivars remain unknown. In this study, we used HPLC-qTOF-ESI-MS/MS to characterize flavan-3-ols and PA profiles in mature berries

in continuous two years of cropping. Our results reveal flavan-3-ol aglycones, flavan-3-ol conjugates, and dimeric PAs in mature berries.

MATERIALS AND METHODS

Chemical agents and standards

All chemicals and standards mentioned below were of either HPLC or LC-MS grade. (+)- Catechin (≥98%, HPLC grade, cat# C1251), (-)- Catechin (≥98%, HPLC grade, cat# C0567), (-)- Epicatechin (≥98%, HPLC grade, cat# E4018), (-)- Epigallcatechin (≥98%, HPLC grade, cat# E3768), (-)- Gallocatechin (≥98%, HPLC grade, cat# G6657), (-)- Catechin gallate (≥98%, HPLC grade, cat# C0692), (-)- Epigallocatechin gallate (≥80%, HPLC grade, cat# E4268) and (-)- Gallocatechin gallate (≥98%, HPLC grade, cat# G6782) were purchased from Sigma-Aldrich® (St Louis, MO, USA). Procyanidin B1 and B2 (HPLC grade, cat# ASB-16230 and 16231, respectively) was purchased from Chroma Dex™ (Irvine, CA, USA). Acetonitrile (LC-MS grade, cat#: 9829-03), glacial acetic acid (HPLC grade, cat#: 9515-03) and methanol (LC-MS grade, cat#: 9830-03) were purchased from Avantor® (Center Valley, PA 18034, USA). Ethyl alcohol, 200 proof (cat#: EX0276-1) was purchased from EMD (Burlington, MA 01803, USA). Water (LC-MC grade, cat#BJLC365) was purchased from VWR® (Radnor, PA, USA).

Plant material

FLH 13-11 and FLH 17-66 vines were grown at the Castle Hayne research station in Wilmington, North Carolina (Elevation: 33 feet, 34.27 °N, 77.9 °W). In this area, berries are fully ripened in the first two weeks of September every year. We collected ripened berries on Sept. 6 in 2011 and Sept. 10 in 2012. Fruits on vines were directly harvested to an ice cooler and

transported to the laboratory. All fresh berries were frozen in liquid nitrogen completely and then stored in -80 freezes. Frozen berries were ground in to fine powder in liquid nitrogen using a steel blender. Powdered samples were completely dried 72 hours via lyophilization from -40°C to -20°C. Dried powder samples were stored in -80°C until extraction of PAs described below.

Extraction of flavan-3-ols and dimeric proanthocyanidins

One hundred milligrams of dry berry powder were suspended in 1.0 ml extraction buffer, which was composed of 0.5% HCl in methanol: dH_2O (50:50, v/v) in a 2 ml Eppendorf tube at room temperature. The tube was vigorously vortexed for 45 s, sonicated for 10 min, and then centrifuged at 10,000 rpm (9,391 rcf) for 10 min. The supernatant was transferred into a new 1.5 ml tube. This step was repeated using 0.5 ml extraction buffer. The two extractions were pooled together in the 1.5 ml tube. To remove chlorophyll and non-polar lipids in the extraction, the 1.5 ml ethanol: water extraction was mixed with 0.5 ml chloroform in a 2 ml tube. The mixture was vortexed vigorously for 45 s and centrifuged at the speed of 10,000 rpm (9,391 rcf) for 5 min. The resulting upper ethanol: water-phase (about 750 µl) containing flavan-3-ols and PAs was pipetted into a new 1.5 ml tube. The bottom chloroform phase containing chlorophyll and non-polar lipids was disposed of into a waste container. These steps were repeated once. The resulting upper phase was stored at - 20°C for flavan-3-ols analysis. Three biological replicates were conducted for the two varieties in this experiment. 720 µl ethanol-water extract was dried off using a SpeedVac Concentrator connected to Refrigerated Condensation Trap for 2 hours. The remaining pellet was dissolved in 720 µl of 0.1% HCl in methanol 100% in a 1.5 ml tube. The tube was centrifuged at 10,000 rpm (9,391 rcf) for 10 min. The resulting clear supernatant was transferred to a new 1.5 ml tube and then stored at - 20°C for flavan-3-ols analysis. Two

hundred µl HCl-methanol extract for each sample was transferred to a glass insert, which was placed in a 1.5 ml glass vial for HPLC and LC-MS analysis.

High performance liquid chromatograph- quadrupole time-of-flight-tandem mass spectrometer (HPLC-qTOF-MS/MS) analysis

HPLC-TOF-MS/MS analysis was performed on an Agilent Technologies (Santa Clara, CA, USA) 6210 time-of-flight LC-MS/MS as reported recently (He, Li et al. 2017). The mobile phase solvents were composed of 1% acetic acid in water (solvent A: 1% HPLC grade acetic acid in LC-MS grade water) and 100% acetonitrile (solvent B) (LC-MS grade), which formed a gradient solvent system to separate flavan-3-ols. A gradient solvent system was composed of ratios of solvent A to B: 85:15 (0-10 min), 85:15 to 80:20 (10-20 min), 80:20 to 75:25 (20-30 min), 75:25 to 65:35 (30-35 min), 65:35 to 60:40 (35-40 min), 60:40 to 50:50 (40-55 min), 50:50 to 10:90 (55-60 min), 10:90 to 90:10 (60-70 min). After the last gradient step, the column was equilibrated and washed 10 min with solvents A: B (85:15). The flow rate was 0.4 ml/min. The injection volume of samples was 5.0 µl. The drying gas flow was set to 12 l/min, and the nebulizer pressure was set to 50 psi. As in our recent report using an optimized protocol for anthocyanin ionization (He, Li et al. 2017), we used the negative mode for ionization of metabolites. The mass spectra were scanned from 100 to 3000 m/z. The acquisition rate: three spectra per second. Fragmentor: 150 v, Skimmer: 65 v, OCT 1 RF Vpp: 750 v, Collision energy: 30. In addition, the UV spectrum was recorded from 190 to 600 nm. (+)-Catechin, (-)-epicatechin, (-)-epigallocatechin, (-)-gallocatechin, (-)-catechin gallate, (-)-epigallocatechin gallate, (-)-gallocatechin gallate, and procyanidin B1 and B2 were used as authentic standards.

Structure annotation

Flavan-3-ols and dimeric PA structure annotation was performed using Agilent MassHunter Software for 6200 Series TOF and 6500 Series G-TOF version B.05.00. To identify flavan-3-ols and dimeric PAs in extracts, retention time, extracted ion chromatogram (EIC), and mass to charge (m/z) ratio for each peak were analyzed to compare with available standards. For those peaks without standards, their EICs and m/z ratios were used for annotation. For each flavan-3-ol and dimeric PA peak detected at 280 nm by HPLC-DAD, their EIC, m/z ratio, retention time, and fragments from CID were integrated for structure annotation. (+)-Catechin, (-)-epicatechin, (-)-epigallocatechin, (-)-gallocatechin, (-)-catechin gallate, (-)-epigallocatechin gallate, (-)-gallocatechin gallate, procyanidin B1, and procyanidin B2 standards were used to generate primary mass spectra (MS1) from ESI and secondary mass spectrum fragments (MS2) from collision induced dissociation, which were used to develop structure annotation protocols. Flavan-3-ol and dimeric PA structures reported in the literature (Fig. 1) were utilized as our references for annotation.

RESULTS AND DISCUSSION

HPLC-qTOF-MS/MS based characterization of flavan-3-ol aglycones, conjugates, and dimeric PAs standards

We used nine standards to develop LC-qTOF-MS/MS protocols for annotation of flavan-3-ols and PAs in samples. These are (+)-catechin, (-)-epicatechin, (-)-epigallocatechin, (-)-gallocatechin, (-)-catechin gallate, (-)-epigallocatechin gallate, (-)-gallocatechin gallate, and procyanidin B1 and B2. Standards were ionized using the negative mode to generate mass-to-charge ratios and then fragmented using collision induced disassociation. The resulting ions

(primary ions) were separated by mass-to-charge ratio in the first stage of mass spectrometry (MS1). Ions of a particular mass-to-charge ratio from each standard were selected to create fragment ions by collision induced dissociation (CID). The resulting fragment ions (secondary ions) were separated and detected in a second stage of mass spectrometry (MS2). Primary and secondary ions were generated for each standard. For example, the molecular weight (MW) of (+)-catechin is 290.26. Its accurate primary ion detected was 289.1574. After CID, five fragment ions obtained were 109.0815, 123.1001, 137.0823, 151.1007, and 247.1028 (Fig. 3). The fragment 247.1028 resulted from the dissociation of ethanol (C_2H_5O) (42.0546) from 289.1574. The fragment ions 109.0815 resulted from cleavage on B or C ring of 289.1574. The fragment ion 123.1001 and its isotopes resulted from the loss of pholoroglucinol (heterocylic ring fission cleavage, 126) and benzofuran forming fission fragmentation (121) of 289.1574. The fragments 137.0823, and 151.1007 resulted from Retro-Diels Alder cleavage from 289.1574. (RDA). Table 1 summarizes the [m/z] ratios and CID profiles for other standards, which form finger printings for annotation of flavan-3-ols and PAs in samples described below.

Metabolite peak profile comparison among FLH 13-11, FLH 17-66, and standards

Flavan-3-ols and dimeric PA profiles were analyzed by HPLC-DAD based profiling. Chromatographic peaks were recorded at 280 nm to compare flavan-3-ols and PA profiles in each variety's berries between two growing seasons. The resulting peak profiles showed that on the one hand, metabolite profiles in each cultivar were slightly different in the two growing seasons; on the other hand, obvious metabolite profile differences existed in the two cultivars (Fig. 2a and b). Based on standards of flavan-3-ols and dimeric PAs, peaks of (+)-catechin, (-)-epicatechin, (-)-epigallocatechin, (-)-gallocatechin, (-)-catechin gallate, (-)-epigallocatechin

gallate, (-)-gallocatechin gallate, and procyanidin B1 and B2 were observed in samples. These peaks and other peaks belonging to flavan-3-ols and PAs were labelled.

Flavan-3-ol aglycone profiles in extracts

HPLC-qTOF-MS/MS analysis identified four flavan-3-ol aglycones in the extracts of FLH 13-11 and FLH 17-66 (Fig. 2). EIC showed that the dominant accurate $[m/z]^-$ ratios for (+)-catechin and (-)-epicatechin were between 289.0359 and 289.1586 (Table 2). In addition, accurate MS fragments generated from collision induced dissociation (CID) were obtained for them. Based on standards and their specific $[m/z]^-$ and MS/MS profiles, the four flavan-3-ol aglycones (Table 2) were identified to be (+)-catechin (Fig. 3), (-)-catechin (S-Fig. 1), (-)-epicatechin (Fig. 4), and (+)-epicatechin (S-Fig. 2). Four flavan-3-ols were detected in FLH 13-11 in two cropping seasons. However, only (-)-epicatechin was detected in FLH 17-66 in two cropping seasons. (+)-epicatechin in FLH17-66 was only detected in one season, but both (+) and (-)-catechin were not detected in the extracts of FLH 17-66.

Flavan-3-ol conjugate profiles in extracts

Regardless of the two cropping years and cultivars, 18 flavan-3-ol conjugates, including eight glucosides and ten gallates (Table 3), were annotated from metabolites in the extracts of all samples via HPLC-qTOF-MS/MS analysis.

Among these 18, only four, (+)-catechin gallate [(+)-CatG], (-)-catechin gallate [(-)-CatG], and (-)-epicatechin gallate [(-)-EpiCatG], were detected in extracts of two cultivars in two consecutive cropping years. This observation suggests that two cultivars from the same parents constitutively biosynthesize these four conjugates. The detection of 14 others was associated

with two cultivars (Table 3). Five were only detected in the extracts of FLH 11-13 berries, while eight were only detected in the extracts of FLH 17-66 berries. Of 18, six are relating to methylated flavan-3-ols. Although which –OH group is methylated remains for further investigation, this observation indicates that methylated anthocyanidins, such as peonidin and petunidin, can be converted to new flavan-3-ols.

In each cultivar, the detection of conjugates was associated with growing seasons (Table 3). Nine were detected in FLH 11-13 berry extracts. Of these, *O*-methylated (-)-gallocatechin gallate [(-)-*O*MegCatG], was detected only in 2011, while four, (+)- catechin 3-*O*-glucoside [(+)- Cat3Glu], (-)-catechin 3-*O*-glucoside [(-)- Cat3Glu], (+)- epicatechin gallate [(+)-EpiCatG], and *O*-methylated (-)- catechin gallate [(-)-*O*MeCatG], were detected only in 2012. Twelve were detected in FLH 17-66 berry extracts. Of these five, (+)-epicatechin [(+)-EpiCat], (+)-gallocatechin 3-*O*-glucoside [(+)-gCat3Glu], (-)-gallocatechin 3-*O*-glucoside [(-)-gCat3Glu], *O*-methylated (+)- epigallocatechin gallate [(+)- *O*MeEpigCatG], and *O*-methylated (-)- epigallocatechin gallate [(-)- *O*MeEpigCatG] were detected only in 2011, while two(-)-epicatechin 3-*O*-glucoside [(-)- EpiCat3Glu], and *O*-methylated (+/-)- epicatechin gallate [(+/-)-*O*MeEpiCatG] were found only in 2012.

Dimeric PA profiles in extracts

Based on two standards (Table 1) and HPLC-qTOF-MS/MS analysis, eight peaks were annotated dimeric PAs, which included one A-type and seven B-type dimers (Table 4). Based on the $[m/z]^-$ value and MS/MS fragment profile, this A-type was annotated as procyanidin A1 (Fig. 9 and Table 4). Seven B-type dimers were characterized to be dimeric procyanidins consisting of catechin and/or epicatechin, in which three have a C4-C8 interflavan bond and four have a C6-

C8 interflavan bond. Although there are two types of interflavan bonds, their mass-to-charge ratios and fragment profiles are almost identical (Table 4, Fig. 10, and S-Figs. 17-22). Regardless of growing years, procyanidin A2, and procyanidin B1, B2, B4, and B5 were detected in both berries (Table 4), indicating that berries of both cultivars can synthesize them. Procyanidin B6-B8 were only detected in berries of FLH 13-11 but not FLH 17-66, indicating the biosynthetic difference between the two cultivars during the two cropping years. Effects of growing seasons on procyanidin profiles were also observed. On the one hand, in FLH 11-13 berry extracts, procyanidin B1 and B8 were detected only in 2011. On the other hand, in FLH 17-66 berry extracts, procyanidin B1, B4, and B5 were found only in 2012.

Discussion

Thirty peaks detected at 280 nm were annotated as four flavan-3-ol aglycones, eighteen flavan-3-ol conjugates, and eight dimeric procyanidins. Our annotation was based on accurate $[m/z]^-$ values, fragment profiles and retention time features of nine standards (Table 1). We have nine standards, therefore, it was not challenging to identify these metabolites in the extracts of samples (Tables 2, 3, and 4). Although no standards were available for 21 others, $[m/z]^-$ values and fragment profiles of each standard and each peak generated by HPLC-qTOF-MS/MS analysis provided highly confident finger printing features for annotation. There are four main fragmentation patterns reported for flavan-3-ols and dimeric PAs, including: Retro-Diels Alder (RDA), heterocylic ring fission (HRF), benzofuran forming fission (BFF) and quinone methide fragmentation (QM, also called as interflavan bond cleavage). We also observed all these in our experiment. For flavan-3-ol aglycones and conjugates, RDA, HRF and BFF were favored for annotation. The fragment profiles from RDA include 137,151, 289, 299, 303, 313, 329, and 465

(*m/z*). The main fragment for HRF is 125 (*m/z*). The main fragment profiles for BFF are 121, 271, and 331 (*m/z*). In addition, fragments ions with 425 (*m/z*) (loss of ethanol), 441 (*m/z*) (presence of epicatechin gallate), 305 (*m/z*) (presence of epigallocatechin), 287 and 179 (*m/z*) (loss of glucose), 169 (*m/z*) (loss of gallic acid), 271 (*m/z*) (loss of water form monomers), 109 (*m/z*) (cleavage on B or C ring), 119 and 331 (*m/z*) (cleavage on glucose residue) were also observed for flavan-3-ol aglycones and conjugates. For dimers, HRF, RDA, and QM cleavages were reported to generate fragments including group:125-163-413-451, group: 151-425, and group 3: 287-289 (*m/z*), respectively (Gu, Kelm et al. 2003; Li and Deinzer 2007; Callemien and Collin 2008; Delcambre and Saucier 2012). Although A- and B-type dimers have linkage and two proton differences, they tend to have identical masses and follow the same fragmentation pathway because of their high structural similarities (Fig. 1). The only variations between individuals of procyanidin dimers is the spatial arrangement due to stereochemistry and the position of the interflavan bond, and elution order (Callemien and Collin 2008).

The annotations of B1, B2, B4, and B5-B8 were based on the two standard samples and HRF, RDA, and QM profiles described above. Based on procyanidin B1 and B2 elution orders (Table 1), procyanidin B1 and B2 were identified in samples (Fig. 10 and S-Fig. 17). Due to the absence of standards for other dimers, we further used these two standards and their retention time as well as our HPLC separation condition to annotate others with a high confidence. For the condition that used a reverse phase column and mobile solutions consisting of 1% acetic acid in water and 100% acetonitrile, four flavan-3-ol monomers were eluted in the order of (+)-catechin, (-)-catechin, (+)-epicatechin, and (-)-epicatechin. Based on these elution features, the elution order for dimers was proposed to be catechin-4,8-catechin, catechin-4, 8-epicatechin, epicatechin-4,8-catechin, and epicatechin-4,8-epicatechin. The order of procyanidin B1

(catechin-4, 8-epicatechin) and B2 (epicatechin-4,8-epicatechin) standards supported this prediction (Tables 1 and 4). The peak between B1 and B2 (Fig. 1) was annotated to be procyanidin B4. Dimers with C4-C6 interflavan bond linkage are eluted later than those with C4-C8 linkage. Therefore, four dimers eluted later than procyanidin B4 were annotated to be procyanidin B5, B6, B7, and B8.

This HPLC-qTOF-MS/MS based profiling provides interesting information to understand effects of cultivars and cropping years on profiles of flavan-3-ols and dimeric PAs. A Venn diagram was generated to characterize metabolic similarity and differences in two cultivars and cropping years (Fig. 11). In 2011, 26 metabolites were detected from two cultivars, but only seven were produced by both of them. In 2012, 24 metabolites were detected, but 10 were produced by both of them. This data revealed biosynthetic differences in berries of two cultivars. In the extracts of FLH 13-11 berries, 22 metabolites were detected in two cropping years and seven of them were differentially produced berries. In the extracts of FLH 17-66, 20 metabolites were detected in two cropping years and 10 of them were differentially produced in berries. These data suggest that muscadine grape is a significant source of diverse flavan-3ols and proanthocyanidin oligomers for studying and answering the questions regarding to precursor of PA extension unites. Significant differences recorded between the two growing seasons in terms of climate conditions such as higher average temperature, drought and lower precipitation revealed that cropping seasons can dramatically affect the composition of flavan-3-ols and dimeric PAs.

In conclusion

A HPLC-qTOF-MS/MS protocol was developed to annotated flavan-3-ols and proanthocyanidins. Four flavan-3-ol aglycones, eighteen flavan-3-ol conjugates, and eight

dimeric procyanidins are annotated from the berry extracts of interspecific hybrids FLH 13-11 FL and FLH 17-66 in two consecutive cropping seasons. These metabolites revealed that both cultivars and cropping seasons affect the composition these favan-3-ols and dimeric PAs.

Acknowledgement

This research was funded by North Carolina State University for Plant Breeding Programs.

REFERENCES

Albert, N. W., D. H. Lewis, et al. (2009). "Light-induced vegetative anthocyanin pigmentation in Petunia." J. Exp. Bot. 60(7): 2191-2202.

Andersen, R. A. and J. A. Sowers (1968). "Optimum conditions for bonding of plant phenols to insoluble polyvinylpyrrolidone." Phytochemistry 7(2): 293-301.

Anderson, J. W. (1968). "Extraction of enzymes and subcellular organelles from plant tissues." Phytochemistry 7(11): 1973-&.

Anderson, J. W. (1968). "Extraction of enzymes and subcellular organelles from plant tissues." Phytochemistry 7(11): 1973-1988.

Ballinger, W. E., E. P. Maness, et al. (1973). "Anthocyanins of black grapes of 10 clones of *Vitis rotundifolia*, MICHX." J Food Sci 38(5): 909-910.

Barchenger, D. W., J. R. Clark, et al. (2015). "Evaluation of physicochemical and storability attributes of muscadine grapes (*Vitis rotundifolia* Michx.)." Hortscience 50(1): 104-111.

Barchenger, D. W., J. R. Clark, et al. (2015). "Nutraceutical Changes in Muscadine Grape and Grape Segments During Storage." Journal of the American Pomological Society 69(2): 66-73.

Blade, C., G. Aragones, et al. (2016). "Proanthocyanidins in health and disease." Biofactors 42(1): 5-12.

Bloor, S. J. and S. Abrahams (2002). "The structure of the major anthocyanin in Arabidopsis thaliana." Phytochemistry 59(3): 343-346.

Borevitz, J. O., Y. J. Xia, et al. (2000). "Activation tagging identifies a conserved MYB regulator of phenylpropanoid biosynthesis." Plant Cell 12(12): 2383-2393.

Brown, W. L. (1940). "The anthocyanin pigment of the hunt muscadine grape." J Am Chem Soc 62: 2808-2810.

Buchanan, B. B., W. Gruissem, et al. (2000). Biochemistry and Molecular Biology of Plants American Society of Plant Physiologists.

Burton, S. G. and S. Kirchmann (1997). "Optimised detergent-based method for extraction of a chloroplast membrane-bound enzyme: Polyphenol oxidase from tea (*Camellia sinensis*)." Biotechnol Tech 11(9): 645-648.

Callemien, D. and S. Collin (2008). "Use of RP-HPLC-ESI(-)-MS/MS to differentiate various proanthocyanidin isomers in lager beer extracts." Journal of the American Society of Brewing Chemists 66(2): 109-115.

Cardona, J. A., J. H. Lee, et al. (2009). "Color and polyphenolic stability in extracts produced from muscadine grape (*Vitis rotundifolia*) pomace." J Agric Food Chem 57(18): 8421-8425.

Carnegie, P. R. (1961). "Separation of low molecular weight peptides from amino acids on DEAE-Sephadex." Nature 192(480): 658-&.

Casado-Vela, J., S. Selles, et al. (2005). "Proteomic approach to blossom-end rot in tomato fruits (*Lycopersicon esculentum* M.): Antioxidant enzymes and the pentose phosphate pathway." Proteomics 5(10): 2488-2496.

Chi, M., B. Bhagwat, et al. (2014). "Reduced polyphenol oxidase gene expression and enzymatic browning in potato (Solanum tuberosum L.) with artificial microRNAs." BMC Plant Biol 14.

Chua, L. S., N. Abd Rahman, et al. (2014). "Plant protein extraction and identification from *Eurycoma longifolia* by gel electrophoresis and mass spectrometry." Curr Proteomics 11(3): 161-170.

Cimini, A., O. Marconi, et al. (2014). "Novel procedure for lager beer clarification and stabilization using sequential enzymatic, centrifugal, regenerable PVPP and crossflow microfiltration processing." Food Bioprocess Technol 7(11): 3156-3165.

Cominelli, E., G. Gusmaroli, et al. (2008). "Expression analysis of anthocyanin regulatory genes in response to different light qualities in *Arabidopsis thaliana*." J Plant Physiol 165: 886-894.

Conner, P. J. and D. MacLean (2013). "Fruit Anthocyanin Profile and Berry Color of Muscadine Grape Cultivars and Muscadinia Germplasm." Hortscience 48(10): 1235-1240.

Delcambre, A. and C. Saucier (2012). "Identification of new flavan-3-ol monoglycosides by UHPLC-ESI-Q-TOF in grapes and wine." Journal of Mass Spectrometry 47(6): 727-736.

Dewick, P. M. (1988). Isoflavonoids. The Flavonoids: Advances in Research Since 1980. J. B. Harborne. London, Chapman and Hall. 5: 125-209.

Dixon, R. A., D. Y. Xie, et al. (2005). "Proanthocyanidins - a final frontier in flavonoid research?" New Phytologist 165(1): 9-28.

Es-Safi, N. E., L. Kerhoas, et al. (2005). "Application of positive and negative electrospray ionization, collision-induced dissociation and tandem mass spectrometry to a study of the fragmentation of 6-hydroxyluteolin 7-O-glucoside and 7-O-glucosyl-(l -> 3)-glucoside." Rapid Commun Mass Spectrom. 19(19): 2734-2742.

Esaka, Y., N. Okumura, et al. (2003). "Electrophoretic analysis of quinone anion radicals in acetonitrile solutions using an on-line radical generator." Electrophoresis 24(10): 1635-1640.

Ferreyra, M. L. F., S. P. Rius, et al. (2012). "Flavonoids: biosynthesis, biological functions, and biotechnological applications." Front Plant Sci 3.

Flores, M., R. A. Isaacson, et al. (2003). "Probing hydrogen bonding to quinone anion radicals by H-1 and H-2 ENDOR spectroscopy at 35 GHz." Chem Phys 294(3): 401-413.

Geng, P., J. H. Sun, et al. (2009). "An investigation of the fragmentation differences of isomeric flavonol-O-glycosides under different collision-induced dissociation based mass spectrometry." Rapid Commun Mass Spectrom 23(10): 1519-1524.

Goldy, R. G., W. E. Ballinger, et al. (1986). "Fruit anthocyanin content of some Euvitis x *Vitis rotundifolia* hybrids." J Am Soc Hortic Sci 111(6): 955-960.

Goldy, R. G., W. E. Ballinger, et al. (1987). "Anthocyanin content of fruit, stem, tendril, leaf, and leaf petioles in muscadine grape." J Am Soc Hortic Sci 112(5): 880-882.

Goldy, R. G., E. P. Maness, et al. (1989). "Pigment quantity and quality characteristics of some native *Vitis rotundifolia* Michx." Am J Enol Vitic 40(4): 253-258.

Goodfriend, L., L. Perelmutter, et al. (1965). "Use of DEAE-Sephadex for fractionation of allergic serum." Nature 205(4972): 718-719.

Gourineni, V., N. F. Shay, et al. (2012). "Muscadine grape (*Vitis rotundifolia*) and wine phytochemicals prevented obesity-associated metabolic complications in C57BL/6J Mice." J Agric Food Chem 60(31): 7674-7681.

Gourineni, V., N. F. Shay, et al. (2012). "Muscadine Grape (Vitis rotundifolia) and Wine Phytochemicals Prevented Obesity-Associated Metabolic Complications in C57BL/6J Mice." Journal of Agricultural and Food Chemistry 60(31): 7674-7681.

Gu, L. W., M. A. Kelm, et al. (2003). "Liquid chromatographic/electrospray ionization mass spectrometric studies of proanthocyanidins in foods." Journal of Mass Spectrometry 38(12): 1272-1280.

Harborne, J. B. (1999). "The comparative biochemistry of phytoalexin induction in plants." Biochem Syst Ecol 27(4): 335-367.

Harborne, J. B. and R. J. Grayer (1988). The Anthocyanins. The Flavonoids: advances in research since 1980. J. B. Harborne. London, Chapman and Hall Ltd: 1-20.

Havelund, J. F., J. J. Thelen, et al. (2013). "Biochemistry, proteomics, and phosphoproteomics of plant mitochondria from non-photosynthetic cells." Front Plant Sci 4.

He, C. F. and Y. M. Wang (2008). "Protein extraction from leaves of *Aloe vera* L., a succulent and recalcitrant plant, for proteomic analysis." Plant Mol Biol Rep 26(4): 292-300.

He, X., Y. Li, et al. (2017). "Metabolic engineering of anthocyanins in dark tobacco varieties" Physiol Plant 159: 2-12.

Hiwada, K., H. Akutsu, et al. (1966). "Separation of plasma angiotensinases by DEAE-Sephadex A-50 column chromatography." Clin Chim Acta 14(3): 410-411.

Hsu, J.-C. and D. A. Heatherbell (1987). "Isolation and characterization of soluble proteins in grapes, grape juice, and wine." Am J Enol Vitic 38(1): 6-10.

Hulme, A. C., J. D. Jones, et al. (1966). "Mitochondrial activity in apple fruits during development of fruit on tree." J Exp Bot 17(50): 135-+.

Hulme, A. C., J. D. Jones, et al. (1963). "Respiration climacteric in apple fruits." Proceedings of the Royal Society Series B-Biological Sciences 158(973): 514-535.

Hulme, A. C., J. D. Jones, et al. (1964). "Mitochondrial preparation from the fruit of the apple. 1. Preparation and general activity." Phytochemistry 3(2): 173-188.

Hulme, A. C. and L. S. C. Wooltorton (1962). "Separation of enzymes present in mitochondrial fraction from apple peel." Nature 196(4852): 388-&.

Ilboudo, O., I. Tapsoba, et al. (2012). "Targeting structural motifs of flavonoid diglycosides using collision-induced dissociation experiments on flavonoid/Pb2+ complexes." Eur J Mass Spectrom 18(5): 465-473.

Jennings, A. C. and W. B. Watt (1967). "Fractionation of plant material. I. Extraction of proteins and nucleic acids from plant tissues and isolation of protein fractions containing hydroxyproline from broad bean (Vicia faba L) leaves." J Sci Food Agric 18(11): 527-&.

Jiang, Z. J., M. Kumar, et al. (2017). "Development of an efficient protein extraction method compatible with LC-MS/MS for proteome mapping in two australian seagrasses *Zostera muelleri* and *Posidonia australis*." Front Plant Sci 8.

Jones, G. and X. H. Qian (1998). "Photochemistry of quinone-bridged amino acids. Intramolecular trapping of an excited charge-transfer state." J Phys Chem A 102(15): 2555-2560.

Jones, J. D., A. C. Hulme, et al. (1964). "Mitochondrial preparations from the fruit of the apple. 2. Oxidative phosphoration." Phytochemistry 3(2): 201-212.

Jonker, A. and P. Q. Yu (2017). "The Occurrence, Biosynthesis, and Molecular Structure of Proanthocyanidins and Their Effects on Legume Forage Protein Precipitation, Digestion and Absorption in the Ruminant Digestive Tract." Int J Mol Sci 18(5).

Khatun, S., M. Ashraduzzaman, et al. (2012). "Purification and characterization of peroxidase from *Moringa oleifera* L. leaves." Bioresources 7(3): 3237-3251.

Kurreck, H. and M. Huber (1995). "Model reactions for photosynthesis-photoinduced charge and energy-transfer between covalently-linked porphyrin and quinone units." Angew Chem-Int Edit 34(8): 849-866.

Lamikanra, O. (1989). "Anthocyanins of *Vitis rotundifolia* hybrid grapes." Food Chem 33(3): 225-237.

Leyko, W. and R. Gondko (1963). "Separation of hemoglobin and cytochrome C by electrophoresis and by chromatography on DEAE-sephadex." Biochimica Et Biophysica Acta 77(3): 500-&.

Li, H. J. and M. L. Deinzer (2007). "Tandem mass spectrometry for sequencing proanthocyanidins." Analytical Chemistry 79(4): 1739-1748.

Lledias, F., F. Hernandez, et al. (2017). "A rapid and reliable method for total protein extraction from succulent plants for proteomic analysis." Protein J 36(4): 308-321.

Loomis, W. D. (1969). Removal of phenolic compounds during the isolation of plant enzymes. Methods in Enzymology, Academic Press. 13: 555-563.

Loomis, W. D. (1974). Overcoming problems of phenolics and quinones in the isolation of plant enzymes and organelles. Methods in Enzymology, Academic Press. 31: 528-544.

Loomis, W. D. and J. Battaile (1966). "Plant phenolic compounds and the isolation of plant enzymes." Phytochemistry 5(3): 423-438.

Lugg, J. W. H. (1939). "The representativeness of extracted samples and the efficiency of extraction of protein from the fresh leaves of plants; and some partial analyses of the whole proteins of leaves." Biochem J. 33: 110-122.

Lugg, J. W. H. and R. A. Weller (1944). "Large-scale extraction of protein samples reasonably representative of the whole proteins in the leaves of some plants: The amide, tyrosine, tryptophan, cystine (plus cysteine) and methionine contents of the preparations." Biochem J 38: 408-411.

Luttge, U. and R. Ratajczak (1997). The physiology, biochemistry and molecular biology of the plant vacuolar ATPase. Advances in Botanical Research Incorporating Advances in Plant Pathology, Vol 25: The Plant Vacuole. R. A. Leigh and D. Sanders. San Diego, Elsevier Academic Press Inc. 25: 253-296.

Mathews, H., S. K. Clendennen, et al. (2003). "Activation tagging in tomato identifies a transcriptional regulator of anthocyanin biosynthesis, modification, and transport." Plant Cell 15(8): 1689-1703.

Matus, J. T., R. Loyola, et al. (2009). "Post-veraison sunlight exposure induces MYB-mediated transcriptional regulation of anthocyanin and flavonol synthesis in berry skins of *Vitis vinifera*." J Exp Bot 60(3): 853-867.

Mayer, A. M. and E. Harel (1979). "Polyphenol oxidases in plants." Phytochemistry 18(2): 193-215.

McCown, B. H., G. E. Beck, et al. (1968). "Plant leaf and stem proteins. I. Extraction and electrophoretic separation of basic water-soluble fraction." Plant Physiol 43(4): 578-&.

Mohammad, M., S. Rauf, et al. (2013). "Kinetic studies on hydrogen bonding in quinone anion radical and the dianion of tetramethyl-1,4-benzoquinone." J Chem Soc Pak 35(3): 654-658.

Mortensen, J. A. (2001). Cultivars. Muscadine Grapes. F. M. Basiounny and D. G. Himelrick. Alexandria VA, ASHS Press: 91-105.

Nanda, C. L., A. C. Kondos, et al. (1975). "Improved technique for plant protein extraction." J Sci Food Agric 26(12): 1917-1924.

Nelsen, S. F., M. N. Weaver, et al. (2007). "Charge localization in a 17-bond mixed-valence quinone radical anion." J Phys Chem A 111(43): 10993-10997.

Nesbitt, W. B., E. P. Maness, et al. (1974). "Relationship of Anthocyanins of Black Muscadine Grapes (Vitis-Rotundifolia Michx) to Wine Color." American Journal of Enology and Viticulture 25(1): 30-32.

Nesbitt, W. B., E. P. Maness, et al. (1974). "Relationship of anthocyanins of black muscadine grapes (*Vitis rotundifolia* Michx) to wine color." Am J Enol Vitic 25(1): 30-32.

Nieman, R. H., D. L. Pap, et al. (1978). "Rapid purification of plant nucleotide extracts with xad-2, polyvinylpolypyrrolidone and charcoal." J Chromatogr A 161(Supplement C): 137-146.

Olien, W. C. (2001). Introduction to the Muscadines. Muacadine Grapes. F. M. Basiouny and D. G. Himelrick. Alexandria, VA, ASHA Press: 1-13.

Parkhey, S., V. Chandrakar, et al. (2015). "Efficient extraction of proteins from recalcitrant plant tissue for subsequent analysis by two-dimensional gel electrophoresis." J Sep Sci 38(20): 3622-3628.

Peng, Q. Z., Y. Zhu, et al. (2012). "An integrated approach to demonstrating the ANR pathway of proanthocyanidin biosynthesis in plants." Planta 236(3): 901-918.

Petrussa, E., E. Braidot, et al. (2013). "Plant Flavonoids-Biosynthesis, Transport and Involvement in Stress Responses." Int J Mol Sci 14(7): 14950-14973.

Pierpoint, W. S. (1996). The extraction of enzymes from plant tissues rich in phenolic compounds. Protein Purification Protocols. S. Doonan. Totowa, NJ, Humana Press: 69-80.

Porter, L. J. (1988). Flavans and Proanthocyanidins. The Flavonoids. J. B. Harborne. London, Chapman and Hall: 21-62.

Queiroz, C., M. L. M. Lopes, et al. (2008). "Polyphenol oxidase: Characteristics and mechanisms of browning control." Food Rev Int 24(4): 361-375.

Quideau, S., D. Deffieux, et al. (2011). "Plant Polyphenols: Chemical Properties, Biological Activities, and Synthesis." Angewandte Chemie-International Edition 50(3): 586-621.

Rene, A. and D. H. Evans (2012). "Electrochemical reduction of some o-quinone anion radicals: Why Is the current intensity so small?" J Phys Chem C 116(27): 14454-14460.

Rinyu, L., L. Nagy, et al. (2001). "The role of the electronic structure of quinones in the charge stabilization in photosynthetic reaction centers." J Mol Struct-THEOCHEM 571: 163-170.

Rodriguez, P. E. A. and F. A. Cumar (1990). "Gangliosides noncovalently bound to DEAE-Sephadex - Application to purification of antiganglioside antibodies." Anal Biochem 188(1): 48-52.

Rowan, D. D., M. Cao, et al. (2009). "Environmental regulation of leaf colour in red 35S:PAP1 *Arabidopsis thaliana*." New Phytol 182(1): 102-115.

Saini, R., N. Kaur, et al. (2014). "Quinones based molecular receptors for recognition of anions and metal ions." Tetrahedron 70(29): 4285-4307.

Sandhu, A. K. and L. W. Gu (2010). "Antioxidant Capacity, Phenolic Content, and Profiling of Phenolic Compounds in the Seeds, Skin, and Pulp of Vitis rotundifolia (Muscadine Grapes) As Determined by HPLC-DAD-ESI-MSn." Journal of Agricultural and Food Chemistry 58(8): 4681-4692.

Sari, Y. W., W. J. Mulder, et al. (2015). "Towards plant protein refinery: Review on protein extraction using alkali and potential enzymatic assistance." Biotechnol J 10(8): 1138-1157.

Schmidt, M. (1962). "Fractionation of acid mucopolysaccharides on DEAE-sephadex anion exchanger." Biochimica Et Biophysica Acta 63(2): 346-&.

Shao, Y. F. and J. S. Bao (2015). "Polyphenols in whole rice grain: Genetic diversity and health benefits." Food Chem 180: 86-97.

Shi, M.-Z. and D.-Y. Xie (2010). "Features of anthocyanin biosynthesis in *pap1-D* and wild-type *Arabidopsis* thaliana plants grown in different light intensity and culture media conditions." Planta 231: 1385-1400.

Shinbuehring, Y. S., M. Drefers, et al. (1978). "Separation of acid and neutral alpha-glucosidase isoenzymes from fetal and adult tissues, cultivated fibroblasts and amniotic-fluid cells by DEAE-Cellulose and Sephadex G-100 column chromatography." Clin Chim Acta 89(3): 393-404.

Sinnecker, S., E. Reijerse, et al. (2004). "Hydrogen bond geometries from electron paramagnetic resonance and electron-nuclear double resonance parameters: Density functional study of quinone radical anion-solvent interactions." J Am Chem Soc 126(10): 3280-3290.

Sisler, E. C. and H. J. Evans (1958). "Comparison of chlorogenic acid and catechol as substrates for the polyphenol oxidase from tobacco and mushroom." Plant Physiol 33: 255-257.

Spranger, I., B. Sun, et al. (2008). "Chemical characterization and antioxidant activities of oligomeric and polymeric procyanidin fractions from grape seeds." Food Chem 108(2): 519-532.

Striegler, R. K., P. M. Carter, et al. (2005). "Yield, quality, and nutraceutical potential of selected muscadine cultivars grown in southwestern Arkansas." Horttechnology 15(2): 276-284.

Sullivan, M. L. (2015). "Beyond brown: polyphenol oxidases as enzymes of plant specialized metabolism." Front Plant Sci 5.

Taiz, L. and E. Zeiger (2010). Plant Physiology. Sunderland, MA, Sinauer Associates, Incorporated.

Taranto, F., A. Pasqualone, et al. (2017). "Polyphenol oxidases in crops: Biochemical, physiological and genetic aspects." Int J Mol Sci 18(2).

Tohge, T., Y. Nishiyama, et al. (2005). "Functional genomics by integrated analysis of metabolome and transcriptome of Arabidopsis plants over-expressing an MYB transcription factor." Plant Journal 42(2): 218-235.

Toth, G. B. and H. Pavia (2001). "Removal of dissolved brown algal phlorotannins using insoluble polyvinylpolypyrrolidone (PVPP)." J Chem Ecol 27(9): 1899-1910.

Tsuji, T., T. Mori, et al. (1985). "Solvent-extraction of plant pigments from leave protein-concentrate." J Chem Eng Jpn 18(6): 539-544.

Wang, W., F. J. Tai, et al. (2008). "Optimizing protein extraction from plant tissues for enhanced proteomics analysis." J Sep Sci 31(11): 2032-2039.

Wang, X., H. R. Tong, et al. (2010). "Chemical characterization and antioxidant evaluation of muscadine grape pomace extract." Food Chem 123(4): 1156-1162.

Wei, Z., J. M. Luo, et al. (2017). "Profile of Polyphenol Compounds of Five Muscadine Grapes Cultivated in the United States and in Newly Adapted Locations in China." Int J Mol Sci 18(3).

Weigel, D., J. H. Ahn, et al. (2000). "Activation tagging in Arabidopsis." Plant Physiology 122(4): 1003-1013.

Welch, C. R., Q. L. Wu, et al. (2008). "Recent advances in anthocyanin analysis and characterization." Current Analytical Chemistry 4(2): 75-101.

Wu, X. L., E. H. Xiong, et al. (2014). "Universal sample preparation method integrating trichloroacetic acid/acetone precipitation with phenol extraction for crop proteomic analysis." Nat Protoc 9(2): 362-374.

Xie, D. Y. and R. A. Dixon (2005). "Proanthocyanidin biosynthesis - still more questions than answers?" Phytochemistry 66(18): 2127-2144.

Xie, D. Y., S. B. Sharma, et al. (2006). "Metabolic engineering of proanthocyanidins through co-expression of anthocyanidin reductase and the PAP1 MYB transcription factor." Plant Journal 45(6): 895-907.

Yang, W. Z., M. Ye, et al. (2012). "Collision-induced dissociation of 40 flavonoid aglycones and differentiation of the common flavonoid subtypes using electrospray ionization ion-trap tandem mass spectrometry and quadrupole time-of-flight mass spectrometry." Eur J Mass Spectrom 18(6): 493-503.

Yoruk, R. and M. R. Marshall (2003). "Physicochemical properties and function of plant polyphenol oxidase: A review." J Food Biochem 27(5): 361-422.

You, Q., F. Chen, et al. (2012). "High-performance liquid chromatography-mass spectrometry and evaporative light-scattering detector to compare phenolic profiles of muscadine grapes." J Chromatogr A 1240: 96-103.

You, Q., F. Chen, et al. (2012). "High-performance liquid chromatography-mass spectrometry and evaporative light-scattering detector to compare phenolic profiles of muscadine grapes." Journal of Chromatography A 1240: 96-103.

You, Q., F. Chen, et al. (2011). "Inhibitory effects of muscadine anthocyanins on alpha-glucosidase and pancreatic lipase activities." J Agric Food Chem 59(17): 9506-9511.

You, Q., F. Chen, et al. (2012). "Analysis of Phenolic Composition of Noble Muscadine (Vitis rotundifolia) by HPLC-MS and the Relationship to Its Antioxidant Capacity." J Food Sci 77(10): C1115-C1123.

Zhang, S. T., L. X. Li, et al. (2017). "Preparative high-speed counter-current chromatography separation of grape seed proanthocyanidins according to degree of polymerization." Food Chem 219: 399-407.

Zhou, L.-L., H.-N. Zeng, et al. (2008). "Development of tobacco callus cultures over expressing *Arabidopsis* PAP1/MYB75 transcription factor and characterization of anthocyanin biosynthesis " Planta 229: 37-51.

Zhou, L. L., H. N. Zeng, et al. (2008). "Development of tobacco callus cultures over expressing Arabidopsis PAP1/MYB75 transcription factor and characterization of anthocyanin biosynthesis." Planta 229(1): 37-51.

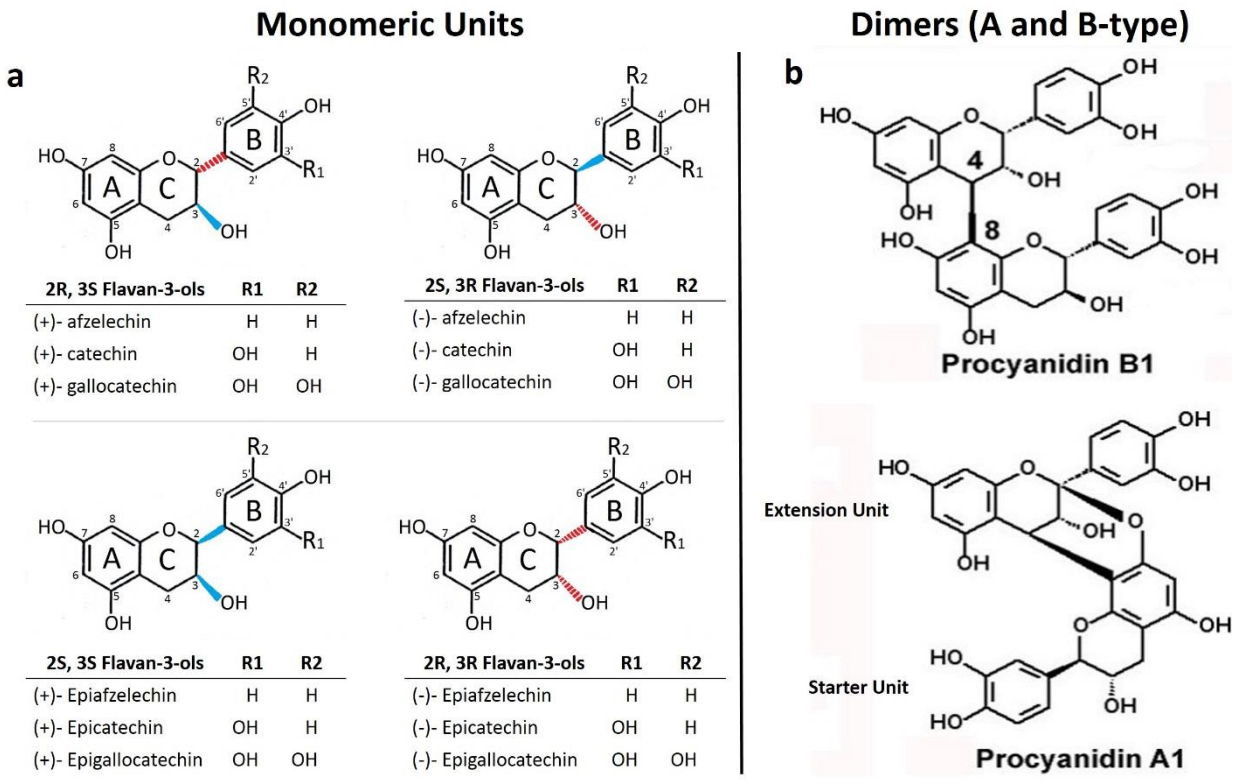

Figure 3.1: Overview of flavan-3-ols (monomers) and dimeric types of proanthocyanidins in grape seed and skins (not grape flesh). (**a**) Four different monomeric units: (+)-catechin, (-)-epicatechin, (-)-epigallocatechin, and (-)-epicatechin 3-*O*-gallate; (**b**) two dimeric oligomers of flavan-3-ols; A-type and B-type procyanidins.

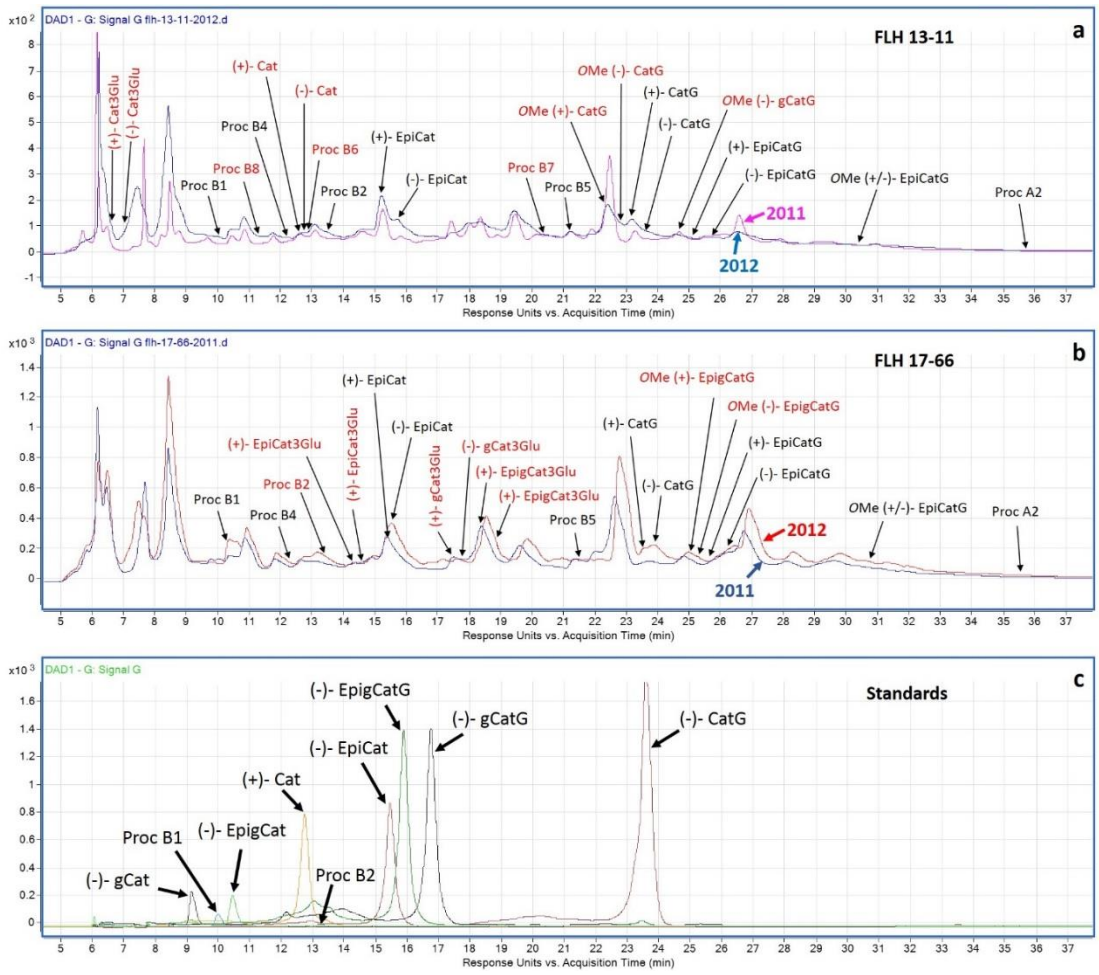

Figure 3.2: **Chromatographic profiles of flavan-3-ols and dimeric types of proanthocyanidin profiles in berries grown in 2011 and 2012.** (**a**) Chromatograms showing peaks annotated to be flavan-3-ols and dimeric proanthocyanidins in berries of FLH 13-11 from 2011 and 2012 cropping years; (**b**) Chromatograms showing peaks annotated to be flavan 3-ols and dimeric proanthocyanidin profiles in berries of FLH 17-66 from 2011 and 2012 cropping years; (**c**) Chromatograms of nine standards including five flavan-3-ol aglycones, two conjugates, and two dimeric proanthocyanidin standards (procyanidin B1 and B2). Compounds detected only in one variety and both varieities were highlighted with red and black color, respectively. Standards: (+)-catechin, (-)-epicatechin, (-)-gallocatechin, (-)-epigallocatechin, (-)-catechin gallate, (-)-epigallocatechin gallate, (-)-gallocatechin gallate, procyanidin B1, and procyanidin B2. Abbreviation, Cat: catechin, EpiCat: epicatechin, Glu: glucoside, G: gallate, g: galloyl, Proc: procyanidin. Me: methylated

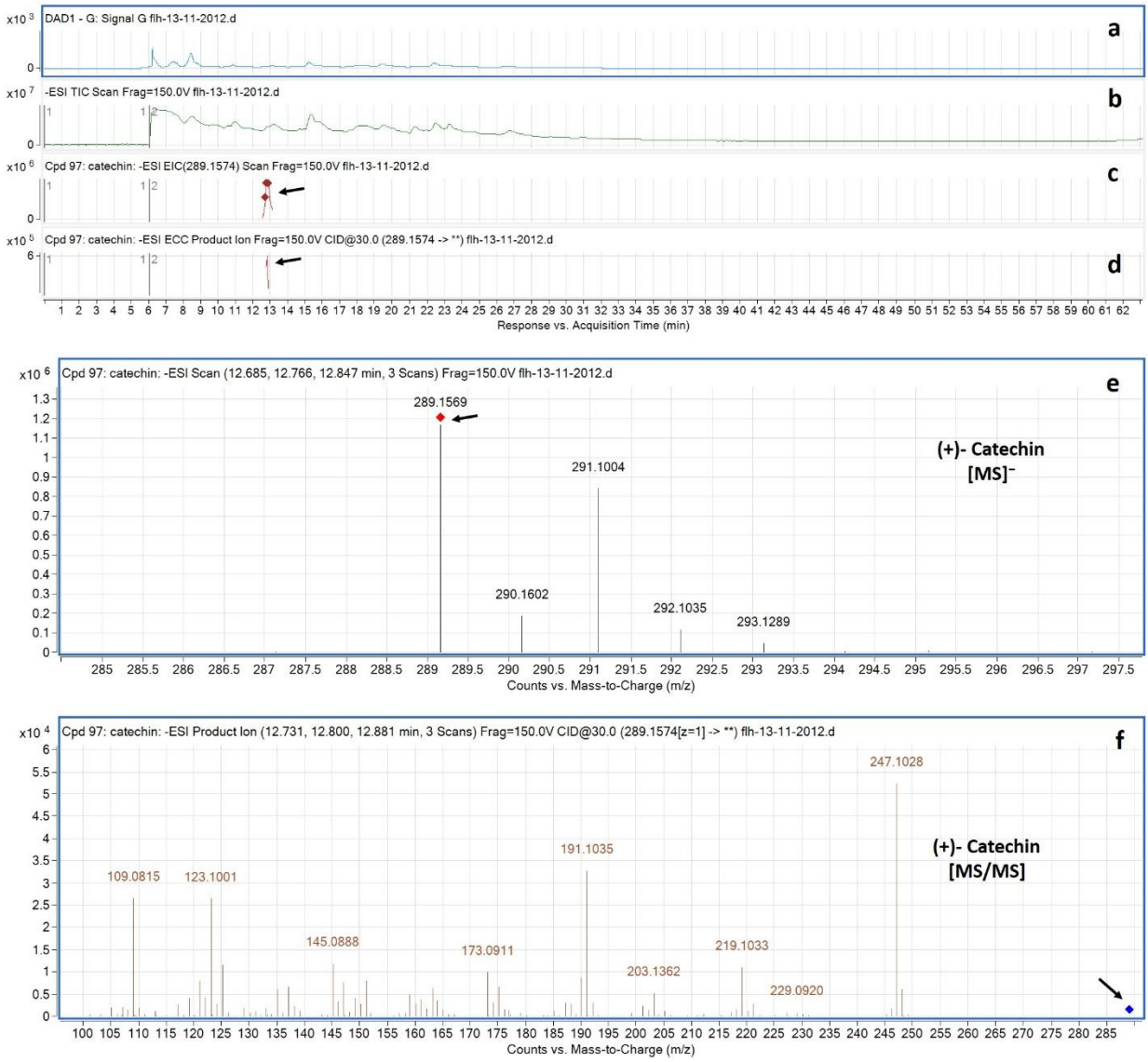

Figure 3.3: Extracted ion chromatogram (EIC) of primary mass spectrum (MS1) and m/z features of secondary ion fragments (MS2) derived from HPLC-qTOF--MS/MS annotate this peak to be (+)- catechin, (MW, 290.26). (**a**) Chromatogram of FLH 13-11extract (2012) recorded at 280 nm; (**b**) Total ion chromatogram of FLH 13-11 extract (2012); (**c**) EIC of primary ion 289.1574 [M-H] $[m/z]^{-}$; (**d**) Enhanced charge capacity (ECC) ion product for 289.1574 $[m/z]^{-}$; (**e**) A MS profile showing an extracted m/z value, 289.1569 $[m/z]^{-}$; (**f**) Fragments from collision-induced dissociation (CID) of 289.1569 showing 109.0815, 123.1001, 137.0823, 151.1007, and 247.1028 $[m/z]^{-}$ (Table 1).

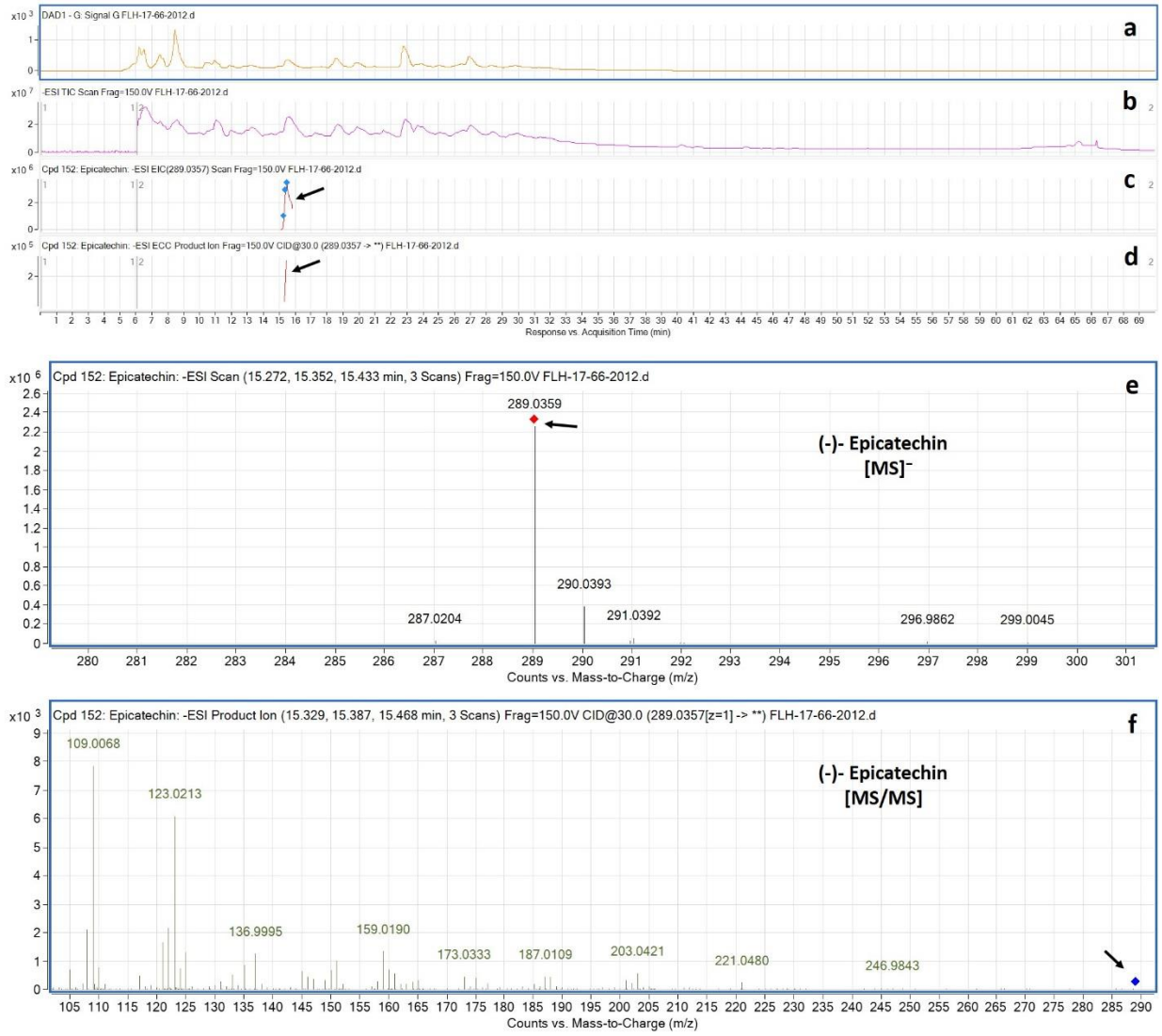

Figure 3.4: Extracted ion chromatogram (EIC) of primary mass spectrum (MS1) and m/z features of secondary ion fragments (MS2) derived from LC-MC/MS annotate this peak to be (-)- Epicatechin, (MW, 290.26). (**a**) Chromatogram of FLH 17-66 extract (2012) recorded at 280 nm; (**b**) Total ion chromatogram of FLH 17-66 extract (2012); (**c**) EIC of primary ion 289.0357 [M-H] $[m/z]^{-}$; (**d**) Enhanced charge capacity (ECC) ion product for 289.0357 $[m/z]^{-}$; (**e**) A MS profile showing an extracted m/z value, 289.0359 $[m/z]^{-}$; (**f**) Fragments from collision-induced dissociation (CID) of 289.0359 showing 109.0068, 123.0213, 136.9995, 151.0132, and 246.9843 $[m/z]^{-}$ (Table 1).

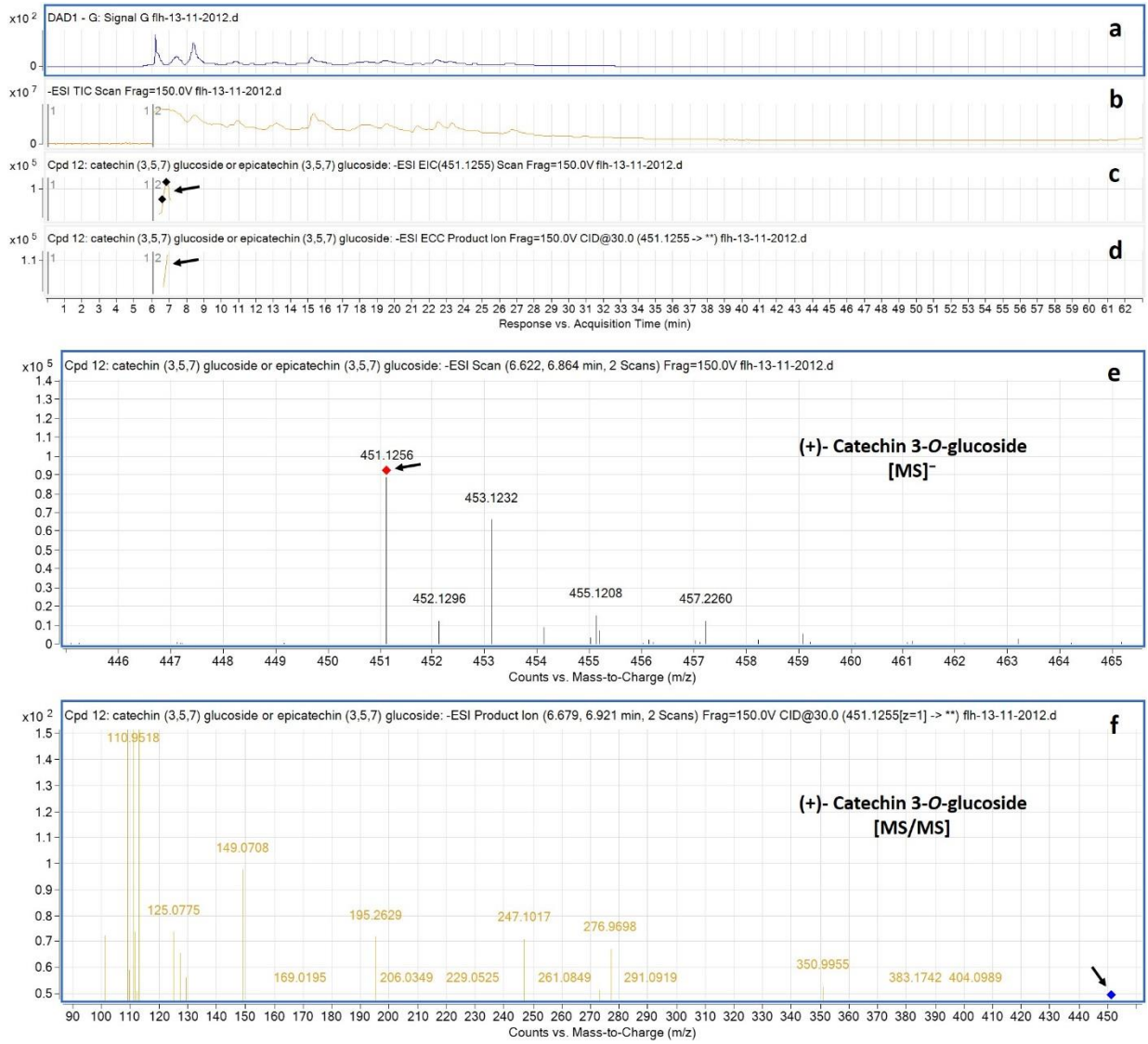

Figure 3.5: Extracted ion chromatogram (EIC) of primary mass spectrum (MS1) and m/z features of secondary ion fragments (MS2) derived from LC-MC/MS annotate this peak to be (+)- Catechin 3-*O*-glucoside, (MW, 452.41). (**a**) Chromatogram of FLH 13-11 extracts (2012) recorded at 280 nm; (**b**) Total ion chromatogram of FLH 13-11 extracts (2012); (**c**) EIC of primary ion 451.1255 [M-H] $[m/z]^{-}$; (**d**) Enhanced charge capacity (ECC) ion product for 451.1255 $[m/z]^{-}$; (**e**) A MS profile showing an extracted m/z value, 451.1256 $[m/z]^{-}$; (**f**) Fragments from collision-induced dissociation (CID) of 451.1256 showing 109.0471, 110.9518, 125.0775, 149.0708- 169.0195, and 247.1017 $[m/z]^{-}$ (Table 1).

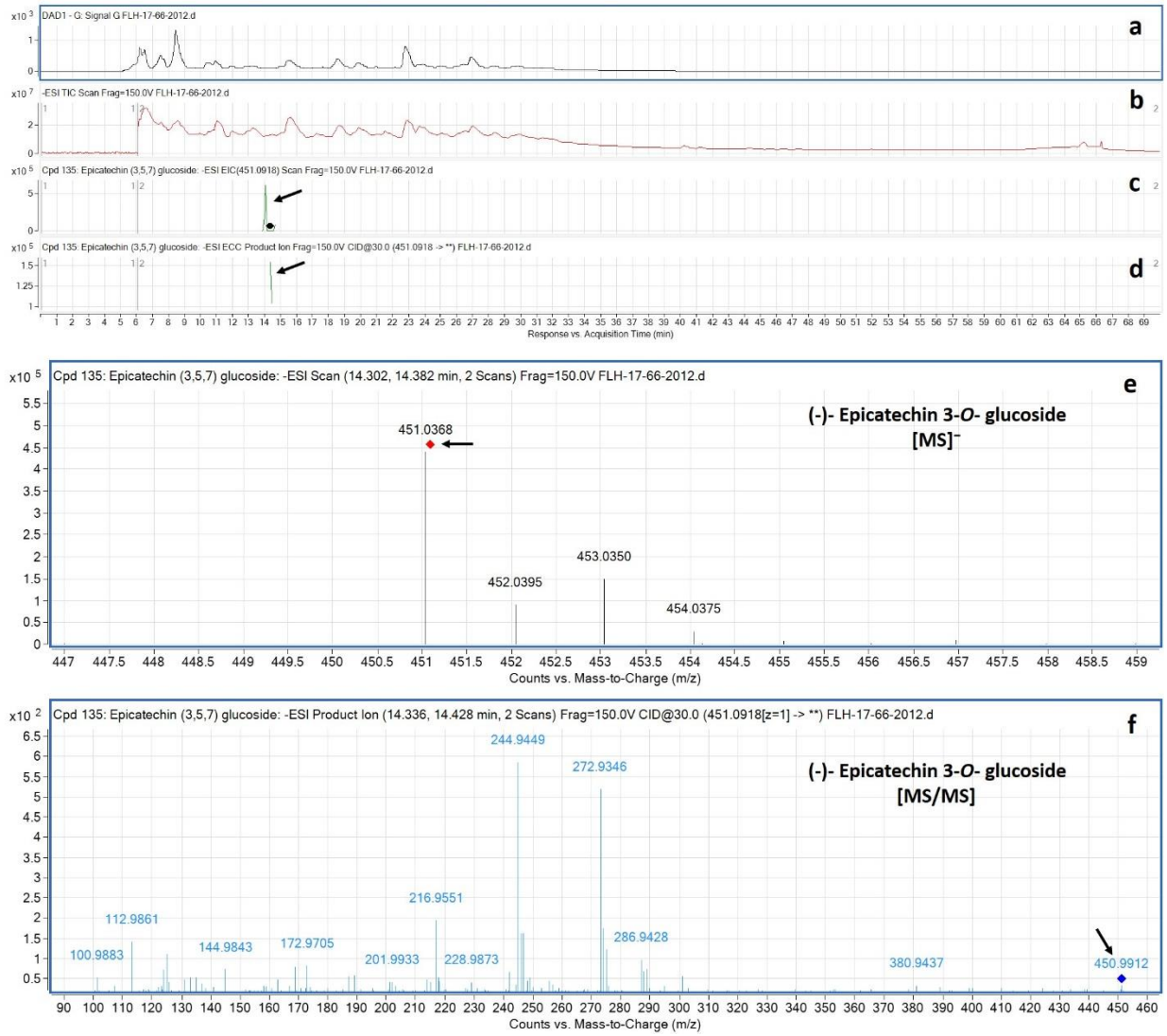

Figure 3.6: Extracted ion chromatogram (EIC) of primary mass spectrum (MS1) and m/z features of secondary ion fragments (MS2) derived from LC-MC/MS annotate this peak to be (-)- Epicatechin 3-*O*-glucoside, (MW, 452.41). (**a**) chromatogram of FLH 17-66 extracts (2012) recorded at 280 nm; (**b**) Total ion chromatogram of FLH 17-66 extract (2012); (**c**) EIC of primary ion 451.0918 [M-H] $[m/z]^{-}$; (**d**) Enhanced charge capacity (ECC) ion product for 451.0918 $[m/z]^{-}$; (**e**) A MS profile showing an extracted m/z value, 451.0368 $[m/z]^{-}$; (**f**) Fragments from collision-induced dissociation (CID) of 451.0368 showing 124.9861, 172.9705, 244.9449, 272.9346, 286.9428, and 300.9102 $[m/z]^{-}$ (Table 1).

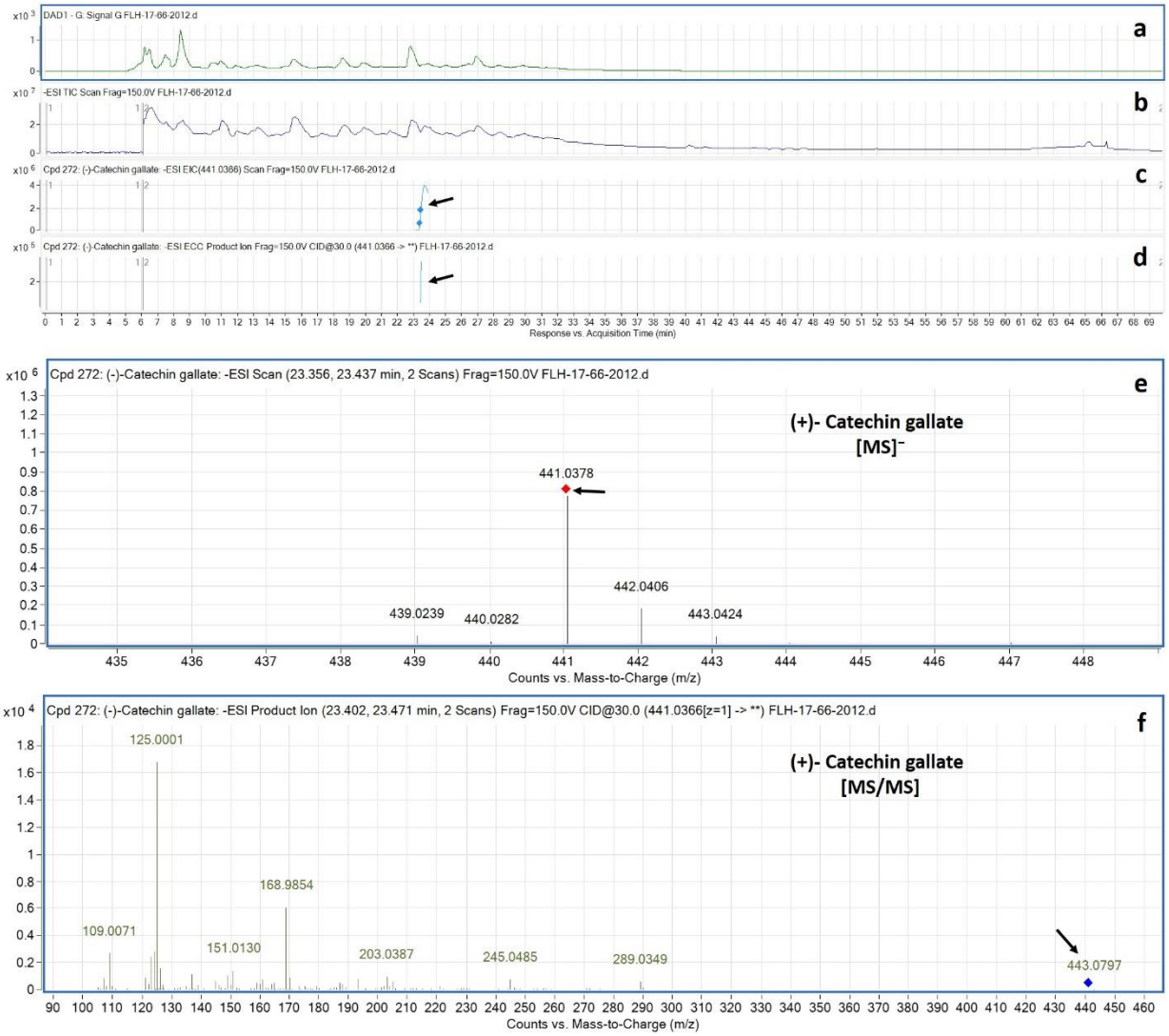

Figure 3.7: Extracted ion chromatogram (EIC) of primary mass spectrum (MS1) and m/z features of secondary ion fragments (MS2) derived from LC-MC/MS annotate this peak to be (+)- Catechin gallate, (MW, 442.37). (**a**) Chromatogram of FLH 17-66 extracts (2012) recorded at 280 nm absorbance; (**b**) Total ion chromatogram of FLH 17-66 extract (2012); (**c**) EIC of primary ion 441.0366 [M-H] $[m/z]^-$; (**d**) Enhanced charge capacity (ECC) ion product for 441.0366 $[m/z]^-$; (**e**) A MS profile showing an extracted m/z value, 441.0378 $[m/z]^-$; (**f**) Fragments from collision-induced dissociation (CID) of 441.0378 showing 109.0071, 125.0001, 136.9989, 151.0130, 179.0047, 245.0485, and 289.0349 $[m/z]^-$ (Table 1).

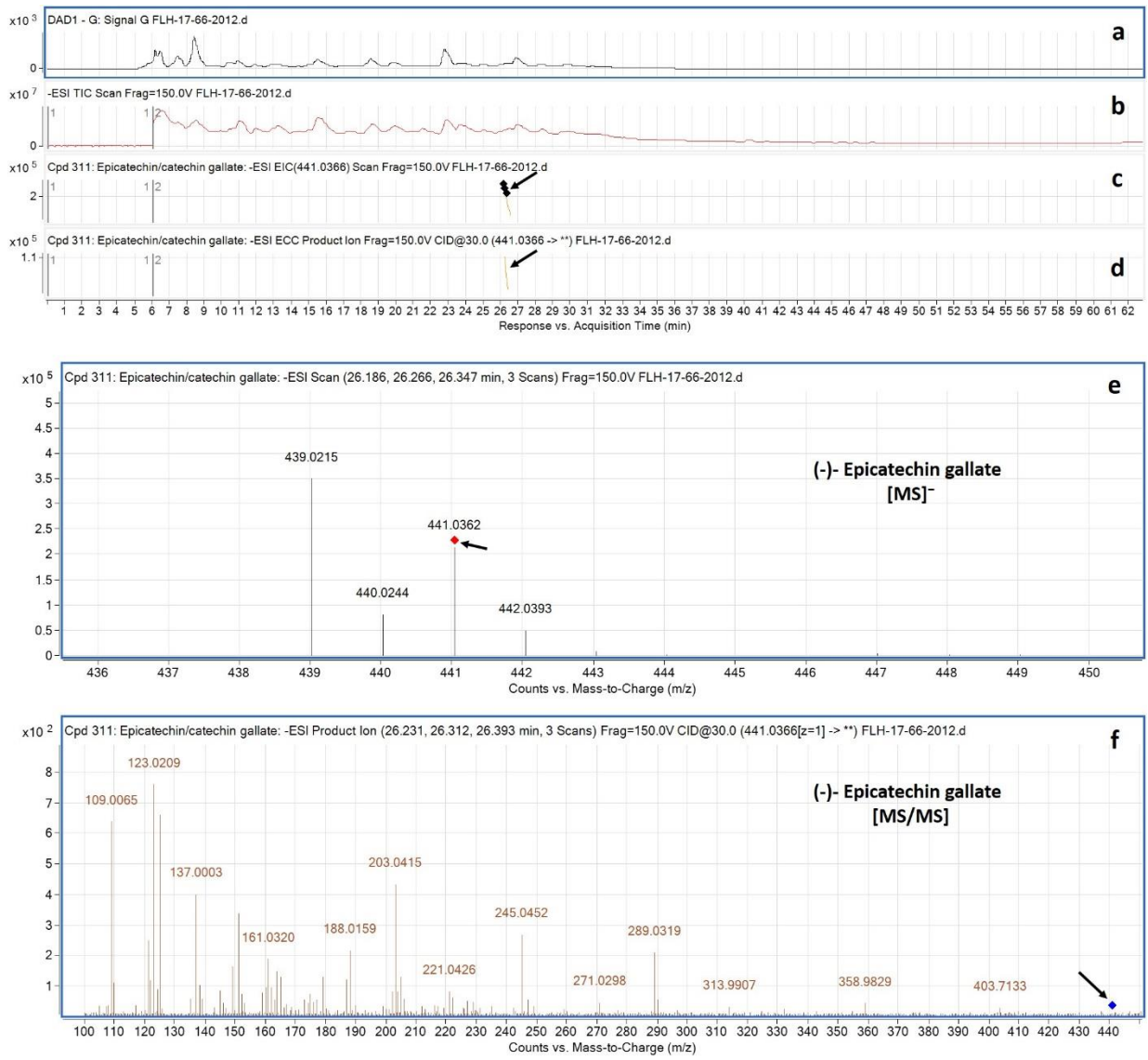

Figure 3.8: Extracted ion chromatogram (EIC) of primary mass spectrum (MS1) and m/z features of secondary ion fragments (MS2) derived from LC-MC/MS annotate this peak to be (-)- Epicatechin gallate, (MW, 442.37). (**a**) Chromatogram of FLH 17-66 extract (2012) recorded at 280 nm; (**b**) Total ion chromatogram of FLH 17-66 extract (2012); (**c**) EIC of primary ion 441.0366 [M-H] $[m/z]^{-}$; (**d**) Enhanced charge capacity (ECC) ion product for 441.0366 $[m/z]^{-}$; (**e**) A MS profile showing an extracted m/z value, 441.0362 $[m/z]^{-}$; (**f**) Fragments from collision-induced dissociation (CID) of 441.0362 showing 109.0065, 123.0209, 137.0003, 151.0112, 179.0064, 245.0452, 271.0298, 289.0319, 313.9907, 331.9910, 358.9829 $[m/z]^{-}$ (Table 1).

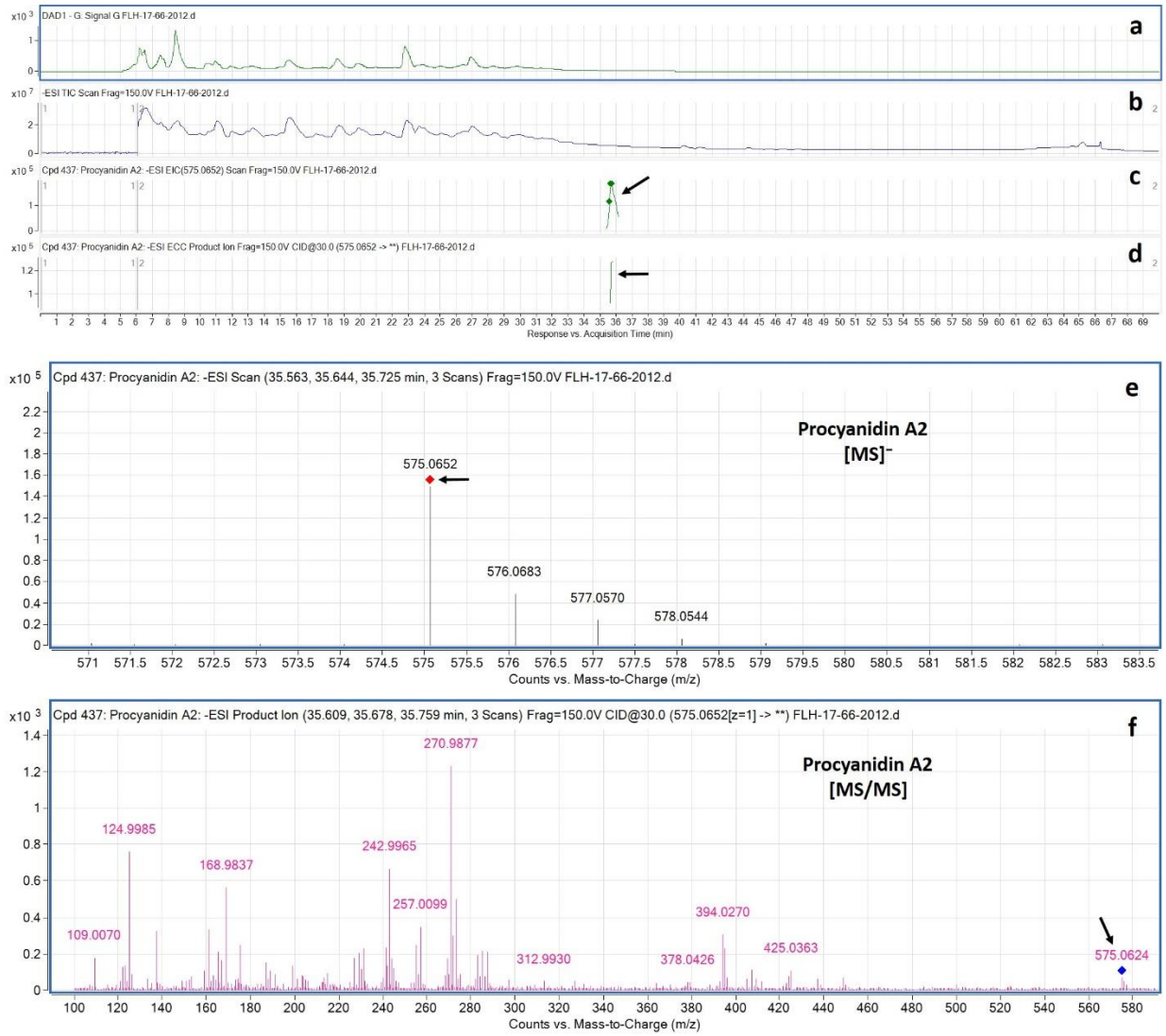

Figure 3.9: Extracted ion chromatogram (EIC) of primary mass spectrum (MS1) and m/z features of secondary ion fragments (MS2) derived from LC-MC/MS annotate this peak to be procyanidin A2, (MW, 576.51). (**a**) Chromatogram of FLH 17-66 extract (2012) recorded at 280 nm; (**b**) Total ion chromatogram of FLH 17-66 extract (2012); (**c**) EIC of primary ion 575.0652 [M-H] $[m/z]^{-}$; (**d**) Enhanced charge capacity (ECC) ion product for 575.0652 $[m/z]^{-}$; (**e**) A MS profile showing an extracted m/z value, 575.0652 $[m/z]^{-}$; (**f**) Fragments from collision-induced dissociation (CID) of 575.0652 showing 109.0070, 124.9985, 136.9988, 152.9935, 168.9837, 242.9965, 270.9877, 285.0011, 296.9985, 327.0119, and 425.0363- $[m/z]^{-}$ (Table 1).

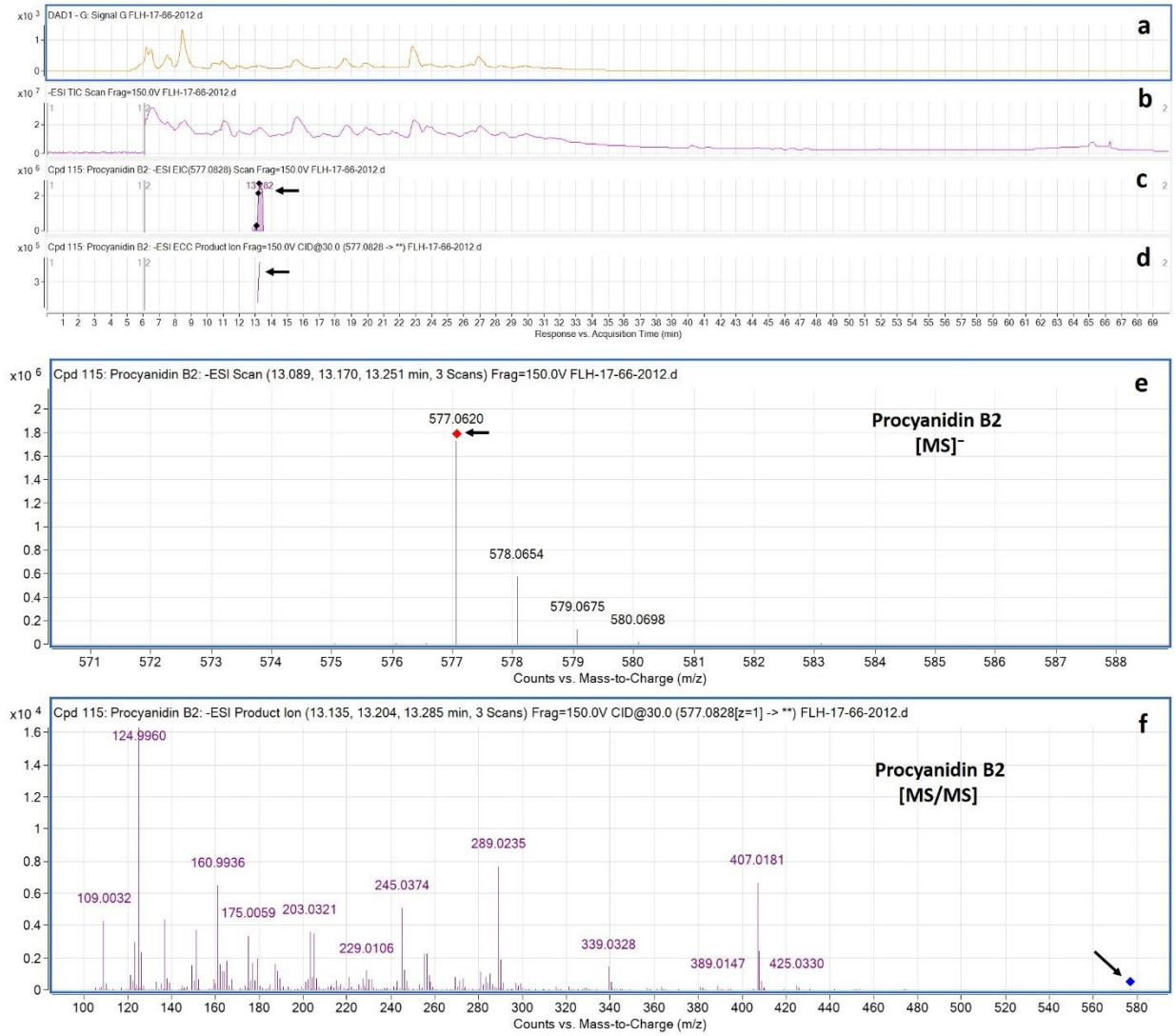

Figure 3.10: Extracted ion chromatogram (EIC) of primary mass spectrum (MS1) and m/z features of secondary ion fragments (MS2) derived from LC-MC/MS annotate this peak to be procyanidin B2, (MW, 578.52). (**a**) Chromatogram of FLH 17-66 extract (2012) recorded at 280 nm; (**b**) Total ion chromatogram of FLH 17-66 extract (2012); (**c**) EIC of primary ion 577.0828 [M-H] $[m/z]^{-}$; (**d**) Enhanced charge capacity (ECC) ion product for 577.0828 $[m/z]^{-}$; (**e**) A MS profile showing an extracted m/z value, 577.0620 $[m/z]^{-}$; (**f**) Fragments from collision-induced dissociation (CID) of 577.0620 showing 109.0032, 124.9960, 136.9946, 151.0073, 160.9936, 245.0374, 289.0235, 407.0181, and 425.0330 $[m/z]^{-}$ (Table 1).

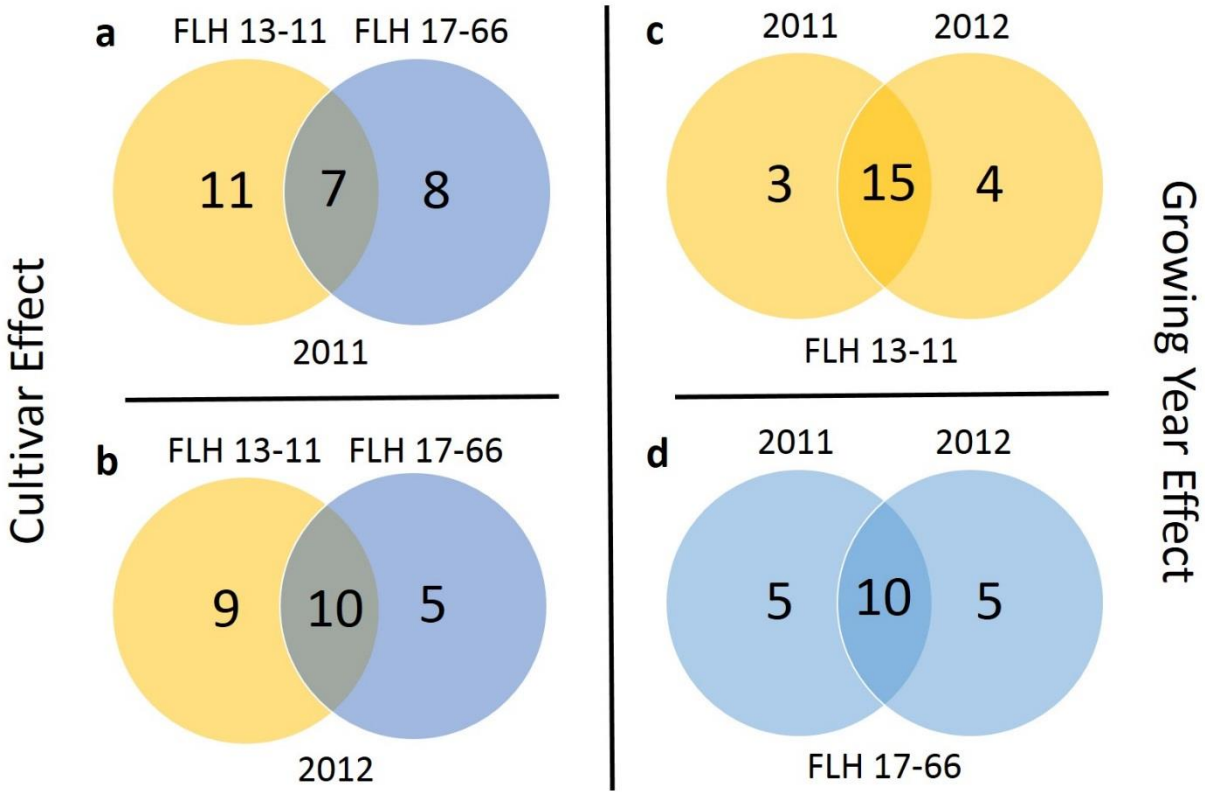

Figure 3.11: A Venn diagram showing effects of cultivars and cropping years on total 30 metabolite compositions. Arabic numerals are metabolites extracted from samples**.**

Table 3.1: Features of mass-to-charge ratios and MS fragmentation profiles generated from HPLC-qTOF-MS/MS of nine standards.

Standards	MW	RT (min)	$[MS]^-$ (m/z)	[MS/MS] (m/z)
(+)-Catechin	290.26	12.761	289.0558	**109.0140- 121.0136- 123.0289- 125.0089- 137.0078- 151.0230**- 159.0238- 187.0227- 203.0529- 212.0308- 221.0634- 245.0640
(-)-Epicatechin	290.27	15.619	289.0558	**109.0137- 121.0131- 123.0286- 125.0089- 137.0079- 151.0218**- 159.0276- 187.0225- 203.0532- 212.0306- 221.0627- 245.0619
(-)-Gallocatechin	306.27	9.166	305.0495	**109.0178- 121.0176- 123.0291- 125.0117- 137.0116- 151.0274- 159.0318- 167.0204**- 175.0250- 179.0199- 186.0174- 203.0183- 219.0500
(-)-Epigallocatechin	306.27	10.338	305.0518	**109.0152- 121.0157- 123.0273- 125.0097- 137.0096- 151.0257- 159.0288- 167.0191**- 175.0235- 179.0157- 189.0375- 203.0180- 219.0513
(-)-Catechin gallate	442.37	23.590	441.0686	**109.0153- 121.0145- 123.0298- 125.0095- 137.0092- 151.0245- 159.0293- 168.9982**- 175.0565- **179.0196**- 189.0382- 203.0543- 221.0658- 245.0653- **271.0450- 289.0552**
(-)-Epigallocatechin gallate	458.00	16.149	457.0565	**109.0146- 121.0144- 122.9944- 125.0088- 137.0081- 151.0229- 159.0277- 168.9973- 179.0193-** 192.9972- 204.0225- 221.0277- 244.0435- 269.0319- **287.0353- 305.0463**
(-)-Gallocatechin gallate	458.00	15.872	457.0577	**109.0152- 121.0145- 122.9962- 125.0097- 137.0087- 151.0233- 159.0286- 168.9982- 179.0194**- 189.0340- 203.0197- 221.0312- 245.0261- 269.0258- **287.0393- 305.0486**
Procyanidin B1	578.52	10.441	577.1225	**109.0138- 121.0139- 123.0284- 125.0081- 137.0077- 151.0232- 159.0269-** 161.0097- **163.0197- 179.0178- 189.0348**- 203.0529- **221.0645-** 245.0625- **271.0448- 287.0327- 289.0541- 299.0364**- 315.0697- 321.0582- 339.0693- 407.0601- **425.0709**
Procyanidin B2	578.52	13.674	577.1224	**109.0132- 121.0146- 123.0283- 125.0082- 137.0086- 151.0221- 159.0269-** 161.0093- **163.0232- 179.0196- 189.0369**- 203.0519- **221.0643**- 245.0621- **271.0435- 286.0298- 289.0535- 297.0203**- 315.0647- 339.0721- 407.0602- **425.0712**

Note: bold values mean highly rich fragments from collision induced dissociation.

Table 3.2: Flavan-3-ol aglycones detected in berries of two interspecific hybrid cultivars FLH 13-11 and FLH 17-66. (Note: "_" means undetected).

Compounds Detected	MW (g/mol)	Cultivar	Year of Harvest 2011	2012	Ret. Tim (min)	MS^- (m/z)	[MS/MS] (m/z) profiles	Figure #
(+)-Catechin	290.26	FLH 13-11	√	√	12.806	289.1574	**109.0815- 123.1001**- **137.0823**- 145.0888- **151.1007**- 163.1031- 173.0911- 191.1035- 203.1362- 219.1033- **247.1028**	Fig. 3
		FLH 17-66	–	–	–	–		
(-)-Catechin	290.26	FLH 13-11	√	√	12.872	289.1586	**109.0824- 123.1012**- **137.0835**- 145.0903- **151.1025**- 163.1047- 173.0926- 191.1046- 203.1395- 219.1048- 247.1045	S-Fig. 1
		FLH 17-66	–	–	–	–		
(+)-Epicatechin	290.27	FLH 13-11	√	√	15.029	289.1574	**109.0817- 123.1005- 137.0835- 151.1017**- 161.1221- 175.1292- 188.1158- 203.1425- 212.1182- 221.1558- 247.1014	S-Fig. 2
		FLH 17-66	√	–	15.277	289.0377	**109.0083- 123.0218**- **137.0031**- 148.9987- 159.0178- 173.0298- 191.0071- 202.0256- 221.0492- 245.0482	
(-)-Epicatechin	290.27	FLH 13-11	√	√	15.629	289.1574	**109.0819- 123.1007- 137.0831- 151.1016**- 159.1082- 175.1354- 187.1087- **203.1421**- 212.1219- 221.1560- 245.1602- 271.1448	Fig. 4
		FLH 17-66	√	√	15.398	289.0357	**109.0068- 123.0213- 136.9995- 151.0132**- 159.0190- 173.0333- 187.0109- 203.0421- 221.0480- 246.9843	

Table 3.3: Eighteen flavan-3-ol conjugates were detected in berries of two interspecific hybrid cultivars FLH 13-11 and FLH 17-66. Four commonly exist in the cultivars and 13 differentially occur in two of them and in growing seasons (Note: "_" means undetected)

Compounds Detected	MW (g/mol)	Cultivar	Year of Harvest 2011	2012	Ret. Tim (min)	$[MS]^-$ (m/z)	[MS/MS] (m/z) profiles	Figure #
(+)-Catechin 3-*O*-glucoside	452.41	FLH 13-11	–	√	6.8	451.1255	**101.0781- 108.9543- 109.0471- 110.9518- 112.9492- 125.0775- 149.0708**- 169.0195- **195.2629**- 206.0349- 229.0525- **247.1017- 276.9698**- 350.9955- 404.0989	Fig. 5
		FLH 17-66	–	–	–	–		
(-)-Catechin 3-*O*-glucoside	452.41	FLH 13-11	–	√	6.991	451.1255	**101.0752- 108.9545- 109.9014- 110.9520- 112.9487**- 132.8862- **149.0722**- 201.1385- 215.1058- **245.1000**- 263.1016- **273.0970**- 301.7091- 337.1560- **350.9861**- 393.1542- 408.0436	S-Fig. 3
		FLH 17-66	–	–	–	–		
(+)-Epicatechin 3-*O*-glucoside	452.41	FLH 13-11	–	–	–	–		S-Fig. 4
		FLH 17-66	√	√	14.185	451.0948	**100.9949- 112.9969- 124.9885**- 136.9909- 152.0334- 168.9777- **188.9751- 216.9631-** 229.9739- **246.9749**- 258.9704- **272.9450**- 287.9723- 300.9451- 343.9958- 391.0083	
(-)-Epicatechin 3-*O*-glucoside	452.41	FLH 13-11	–	–	–	–		Fig. 6
		FLH 17-66	–	√	14.382	451.0918	**100.9883**- **112.9861**- **124.9861-** 144.9843- 162.9523- 172.9705- **188.9668**- 201.9933- **216.9551**- 228.9873- **244.9449**- 255.4556- **272.9346-** 286.9428- 300.9102- 380.9437	
(+)-Catechin gallate	442.37	FLH 13-11	√	√	23.159	441.1883	**109.0819- 125.0805- 137.0829- 151.1012**- 161.1235- **169.0794**- 179.1017- 193.0835- **203.1424**- 221.1560- **245.1601**- 259.1415- 271.1424- **289.1571**- 303.1370- 331.1358-	Fig. 7
		FLH 17-66	√	√	23.436	441.0366	**109.0071- 125.0001**- 136.9989- 151.0130- 161.0310- **168.9854**- 179.0047- 192.9813- 203.0387- 211.0086- 221.0537- 245.0485- 256.0208- 289.0349	
(-)-Catechin gallate	442.37	FLH 13-11	√	√	23.795	441.1883	**109.0820- 125.0805- 137.0833- 151.1014**- 169.0795- 179.1017- 193.0838- **203.1422**- 221.1563- **245.1603**- 271.1434- **289.1570**- 303.1388- 331.1365	S-Fig. 5
		FLH 17-66	√	√	23.84	441.04	**109.0075- 125.0004-** 136.9990- 151.0140- 161.0307- **168.9855**- 187.0088- 203.0416- 221.0477- 245.0471- 259.0269- 271.0268- 289.0332	
(+)-Epicatechin gallate	442.37	FLH 13-11	–	√	25.094	441.1883	**109.0821- 125.0805- 137.0831- 151.1013- 169.0792**- 179.1019- 188.1141- 193.0832- **203.1421**- 209.1312- 221.1577- **245.1607**- 259.1414- 271.1441- **289.1568**- 303.1366	S-Fig. 6
		FLH 17-66	√	√	25.665	441.0366	**109.0070- 125.0005-137.0002**- 146.0097- **151.0127**- 163.0083- 188.0163- **203.0384**- 221.0529- 235.1838- **245.0512**- 265.3904- **289.0262**- 342.0549- 379.8921	
(-)-Epicatechin gallate	442.37	FLH 13-11	√	√	25.818	441.1892	**109.0836- 125.0810- 137.0830- 151.1038**- 164.0731- 179.1025- 187.1074- 195.0042- **203.1427**- 221.1591- **245.1588**- 254.1340- 275.1032- **289.1590**- 301.1176- 315.1329-	Fig. 8
		FLH 17-66	√	√	26.312	441.0366	**109.0065- 123.0209**- **137.0003**- 145.0019- **151.0112**- 161.0320- 179.0064- 188.0159- **203.0415**- 221.0426- 235.0150- **245.0452**- 258.9808- 271.0298- **289.0319**- 313.9907- 331.9910- 358.9829- 403.7133	
(+)-Gallocatechin 3-*O*-glucoside	468.00	FLH 13-11	–	–	–	–		S-Fig. 7
		FLH 17-66	√	–	17.476	467.9999	**106.9921- 125.0015-** 133.9739- 157.0012- **168.9887**- 179.0102- 200.9870- 228.9835- 246.9902- 274.9884- **300.9626-** 317.0175- 346.9813- 367.9021- 432.2409- 465.6268	
(-)-Gallocatechin 3-*O*-glucoside	468.00	FLH 13-11	–	–	–	–		S-Fig. 8
		FLH 17-66	√	–	17.656	467.9999	**106.9969- 125.0027**- 135.0205- **168.9884**- 184.9934- 210.9862- 228.9798- 250.0131- 274.9883- 283.9547- **300.9604**- 315.9707- 338.4035- 367.0427-	

Table 3.3: (continued).

(+)-Epigallocatechin 3-*O*-glucoside	468.00	FLH 13-11	–	–	–	–		S-Fig. 9
		FLH 17-66	√	√	18.234	467.9974	**106.9919- 124.9998**- 145.0057- 156.9997- **168.1867**- 184.9947- 200.9880- 228.9807- 244.9756- 256.9695- 274.9827- 290.9684- **300.9618**- 313.0098	
(-)-Epigallocatechin 3-*O*-glucoside	468.00	FLH 13-11	–	–	–	–		S-Fig. 10
		FLH 17-66	√	√	18.875	467.9974	**106.9919- 125.0000- 145.0007**- 159.0135- **168.9849**- 184.9949- 200.9831- 228.9837- 256.9720- 274.9860- **300.9609**- 313.0135- 340.0573- 465.0236	
O-Methylated (+)-Catechin gallate	456.00	FLH 13-11	√	√	22.362	455.3199	**101.0748- 113.0764- 125.0799- 131.0919-** 143.0946- **161.1074**- 169.0767- 189.0931- **217.0827**- 245.1269- **263.2316**- 274.0943- 283.1247- 291.0934- 301.0835- 311.6865- 329.1163- **340.0422**- 355.0671- 399.0656	S-Fig. 11
		FLH 17-66	–	–	–	–		
O-Methylated (-)-Catechin gallate	456.00	FLH 13-11	–	√	22.928	455.3199	**101.0749- 113.0780- 125.0801- 132.0988**- 143.0908- **161.1085**- 173.0920- 191.0647- **217.0746**- 247.0945- **263.2333**- 295.0561- 311.1188- **340.0548**- 355.0660- 375.2308- 399.0789	S-Fig. 12
		FLH 17-66	–	–	–	–		
O-Methylated (+/-)-Epicatechin gallate	456.00	FLH 13-11	√	√	30.36	455.2054	107.0648- 11.0601- **125.0799**- 139.1013- 149.0834- **169.0778**- 173.0796- 185.1217- **191.1028**- 202.1402- **217.0770**- 226.1377- 235.1698- 259.1825- **270.1331**- **285.1589- 303.1738**- 315.0628- 335.0702- 361.2071	S-Fig. 13
	456.00	FLH 17-66	–	√	30.839	455.0504	**106.9945- 124.9977- 136.9965**- **148.9984- 168.9866**- 177.0170- 183.0117- 196.8803- **202.0292**- 217.0550- 220.0302- **228.0043- 241.0177**- 253.9952- 269.0249- 274.9825- 285.0435- 303.0430- 310.9758- 348.2291- 387.2122- 446.0391	
O-Methylated (-)-Gallocatechin gallate	472.40	FLH 13-11	√	–	24.923	471.2039	107.0656- 109.0812- **125.0809**- 137.0832- 145.0904- **151.1014**- **161.0884- 169.0798**- 183.1141- 201.1258- 213.1294- 225.1304- 243.1426- 257.1262- **269.1280- 287.1421**- 303.1401- 313.1232	S-Fig. 14
		FLH 17-66	–	–	–	–		
O-Methylated (+)-Epigallocatechin gallate	472.40	FLH 13-11	–	–	–	–		S-Fig. 15
		FLH 17-66	√	–	25.018	471.0486	**106.9918- 125.0014- 151.0132- 160.9981- 168.9872-** 183.0166- 201.0280- 213.0195- 225.0247- 243.0342- 257.0042- 269.0087- 288.0210- 303.0141	
O-Methylated (-)-Epigallocatechin gallate	472.40	FLH 13-11	–	–	–	–		S-Fig. 16
		FLH 17-66	√	–	25.347	471.0486	**106.9950- 124.9992**- 133.0056- **151.0090**- **160.9945**- 164.9891- **168.9837**- 173.0359- 178.9967- 183.0169- 188.0060- 199.0158- 213.0245- 241.0151- 269.0020- 297.9831- 313.9682- 337.9594	

Table 3.4: Eight dimeric proanthocyanidins were detected in berries of two interspecific hybrid cultivars FLH 13-11 and FLH 17-66. (Note: "_" means not detected).

Compounds Detected	MW (g/mol)	Cultivar	Year of Harvest 2011	Year of Harvest 2012	Ret. Tim (min)	MS^- (m/z)	[MS/MS] (m/z) profiles	Figure #
Procyanidin A2	576.51	FLH 13-11	√	√	35.193	575.2385	**125.0804- 137.0830-** 151.0966- **161.0901**- 169.0802- 175.1030- 191.0990- 201.1213- 217.1222- **229.1250**- 243.1107- 257.1236- **271.1085**- 287.1407- 351.0316- **394.1682**- 407.1760- 449.1959	Fig. 9
		FLH 17-66	√	√	35.684	575.0652	**109.0070- 124.9985- 136.9988**- 152.9935- **160.9962- 168.9837**- 175.0088- 187.0083- 199.0077- 215.0015- 227.000- 230.9939- **242.9965- 257.0099- 270.9877**- 285.0011- 296.9985- 312.9930- 327.0119- 378.0426- **394.0270-** 407.0324- 425.0363- 449.0414	
Procyanidin B1 [epicatechin-(4β→8)-catechin]	578.52	FLH 13-11	√	–	10.008	577.2579	**109.0823- 125.0812- 137.0845**- 151.0997- **161.0911**- 179.1013- 187.1092- **205.1215-** 217.1259- 229.1257- **245.1596**- 256.1226- 273.1247- 281.1328- **289.1590**- 297.1640- 339.1805- 381.1925- 393.1828- **407.1804**- 425.1916- 451.2157	S-Fig. 17
		FLH 17-66	–	√	10.068	577.0828	**108.9944- 124.9868- 136.9845**- 152.9751- **160.9802**- 174.9912- 203.0163- 229.9978- **245.0179**- 254.9655- 272.9779- **289.0023**- 297.9319- 312.9674- 339.0092- **406.9878**	
Procyanidin B2 [epicatechin-(4β→8)-epicatechin]	578.52	FLH 13-11	√	√	13.528	577.2551	**109.0809- 125.0801- 137.0810**- 149.0838- 161.0938- **165.0838-** 175.1065- 191.1055- 205.1202- 229.1258- 245.1590- 269.1261- **289.1558**- 329.1543- 367.2092- 393.1943- **407.1765**- 439.2095- 533.2681	Fig. 10
		FLH 17-66	√	√	13.21	577.0828	**109.0032- 124.9960- 136.9946**- 151.0073- **160.9936**- 175.0059- 187.0037- 203.0321- 221.0419- 229.0106- **245.0374**- 254.9878- 268.9982- 280.9984- **289.0235**- 339.0328- 389.0147- **407.0181**- 425.0330	
Procyanidin B4 [catechin-(4β→8)-epicatechin]	578.52	FLH 13-11	√	√	12.24	577.2551	**109.0814- 125.0805- 137.0823- 149.0852- 165.0824**- 179.1032- **191.1036- 201.1267**- 205.1212- 227.1137- **247.1403- 269.1262**- 289.1557- 329.1593- 353.1942- 367.2122- **393.1957**- 407.1776- 425.1887- **439.2070**	S-Fig.18
		FLH 17-66	–	√	12.407	577.0828	**109.0231- 125.0156- 137.0162**- 149.0119- **163.0261- 165.0054**- 177.0335- **191.0167**- 201.0358- 215.0238- **227.0187- 241.0249**- 269.0177- **289.0338**- 367.0710- 404.0440- 439.0388- 541.0047	
Procyanidin B5 [epicatechin-(4β→6)-epicatechin]	578.52	FLH 13-11	√	√	21.369	577.2193	**109.0808- 125.0802- 137.0823- 151.1006- 161.0891**- 165.0832- 179.0649- 187.1050- 205.1192- 229.1270- **245.1575**- 271.1073- **289.1563- 316.1109-** 329.1598- 339.1809- 359.1454- 381.1959- **407.1782**- 425.1849- 439.2071- 451.2220- **463.1951**	S-Fig.19
		FLH 17-66	–	√	21.467	577.0828	**109.0011- 124.9934- 136.9912**- 151.0032- **160.9909**- 175.0013- 187.0008- 203.0265- 214.9922- 227.0197- 245.0321- 255.9888- 270.9718- 280.9948- **289.0166- 315.9665**- 339.0265- 407.0129- 463.0166	
Procyanidin B6 [catechin-(4β→6)-catechin]	578.52	FLH 13-11	√	√	12.886	577.2551	**109.0813- 125.0800- 137.0824- 151.1011- 161.0883**- 165.0837- **179.1019**- 187.1074- **205.1203**- 229.1273- **245.1579**- 273.1228- **289.1562**- 329.1583- **339.1792**- 357.1931- **407.1774**- **425.1894**-439.2095- 451.2070	S-Fig. 20
		FLH 17-66	–	–	–	–		
Procyanidin B7 [epicatechin-(4β→6)-catechin]	578.52	FLH 13-11	√	√	20.289	577.2551	**109.0793- 125.0802- 137.0822**- 149.0840- **165.0846**- 179.1029- **189.1219**- 207.1402- 229.1203- **243.1446**- 271.1450- **289.1552**- 301.1616- **329.1578**- 353.1956- 377.1962- 407.1900- 425.1968- **439.2060**- 449.2324- 475.2127- 509.2548- 533.2597- 559.2447	S-Fig. 21
		FLH 17-66	–	–	–	–		
Procyanidin B8 [catechin-(4β→6)-epicatechin]	578.52	FLH 13-11	√	–	11.255	577.2579	**109.0822- 125.0815- 137.0833- 151.1016**- **161.0898**- 165.0855- 175.1072- 187.1098- **205.1217**- 229.1266- **245.1602**- 256.1230- 273.1279- **289.1577**- 299.1461- 329.1573- **339.1795**- 381.2008- **407.1800**- 425.1916- 439.2084- 451.2077	S-Fig. 22
		FLH 17-66	–	–	–	–		

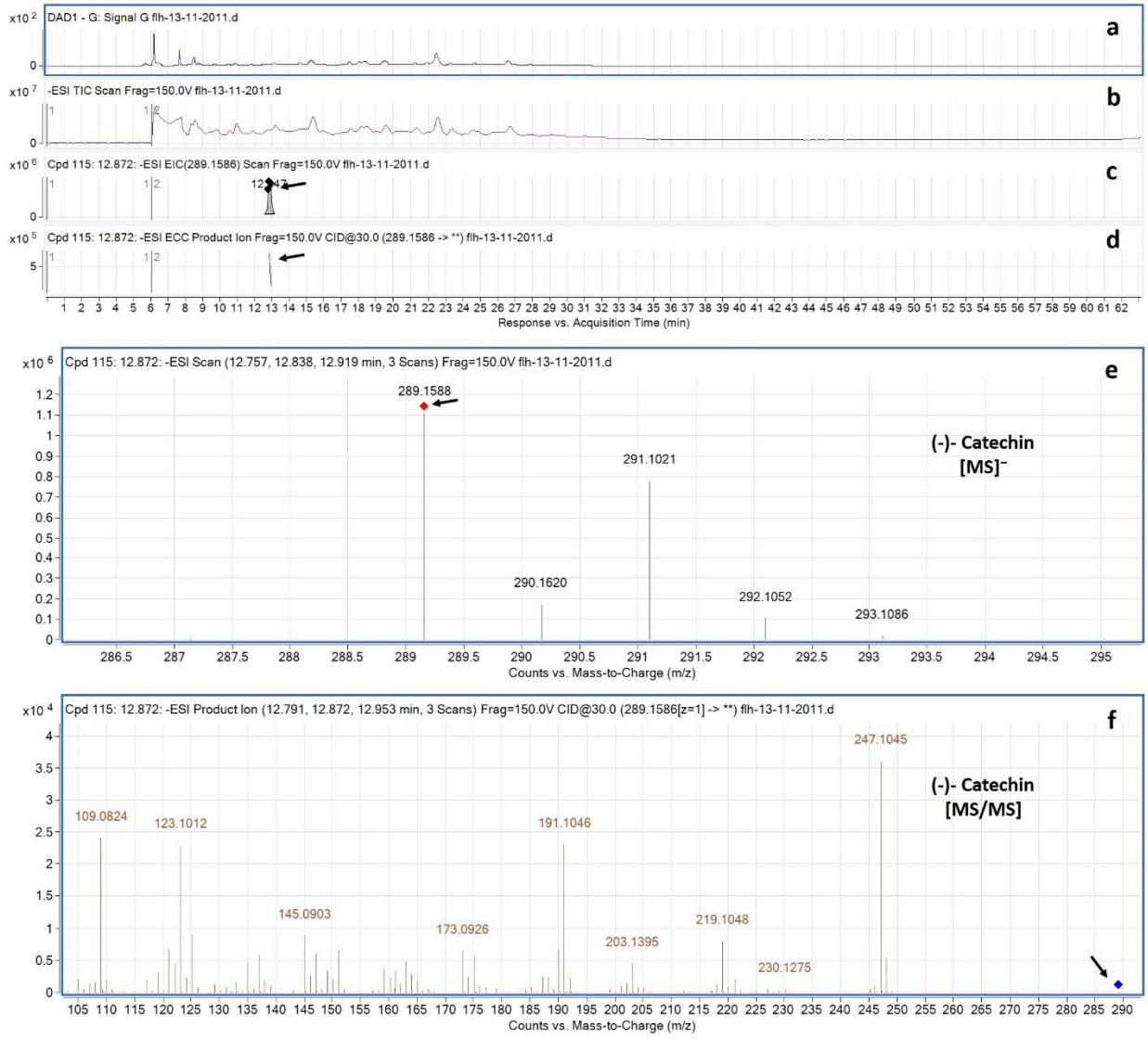

Supplementary Figure 3.1: Extracted ion chromatogram (EIC) of primary mass spectrum (MS1) and m/z features of secondary ion fragments (MS2) derived from LC-MC/MS annotate this peak to be (-)- Catechin, (MW, 290.26). (**a**) Chromatogram of FLH 13-11 extracts (2011) recorded at 280 nm absorbance; (**b**) Total ion chromatogram of FLH 13-11 extract (2011); (**c**) EIC of primary ion 289.1586 [M-H] $[m/z]^{-}$; (**d**) Enhanced charge capacity (ECC) ion product for 289.15836 $[m/z]^{-}$; (**e**) A MS profile showing an extracted m/z value, 289.1588 $[m/z]^{-}$; (**f**) Fragments from collision-induced dissociation (CID) of 289.1588 showing 109.0824, 123.1012, 137.0835, 145.0903, 151.1025, 163.1047, 173.0926, 191.1046, 203.1395, 219.1048, and 230.1275 $[m/z]^{-}$ (Table 2).

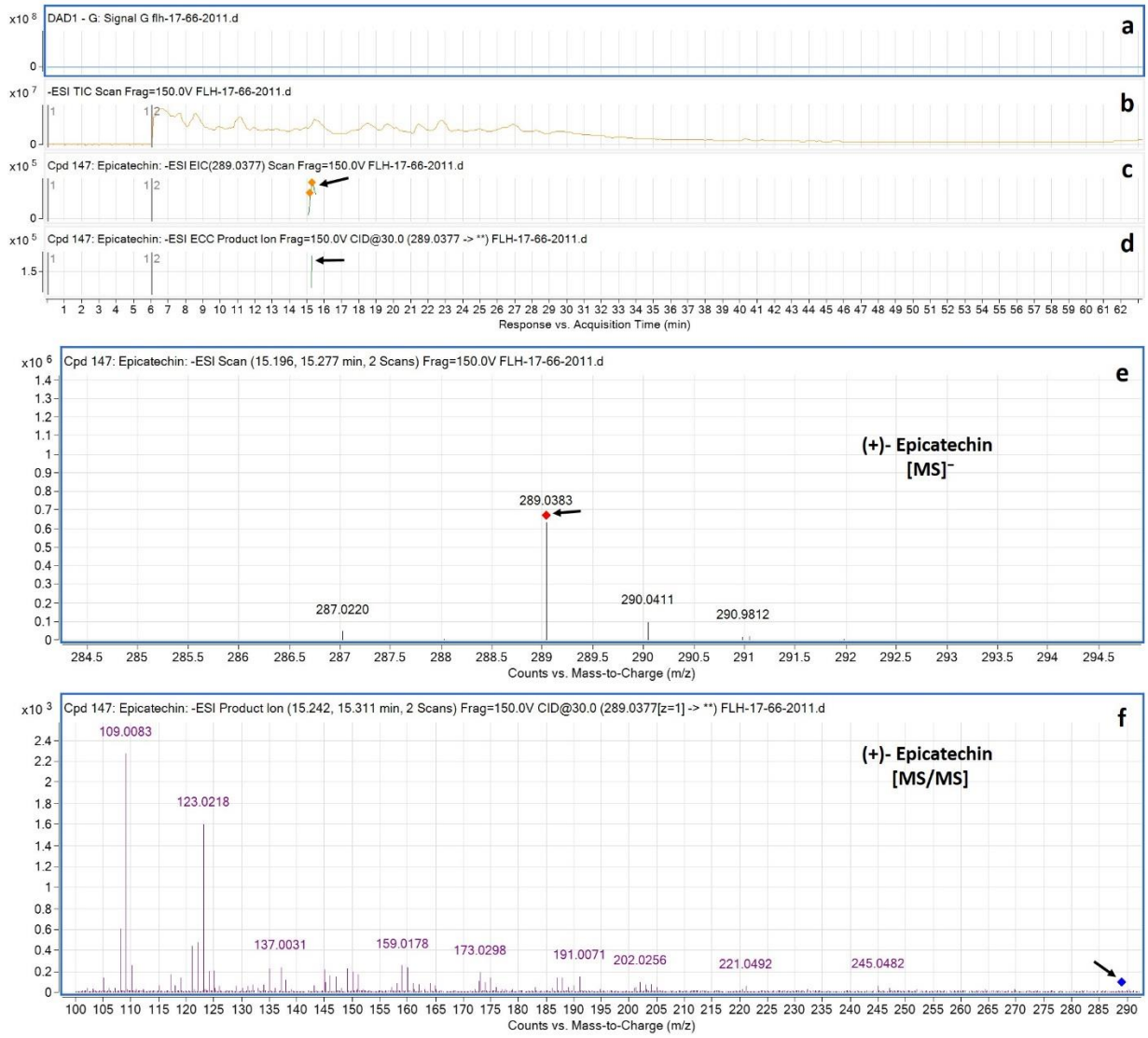

Supplementary Figure 3.2: Extracted ion chromatogram (EIC) of primary mass spectrum (MS1) and m/z features of secondary ion fragments (MS2) derived from LC-MC/MS annotate this peak to be (+)- Epicatechin, (MW, 290.26). (**a**) Chromatogram of FLH 17-66 extracts (2011) recorded at 280 nm absorbance; (**b**) Total ion chromatogram of FLH 17-66 extract (2011); (**c**) EIC of primary ion 289.0377 [M-H] $[m/z]^{-}$; (**d**) Enhanced charge capacity (ECC) ion product for 289.0377 $[m/z]^{-}$; (**e**) A MS profile showing an extracted m/z value, 289.0383 $[m/z]^{-}$; (**f**) Fragments from collision-induced dissociation (CID) of 289.0383 showing 109.0083, 123.0218, 137.0031, 148.9987, 159.0178, 173.0298, 191.0071, 202.0256, 221.0492, and 245.0482 $[m/z]^{-}$ (Table 2).

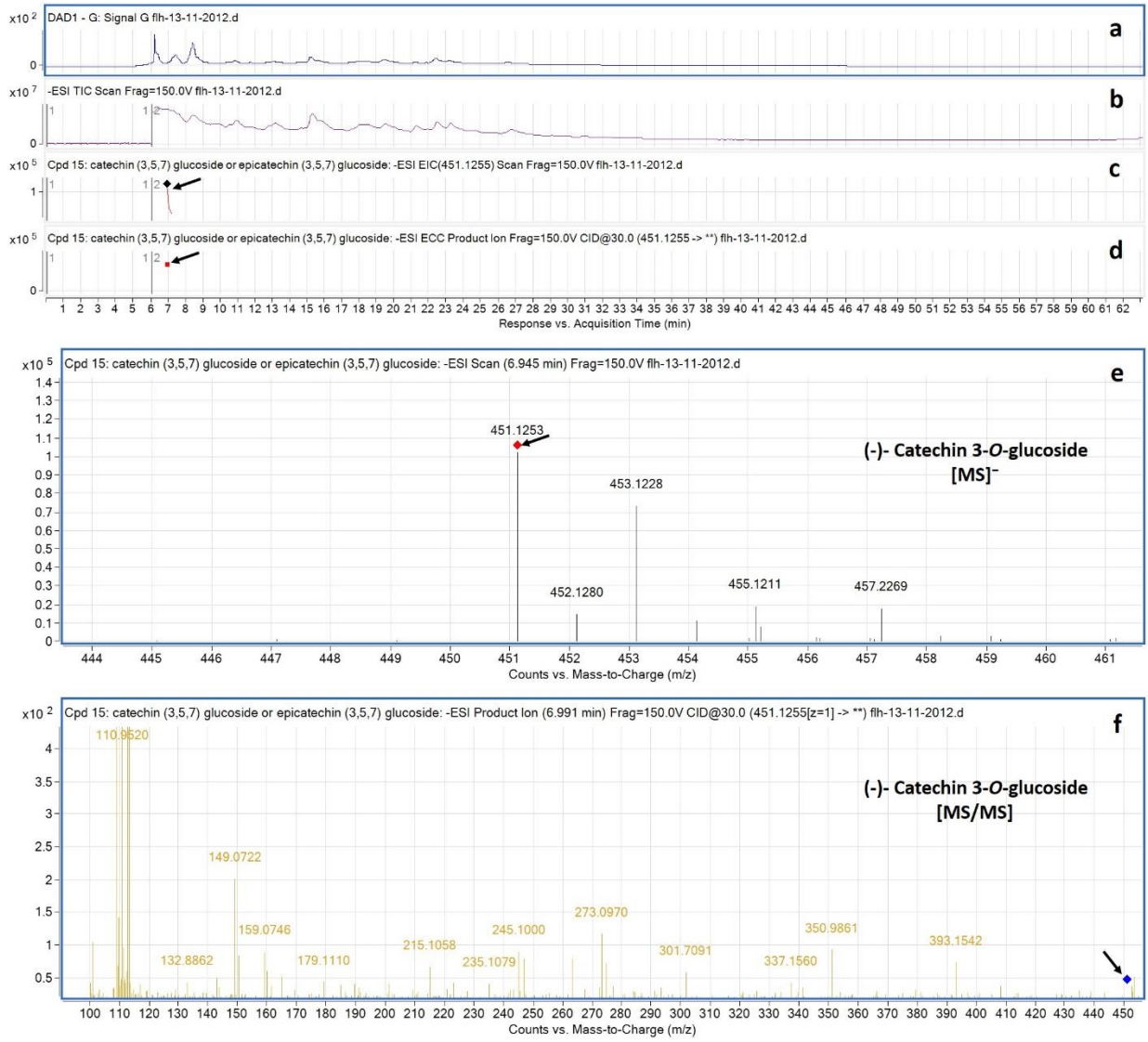

Supplementary Figure 3.3: Extracted ion chromatogram (EIC) of primary mass spectrum (MS1) and m/z features of secondary ion fragments (MS2) derived from LC-MC/MS annotate this peak to be (-)- Catechin 3-*O*-glucoside, (MW, 452.41). (**a**) Chromatogram of FLH 13-11 extracts (2012) recorded at 280 nm absorbance; (**b**) Total ion chromatogram of FLH 13-11 extract (2012); (**c**) EIC of primary ion 451.1255 [M-H] $[m/z]^{-}$; (**d**) Enhanced charge capacity (ECC) ion product for 451.1255 $[m/z]^{-}$; (**e**) A MS profile showing an extracted m/z value, 451.1253 $[m/z]^{-}$; (**f**) Fragments from collision-induced dissociation (CID) of 451.1253 showing 101.0752, 108.9545, 109.9014, 110.9520, 112.9487, 132.8862, 149.0722, 201.1385, 215.1058, 245.1000, 263.1016, 273.0970, 301.7091, 337.1560, 350.9861, and 393.1542 $[m/z]^{-}$ (Table 3).

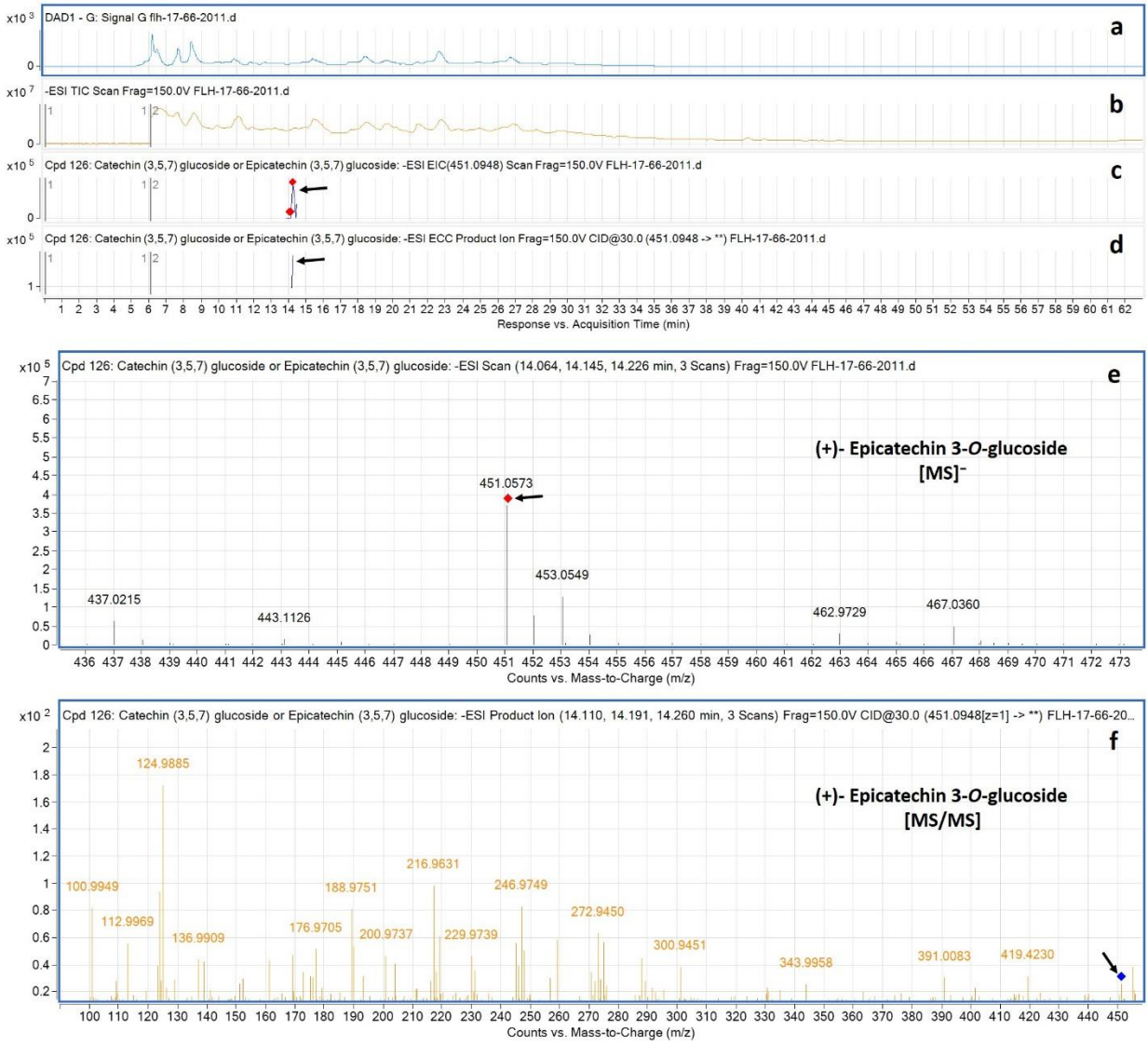

Supplementary Figure 3.4: Extracted ion chromatogram (EIC) of primary mass spectrum (MS1) and m/z features of secondary ion fragments (MS2) derived from LC-MC/MS annotate this peak to be (+)- Epicatechin 3-*O*-glucoside, (MW, 452.41). (**a**) Chromatogram of FLH 17-66 extracts (2011) recorded at 280 nm absorbance; (**b**) Total ion chromatogram of FLH 17-66 extract (2011); (**c**) EIC of primary ion 451.0948 [M-H] $[m/z]^{-}$; (**d**) Enhanced charge capacity (ECC) ion product for 451.0948 $[m/z]^{-}$; (**e**) A MS profile showing an extracted m/z value, 451.0573 $[m/z]^{-}$; (**f**) Fragments from collision-induced dissociation (CID) of 451.0573 showing 100.9949, 112.9969, 124.9885, 136.9909, 152.0334, 168.9777, 188.9751, 216.9631, 229.9739, 246.9749, 258.9704, 272.9450, 287.9723, 300.9451, 343.9958, and 391.0083 $[m/z]^{-}$ (Table 3).

Supplementary Figure 3.5: Extracted ion chromatogram (EIC) of primary mass spectrum (MS1) and m/z features of secondary ion fragments (MS2) derived from LC-MC/MS annotate this peak to be (-)- Catechin gallate, (MW, 442.37). (**a**) Chromatogram of FLH 17-66 extracts (2011) recorded at 280 nm absorbance; (**b**) Total ion chromatogram of FLH 17-66 extract (2011); (**c**) EIC of primary ion 441.0400 [M-H] $[m/z]^{-}$; (**d**) Enhanced charge capacity (ECC) ion product for 441.0400 $[m/z]^{-}$; (**e**) A MS profile showing an extracted m/z value, 441.0359 $[m/z]^{-}$; (**f**) Fragments from collision-induced dissociation (CID) of 441.0359 showing 109.0075, 125.0004, 136.9990, 151.0140, 161.0307, 168.9855, 187.0088, 203.0416, 221.0477, 245.0471, 259.0269, 271.0268, and 289.0332 $[m/z]^{-}$ (Table 3).

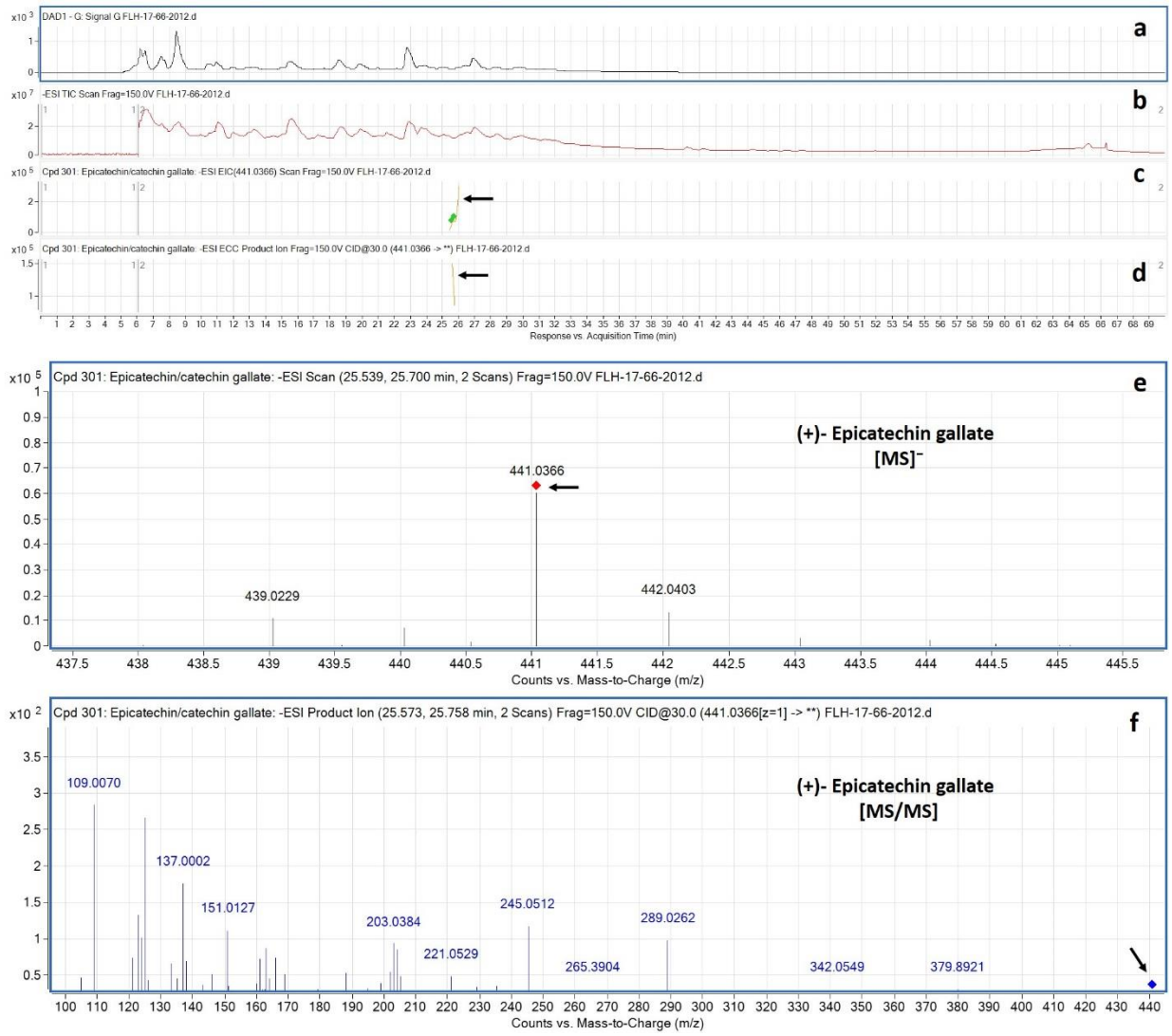

Supplementary Figure 3.6: Extracted ion chromatogram (EIC) of primary mass spectrum (MS1) and m/z features of secondary ion fragments (MS2) derived from LC-MC/MS annotate this peak to be (+)- Epicatechin gallate, (MW, 442.37). (**a**) Chromatogram of FLH 17-66 extracts (2011 and 2012) recorded at 280 nm absorbance; (**b**) Total ion chromatogram of FLH 17-66 extract (2012); (**c**) EIC of primary ion 441.0366 [M-H] $[m/z]^{-}$; (**d**) Enhanced charge capacity (ECC) ion product for 441.0366 $[m/z]^{-}$; (**e**) A MS profile showing an extracted m/z value, 441.0366 $[m/z]^{-}$; (**f**) Fragments from collision-induced dissociation (CID) of 441.0366 showing 109.0070, 125.0005, 137.0002, 146.0097, 151.0127, 163.0083, 188.0163, 203.0384, 221.0529, 235.1838, 245.0512, 265.3904, 289.0262, 342.0549, and 379.8921 $[m/z]^{-}$ (Table 3).

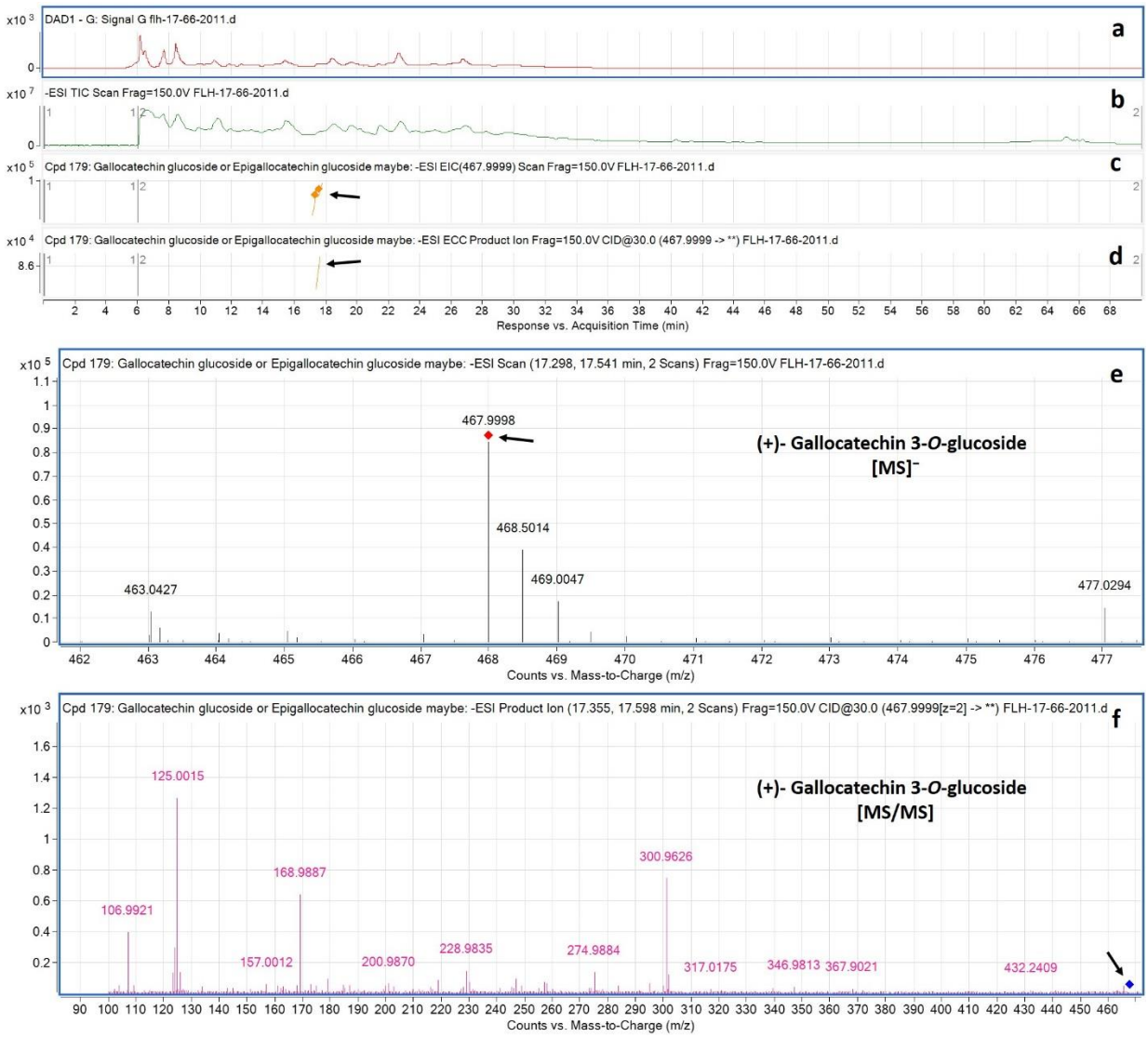

Supplementary Figure 3.7: Extracted ion chromatogram (EIC) of primary mass spectrum (MS1) and m/z features of secondary ion fragments (MS2) derived from LC-MC/MS annotate this peak to be (+)- Gallocatechin 3-*O*-glucoside, (MW, 468.0). (**a**) Chromatogram of FLH 17-66 extracts (2011) recorded at 280 nm absorbance; (**b**) Total ion chromatogram of FLH 17-66 extract (2011); (**c**) EIC of primary ion 467.9999 [M-H] $[m/z]^{-}$; (**d**) Enhanced charge capacity (ECC) ion product for 467.9999 $[m/z]^{-}$; (**e**) A MS profile showing an extracted m/z value, 467.9998 $[m/z]^{-}$; (**f**) Fragments from collision-induced dissociation (CID) of 467.9998 showing 106.9921, 125.0015, 133.9739, 157.0012, 168.9887, 179.0102, 200.9870, 228.9835, 246.9902, 274.9884, 300.9626, 317.0175, 346.9813, 367.9021, and 432.2409 $[m/z]^{-}$ (Table 3).

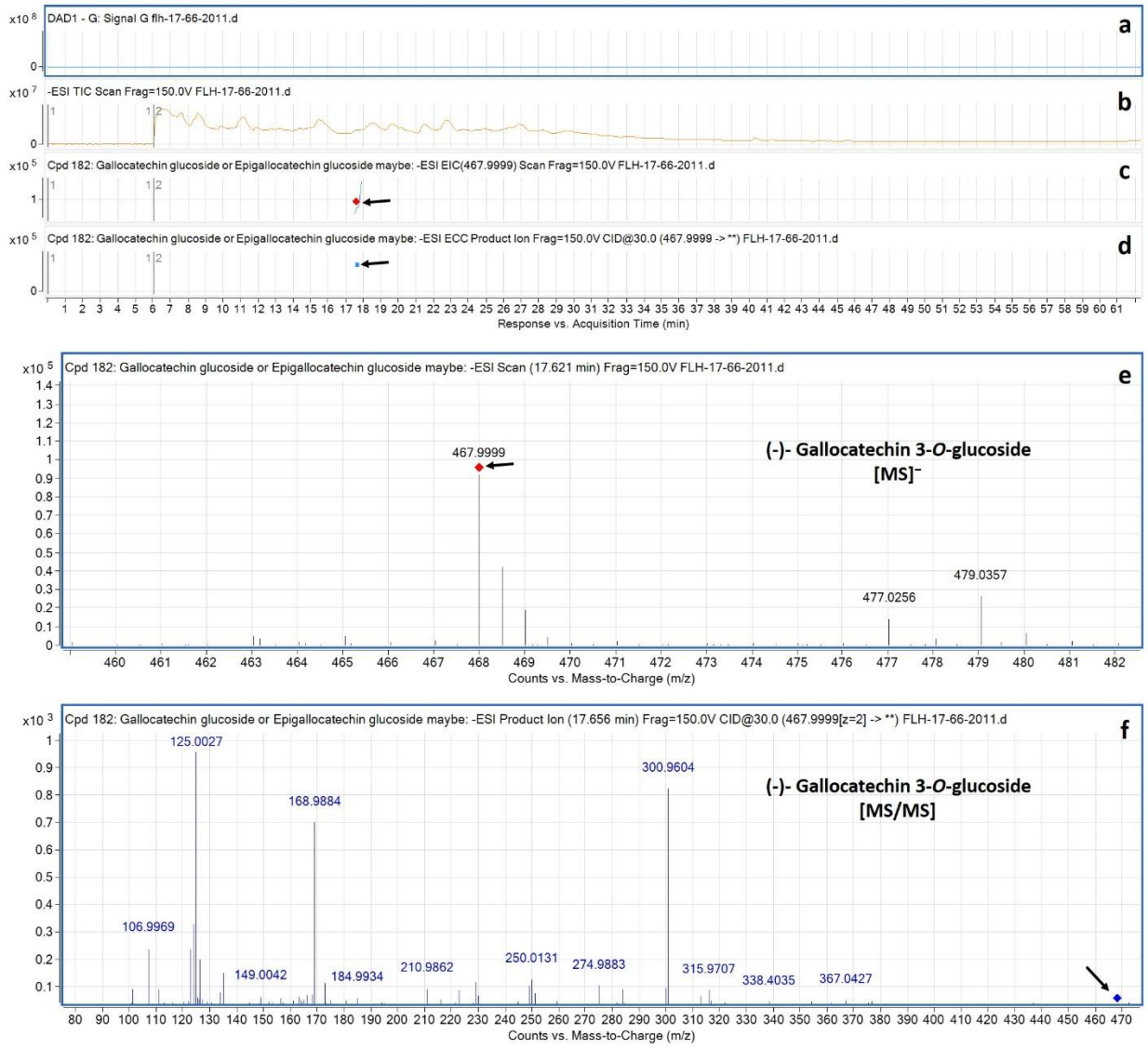

Supplementary Figure 3.8: Extracted ion chromatogram (EIC) of primary mass spectrum (MS1) and m/z features of secondary ion fragments (MS2) derived from LC-MC/MS annotate this peak to be (-)- Gallocatechin 3-*O*-glucoside, (MW, 468.0). (**a**) Chromatogram of FLH 17-66 extracts (2011) recorded at 280 nm absorbance; (**b**) Total ion chromatogram of FLH 17-66 extract (2011); (**c**) EIC of primary ion 467.9999 [M-H] $[m/z]^{-}$; (**d**) Enhanced charge capacity (ECC) ion product for 467.9999 $[m/z]^{-}$; (**e**) A MS profile showing an extracted m/z value, 467.9999 $[m/z]^{-}$; (**f**) Fragments from collision-induced dissociation (CID) of 467.9999 showing 106.9969, 125.0027, 135.0205, 168.9884, 184.9934, 210.9862, 228.9798, 250.0131, 274.9883, 283.9547, 300.9604, 315.9707, 338.4035, and 367.0427 $[m/z]^{-}$ (Table 3).

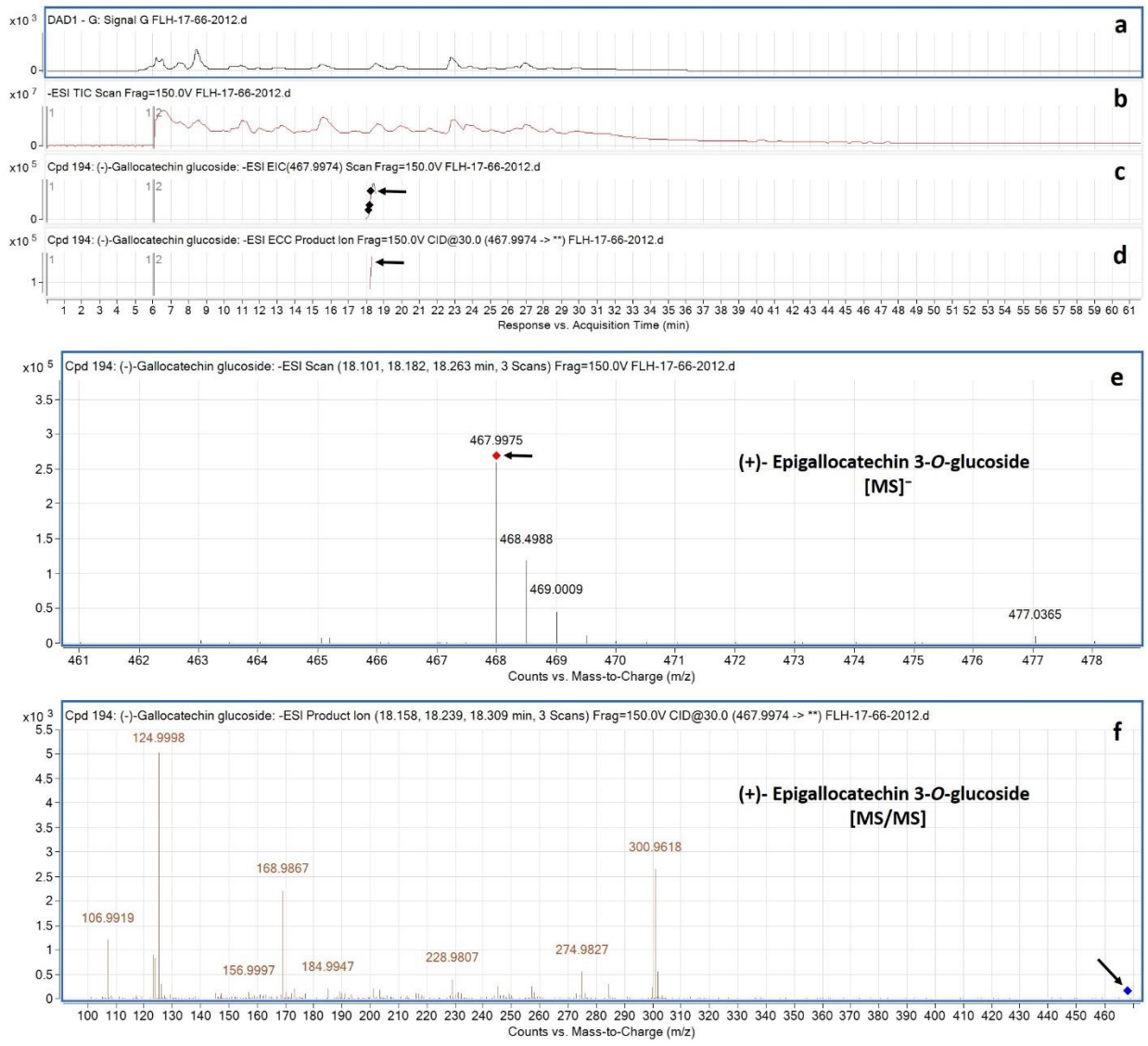

Supplementary Figure 3.9: Extracted ion chromatogram (EIC) of primary mass spectrum (MS1) and m/z features of secondary ion fragments (MS2) derived from LC-MC/MS annotate this peak to be (+)- Epigallocatechin 3-*O*-glucoside, (MW, 468.0). (**a**) Chromatogram of FLH 17-66 extracts (2011 and 2012) recorded at 280 nm absorbance; (**b**) Total ion chromatogram of FLH 17-66 extract (2012); (**c**) EIC of primary ion 467.9974 [M-H] $[m/z]^{-}$; (**d**) Enhanced charge capacity (ECC) ion product for 467.9974 $[m/z]^{-}$; (**e**) A MS profile showing an extracted m/z value, 467.9975 $[m/z]^{-}$; (**f**) Fragments from collision-induced dissociation (CID) of 467.9975 showing 106.9919, 124.9998, 145.0057, 156.9997, 168.1867, 184.9947, 200.9880, 228.9807, 244.9756, 256.9695, 274.9827, 290.9684, and 300.9618 $[m/z]^{-}$ (Table 3).

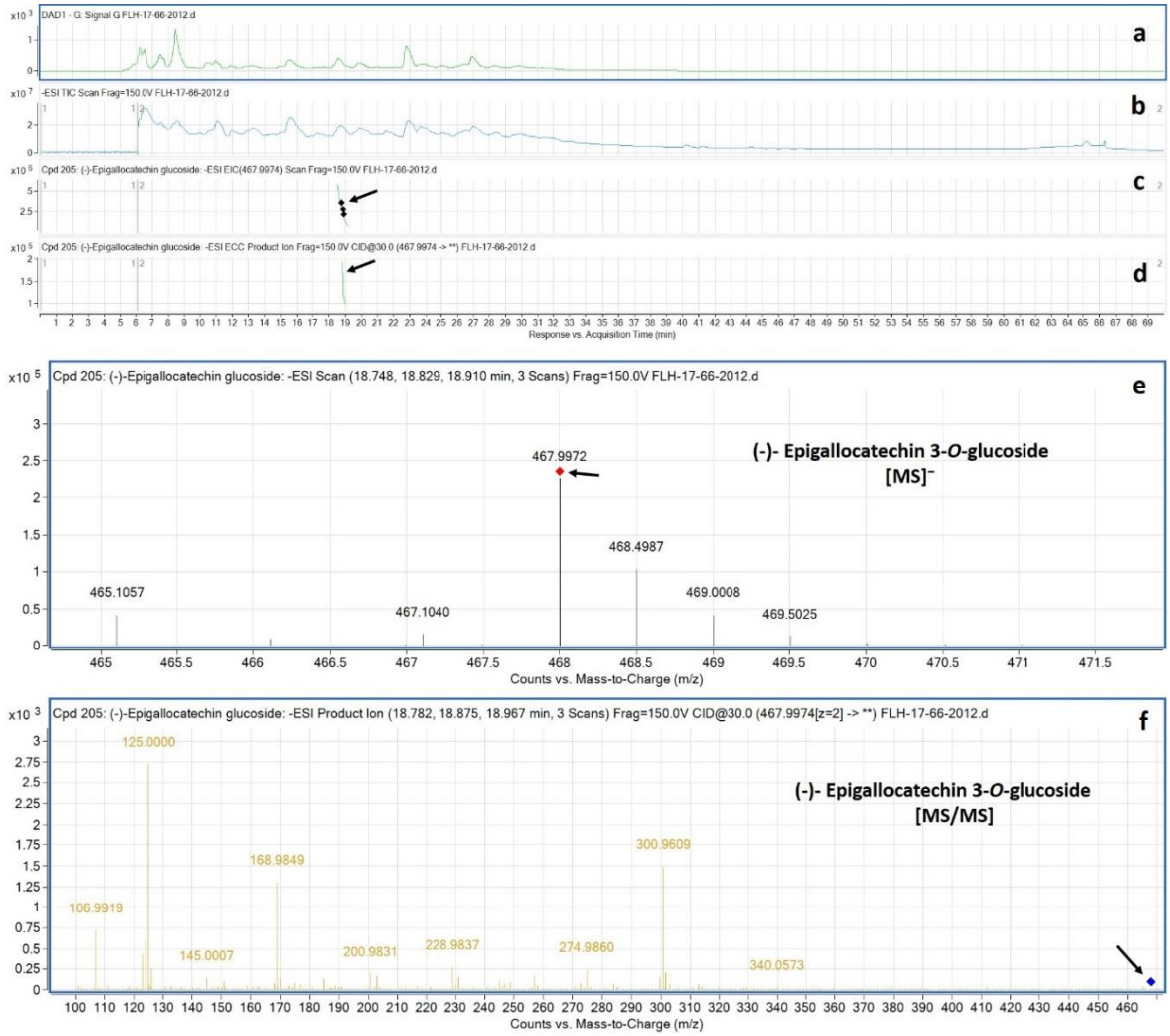

Supplementary Figure 3.10: Extracted ion chromatogram (EIC) of primary mass spectrum (MS1) and m/z features of secondary ion fragments (MS2) derived from LC-MC/MS annotate this peak to be (-)- Epigallocatechin 3-*O*-glucoside, (MW, 468.0). (**a**) Chromatogram of FLH 17-66 extracts (2011 and 2012) recorded at 280 nm absorbance; (**b**) Total ion chromatogram of FLH 17-66 extract (2012); (**c**) EIC of primary ion 467.9974 [M-H] $[m/z]^{-}$; (**d**) Enhanced charge capacity (ECC) ion product for 467.9974 $[m/z]^{-}$; (**e**) A MS profile showing an extracted m/z value, 467.9972 $[m/z]^{-}$; (**f**) Fragments from collision-induced dissociation (CID) of 467.9972 showing 106.9919, 125.0000, 145.0007, 159.0135, 168.9849, 184.9949, 200.9831, 228.9837, 256.9720, 274.9860, 300.9609, 313.0135, and 340.0573 $[m/z]^{-}$ (Table 3).

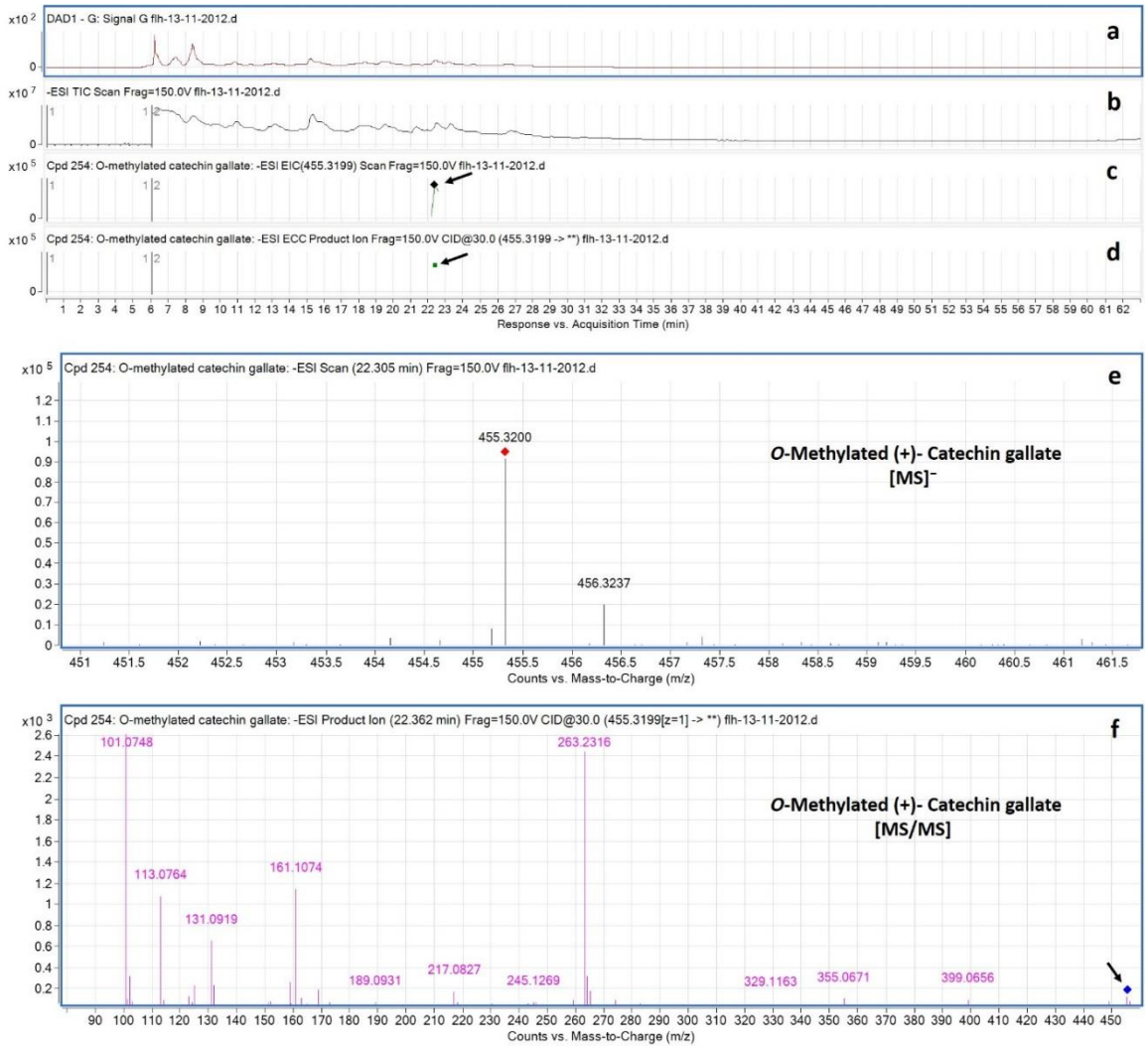

Supplementary Figure 3.11: Extracted ion chromatogram (EIC) of primary mass spectrum (MS1) and m/z features of secondary ion fragments (MS2) derived from LC-MC/MS annotate this peak to be *O*-methylated (+)- Catechin gallate, (MW, 456.0). (**a**) Chromatogram of FLH 13-11 extracts (2012) recorded at 280 nm absorbance; (**b**) Total ion chromatogram of FLH 13-11 extract (2012); (**c**) EIC of primary ion 455.3199 [M-H] $[m/z]^{-}$; (**d**) Enhanced charge capacity (ECC) ion product for 455.3199 $[m/z]^{-}$; (**e**) A MS profile showing an extracted m/z value, 455.3200 $[m/z]^{-}$; (**f**) Fragments from collision-induced dissociation (CID) of 455.3200 showing 101.0748, 113.0764, 125.0799, 131.0919, 143.0946, 161.1074, 169.0767, 189.0931, 217.0827, 245.1269, 263.2316, 274.0943, 283.1247, 291.0934, 301.0835, 329.1163, 355.0671, and 399.0656 $[m/z]^{-}$ (Table 3).

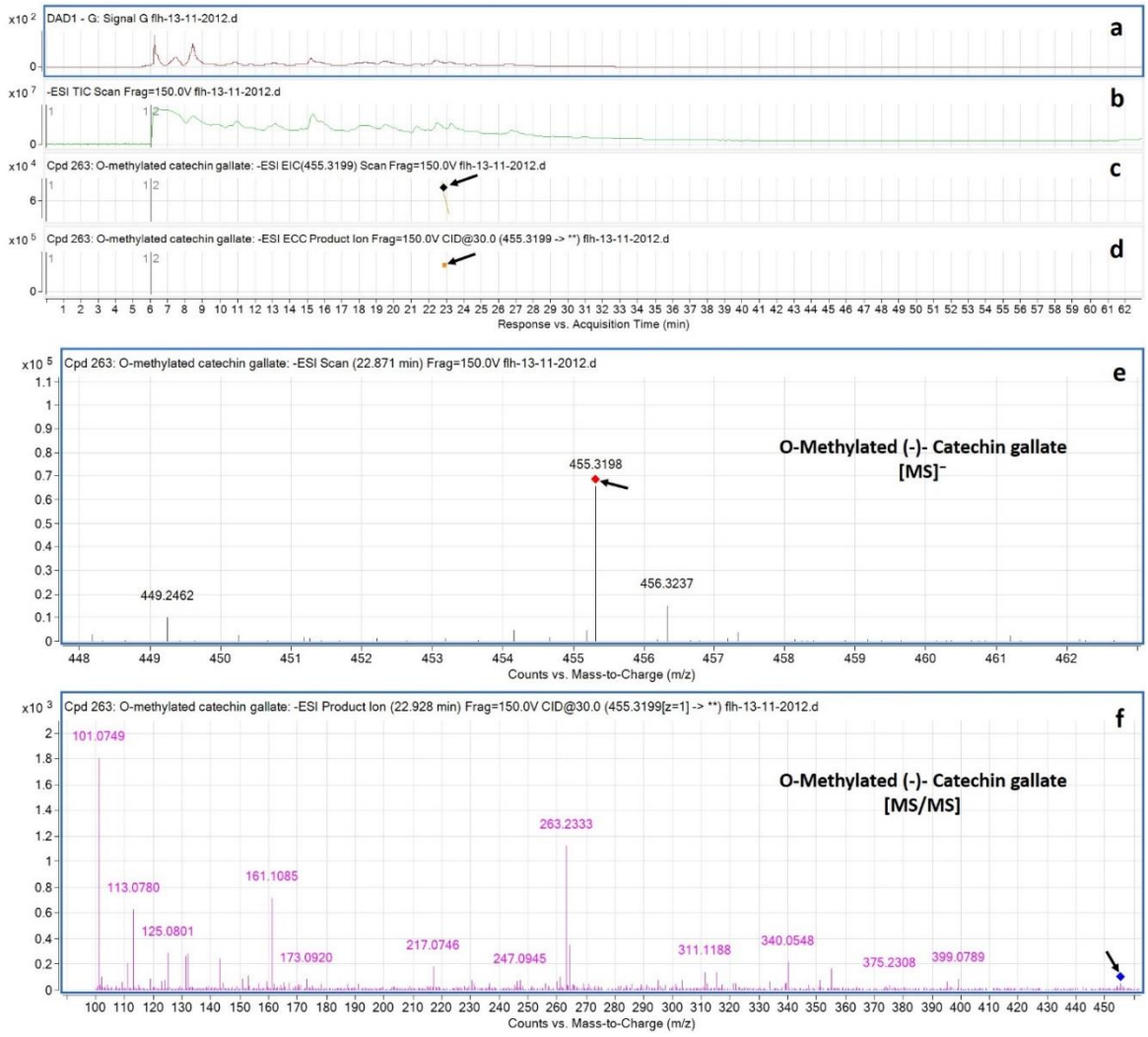

Supplementary Figure 3.12: Extracted ion chromatogram (EIC) of primary mass spectrum (MS1) and m/z features of secondary ion fragments (MS2) derived from LC-MC/MS annotate this peak to be *O*-methylated (-)- Catechin gallate, (MW, 456.0). (**a**) Chromatogram of FLH 13-11 extracts (2012) recorded at 280 nm absorbance; (**b**) Total ion chromatogram of FLH 13.11 extract (2012); (**c**) EIC of primary ion 455.3199 [M-H] $[m/z]^{-}$; (**d**) Enhanced charge capacity (ECC) ion product for 455.3199 $[m/z]^{-}$; (**e**) A MS profile showing an extracted m/z value, 455.3198 $[m/z]^{-}$; (**f**) Fragments from collision-induced dissociation (CID) of 455.3198 showing 101.0749, 113.0780, 125.0801, 132.0988, 143.0908, 161.1085, 173.0920, 191.0647, 217.0746, 247.0945, 263.2333, 295.0561, 311.1188, 340.0548, 355.0660, 375.2308, and 399.0789 $[m/z]^{-}$ (Table 3).

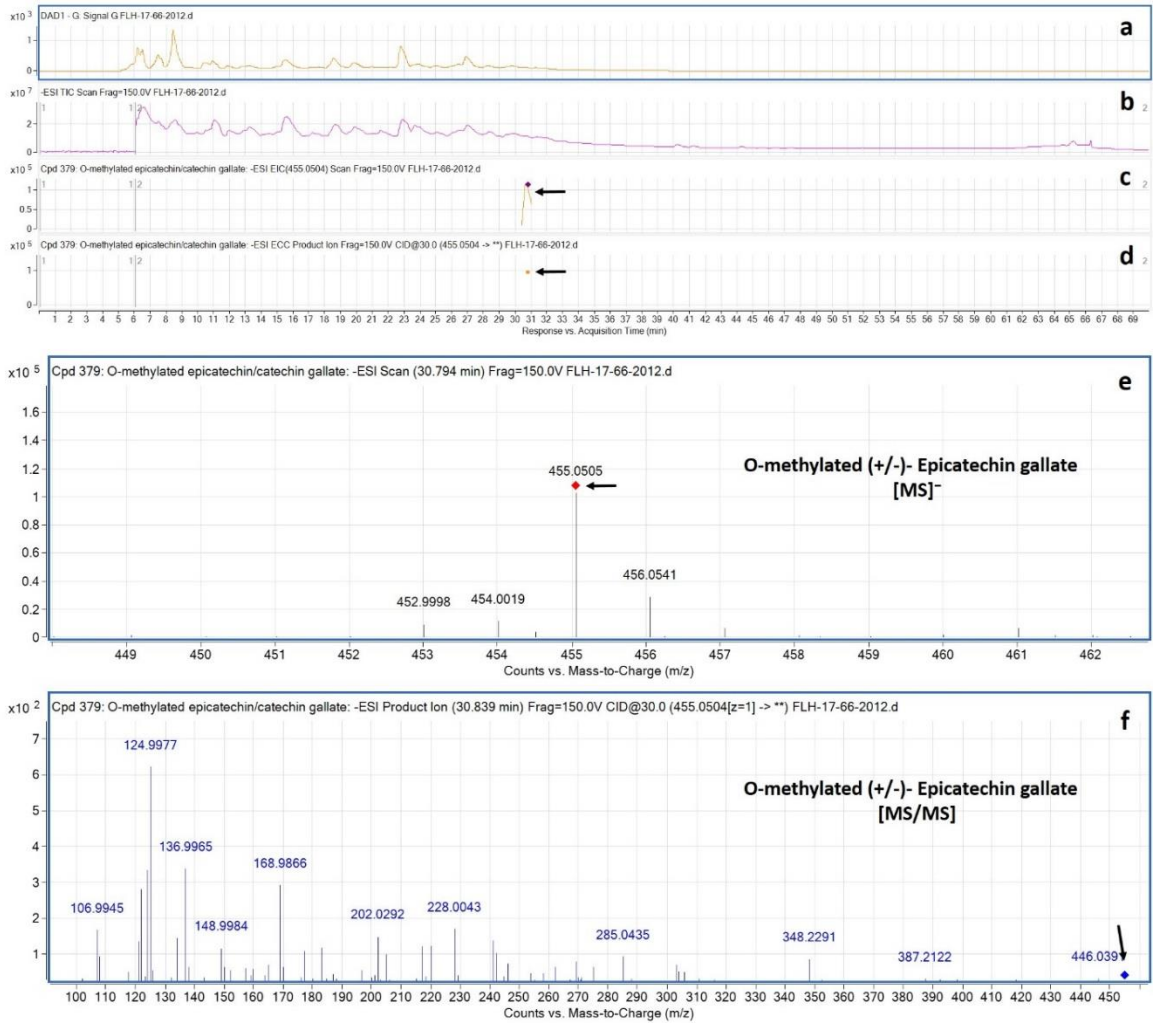

Supplementary Figure 3.13: Extracted ion chromatogram (EIC) of primary mass spectrum (MS1) and m/z features of secondary ion fragments (MS2) derived from LC-MC/MS annotate this peak to be *O*-methylated (+/-)- Epicatechin gallate, (MW, 456.0). (**a**) Chromatogram of FLH 17-66 extracts (2012) recorded at 280 nm absorbance; (**b**) Total ion chromatogram of FLH 17-66 extract (2012); (**c**) EIC of primary ion 455.0504 [M-H] $[m/z]^{-}$; (**d**) Enhanced charge capacity (ECC) ion product for 455.0504 $[m/z]^{-}$; (**e**) A MS profile showing an extracted m/z value, 455.0505 $[m/z]^{-}$; (**f**) Fragments from collision-induced dissociation (CID) of 455.0505 showing 106.9945, 124.9977, 136.9965, 148.9984, 168.9866, 177.0170, 183.0117, 196.8803, 202.0292, 217.0550, 220.0302, 228.0043, 241.0177, 253.9952, 269.0249, 274.9825, 285.0435, 303.0430, 310.9758, 348.2291, and 387.2122 $[m/z]^{-}$ (Table 3).

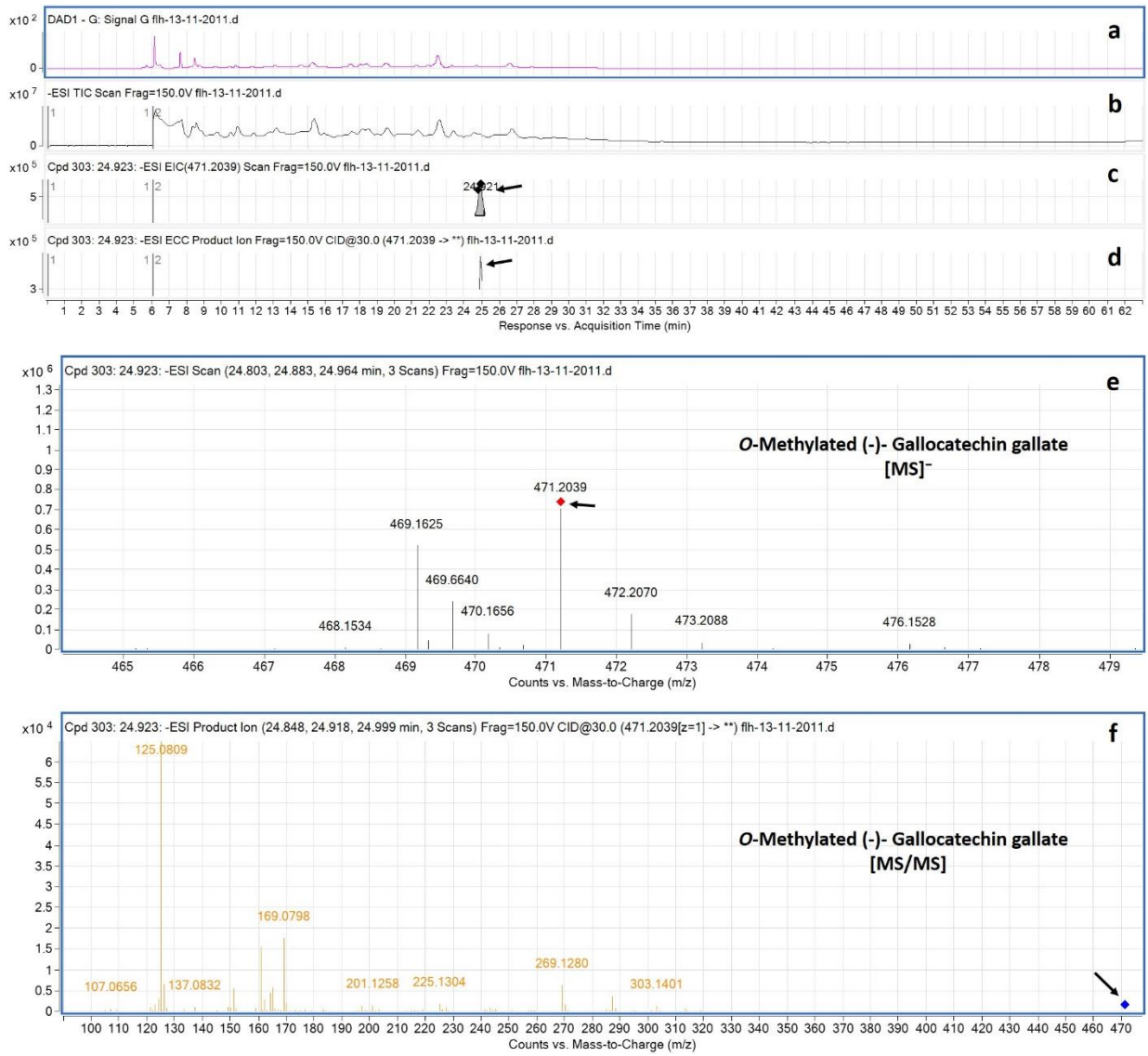

Supplementary Figure 3.14: Extracted ion chromatogram (EIC) of primary mass spectrum (MS1) and m/z features of secondary ion fragments (MS2) derived from LC-MC/MS annotate this peak to be *O*-methylated (-)- Gallocatechin gallate, (MW, 472.4). (**a**) Chromatogram of FLH 13-11 extracts (2011) recorded at 280 nm absorbance; (**b**) Total ion chromatogram of FLH 13-11 extract (2011); (**c**) EIC of primary ion 471.2039 [M-H] $[m/z]^{-}$; (**d**) Enhanced charge capacity (ECC) ion product for 471.2039 $[m/z]^{-}$; (**e**) A MS profile showing an extracted m/z value, 471.2039 $[m/z]^{-}$; (**f**) Fragments from collision-induced dissociation (CID) of 471.2039 showing 107.0656, 109.0812, 125.0809, 137.0832, 145.0904, 151.1014, 161.0884, 169.0798, 183.1141, 201.1258, 213.1294, 225.1304, 243.1426, 257.1262, 269.1280, 287.1421, 303.1401, and 313.1232 $[m/z]^{-}$ (Table 3).

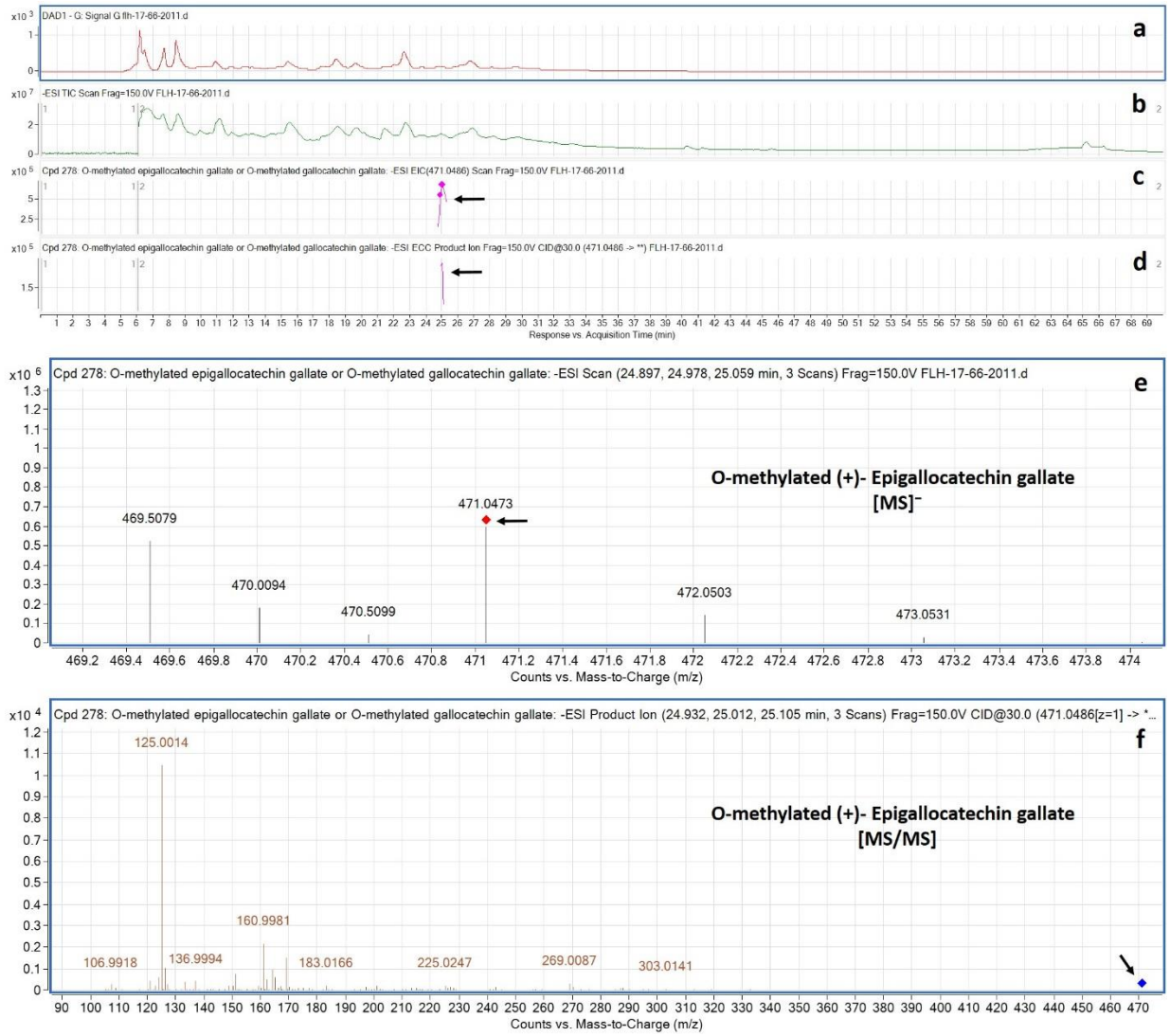

Supplementary Figure 3.15: Extracted ion chromatogram (EIC) of primary mass spectrum (MS1) and m/z features of secondary ion fragments (MS2) derived from LC-MC/MS annotate this peak to be *O*-methylated (+)- Epigallocatechin gallate, (MW, 472.4). (**a**) Chromatogram of FLH 17-66 extracts (2011) recorded at 280 nm absorbance; (**b**) Total ion chromatogram of FLH 17-66 extract (2011); (**c**) EIC of primary ion 441.0366 [M-H] $[m/z]^{-}$; (**d**) Enhanced charge capacity (ECC) ion product for 471.0486 $[m/z]^{-}$; (**e**) A MS profile showing an extracted m/z value, 471.0486 $[m/z]^{-}$; (**f**) Fragments from collision-induced dissociation (CID) of 471.0473 showing 106.9918, 125.0014, 151.0132, 160.9981, 168.9872, 183.0166, 201.0280, 213.0195, 225.0247, 243.0342, 257.0042, 269.0087, 288.0210, and 303.0141 $[m/z]^{-}$ (Table 3).

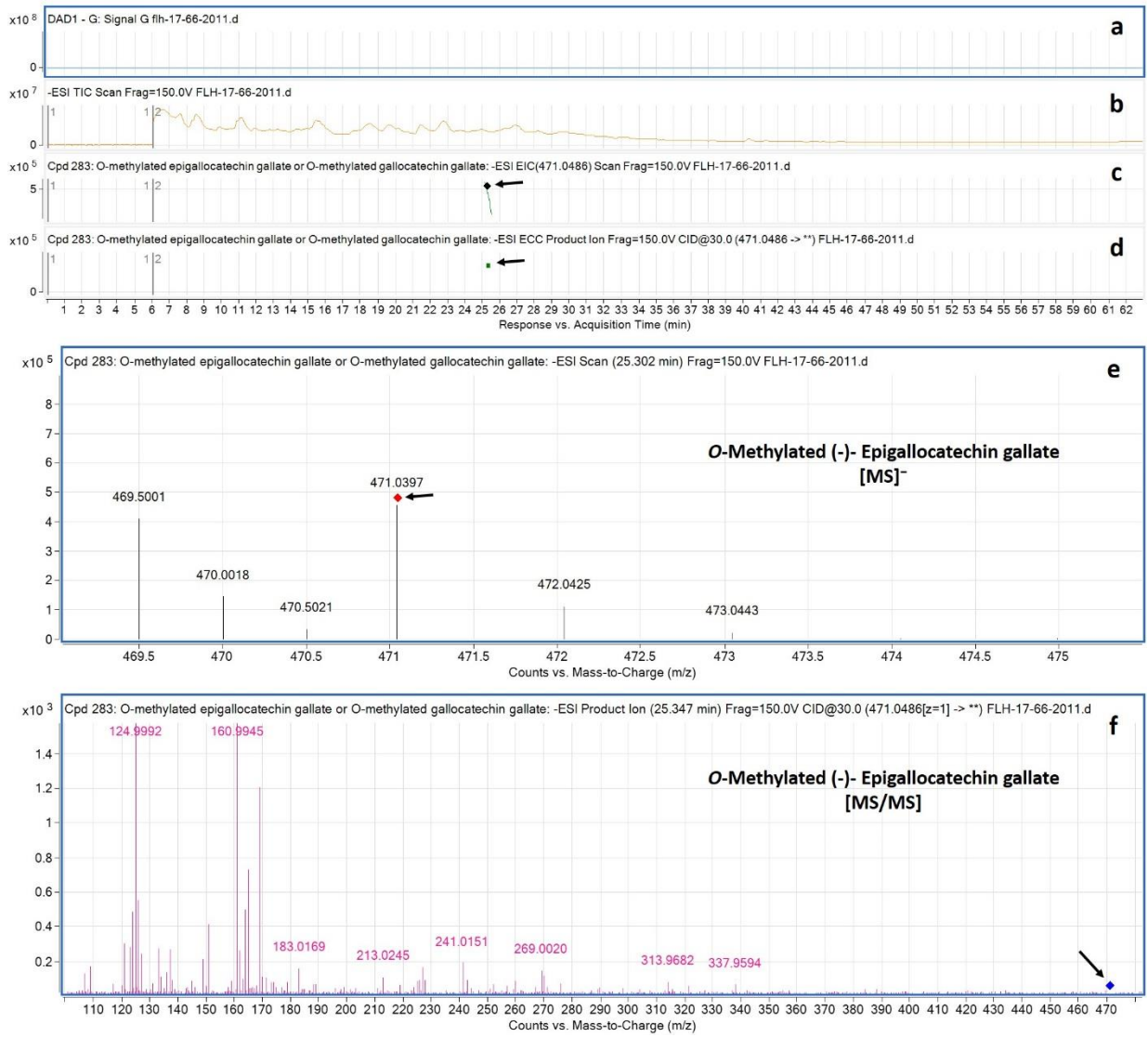

Supplementary Figure 3.16: Extracted ion chromatogram (EIC) of primary mass spectrum (MS1) and m/z features of secondary ion fragments (MS2) derived from LC-MC/MS annotate this peak to be *O*-methylated (-)- Epigallocatechin gallate, (MW, 472.4). (**a**) Chromatogram of FLH 17-66 extracts (2011) recorded at 280 nm absorbance; (**b**) Total ion chromatogram of FLH 17-66 extract (2011); (**c**) EIC of primary ion 471.0486 [M-H] $[m/z]^{-}$; (**d**) Enhanced charge capacity (ECC) ion product for 471.0486 $[m/z]^{-}$; (**e**) A MS profile showing an extracted m/z value, 471.0397 $[m/z]^{-}$; (**f**) Fragments from collision-induced dissociation (CID) of 471.0397 showing 106.9950, 124.9992, 133.0056, 151.0090, 160.9945, 164.9891, 168.9837, 173.0359, 178.9967, 183.0169, 188.0060, 199.0158, 213.0245, 241.0151, 269.0020, 297.9831, 313.9682, and 337.9594 $[m/z]^{-}$ (Table 3).

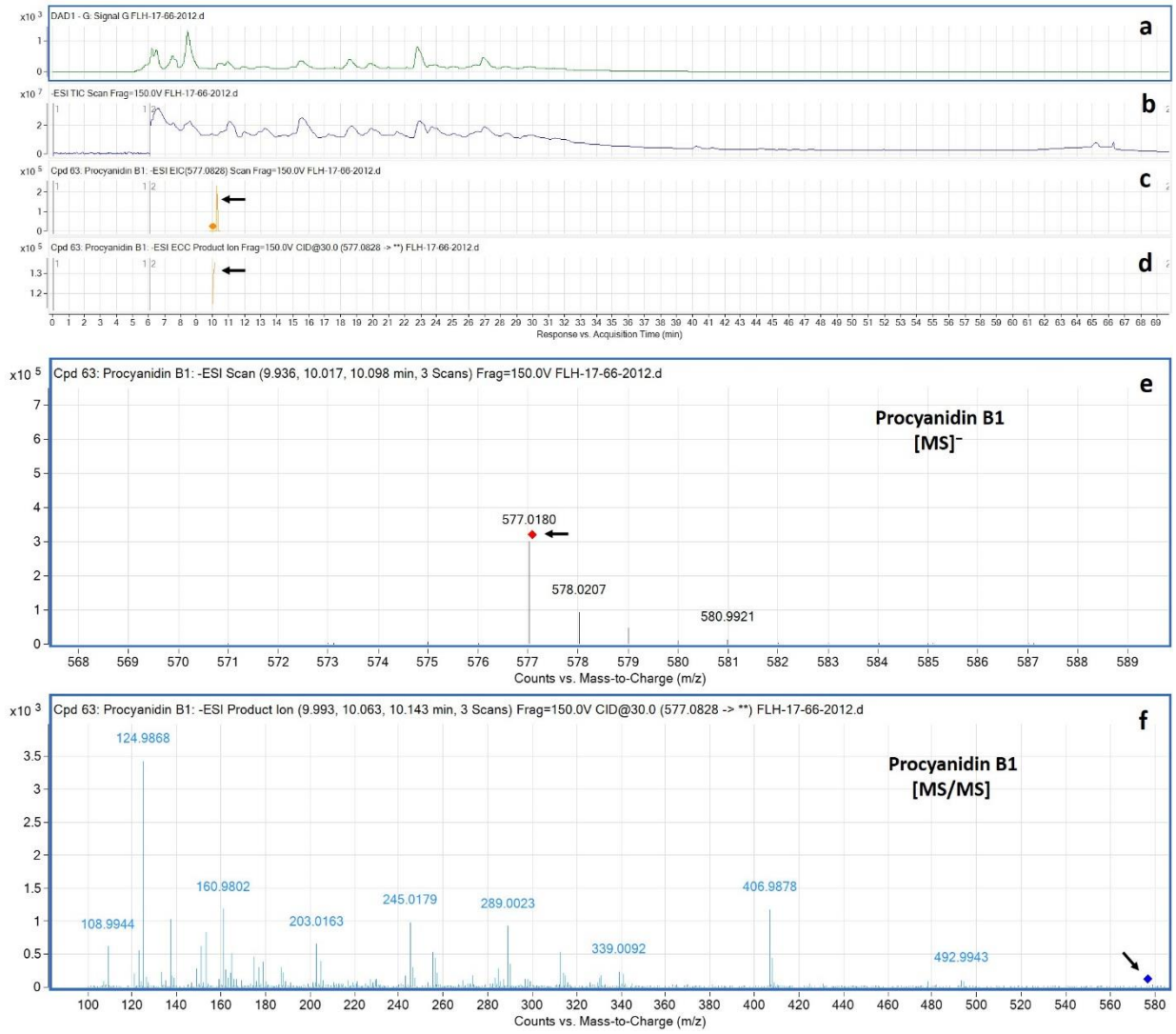

Supplementary Figure 3.17: Extracted ion chromatogram (EIC) of primary mass spectrum (MS1) and m/z features of secondary ion fragments (MS2) derived from LC-MC/MS annotate this peak to be Procyanidin B1, (MW, 578.52). (**a**) Chromatogram of FLH 17-66 extracts (2012) recorded at 280 nm absorbance; (**b**) Total ion chromatogram of FLH 17-66 extract (2012); (**c**) EIC of primary ion 577.0828 [M-H] $[m/z]^{-}$; (**d**) Enhanced charge capacity (ECC) ion product for 577.0828 $[m/z]^{-}$; (**e**) A MS profile showing an extracted m/z value, 577.0180 $[m/z]^{-}$; (**f**) Fragments from collision-induced dissociation (CID) of 577.0180 showing 108.9944, 124.9868, 136.9845, 152.9751, 160.9802, 174.9912, 203.0163, 229.9978, 245.0179, 272.9779, 289.0023, 297.9319, 312.9674, 339.0092, and 406.9878 $[m/z]^{-}$ (Table 4).

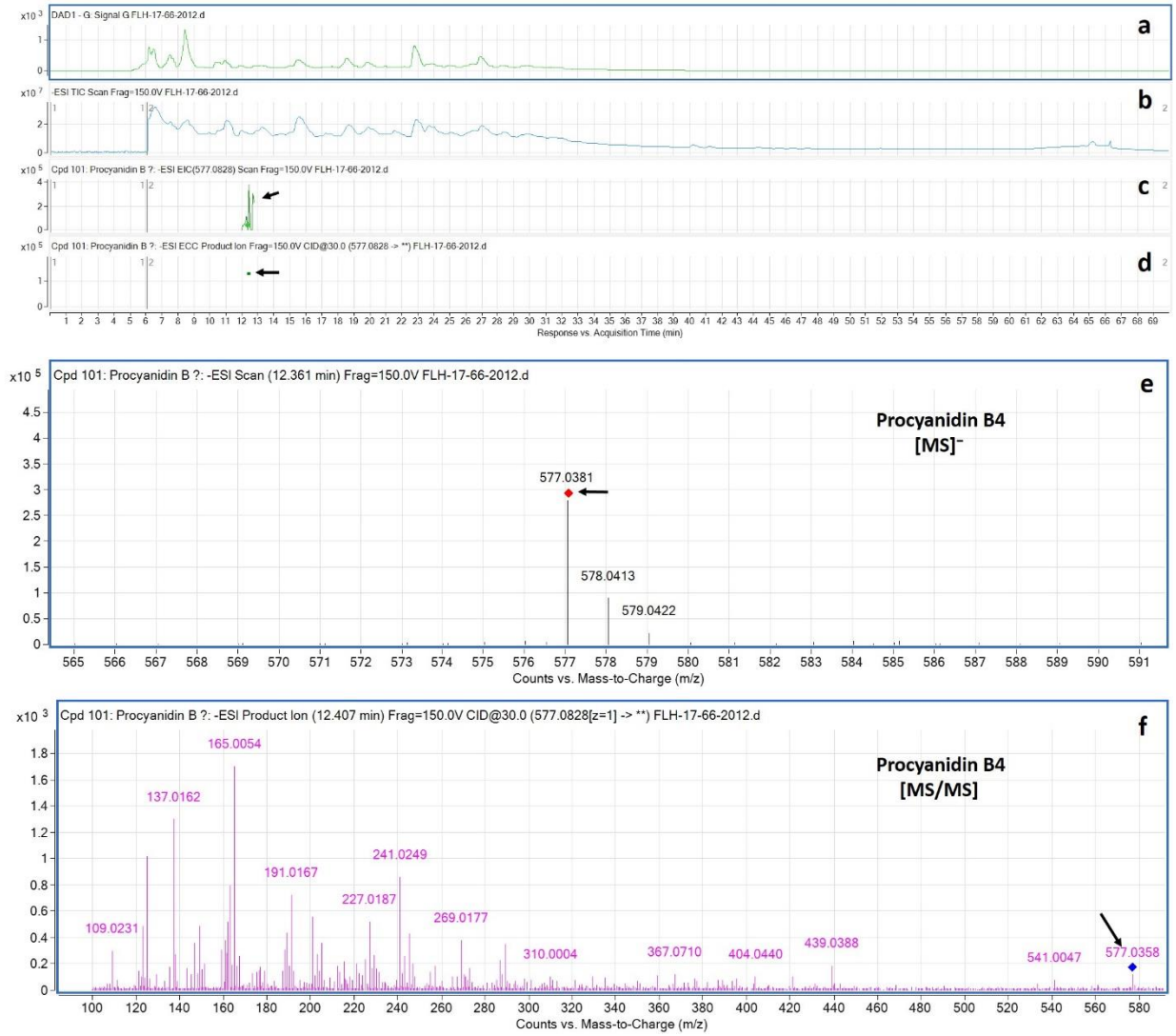

Supplementary Figure 3.18: Extracted ion chromatogram (EIC) of primary mass spectrum (MS1) and m/z features of secondary ion fragments (MS2) derived from LC-MC/MS annotate this peak to be Procyanidin B4, (MW, 578.52). (**a**) Chromatogram of FLH 17-66 extracts (2012) recorded at 280 nm absorbance; (**b**) Total ion chromatogram of FLH 17-66 extract (2012); (**c**) EIC of primary ion 577.0828 [M-H] $[m/z]^{-}$; (**d**) Enhanced charge capacity (ECC) ion product for 577.0828 $[m/z]^{-}$; (**e**) A MS profile showing an extracted m/z value, 577.0381 $[m/z]^{-}$; (**f**) Fragments from collision-induced dissociation (CID) of 577.0358 showing 109.0231, 125.0156, 137.0162, 149.0119, 163.0261, 165.0054, 179.0335, 191.0167, 201.0358, 241.0249, 269.0177, 289.0338, 404.0440, and 439.0388 $[m/z]^{-}$ (Table 4).

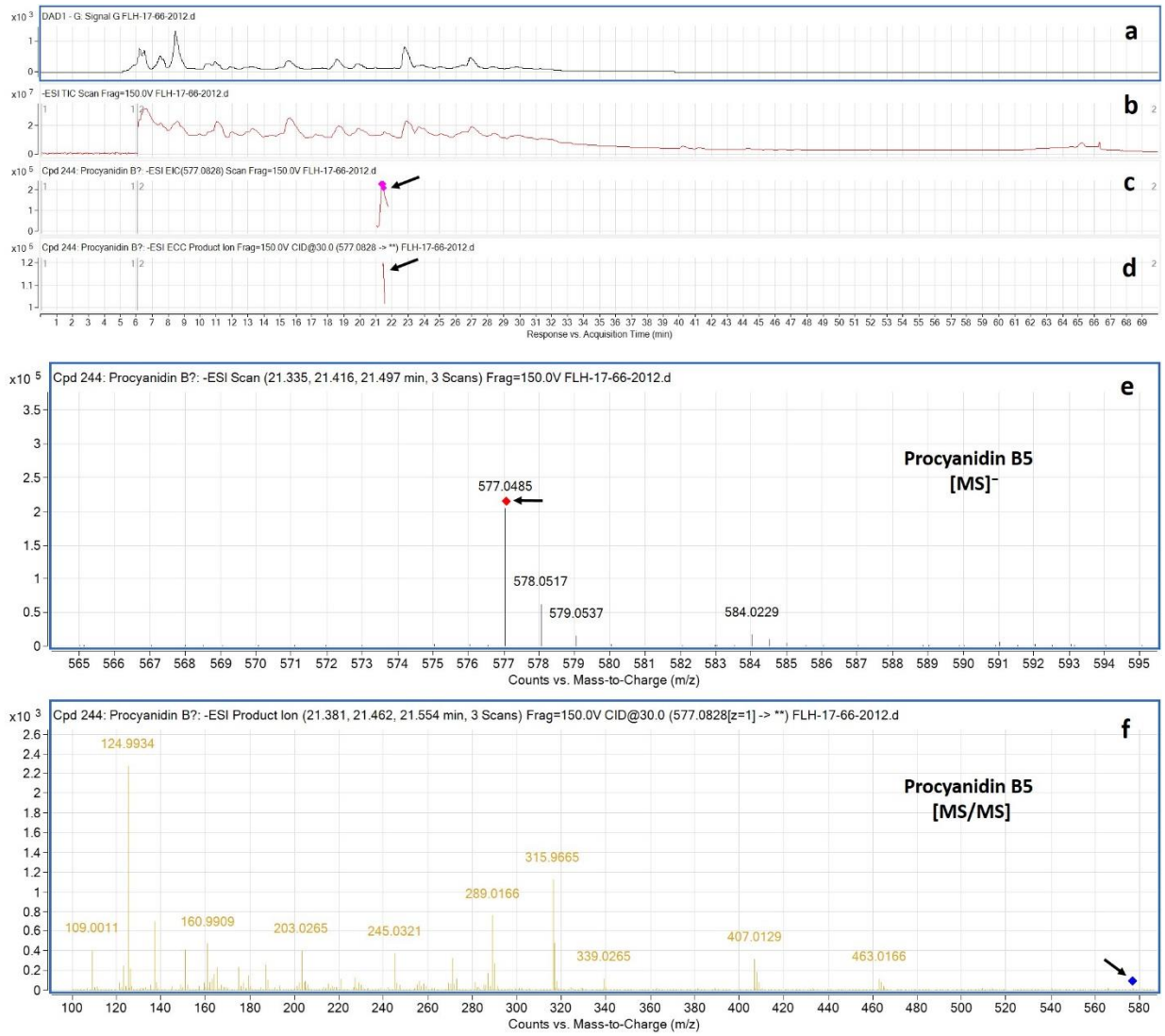

Supplementary Figure 3.19: Extracted ion chromatogram (EIC) of primary mass spectrum (MS1) and m/z features of secondary ion fragments (MS2) derived from LC-MC/MS annotate this peak to be Procyanidin B5, (MW, 578.52). (**a**) Chromatogram of FLH 17-66 extracts (2012) recorded at 280 nm absorbance; (**b**) Total ion chromatogram of FLH 17-66 extract (2012); (**c**) EIC of primary ion 577.0828 [M-H] $[m/z]^{-}$; (**d**) Enhanced charge capacity (ECC) ion product for 577.0828 $[m/z]^{-}$; (**e**) A MS profile showing an extracted m/z value, 577.0485 $[m/z]^{-}$; (**f**) Fragments from collision-induced dissociation (CID) of 577.0485 showing 109.0011, 124.9934, 136.9912, 151.0032, 179.0013, 189.0008, 203.0265, 227.0197, 245.0321, 270.9718, 289.0166, 315.9665, 339.0265, and 407.0129 $[m/z]^{-}$ (Table 4).

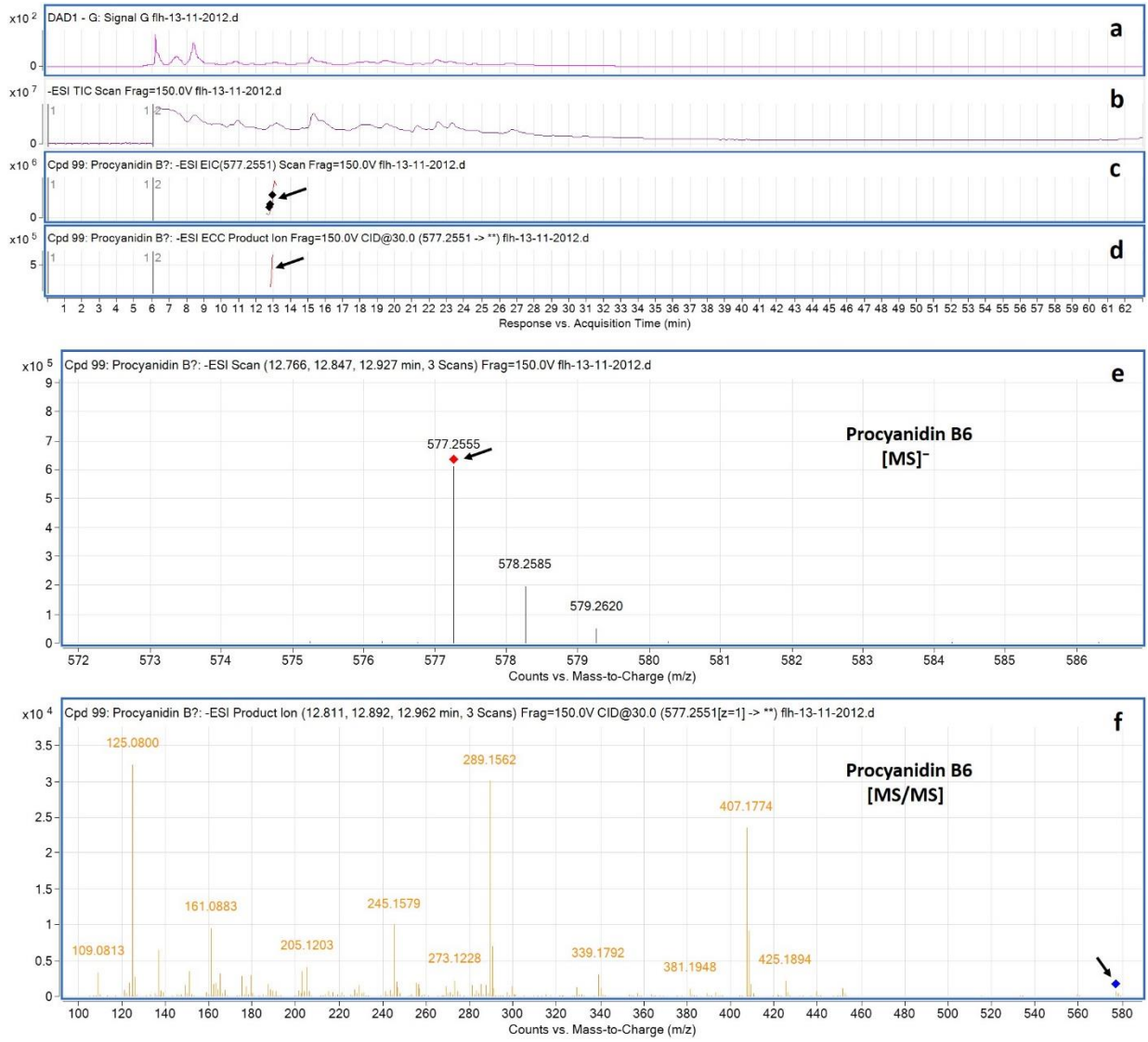

Supplementary Figure 3.20: Extracted ion chromatogram (EIC) of primary mass spectrum (MS1) and m/z features of secondary ion fragments (MS2) derived from LC-MC/MS annotate this peak to be Procyanidin B6, (MW, 578.52). (**a**) Chromatogram of FLH 13-11 extracts (2012) recorded at 280 nm absorbance; (**b**) Total ion chromatogram of FLH 13-11 extract (2012); (**c**) EIC of primary ion 577.2551 [M-H] $[m/z]^{-}$; (**d**) Enhanced charge capacity (ECC) ion product for 577.2551 $[m/z]^{-}$; (**e**) A MS profile showing an extracted m/z value, 577.2555 $[m/z]^{-}$; (**f**) Fragments from collision-induced dissociation (CID) of 577.2555 showing 109.0813, 125.0800, 137.0824, 151.1011, 161.0883, 165.0837, 179.1019, 187.1074, 205.1203, 229.1273, 245.1579, 289.1562, 339.1792, 407.1774 and 425.1894 $[m/z]^{-}$ (Table 4).

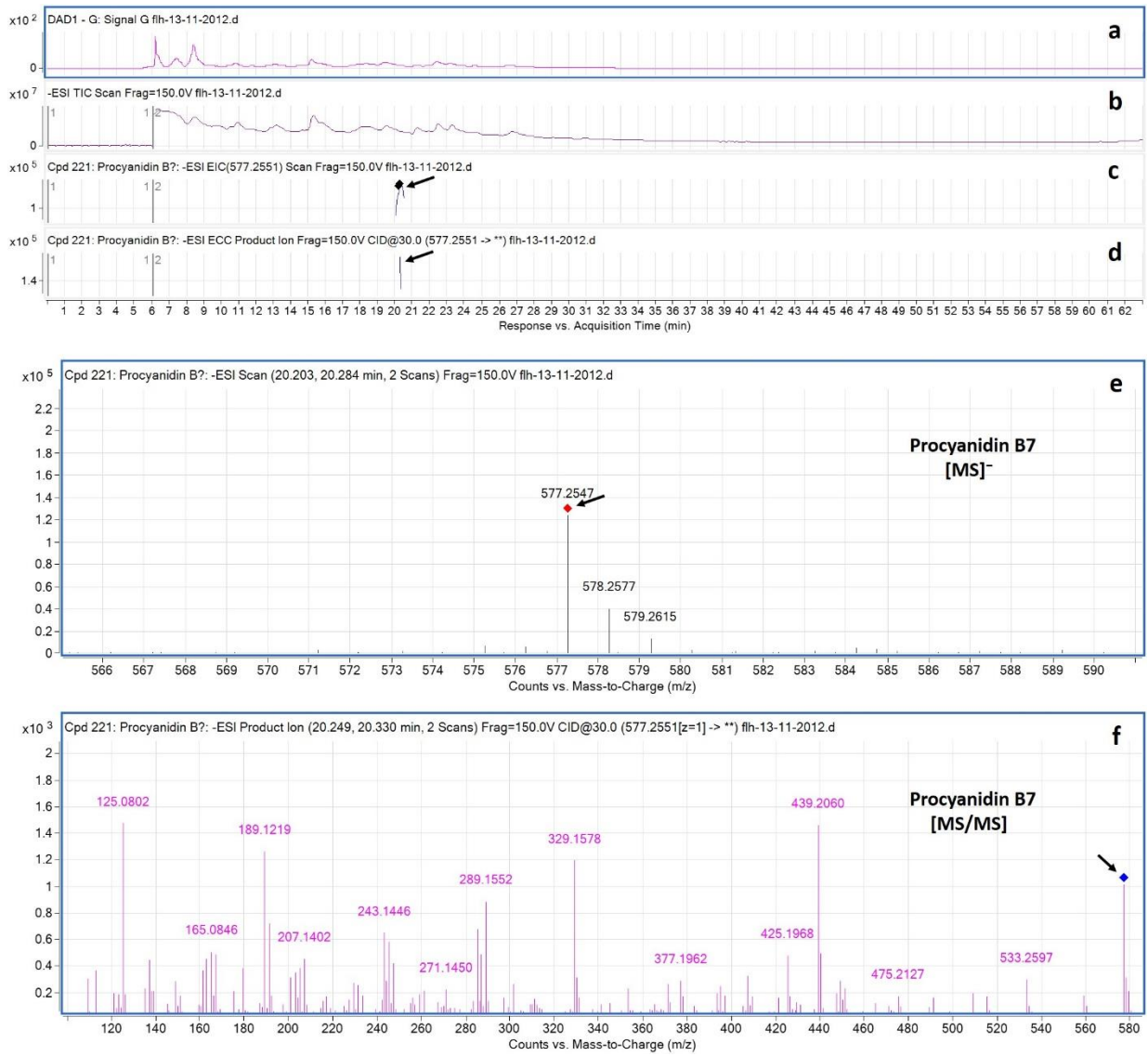

Supplementary Figure 3.21: Extracted ion chromatogram (EIC) of primary mass spectrum (MS1) and m/z features of secondary ion fragments (MS2) derived from LC-MC/MS annotate this peak to be Procyanidin B7, (MW, 578.52). (**a**) Chromatogram of FLH 13-11 extracts (2012) recorded at 280 nm absorbance; (**b**) Total ion chromatogram of FLH 13-11 extract (2012); (**c**) EIC of primary ion 577.2551 [M-H] $[m/z]^{-}$; (**d**) Enhanced charge capacity (ECC) ion product for 577.2551 $[m/z]^{-}$; (**e**) A MS profile showing an extracted m/z value, 577.2547 $[m/z]^{-}$; (**f**) Fragments from collision-induced dissociation (CID) of 577.2547 showing 109.0793, 125.0802, 137.0822, 165.0846, 179.1029, 189.1219, 243.1446, 271.1450, 289.1552, 329.1578, 407.1900, 425.1968, and 439.2060 $[m/z]^{-}$ (Table 4).

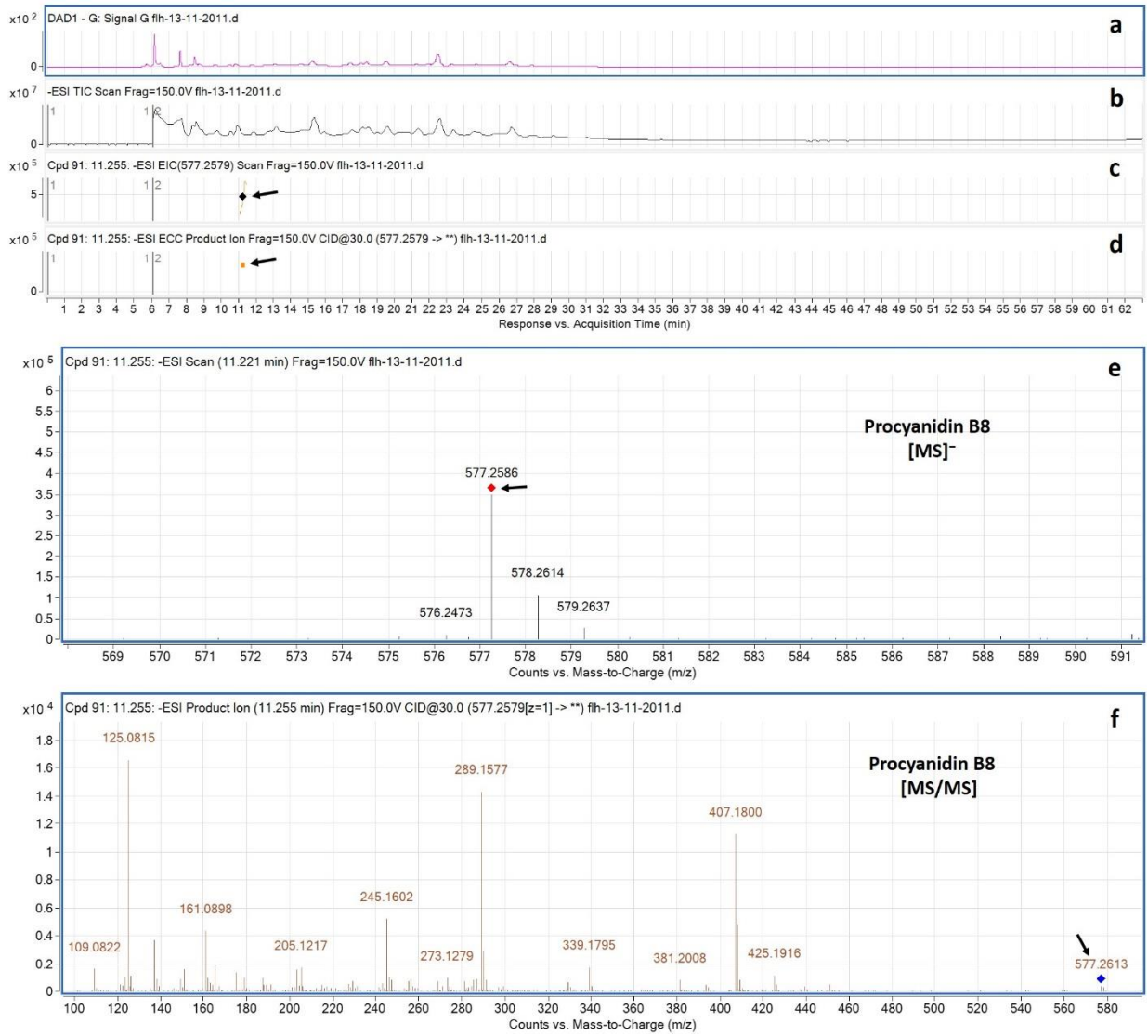

Supplementary Figure 3.22: Extracted ion chromatogram (EIC) of primary mass spectrum (MS1) and m/z features of secondary ion fragments (MS2) derived from LC-MC/MS annotate this peak to be Procyanidin B8, (MW, 578.52). (**a**) Chromatogram of FLH 13-11 extracts (2011) recorded at 280 nm absorbance; (**b**) Total ion chromatogram of FLH 13-11 extract (2011); (**c**) EIC of primary ion 577.2579 [M-H] $[m/z]^{-}$; (**d**) Enhanced charge capacity (ECC) ion product for 577.2579 $[m/z]^{-}$; (**e**) A MS profile showing an extracted m/z value, 577.2586 $[m/z]^{-}$; (**f**) Fragments from collision-induced dissociation (CID) of 577.2613 showing 109.0822, 125.0815, 137.0833, 151.1016, 161.0898, 205.1217, 245.1602, 289.0349, 289.1577, 339.1795, and 407.1800 $[m/z]^{-}$ (Table 4).

CHAPTER 4

An Efficient Protocol for the Extraction of Pigment-Free Active Polyphenol Oxidase and Soluble Proteins from Plant Cells

Seyit Yuzuak and De-Yu Xie*

Department of Plant and Microbial Biology, North Carolina State University, Raleigh, NC 27695

*Corresponding author: dxie@ncsu.edu

Abstract

Background

The elimination of brownish pigments from plant protein extracts has been a challenge in plant biochemistry studies. Although numerous approaches have been developed to reduce pigments for enzyme assays, none have been able to completely remove pigments from plant protein extracts for biochemical studies.

Results

A simple and effective protocol was developed to completely remove pigments from plant protein extracts. Proteins were extracted from red anthocyanin-rich transgenic and greenish wild-type tobacco cells cultured on agar-solidified MS medium. Protein extracts from these cells were brownish or dark color due to the pigments. Four approaches were comparatively tested to show that diethylaminoethyl (DEAE)-Sephadex anion exchange gel column was effective for completely removing pigments to obtain transparent pigment-free protein extracts. Millipore

Amicon® Ultra 10K cut-off filter unit was used to effectively desalt proteins. Moreover, the removal of pigments significantly increased soluble protein recovery. Furthermore, enzymatic assays using catechol as a substrate coupled with high-performance liquid chromatography analysis demonstrated that the pigment-free polyphenol oxidase (PPO) were active, and the complete removal of pigments enhanced catalytic activity of PPO.

Conclusion

A simple and effective protocol was successfully developed to not only completely remove anthocyanin and polyphenolics-derived quinone pigments from plant protein extracts but also to increase the final recovery of total soluble active proteins. This robust protocol will enhance plant biochemical studies using native proteins.

Key words: Plant protein extraction-anthocyanin-polyphenolics-quinones-pigments-diethylaminoethyl (DEAE)-Sephadex anion exchange gel column

Introduction

Plant protein extraction (PPE) is the first essential step in plant biochemistry studies. In the past, a major research effort was focused on the development of extraction methods to yield high quality of plant proteins (Lugg 1939; Lugg and Weller 1944; Jennings and Watt 1967; Anderson 1968; McCown, Beck et al. 1968; Nanda, Kondos et al. 1975; Wu, Xiong et al. 2014; Parkhey, Chandrakar et al. 2015; Sari, Mulder et al. 2015). To date, numerous protocols have been reported for protein extraction from different plant species and materials for variable biochemical study purposes, such as enzyme characterization, Krebs cycle and other metabolic pathway analyses, and proteomics (Hulme and Wooltorton 1962; Hulme, Jones et al. 1963; Hulme, Jones et al. 1964; Jones, Hulme et al. 1964; Loomis and Battaile 1966; Nanda, Kondos et al. 1975; Pierpoint 1996; Casado-Vela, Selles et al. 2005; He and Wang 2008; Peng, Zhu et al. 2012; Wu, Xiong et al. 2014; Lledias, Hernandez et al. 2017). Moreover, the past improvements of PPE for native protein research have provided fundamental knowledge to understand biochemical processes from molecular and cellular levels to physiology and ecology (Hulme and Wooltorton 1962; Jones, Hulme et al. 1964; Luttge and Ratajczak 1997; Harborne 1999; Buchanan, Gruissem et al. 2000; Havelund, Thelen et al. 2013). In fact, the past efforts also indicate that more effective PPE methods will be necessary to refine our current understanding of plant biochemical events that occur in single cells, tissues, development, and different environmental conditions.

One of the main past PPE efforts has been focusing on developing effective techniques to remove plant secondary metabolites from protein extracts (Anderson 1968; Tsuji, Mori et al. 1985; Wang, Tai et al. 2008; Peng, Zhu et al. 2012; Chua, Abd Rahman et al. 2014; Lledias, Hernandez et al. 2017), especially plant polyphenolics. Plant polyphenolics, a large family of

plant secondary metabolites, are characterized by diverse structures, such as proanthocyanidins, flavanols, and anthocyanins (Dewick 1988; Harborne and Grayer 1988; Porter 1988; Shao and Bao 2015; Taranto, Pasqualone et al. 2017).

Plant polyphenolics commonly exist in the plant kingdom. When plant tissues are used to extract proteins, the presence of polyphenolics is a common problem because during enzyme extraction, the easy oxidation of polyphenolics always leads to light to severe browning pigmentation (Hulme and Wooltorton 1962; Anderson 1968; Loomis 1969; Sullivan 2015; Jiang, Kumar et al. 2017; Taranto, Pasqualone et al. 2017). The browning pigmentation can commonly lead to difficulties in enzyme assays because polyphenolics and their derived pigments can bind proteins either reversibly via hydrogen bonding or irreversibly via covalent linkage, thus resulting in extreme difficulty in obtaining pigment-free crude extracts and the inactivation of enzymes (Loomis and Battaile 1966; Anderson 1968; Loomis 1969; Loomis 1974).

To obtain an appropriate quality of plant enzyme extracts, different chemical reagents and methods have been tested to remove polyphenolics and quinones to overcome this browning pigmentation or other pigmentation problems (Loomis and Battaile 1966; Andersen and Sowers 1968; Loomis 1969; Loomis 1974). Common chemical reagent examples tested previously and being used currently include vitamin C, β-mercaptoethanol, dithiothreitol, polyvinylpyrrolidone (PVP), polyvinylpolypyrrolidone (PVPP), and others (Loomis and Battaile 1966; Toth and Pavia 2001; Peng, Zhu et al. 2012; Cimini, Marconi et al. 2014). Accordingly, numerous promising methods for the reduction of browning pigmentation have been optimized for different purposes. For example, PVPP and PVP are commonly used in protein extractions for enzyme assays, given that both have been reported to remove brownish pigments from protein extracts (Hulme, Jones et al. 1964; Hulme, Jones et al. 1966; Anderson 1968; Loomis 1969; Loomis 1974; Burton and

Kirchmann 1997; Toth and Pavia 2001; Khatun, Ashraduzzaman et al. 2012; Cimini, Marconi et al. 2014; Jiang, Kumar et al. 2017). However, to our knowledge, none of the chemical reagents can completely remove anthocyanins and polyphenolics-derived brownish pigments in plant enzyme extracts.

In this study, we report the development of an effective protocol to obtain pigment-free plant enzyme extracts. We have developed anthocyanin-rich transgenic tobacco calli to characterize metabolism-programmed biochemical processes (Zhou, Zeng et al. 2008). Extracts of soluble proteins are highly abundant with anthocyanin, oxidized anthocyanin derivatives, and other polyphenolics and quinones, which cause deeply dark brownish color. To remove all pigments, a quick and effective protocol has been developed to obtain high quality pigment-free colorless protein extracts. Further enzyme assays for polyphenol oxidase (PPO) activity demonstrate that this robust protocol recovers active enzymes.

MATERIAL and METHODS

Reagents and chemicals

Reagents and chemicals used in our experiments include: acetonitrile (LC-MS grade, cat#: 9829-03), glacial acetic acid (HPLC grade, cat#: 9515-03), and methanol (LC-MS grade, cat#: 9830-03) from Avantor® (Center Valley, PA 18034, USA); catechol (1,2-dihydroxybenzene, ≥99% cat#: 135011), polyvinylpolypyrrolidone (PVPP, cross-linked ~110 μm particle size, cat#: 77627), ammonium persulphate (APS, ≥98% , cat#: A3678), and diethylaminoethyl (DEAE)-Sephadex A-25 anion exchange (cat#: A25120) from Sigma-Aldrich® (St. Louis County, MO 63178, USA); Tris powder (≥99.8%, cat#: 17926) and sodium

dodecyl sulfate (SDS, cat#: BP166-500) from Fisher Scientific (Waltham, MA 02451, USA); acrylamide/bisacrylamide (37.5:1) 30% solvent (cat#: J61505) and ammonium sulphate [$(NH_4)_2SO4$, 99.0 % min, cat#: A11682] from Alfa Aesar (Reston, VA 20191 USA); polyvinylpyrrolidone (PVP, white powder, cat#: 02102787) from MP Biomedicals (Solon, OH 44139, USA); ethylenediaminetetraacetic acid (EDTA, cat#:BDH9232) from VWR Analytical (Radnor, PA 19087, USA); bovine serum albumin (BSA, 10mg/mL, cat#: R3961) from Promega Bio Sciences (San Luis Obispo, CA 93401, USA); tetramethylethylenediamine (TEMED, cat#:1610801) and R250 Coomassie Brilliant Blue (cat#: 1610400) from Bio-Rad (Hercules, CA 94547,USA); β-mercaptoethanol (cat#: 41300000-1) from bioWORLD (Dublin, OH 43017, USA); ethyl acetate (cat#: EX0240-3) from EMD Millipore (Burlington, MA 01803, USA), and bromophenol blue (cat# 151350250) from Acros Organics (New Jersey, USA).

Red and green tobacco calli and cells

We have developed different transgenic versus wild-type cell lines to understand anthocyanin biosynthesis in callus and cell cultures (Zhou, Zeng et al. 2008). Red cell lines were cloned from *PAP1* (*Production of Anthocyanin Pigment 1* encoding a R2R3-MYB transcription factor) transgenic tobacco (*Nicotiana tabacum* var. Xanthi) plants. One cell line, namely 6R that overexpresses *PAP1* and yields high production of anthocyanins (Zhou, Zeng et al. 2008), has been continuously subcultured for different research purposes. This cell line (Fig. 1 a) was used for protein extraction in this study. In addition, different cell lines were developed from wild-type tobacco plants as controls (Zhou, Zeng et al. 2008). One greenish wild type cell line, namely P3 (Fig. 1 c), was used for protein extraction in this study. Callus subculture and medium components were as described previously (Zhou, Zeng et al. 2008). In brief, calli were

aseptically inoculated onto phytoagar-solidified 0.8% (w/v) Murashige and Skoog (MS) basal medium (pH 5.7) containing 0.25 mg L^{-1} 2,4-dichlorophenoxyacetic acid, 0.10 mg L^{-1} kinetin, and 30 g L^{-1} sucrose in petri dishes. All petri dishes were placed in a growth chamber facilitated with a 22 °C temperature and a 16 h/8 h light/dark photoperiod. Calli cultured for 15 days were collected, immediately frozen in liquid nitrogen, grounded into a fine powder, and stored at -80 °C until use.

Total crude protein extraction

Soluble proteins were extracted from powdered 6R and P3 samples following these steps. The extraction buffer was composed of 0.1 M Tris-Cl (pH 7.0) and 10 mM EDTA. Five grams of fresh powdered sample were suspended in 30 mL of a protein extraction buffer contained in a 50 mL polyethylene centrifuge tube. The tube was vortexed for one min thoroughly, sonicated for 15 min in a Fisher Scientific FS60H Ultrasonic Cleaner, and then shaken at 100 rpm for 15 min at 4°C. The tube was centrifuged for 15 min at 6,500 rpm (5,820 rcf) on Beckman Coulter Avanti JXN-26 centrifuge with JA-17 rotor. The resulting supernatant with total soluble proteins was transferred to a new tube (Fig. 1 b and d). All protein extracts from P3 cells were brownish due to polyphenol oxidation. All protein extracts from 6R cells were deeply dark brownish due to high production of anthocyanins and oxidation of other polyphenolics. All protein extracts were stored at 4 °C for the following experiments.

Method I: removal of pigment with polyvinylpyrrolidone

Polyvinylpyrrolidone (PVP) was used to remove pigments from crude protein extracts (Fig. 2 a). Three steps, I-1, 2, and 3, were carried out using this method. The I-1 step was the treatment of protein extracts with PVP. PVP (60, 120, and 180 mg) was added into nine mL of crude protein extract contained in a 15 mL tube. The tubes were shaken for 15 min at 100 rpm at room temperature and then placed on ice for an additional 30 min. The I-2 step was the centrifugation of tubes. All tubes were centrifuged at 15,000 rpm (31,000 rcf) for 10 min at 4°C. The resulting supernatant in each tube was transferred to a new one. The I-3 step was the reduction of protein extract volume and further removal of pigments using a 15 mL Millipore Amicon® Ultra 10K cut-off filter unit. An approximately nine ml protein extract was pipetted to a cut-off filter unit. The filter unit was centrifuged at 4,000 rpm (3,220 rcf) for 30 min at 4°C. Salt and certain pigments were filtered to the bottom of the filter unit and then removed to a waste container. An approximately 1.0 mL protein extract remained in the upper section of the filter unit. This procedure removed lower molecular weight metabolites including certain pigments and was repeated several (4-5) times by adding fresh buffer until no pigments were filtered to the bottom. The protein extract volume was maintained to 1.0 mL, transferred to a 1.5 mL Eppendorf tube, and then stored at 4 °C until use.

Methods II and III: removal of pigment with polyvinylpolypyrrolidone

Polyvinylpolypyrrolidone (PVPP) was tested to remove pigments in crude protein extractions in methods II and III. Method II had three steps, II-1, 2, and 3 (Fig. 2 a). The II-1 step was addition of PVPP into crude protein extracts. Three amounts of PVPP (60, 120, and 180 mg)

were tested. PVPP was added into nine mL of crude protein extracts as described in the I-1 step of PVP treatment. The II-2 was the same as the I-2 step described above. The II-3 step was also the same as the I-3 step described above.

Method III had four steps, III-1, 2, 3, and 4 (Fig. 2 a). The III-1 and 2 steps were the same as the II-1 and II described above. The III-3 step was precipitation of crude proteins using ammonium sulfate [$(NH_4)_2SO_4$]. After nine mL of protein extracts were obtained from the III-2 step and transferred to a new tube, three amounts of $(NH_4)_2SO_4$ (2.0, 4.0, and 5.0 g) were tested for precipitation. $(NH_4)_2SO_4$ was added into the tube until completely dissolved with a magnate stirring bar at 4°C. The tube was centrifuged at 15,000 rpm (31,000 rcf) for 10 min at 4°C. After the supernatant was removed, the precipitated proteins were completely dissolved in nine mL of 0.02 M (pH 7.0) Tris-HCl buffer. The III-4 step was to further remove $(NH_4)_2SO_4$ and pigments. The resulting protein extract from the III-3 step was gently transferred to a 15 mL Millipore Amicon® Ultra 10K cut-off filter unit to remove salts and certain pigments as described in the I-3 step above. The resulting upper protein extract was pipetted into a new 1.5 mL Eppendorf tube and then stored at 4°C until use.

Method IV: removal of pigments using DEAE-Sephadex gel

Method IV included column preparation and three steps of pigment removal, IV-1, 2, and 3 (Fig. 2 b). DEAE-Sephadex A-25 anion exchange matrix was used to prepare pigment removal columns. One gram of matrix powder was fully suspended in 25 mL 0.02 M Tris-HCl extraction buffer (pH 7.0) and then incubated in boiling water for one hour. Ten mL of suspended matrix mix including 1.0 gram of matrix powder was cooled down to room

temperature and then loaded into a new 15 mL polyethylene syringe (height: 8.0 cm and diameter: 1.5 cm), the outlet of which was appropriately inserted in a cotton ball. After most of the buffer was flown through at a rate of 1.0 mL/min, 30 mL 0.02 M Tris-Cl (pH 7.0) was added to equilibrate and wash the matrix. This flow-through of buffer was not stopped until approximately 1.0 mL was left above the top of the matrix. No air bubble was allowed through matrix. The column was ready for the removal of the pigment described below.

The IV-1 step was the reduction of the protein extract volume. Nine mL of protein extract was reduced to 1.0 mL using a 15 mL Millipore Amicon® Ultra 10K cut-off filter unit, the procedure of which was as described above in the I-3 step. After this step, the volume of protein extract was reduced to approximately 1.0 mL. The IV-2 step was the removal of pigments using the DEAE-Sephadex A-25 anion exchange gel column prepared. Concentrated protein extract was loaded on the top of the column and allowed to completely flow into the matrix with a rate of 1.0 mL/min. Four elution buffers, 0.0 M, 0.10 M, 0.20 M and 0.25 M NaCl dissolved in 0.02 M Tris-HCl (pH 7.0), were prepared to elute proteins. For each elution buffer, 30 mL was sequentially used to elute proteins at a flow rate of 1.0 mL/min. The flow-through buffer was collected from each elution and then combined together to obtain approximately 120 mL of collection. The step IV-3 was that this final protein collection was concentrated and desalted using a 15 mL Millipore Amicon® Ultra 10K cut-off filter unit as described above in the I-3 step. After concentration, the final protein extract volume was adjusted to be 1.0 mL and then stored at 4 °C until use.

Measurement of protein concentrations

The total protein concentration was measured using the Bio-Rad Bradford protein assay after protein extracts were adjusted to 1.0 mL in each step in methods I, II, III, IV. Four µL of protein extract concentrated was added to 76 µL 0.02 M Tris-HCl (pH 7.0) buffer and then thoroughly mixed to obtain 80 µL mixture, from which 20 µL was added to 980 µL (1X) Bradford buffer contained in a 1.5 mL Eppendorf tube. The mixture was gently and thoroughly mixed via pipetting and incubated for 5 min at room temperature. The absorbent values of mixtures was recorded at 595 nm on a NanoDrop™ 2000C Spectrophotometer (Thermo Fisher Scientific, USA). In addition, bovine serum albumin (BSA) was used to develop a standard curve to calculate protein concentrations.

Protein analysis using sodium dodecyl sulfate polyacrylamide gel electrophoresis

Protein extract quality was examined using sodium dodecyl sulfate polyacrylamide gel electrophoresis (SDS-PAGE). SDS-PAGE (12.5 %) was freshly prepared prior to electrophoresis. The separation gel was prepared using 2.9 mL of 30% acrylamide/bisacrylamide solvent, 1.75 mL of 4X Tris/0.4% SDS (pH 8.8), 2.4 mL of dH_2O, 40 µL of 10% (w/v) ammonium persulphate (APS), and 10 µL of tetramethylethylenediamine (TEMED). The stacking gel was prepared using 312 µL of 30% acrylamide/bisacrylamide solvent, 750 µL of 4X Tris/0.4% SDS (pH 6.8), 1.9 mL of dH2O, 20 µL of 10% APS, and 8.0 µL of TEMED. The size of the comb created 40 µL volume wells for sample loading. SDS-PAGE was prepared using a caster (10 x 8 cm). SDS-PAGE was then installed in a Bio-Rad Mini Protean® Tetra Cell Electrophoresis apparatus (Bio-Rad, USA).

Twenty µg of the protein sample was mixed with 10 uL of the protein loading buffer, which was composed of 25% glycerol, 10% SDS, 0.5 M Tris-Cl (pH 7.0), 0.15 µM bromophenol blue (Bio-Rad), dH_2O, and 0.15 mM β-mercaptoethanol (bioWORLD). The resulting mixture was incubated for 5 min at 95°C. After samples were cooled down to room temperature, they were loaded to SDS-PAGE. The polyacrylamide gel and 1 L of 1 X Tris-Glycine-SDS running buffer including 3.03 g of Tris, 14 g of Glycine and 5.0 mL of 20% SDS were placed in an electrophoresis chamber. In addition, 10 µg of Bio-Rad Precision Plus Protein™ ladder was loaded to a molecular weight standard. The electrodes of the electrophoresis apparatus was wired to a power source. The voltage of electrophoresis was set at 70 Volt for 25 min and then increased to 120 Volt for 90 min. After the completion of electrophoresis, the gel was rinsed using dH_2O and then placed into in a glass tank containing a protein staining buffer, which was prepared using 450 mL of dH_2O, 450 mL of MeOH, 100 mL of glacial acetic acid (9:9:2, V:V:V) and 1.0 g of R250 Coomassie Brilliant Blue (Bio-Rad). The staining tank was placed on a shaker with a speed of 100 rpm for overnight gel staining. The stained gel was de-stained with a buffer consisting of 500 mL of dH_2O, 400 mL of MeOH, and 100 mL of glacial acetic acid (5:4:1 V/V/V). After excess dye was removed, the gel was photographed using the 8-megapixel camera of an Iphone 5S or placed in a G-Box F3 Gel Doc System (Syngene) for photographing better images.

Polyphenol oxidase assay and high performance liquid chromatograph analysis

Polyphenol oxidase (PPO) activity was assayed using catechol, a common *o*-diphenol substrate. Catechol (99.99%) was freshly dissolved in methanol to prepare a 1.0 M stock solution. An enzymatic reaction was carried out in 1.0 mL volume, which was composed of 899

µL of 0.02 M Tris-HCl (pH 7.0) buffer, 100 µL of protein extracts (125 µg) after the treatment of pigment removal from methods I, II, III, and IV, and 1.0 µL of 1.0 M catechol (110 µg) contained in a 15 mL polyethylene tube. In addition, control reactions without catechol or a substituting protein extract with 100 µL buffer or BSA (125 µg) were performed. Each assay was repeated three times. All reactions were incubated for 45 min at room temperature and stopped by adding three mL of ethyl acetate (EA). After adding EA, each tube was thoroughly vortexed for two min and then centrifuged at 8,000 rpm (8,820 rcf) for five min at 22°C. The resulting upper ethyl acetate phase was gently transferred to a new tube and dried using a savant speed vacuum concentrator. The remaining pellet was dissolved in 200 µL of methanol (LC/MS grade) for high performance liquid chromatography (HPLC) analysis.

HPLC analysis was completed on a Shimadzu LCMS-2010 EV instrument. Metabolites in samples were separated on an Eclipse XDB-C18 analytical column (250 mm × 4.6 mm, 5.0 µm, Agilent, Santa Clara, CA, USA). The mobile phase solvents used for metabolite elution included 1% acetic acid in water (solvent A, HPLC-grade acetic acid, LC/MS-grade water) and 100% acetonitrile (solvent B, LC/MS-grade). A gradient solvent system, which was developed to separate products, was composed of ratios of solvent A to B: 80:20 (0–5 min), 80:20 to 70:30 (5–10 min), 70:30 to 65:35 (10–20 min), 65:35 to 60:40 (20–30 min), 60:40 to 55:45 (30–40 min), 55:45 to 50:50 (40–45 min), 50:50 to 48:52 (45–50 min), 48:52 to 45:55 (50–55 min), 45:55 to 40:60 (55–58 min) and 40:60 to 10:90 (58–58.5 min). After each elution, the column was washed for 11.5 min with a mixture of elution buffer including 20% of solvent B and 80% solvent A. The flow rate was 0.4 mL/min and the injection volume was 1.0 uL. Chromatographs of metabolites were recorded from 190 to 800 nm. Prior to and after enzymatic reactions, peak

values of catechol were recorded at 280 nm for each reaction and used to evaluate PPO catalytic activity.

PPO assay using ultra-violet spectrophotometer

PPO activity in crude protein extracts from four methods were compared using absorbance values of enzymatic products. Crude proteins extracted from methods I, II, III, and IV were used in this assay. Crude proteins extracted using methods I, II, and III and then using method IV were also used in this assay. The total volume of incubation reactions for PPO activity was 1.0 mL including 0.02 M Tris-Cl (pH 7.0) buffer, 20 µg of protein extracts, and 100 mM catechol. The reaction in each tube did not start until each crude protein extract was added. After crude protein was added, each tube was immediately placed in a Thermo Electron Corporation Spectronic Helios Alpha Beta UV-Visible Spectrophotometer to measure the absorbance value (ABS) at 420 nm (A_{420nm}), the wavelength of which has been used to measure PPO activity (Chi, Bhagwat et al. 2014). ABS was recorded every 30 seconds for 5 min at 25 °C. Dynamic ABS values were used to evaluate PPO activity. This enzymatic assay for each crude protein extract was repeated three times, each with three technical replicates. Meanwhile, negative control reactions, including one combination of catechol and buffer only and the other combination of bovine serum albumin (BSA) protein and catechol, were carried out to record absorbance values and repeated three times. One unit of PPO activity was defined as the amount of enzyme necessary to change A_{420nm} in 0.001/min at 25 °C. The enzymatic activity was calculated as ABS units per minute.

Statistical analysis

Each pigment-removal experiment for Method I, II, III and IV was repeated at least five times. Each enzyme assay was repeated with three biological replicates, each with three technical replicates. All data were expressed as means ± standard deviations, and subjected to the statistical analyses by using Microsoft Excel software package (Microsoft Corp.). Student's *t* test was carried out to examine statistical significance at the 95% confidence level (p-value ≤ 0.05).

RESULTS and DISCUSSION

DEAE-Sephadex gel column produces pigment-free and transparent protein extracts

Crude protein extracts from greenish wild-type P3 calli and red transgenic 6R calli were brownish and extremely dark brownish, respectively (Fig. 1 b and d). The dark brownish color in 6R protein extracts resulted from water-soluble anthocyanins and oxidation of other polyphenolics. The brownish pigmentation in P3 protein extracts likely resulted from the oxidation of polyphenolics. To remove these pigments in protein extracts, we compared four methods (Fig. 2). Methods I and II were designed to use PVP and PVPP, respectively. These two reagents have been commonly reported for the removal of pigments from protein extracts. In addition, we used a Millipore Amicon® Ultra 10K cut-off filter unit to remove small molecules including pigments. The resulting data showed that the two combinations of PVP (Method I) and PVPP (Method II) with the Millipore Amicon® Ultra 10K cut-off filter unit were ineffective for removing pigments from protein extracts (Fig. 3 a and b). In addition, a combination of PVPP, $(NH_4)_2SO_4$ precipitation, and the Millipore Amicon® Ultra 10K cut-off filter unit was tested in

our method III. This method was also unable to improve pigment removal from protein extracts (Fig. 3 c).

Method IV is a new approach. A simple DEAE-Sephadex gel A-25 column was prepared to remove pigments. After dark brownish protein extracts from red 6R calli were loaded onto the column, all pigments were bound to a gel matrix (Supplementary Fig. 1 a). In addition, brownish pigments in P3 protein extracts were bound to a gel matrix. The resulting protein extracts from both P3 and 6R calli were colorless and transparent (Fig. 3 d). This result demonstrated that method IV was effective to remove all pigments from protein extracts from two types of tissues. Furthermore, dark protein extracts treated using methods I, II, and III (Fig. 3 a, b, and c) were also loaded onto DEAE-Sephadex gel A-25 gel columns. All pigments in these dark extracts were also completely removed from proteins (Fig. 3 e and Supplementary Fig. 1 b). These results demonstrated that the new method IV using DEAE-Sephadex gel A-25 was highly effective for removing of pigments from protein extracts (Fig. 3).

Protein quality and production

All protein extracts treated for pigment removal with methods I, II, III, and IV (Fig. 3 a-e) were examined using SDS-PAGE to check band profile quality. Gels were photographed to compare protein band profiles. The resulting images showed that apparent protein bands were obtained from protein extracts treated with method IV (Fig. 4). There was no pigment migrating contamination in the gels. By contrast, images showed that proteins from extracts treated with methods I, II, and III were darkly smeared in gel. Pigment migrating contamination was highly severe in gels. After these extracts treated with methods I, II, and III were further re-treated with

the new method IV to obtain pigment-free proteins, gel images showed that the severe smearing problem was completely eliminated to result in apparent protein band profiles. Accordingly, pigments in the protein extracts from methods I, II, and III caused the smearing problem, which was solved by the new method IV. In conclusion, all results demonstrate that the new method IV using DEAE-Sephadex gel is effective to remove pigments to obtain high quality proteins.

Protein concentrations were measured to calculate productions recovered from the new method IV. It was interesting that after the removal of pigments, the total soluble protein concentrations from both P3 and 6R calli were significantly increased (Table 1). The yield of the total soluble proteins recovered from P3 and 6R calli were increased 17% and 65%, respectively. Accordingly, the removal of pigments recovered more soluble proteins. Moreover, protein productions were measured for extracts treated with methods I, II, and III and then re-treated with the new method IV (Fig. 3 a-c). The removal of pigments with method IV also significantly increased recovery of total soluble proteins from those extracts treated with methods I, II, and III. These results demonstrate that the new method IV using DEAE-Sephadex gel is effective to recover more soluble proteins bound with pigments, thus increases the final yield.

Polyphenol oxidase activity

Our goal is to remove pigments to obtain high quality soluble proteins with biochemical activities, such as active enzymes. Browning pigmentation occurring during protein extractions has been reported to result from oxidation of phenolics or polyphenolics catalyzed by polyphenol oxidase (PPO) (Yoruk and Marshall 2003; Queiroz, Lopes et al. 2008; Sullivan 2015). We hypothesized that the pigment-free protein extracts had PPO activity. Given that catechol, an

ortho-diphenol, is the commonest substrate of PPO (Sisler and Evans 1958; Mayer and Harel 1979; Yoruk and Marshall 2003), we used this metabolite as a substrate to test PPO activity in the pigment-free protein extracts. When an incubation of a pigment-free protein extract listed in Fig. 3 and catechol started at room temperature, a yellowish pigmentation immediately occurred in the reaction. As the incubation continued, the pigmentation apparently changed to deep yellow and then brown. However, these yellowish and brownish pigmentations were not observed in control experiments. To understand the formation of metabolites from the incubation, HPLC was performed to reveal metabolite profiles. The resulting HPLC data showed that in addition to catechol detected at 16.53 min, three different major peaks were detected at 10.17, 17.71, and 24.91 min (Fig. 5 a). However, these three peaks were not detected from control incubations. Although we did not have standards, based on their UV-spectra features, we predict that these peaks are quinones from catechol. Furthermore, peak values of catechol in reactions prior to and after adding PPO were recorded at 280 nm. The resulting data showed that the concentrations of catechol were significantly reduced in the reactions (Fig. 5 b). These results demonstrate that pigment-free proteins are active for biochemical analysis.

Enhancement of PPO activity after removal of pigments

PPO activity in four types of different protein extracts from Methods I, II, III and IV were compared using product absorbance values recorded at 420 nm on a UV spectrophotometer. After reactions started, the live products' absorbance was recorded every 30 seconds to reflect initial velocity. The resulting data showed that the products' absorbance values were similar in crude protein extract non-treated and three types of protein extracts treated by Method I, II, and III (Fig. 5 c). After the removal of pigments using Method IV, PPO activity in all protein extracts

was significantly increased. These results demonstrate that the complete removal of pigments enhances PPO activity.

Discussion

DEAE-Sephadex powder is a type of bead-formed gel that is prepared by cross-linking between dextran and epichlorohydrin, and contains a diethylaminoethyl (DEAE) functional group inside the beads (Carnegie 1961). In the gel, the DEAE functional group is positively charged at the nitrogen (N) atom and the beads are coated with chloride as a counter ion. To date, different types of anion DEAE-Sephadex and other DEAE types have been successfully applied to isolate anion amino acids (Carnegie 1961; Schmidt 1962) and proteins for different study purposes (Leyko and Gondko 1963; Goodfriend, Perelmutter et al. 1965; Hiwada, Akutsu et al. 1966; Shinbuehring, Drefers et al. 1978; Rodriguez and Cumar 1990). However, to our knowledge, no studies have reported the use of anion DEAE-Sephadex column to remove plant pigments for protein extraction.

In our experiments, we compared four different methods, three of which are commonly used to reduce pigment concentrations in extracts as described in the introduction and results above. In the new method IV, we used DEAE-Sephadex A-25, because this type is an appropriate anion exchange choice to remove small molecules with less than 30,000 Dalton molecular weights. Anthocyanins and most quinones derived from polyphenolics either via PPO oxidation or via spontaneous oxidation follow in this molecular weight range. In the four methods compared, the new method IV using a simple DEAE-Sephadex anion exchange gel column showed the best result to obtain transparent and pigment-free protein extracts. All

brownish pigments were completely removed from all types of extracts (Fig. 3) to result in high quality proteins (Fig. 4). In addition, although we used buffers (pH 7.0) to heavily wash the column to maximize the release of bound proteins, all pigments remained in the top section of column (S-Fig. 1), indicating that this strong linkage most likely resulted from a covalently cross-linking between pigments and DEAE. Although it is unclear what reaction mechanism is behind this result, we hypothesize that all pigments likely covalently react with DEAE. One indirect evidence is all separation results using sephadex gel G25-100 alone tested in our experiments. When brownish protein extracts were loaded onto different sephadex column, all pigments were co-eluted with proteins. Moreover, the past photochemistry studies have provided certain evidence to support this hypothesis.

As written in the current textbooks, such as Plant Physiology (Taiz and Zeiger 2010), quinones are acceptors of electrons and play an essential electron transferring role in plant photosynthesis (Kurreck and Huber 1995; Rinyu, Nagy et al. 2001). Particularly, different photochemistry studies on benzoquinones and their semiquinone structures have demonstrated that quinones exist as anion radical ions in different solvents (including water) (Jones and Qian 1998; Esaka, Okumura et al. 2003; Sinnecker, Reijerse et al. 2004; Nelsen, Weaver et al. 2007; Rene and Evans 2012; Saini, Kaur et al. 2014). This type of anion charge is associated with hydrogen bonding reactions between quinones and others metabolites in chemical and biological processes (Flores, Isaacson et al. 2003; Sinnecker, Reijerse et al. 2004; Mohammad, Rauf et al. 2013). Based on these previous reports, we suggest that pigments in protein extracts are negatively charged to form anion ions in our experiments. When brownish protein extracts are loaded to anion DEAE-Sephadex column, DEAE can covalently link to anion pigments and then substitute those anion proteins and other soluble proteins extracted from plant cells. In the next

step, we expect to further undertake chemical experiments to elucidate the mechanism in the future.

The new method IV can increase the final recovery production of active soluble proteins after the complete removal of all pigments. In our experiments, we obtained brownish protein extracts (Figs. 1 and 3), which were completely soluble in buffer. However, pigments could not be removed by PVP and PVPP and Millipore Amicon® Ultra 10K cut-off filter unit used in methods I, II, and III (Fig. 3). This result suggests that anion pigments are most likely linked with cation proteins. In addition to our observation, numerous past experiments have demonstrated linkages between brownish quinones and proteins (Loomis and Battaile 1966; Loomis 1969; Loomis 1974). One linkage is reversibly cross binding via hydrogen bounding, and the other is irreversibly cross-linking via a covalently binding reaction (Anderson 1968; Loomis 1969). Both linkages decrease extraction efficiency for high quality proteins. Moreover, the covalent linkage not only reduces protein recovery, but also leads to severe inactivation of enzymes. This was the rationale that different chemical reagents such as PVP were tested and identified to remove pigments from protein extracts.

To date, although PVPP and PVP or other quinone-binding reagents have been used to reduce this problem, to our knowledge, none of them can completely eliminate pigments from protein extracts due to their cross-linking (Andersen and Sowers 1968; Anderson 1968; Loomis 1974; Nieman, Pap et al. 1978; Hsu and Heatherbell 1987). Our experiments herein also showed that the use of PVPP, PVP, and other reagents couldn’t obtain pigment-free enzyme extracts, indicating that many proteins were bound to pigments. We hypothesized that a breakdown of the cross-linking of proteins and pigments might release more soluble proteins. Our data

demonstrated that after the DEAE-Sephadex linked pigments and completely substituted all bound proteins, the recovery of total soluble protein was significantly increased (Table 1).

Furthermore, the new method IV produces active proteins for biochemical studies. Quinones and phenolics can strongly inactivate enzyme activities, such as phenol oxidases (Hulme and Wooltorton 1962; Hulme, Jones et al. 1966; Loomis 1969). In our experiments, after the removal of pigments, our enzyme assay demonstrated a PPO activity to catalyze catechol to quinones (Fig. 5 a-b). Moreover, PPO extracted from the new method IV had significantly higher activity than those extracted from other methods (Fig. 5 c). These results show that the new method IV is effective for reducing or eliminating inhibiting effects of brownish pigments on enzyme activity and to recover biochemically active proteins. In summary, the new method IV developed herein is effective for extracting active pigment-free soluble proteins with a high yield. This robust protocol will enhance plant biochemistry study using native proteins.

Conclusion

A new effective protocol has been developed to extract pigment-free soluble and desalted plant proteins. Anion DEAE-Sephadex is the main component to covalently bind anthocyanins and polyphenolics-derived quinones, the main components of pigments in plant protein extracts. Millipore Amicon® Ultra 10K cut-off filter unit is effective for removing salts from protein extracts and reducing volumes. The pigment-free soluble proteins are biochemically active.

REFERENCES

Andersen, R. A. and J. A. Sowers (1968). "Optimum conditions for bonding of plant phenols to insoluble polyvinylpyrrolidone." Phytochemistry 7(2): 293-301.

Anderson, J. W. (1968). "Extraction of enzymes and subcellular organelles from plant tissues." Phytochemistry 7(11): 1973-&.

Anderson, J. W. (1968). "Extraction of enzymes and subcellular organelles from plant tissues." Phytochemistry 7(11): 1973-1988.

Buchanan, B. B., W. Gruissem, et al. (2000). Biochemistry and Molecular Biology of Plants American Society of Plant Physiologists.

Burton, S. G. and S. Kirchmann (1997). "Optimised detergent-based method for extraction of a chloroplast membrane-bound enzyme: Polyphenol oxidase from tea (*Camellia sinensis*)." Biotechnol Tech 11(9): 645-648.

Carnegie, P. R. (1961). "Separation of low molecular weight peptides from amino acids on DEAE-Sephadex." Nature 192(480): 658-&.

Casado-Vela, J., S. Selles, et al. (2005). "Proteomic approach to blossom-end rot in tomato fruits (*Lycopersicon esculentum* M.): Antioxidant enzymes and the pentose phosphate pathway." Proteomics 5(10): 2488-2496.

Chi, M., B. Bhagwat, et al. (2014). "Reduced polyphenol oxidase gene expression and enzymatic browning in potato (Solanum tuberosum L.) with artificial microRNAs." BMC Plant Biol 14.

Chua, L. S., N. Abd Rahman, et al. (2014). "Plant protein extraction and identification from *Eurycoma longifolia* by gel electrophoresis and mass spectrometry." Curr Proteomics 11(3): 161-170.

Cimini, A., O. Marconi, et al. (2014). "Novel procedure for lager beer clarification and stabilization using sequential enzymatic, centrifugal, regenerable PVPP and crossflow microfiltration processing." Food Bioprocess Technol 7(11): 3156-3165.

Dewick, P. M. (1988). Isoflavonoids. The Flavonoids: Advances in Research Since 1980. J. B. Harborne. London, Chapman and Hall. 5: 125-209.

Esaka, Y., N. Okumura, et al. (2003). "Electrophoretic analysis of quinone anion radicals in acetonitrile solutions using an on-line radical generator." Electrophoresis 24(10): 1635-1640.

Flores, M., R. A. Isaacson, et al. (2003). "Probing hydrogen bonding to quinone anion radicals by H-1 and H-2 ENDOR spectroscopy at 35 GHz." Chem Phys 294(3): 401-413.

Goodfriend, L., L. Perelmutter, et al. (1965). "Use of DEAE-Sephadex for fractionation of allergic serum." Nature 205(4972): 718-719.

Harborne, J. B. (1999). "The comparative biochemistry of phytoalexin induction in plants." Biochem Syst Ecol 27(4): 335-367.

Harborne, J. B. and R. J. Grayer (1988). The Anthocyanins. The Flavonoids: advances in research since 1980. J. B. Harborne. London, Chapman and Hall Ltd: 1-20.

Havelund, J. F., J. J. Thelen, et al. (2013). "Biochemistry, proteomics, and phosphoproteomics of plant mitochondria from non-photosynthetic cells." Front Plant Sci 4.

He, C. F. and Y. M. Wang (2008). "Protein extraction from leaves of *Aloe vera* L., a succulent and recalcitrant plant, for proteomic analysis." Plant Mol Biol Rep 26(4): 292-300.

Hiwada, K., H. Akutsu, et al. (1966). "Separation of plasma angiotensinases by DEAE-Sephadex A-50 column chromatography." Clin Chim Acta 14(3): 410-411.

Hsu, J.-C. and D. A. Heatherbell (1987). "Isolation and characterization of soluble proteins in grapes, grape juice, and wine." Am J Enol Vitic 38(1): 6-10.

Hulme, A. C., J. D. Jones, et al. (1966). "Mitochondrial activity in apple fruits during development of fruit on tree." J Exp Bot 17(50): 135-+.

Hulme, A. C., J. D. Jones, et al. (1963). "Respiration climacteric in apple fruits." Proceedings of the Royal Society Series B-Biological Sciences 158(973): 514-535.

Hulme, A. C., J. D. Jones, et al. (1964). "Mitochondrial preparation from the fruit of the apple. 1. Preparation and general activity." Phytochemistry 3(2): 173-188.

Hulme, A. C. and L. S. C. Wooltorton (1962). "Separation of enzymes present in mitochondrial fraction from apple peel." Nature 196(4852): 388-&.

Jennings, A. C. and W. B. Watt (1967). "Fractionation of plant material. I. Extraction of proteins and nucleic acids from plant tissues and isolation of protein fractions containing hydroxyproline from broad bean (Vicia faba L) leaves." J Sci Food Agric 18(11): 527-&.

Jiang, Z. J., M. Kumar, et al. (2017). "Development of an efficient protein extraction method compatible with LC-MS/MS for proteome mapping in two australian seagrasses *Zostera muelleri* and *Posidonia australis*." Front Plant Sci 8.

Jones, G. and X. H. Qian (1998). "Photochemistry of quinone-bridged amino acids. Intramolecular trapping of an excited charge-transfer state." J Phys Chem A 102(15): 2555-2560.

Jones, J. D., A. C. Hulme, et al. (1964). "Mitochondrial preparations from the fruit of the apple. 2. Oxidative phosphoration." Phytochemistry 3(2): 201-212.

Khatun, S., M. Ashraduzzaman, et al. (2012). "Purification and characterization of peroxidase from *Moringa oleifera* L. leaves." Bioresources 7(3): 3237-3251.

Kurreck, H. and M. Huber (1995). "Model reactions for photosynthesis-photoinduced charge and energy-transfer between covalently-linked porphyrin and quinone units." Angew Chem-Int Edit 34(8): 849-866.

Leyko, W. and R. Gondko (1963). "Separation of hemoglobin and cytochrome C by electrophoresis and by chromatography on DEAE-sephadex." Biochimica Et Biophysica Acta 77(3): 500-&.

Lledias, F., F. Hernandez, et al. (2017). "A rapid and reliable method for total protein extraction from succulent plants for proteomic analysis." Protein J 36(4): 308-321.

Loomis, W. D. (1969). Removal of phenolic compounds during the isolation of plant enzymes. Methods in Enzymology, Academic Press. 13: 555-563.

Loomis, W. D. (1974). Overcoming problems of phenolics and quinones in the isolation of plant enzymes and organelles. Methods in Enzymology, Academic Press. 31: 528-544.

Loomis, W. D. and J. Battaile (1966). "Plant phenolic compounds and the isolation of plant enzymes." Phytochemistry 5(3): 423-438.

Lugg, J. W. H. (1939). "The representativeness of extracted samples and the efficiency of extraction of protein from the fresh leaves of plants; And some partial analyses of the whole proteins of leaves." Biochem J. 33: 110-122.

Lugg, J. W. H. and R. A. Weller (1944). "Large-scale extraction of protein samples reasonably representative of the whole proteins in the leaves of some plants: The amide, tyrosine, tryptophan, cystine (plus cysteine) and methionine contents of the preparations." Biochem J 38: 408-411.

Luttge, U. and R. Ratajczak (1997). The physiology, biochemistry and molecular biology of the plant vacuolar ATPase. Advances in Botanical Research Incorporating Advances in Plant

Pathology, Vol 25: The Plant Vacuole. R. A. Leigh and D. Sanders. San Diego, Elsevier Academic Press Inc. 25: 253-296.

Mayer, A. M. and E. Harel (1979). "Polyphenol oxidases in plants." Phytochemistry 18(2): 193-215.

McCown, B. H., G. E. Beck, et al. (1968). "Plant leaf and stem proteins. I. Extraction and electrophoretic separation of basic water-soluble fraction." Plant Physiol 43(4): 578-&.

Mohammad, M., S. Rauf, et al. (2013). "Kinetic studies on hydrogen bonding in quinone anion radical and the dianion of tetramethyl-1,4-benzoquinone." J Chem Soc Pak 35(3): 654-658.

Nanda, C. L., A. C. Kondos, et al. (1975). "Improved technique for plant protein extraction." J Sci Food Agric 26(12): 1917-1924.

Nelsen, S. F., M. N. Weaver, et al. (2007). "Charge localization in a 17-bond mixed-valence quinone radical anion." J Phys Chem A 111(43): 10993-10997.

Nieman, R. H., D. L. Pap, et al. (1978). "Rapid purification of plant nucleotide extracts with xad-2, polyvinylpolypyrrolidone and charcoal." J Chromatogr A 161(Supplement C): 137-146.

Parkhey, S., V. Chandrakar, et al. (2015). "Efficient extraction of proteins from recalcitrant plant tissue for subsequent analysis by two-dimensional gel electrophoresis." J Sep Sci 38(20): 3622-3628.

Peng, Q. Z., Y. Zhu, et al. (2012). "An integrated approach to demonstrating the ANR pathway of proanthocyanidin biosynthesis in plants." Planta 236(3): 901-918.

Pierpoint, W. S. (1996). The extraction of enzymes from plant tissues rich in phenolic compounds. Protein Purification Protocols. S. Doonan. Totowa, NJ, Humana Press: 69-80.

Porter, L. J. (1988). Flavans and Proanthocyanidins. The Flavonoids. J. B. Harborne. London, Chapman and Hall: 21-62.

Queiroz, C., M. L. M. Lopes, et al. (2008). "Polyphenol oxidase: Characteristics and mechanisms of browning control." Food Rev Int 24(4): 361-375.

Rene, A. and D. H. Evans (2012). "Electrochemical reduction of some o-quinone anion radicals: Why Is the current intensity so small?" J Phys Chem C 116(27): 14454-14460.

Rinyu, L., L. Nagy, et al. (2001). "The role of the electronic structure of quinones in the charge stabilization in photosynthetic reaction centers." J Mol Struct-THEOCHEM 571: 163-170.

Rodriguez, P. E. A. and F. A. Cumar (1990). "Gangliosides noncovalently bound to DEAE-Sephadex - Application to purification of antiganglioside antibodies." Anal Biochem 188(1): 48-52.

Saini, R., N. Kaur, et al. (2014). "Quinones based molecular receptors for recognition of anions and metal ions." Tetrahedron 70(29): 4285-4307.

Sari, Y. W., W. J. Mulder, et al. (2015). "Towards plant protein refinery: Review on protein extraction using alkali and potential enzymatic assistance." Biotechnol J 10(8): 1138-1157.

Schmidt, M. (1962). "Fractionation of acid mucopolysaccharides on DEAE-sephadex anion exchanger." Biochimica Et Biophysica Acta 63(2): 346-&.

Shao, Y. F. and J. S. Bao (2015). "Polyphenols in whole rice grain: Genetic diversity and health benefits." Food Chem 180: 86-97.

Shinbuehring, Y. S., M. Drefers, et al. (1978). "Separation of acid and neutral alpha-glucosidase isoenzymes from fetal and adult tissues, cultivated fibroblasts and amniotic-fluid cells by DEAE-Cellulose and Sephadex G-100 column chromatography." Clin Chim Acta 89(3): 393-404.

Sinnecker, S., E. Reijerse, et al. (2004). "Hydrogen bond geometries from electron paramagnetic resonance and electron-nuclear double resonance parameters: Density functional study of quinone radical anion-solvent interactions." J Am Chem Soc 126(10): 3280-3290.

Sisler, E. C. and H. J. Evans (1958). "Comparison of chlorogenic acid and catechol as substrates for the polyphenol oxidase from tobacco and mushroom." Plant Physiol 33: 255-257.

Sullivan, M. L. (2015). "Beyond brown: polyphenol oxidases as enzymes of plant specialized metabolism." Front Plant Sci 5.

Taiz, L. and E. Zeiger (2010). Plant Physiology. Sunderland, MA, Sinauer Associates, Incorporated.

Taranto, F., A. Pasqualone, et al. (2017). "Polyphenol oxidases in crops: Biochemical, physiological and genetic aspects." Int J Mol Sci 18(2).

Toth, G. B. and H. Pavia (2001). "Removal of dissolved brown algal phlorotannins using insoluble polyvinylpolypyrrolidone (PVPP)." J Chem Ecol 27(9): 1899-1910.

Tsuji, T., T. Mori, et al. (1985). "Solvent-extraction of plant pigments from leave protein-concentrate." J Chem Eng Jpn 18(6): 539-544.

Wang, W., F. J. Tai, et al. (2008). "Optimizing protein extraction from plant tissues for enhanced proteomics analysis." J Sep Sci 31(11): 2032-2039.

Wu, X. L., E. H. Xiong, et al. (2014). "Universal sample preparation method integrating trichloroacetic acid/acetone precipitation with phenol extraction for crop proteomic analysis." Nat Protoc 9(2): 362-374.

Yoruk, R. and M. R. Marshall (2003). "Physicochemical properties and function of plant polyphenol oxidase: A review." J Food Biochem 27(5): 361-422.

Zhou, L.-L., H.-N. Zeng, et al. (2008). "Development of tobacco callus cultures over expressing *Arabidopsis* PAP1/MYB75 transcription factor and characterization of anthocyanin biosynthesis " Planta 229: 37-51.

Zhou, L. L., H. N. Zeng, et al. (2008). "Development of tobacco callus cultures over expressing Arabidopsis PAP1/MYB75 transcription factor and characterization of anthocyanin biosynthesis." Planta 229(1): 37-51.

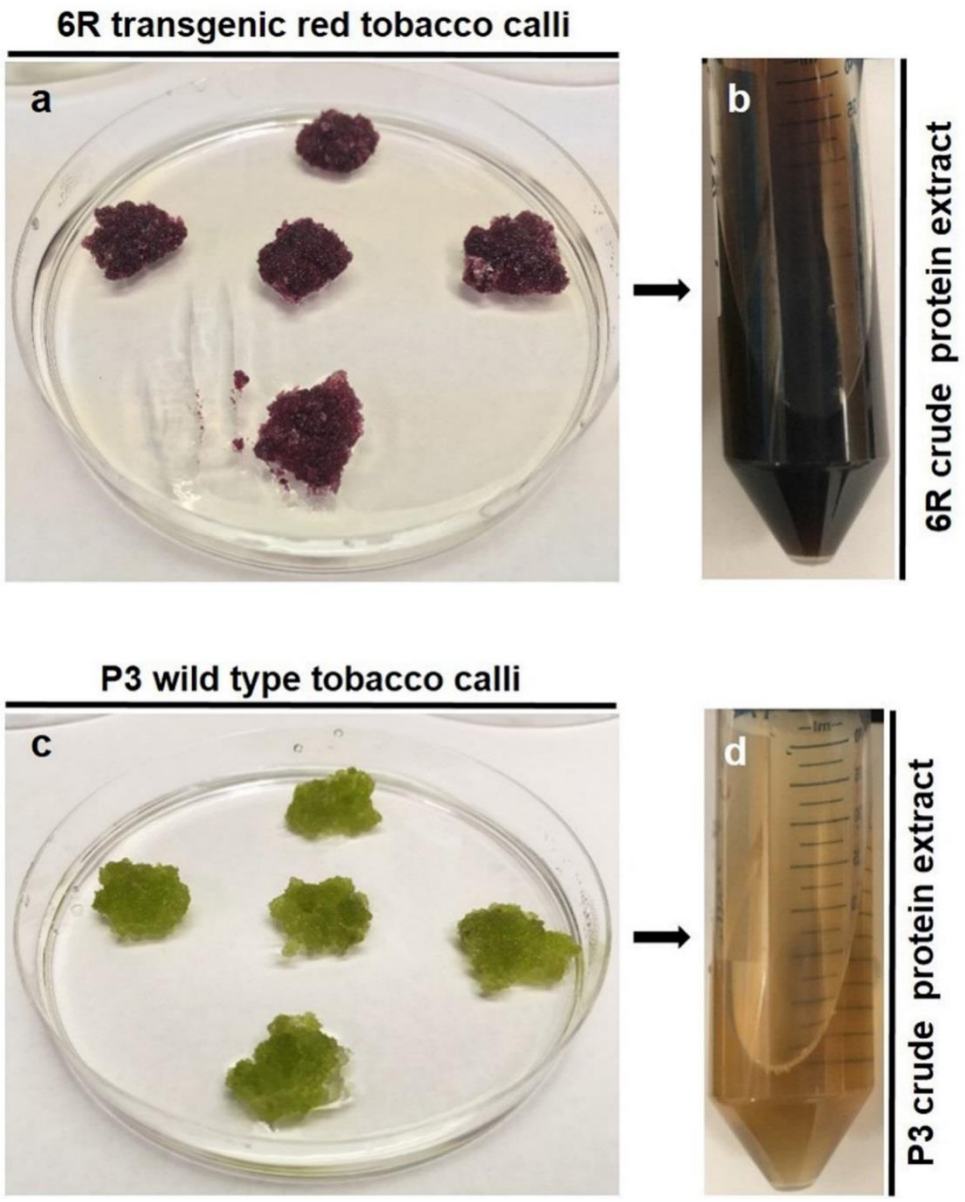

Figure 4.1: Different calli cultured on agar-solidified medium and colors of their crude protein extracts. a-b transgenic red calli cultured 15 days (**a**) and crude protein extract with dark color (**b**). **c-d** greenish wild type calli cultured 15 days (**c**) and crude protein extract with light brownish color (**d**)

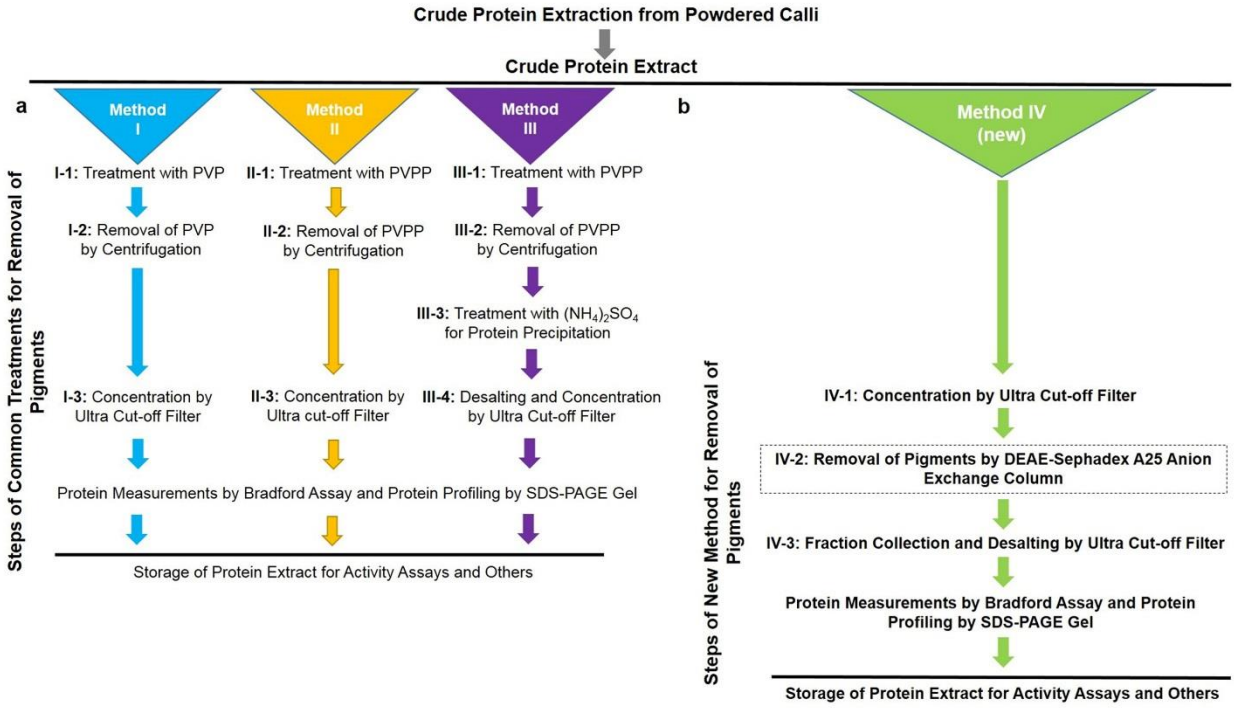

Figure 4.2: Four methods and steps used to remove pigments from crude protein extracts. a steps of methods I, II, and III reported in in literature for removal of pigments using PVP and PVPP; **b** steps of our new method (IV) for removal of pigments.

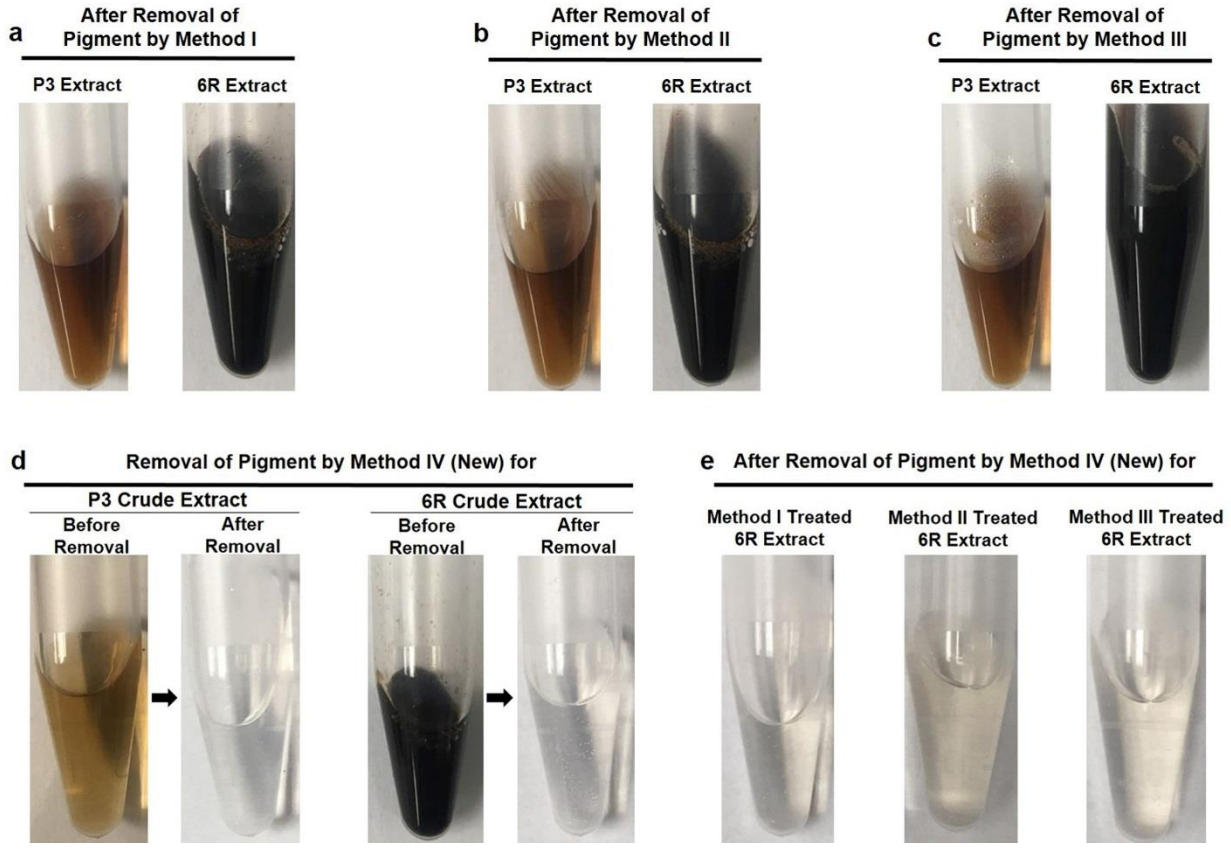

Figure 4.3: Comparison of pigment removal results obtained with different methods. a-c colors of crude protein extracts from P3 and 6R calli after treatment with PVP (method I) (**a**), PVPP (method II) (**b**), PVPP and $(NH4)_2SO4$ (method III) (**c**); **d** colors of crude protein extracts from P3 and 6R calli after pigment removal using the new method IV; **e** pigment-free protein extracts were obtained after re-treated of crude protein extracts in (**a**), (**b**), and (**c**) resulted from treatment of PVP, PVPP, and PVPP and $(NH4)_2SO_4$ using the new method IV.

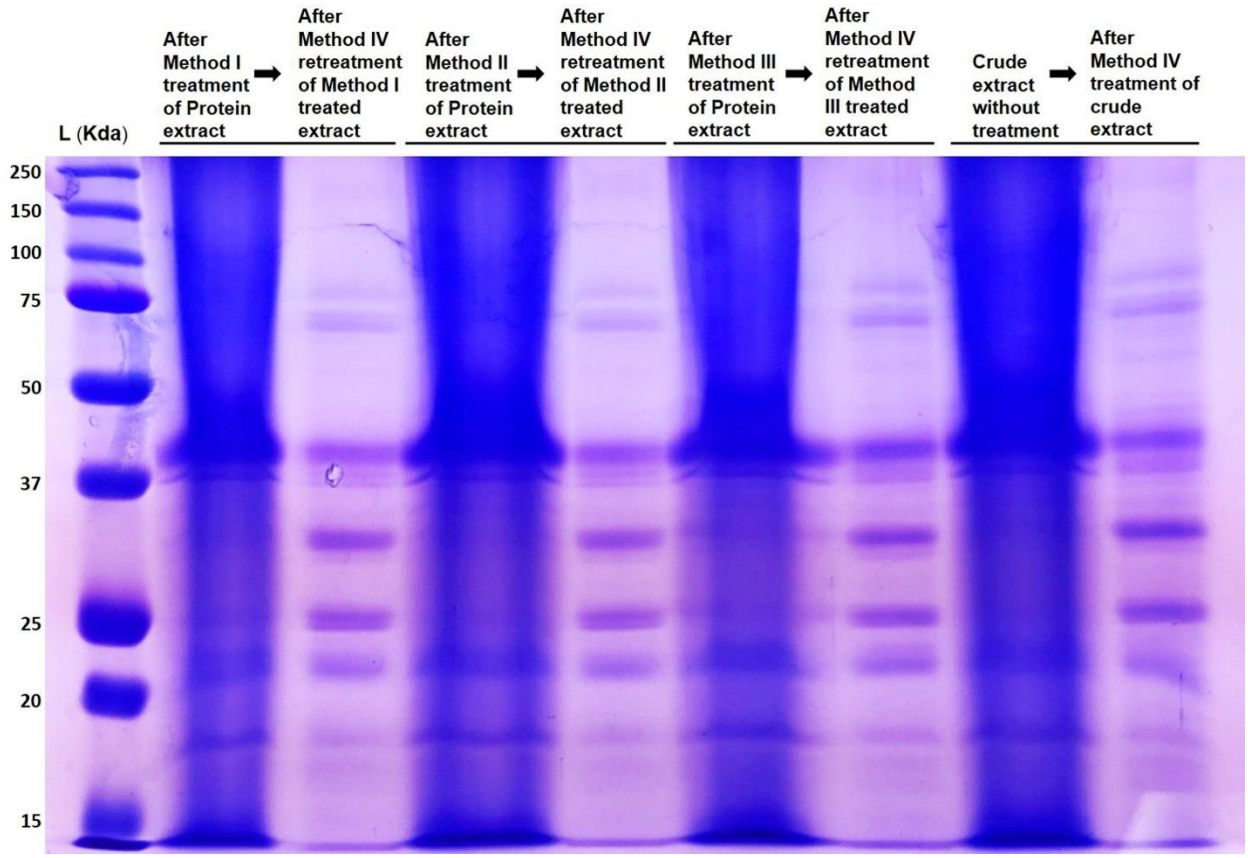

Figure 4.4: A SDS-PAGE image shows band profiles from protein extracts using four different methods. All crude proteins were extracted from red 6R cells. Protein extracts from methods I, II, and III were retreated with the new method IV. Protein extracts prior to and after treatment using the method IV were loaded gels side by side. 20 ug of protein sample was loaded to each line.

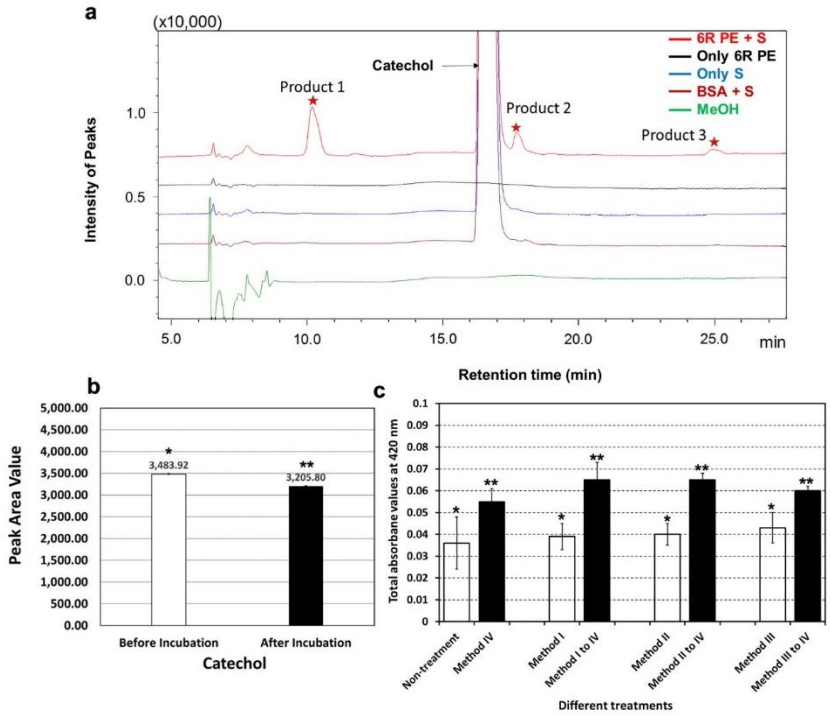

Figure 4.5: Polyphenol oxidase assay using catechol as substrate. a HPLC profiles showing catalytic products from incubations of catechol and pigment-free crude protein extracts from the new method IV. Catechol (1.0 mM) was incubated with pigment-free crude protein extracts (PE) and bovine serum albumin (BSA) for 45 min, respectively. Catechol (substrate, S) and pigment-free crude protein extract (PE) alone were used as controls, respectively. Absorbance values and chromatographs were recorded at 280 nm. Three new products 1, 2, and 3 are formed from catechol catalyzed by PPO. 6R PE+S: 6R protein extract from method IV was incubated with substrate catechol, 6R PE: 6R protein extract from method IV without substrate, S: substrate alone without protein extract, BSA+S: BSA was incubated with substrate, and MeOH: methanol solvent used as control. **b** comparison of peak area values of catechol before and after incubation ("*" and "**" mean significant difference, p-value ≤0.05, t-value: 2.07). **c** Production comparison of reaction products from crude enzyme extracts before and after the pigment removal using new Method IV. Reaction using catechol was carried out in one minute and absorbance values for products were recorded at 420 nm on a UV spectrophotometry. Four bars labeled "*" or "**" alone mean no significant difference. Bars between labels with "*" and "**" means significant difference (p-value ≤0.05, t-value: 2.77).

Table 4.1: Protein yields show that the new Method IV increases the recovery of total soluble proteins from pigments.

Calli	Extracts	Total soluble protein concentration (μg/μL)	Total soluble protein recovery production from fresh cells (mg/g)	Percentage of total soluble protein in per gram fresh cells	Recovery yield increase of total soluble protein by the new method
P3 (green)	Crude extract prior to the new method	0.2792 ± 0.006	1.530^{a} ± 0.012	0.153%	
	After removal of pigment by the new method	5.4776 ± 0.125	1.780^{b} ± 0.049	0.178%	16%
6R (red)	Crude extract prior to the new method	0.2657 ± 0.009	1.541^{c} ± 0.07	0.154%	
	After removal of pigment by the new method	7.8236 ± 0.069	2.543^{d} ± 0.027	0.254%	65%

Numbers labeled with “a” and “b” means significant difference. Numbers labeled with “c” and “d” means significant difference (*p*-value ≤0.05, Student’s *t* test)

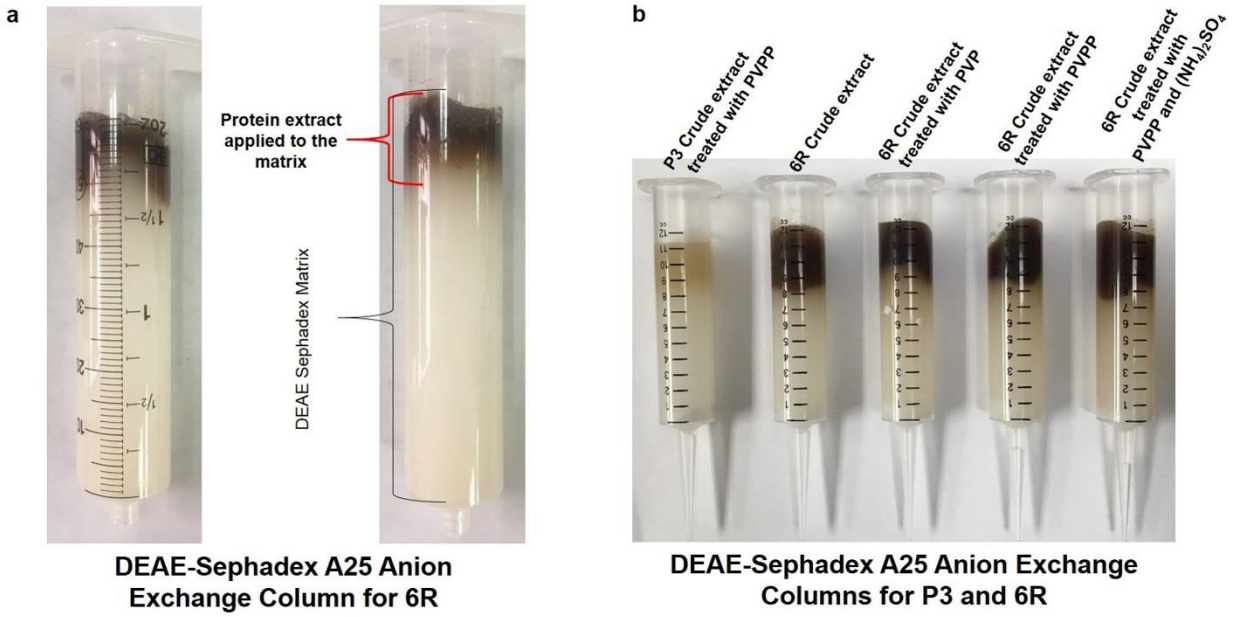

Supplementary Figure 1: DEAE-Sephadex A25 anion exchange column prepared in the laboratory and pigment removal from protein extracts. a two columns show that pigments in 6R protein extracts are bound to gel matrix. **b** five columns show that pigments in protein extracts after treatment with methods I, II, and III are bound to gel matrix.

CHAPTER 5

Purification of Putative Plant Polyphenol Oxidase from Red Cells: A Putative Condensing Synthase of Proanthocyanidins

Abstract

As described in the introduction, although the condensation mechanism of PA formation is unknown, plant polyphenol oxidase (PPO), laccase, and peroxidase have been proposed to be three groups of candidates that exhibit condensing synthase activity. In this chapter, I summarize a condensing synthase purification and preliminary enzymatic activity analysis. Our laboratory has developed transgenic red callus and cell suspension culture as a model system to understand mechanisms of PA polymerization. Red tobacco cells were previously engineered from PAP1 (R2R3-MYB member, a master regulator) transgenic plants, which highly produced anthocyanins. According to our previous preliminary data, our hypothesis is that transgenic red tobacco cells express a condensing synthase involved in the polymerization of flavan-3-ols. To test this hypothesis, I performed large scale red cell suspension culture and extracted crude proteins. In addition, as described in Chapter IV, I developed an effective protocol to remove pigments from crude proteins. I then developed a purification protocol to purify a condensing synthase candidates. Both denatured and native protein electrophoreses were performed to demonstrate that a condensing synthase was purified from crude proteins. Further native gel staining using the substrate (-)-epicatechin demonstrated that this candidate syntahse converted the substrate to new compounds. Further, preliminary *in vitro* enzyme assay coupled with thin-layer chromatograph and HPLC showed that the condensing synthase with PPO

function catalyzed (-)-epicatechin to new dimeric compounds. These preliminary data show that red cells express a condensing synthase, which polymerizes flavan-3-ols to PA-like oligomers.

INTRODUCTION

Current hypotheses of polymerization mechanism for PA formation

The last step of PA formation is polymerization. Since I have described three current hypotheses of PA polymerization in the introduction (Chapter 1), here I briefly summarize mechanisms proposed in the second hypothesis for PA polymerization (Figure 1). For the second hypothesis, two general questions remain unanswered about building blocks of polymerization and condensing synthase. The first question is what types of precursors are the extension units in PAs? As introduced in the introduction chapter, a long-term hypothesis is that leucoanthocyanidins (a 2R,3S-2, 3-*trans* configuration) are the precursors of the extension units. However, this model has been questioned by the fact that predominant extension units found in PAs isolated from different plants are (-)- epicatechin (a 2R, 3R-2, 3-*cis* configuration) monomers. The second question is what type of condensing synthase catalyzes the polymerization step. To answer these two essential questions, flavan-3-ols and anthocyanidins were proposed to be precursors of extension units of PAs (Xie and Dixon 2005). In this new model, flavan-3-ols {such as (+)-catechin and (-)-epicatechin)} and anthocyanidins are converted to their corresponding *o*-quinone and quinone methides by an enzymatic reaction. Three groups of enzymes, polyphenol oxidase (PPO), laccase, and peroxidase are proposed to be condensing synthase to catalyze polymerization in this new model (Dixon, Xie et al. 2005). Although direct

evidence for this new model is still lacking, our preliminary data obtained previously and in this study provides biochemical evidence to support that flavan-3-ols can be used as extension unit precursors to form dimeric PAs and a condensing synthase with a putative PPO function can catalyze polymerization of flavan-3-ols to form PA-like oligomers.

Transgenic red tobacco cells: A model system

Transgenic red tobacco cell cultures have been developed as a model system to study PA polymerization in our laboratory (Zhou, Zeng et al. 2008). *Nicotiana tabacum* is a well-established model organism to test many hypotheses (Mathews, Clendennen et al. 2003). Our lab previously overexpressed *Arabidopsis PAP1* (*Production of Anthocyanin Pigment 1* gene (At1g56650) in tobacco plants. PAP1 encoded the MYB75 transcription factor of the biosynthetic pathway of anthocyanins (Borevitz, Xia et al. 2000; Weigel, Ahn et al. 2000). The overexpression of *PAP1* activates the entire anthocyanin pathway, which leads to high production of anthocyanins in all tissues. (Borevitz, Xia et al. 2000; Tohge, Nishiyama et al. 2005; Xie, Sharma et al. 2006).

In addition, the PAP1 transgenic tobacco plants produced new anthocyanidin molecules such as delphinidins and pelargonidins (Xie, Sharma et al. 2006). To engineer the ANR pathway (Fig. 1 in Chapter 1), *ANR* was introduced into the PAP1 transgenic red tobacco plants. The resulting PAP1::ANR transgenic plants not only produce flavan-3-ols but also PAs (Xie, Sharma et al. 2006). The formation of PAs indicates that red cells not only provide anthocyanidin substrates but also express condensing enzymes to catalyze the polymerization of flavan-3-ols to form PAs. To test the polymerization activity in red cells, our lab previously engineered red cells from red tobacco leaves and developed these cells as a model system to test polymerization

mechanisms of PAs (Zhou, Zeng et al. 2008). In my study, I have continued red cell culture to isolate proteins to test polymerization reactions.

MATERIALS and METHODS

Plant Material

Two types of cell lines have been maintained in the lab (Figure 2 a). One is named 6R, which overexpresses PAP1 and highly produces anthocyanins, and the other is named P3, which is wild type control (Zhou, Zeng et al. 2008). Cells (callus) have been maintained on agar-solidified subculture medium at 22 °C and 16 h/8 h light/dark photoperiod in a growth chamber in a 15-day interval. The sub-culture medium is composed of basal MS medium (pH 5.7) containing 0.25 mg L^{-1} 2,4-dichlorophenoxyacetic acid, 0.10 mg L^{-1} kinetin, 30 g L^{-1} sucrose and 0.8% (w/v) phyto agar. Calli were used to establish cell suspension culture using liquid subculture medium in 4 liters E-flasks, which were shaked at a speed of 100 rpm/min (Figure 2). Temperature and photoperiod conditions were the same as used for cell subculture on solid medium. Suspension culture was subcultured in every 15 days, as well. After 15 days of culture, suspension-cultured cells were collected as shown in Figure 2, immediately frozen in liquid nitrogen, ground to a fine powder in liquid nitrogen, and the stored at -80 °C until use. Liquid medium was also collected for precipitation of proteins. Furthermore, calli subcultured on solid medium were collected and stored at -80 °C to extract proteins.

Extraction of a putative condensing synthase with PPO function

Soluble proteins were extracted from powdered 6R and P3 cell samples as follows (Figure 3). The extraction buffer was composed of 0.1 M Tris-Cl (pH 7.0) and 10 mM EDTA. Thirty grams of fresh powdered sample were suspended in 150 mL extraction buffer contained in a 500 mL polyethylene centrifuge tube. The tube was vortexed one min thoroughly, sonicated 30 min in a water bath in Fisher Scientific FS60H Ultrasonic Cleaner, and then shaken at 100 rpm 20 min at 4°C. The tube was centrifuged 15 min at 6,500 rpm (5,820 rcf) and 15 °C on Beckman Coulter Avanti JXN-26 centrifuge. The resulting supernatant with total soluble proteins was transferred to a new tube. The supernatant was centrifuged for another 20 min at 9,900 rpm (13,500 rcf) and 15 °C. The flow-through contained total soluble proteins. As shown in Chapter 4, soluble protein extracts from P3 cells were brownish due to polyphenol oxidation and those from 6R cells were deeply dark brownish due to high production of anthocyanins and oxidation of other polyphenolics. Twelve mL crude extracts were placed in Millipore 15 mL 10K filters by following the manufacturer's instructions, which were centrifuged 35 min at 4,000 rpm (3,220 rcf) and 15 °C. The resulting flow-through containing small molecules and pigments was disposed into waste container. The remaining protein extracts were stored at 4 °C for the following experiments.

The total protein concentration was measured using the Bio-Rad Bradford protein assay. Four µL of protein extract concentrated was added to 76 µL 0.02 M Tris-HCl (pH 7.0) buffer and then thoroughly mixed to obtain 80 µL mixture, from which 20 µL was added to 980 µL (1X) Bradford buffer contained in a 1.5 mL Eppendorf tube. The mixture was gently and thoroughly mixed via pipetting and incubated 5 min at room temperature. The absorbent values of mixtures were recorded at 595 nm on a NanoDrop™ 2000C Spectrophotometer (Thermo

Fisher Scientific, USA). In addition, bovine serum albumin (BSA) was used to develop a standard curve to calculate protein concentrations.

Purification of a putative condensing synthase with PPO function

Our previous experiments have shown that the PPO activity in cultured cells are tolerant to boiling. In addition, our previous experiments obtained partial amino acid sequences of a few of boiling-tolerant proteins from suspension-cultured 6R cell protein extracts. Based on these sequences, we found that temperature-tolerant proteins were featured by lower than 7 isoelectric point (pI), the pH at which the net charge of the protein is zero. To simplify purification steps, I used a water boiling step to remove many temperature-sensitive proteins. The crude protein extract was heated 1-3 min at 100 °C in boiling water and then centrifuged 10 min at 12,500 rpm (21,520 rcf). The resulting supernatant was used for condensing enzyme purification. Because the isoelectric point value of the protein was lower than 7, it was considered as an acidic protein. Therefore, I used a DEAE Sephadex A20-120 ion-exchange (IE) column, which was weak anion exchanger at the pH 7.0 using 0.02 M Tris-HCl as the start buffer. Ten grams of DEAE Sephadex powder were loaded into a glass column (4 x 10 cm, diameter x height). The resulting column was washed with 40 mL protein extraction buffer (starter buffer). Boiling-tolerant proteins were loaded on the top of the IE column and flow through via gravity of buffer. A series of Tris-HCl buffers containing 0 M, 0.10 M and 0.20 M NaCl were used to elute proteins. For each specific NaCl concentration, three column volumes were used for elution. Each flow-through fraction was collected and was tested using (-)-epicatechin. The flow-through with catalytic activity was collected together for further analysis. We found that active proteins were eluted using the 0.10 M NaCl and 0.20 M NaCl elution

fractions. This result indicated that 0.10 M NaCl and 0.20 M NaCl in pH7.0 buffer were effective to elute target condensing synthases from the DEAE-Sephadex. Proteins in this flow-through fractions were further separated on a Sephadex G-75 column for size-exclusion chromatography. As prepared for DEAE sephadex column, G-75 powder was used to prepare column and washed with three column volumes of Tris-HCl buffer. After the DEAE protein fraction was loaded to this column and eluted using Tris-HCl buffer, the flow-through was collected every 30 seconds. Protein band (numbered as 1) on SDS-PAGE gel (Figure 5) was used for peptide sequence analysis.

Sodium dodecyl sulfate polyacrylamide gel electrophoresis (SDS-PAGE)

Protein extracts from each step in Figure 3 were used for SDS-PAGE. The concentration of **s**odium dodecyl sulfate polyacrylamide gel was 10% to check protein quality. Twenty µg proteins for each step were loaded onto a gel. Fifteen µg protein standard ladder was loaded to estimate protein sizes. After electrophoresis, the gel was stained with 0.25% Coomassie brilliant blue (R250). The protein band numbered as "1" (Figure 5) was cut from the gel, then sequenced for peptide anaylsis.

Proteinase K treatment for denaturation of a putative condensing synthase

Proteinase K (Cat #V3021, Promega) treatment was applied for putative condensing synthase with PPO activity to test weather *in vitro* incubation catalysis was emerged due to an enzymatic activity. 10 µg of condensing synthase protein extracted and purified from 6R was dissolved in 0.05 M Tris-Cl (pH 7.0) buffer and 0.05 M $CaCl_2$ in a reaction volume of up to 100

µL. 10 µg of proteinase K was then added to the reaction to a final concentration of 100 µg/mL. The reaction mixture was incubated at 37 °C for overnight. After denaturation, the reaction mixtures was loaded on SDS-PAGE gel to demonstrate digestion of target protein by proteinase K. Protein targets treated (digested) with proteinase K were then incubated with (+)-catechin and (-)-epicatechin substrates on Native-PAGE gels to demonstrate an expected inhibition of *in vitro* condensing activity.

In vitro **enzyme assays**

Condensing (polymerization) activity was assayed by *in vitro* incubations. Our lab previously showed condensing activity using crude extraction of proteins and two substrates, (+)-catechin and (-)-epicatechin. Herein, the two substrates were used to testa condensing synthase purified from crude extracts. Two metabolites were freshly dissolved in methanol to prepare a 1.0 mg/mL stock solution. An enzymatic reaction was carried out in 500 µl volume, which was composed of 475 µL of 0.02 M Tris-HCl (pH 7.0) buffer, 15 µL of protein extracts (10 µg) and 10.0 µL of 1.0 µg/µL substrates (10 µg) contained in a 1.5 ml polyethylene tube. In addition, control reactions without substrates and without protein extracts (only substrate and buffer) were performed. All reactions were incubated for 30 min at room temperature and stopped by adding one ml of ethyl acetate (EA) (Figure 8). Each tube was thoroughly vortexed two min and then centrifuged at 8,000 rpm (8,820 rcf) five min at 22°C. The resulting upper ethyl acetate phase was gently transferred to a new tube and dried in a savant speed vacuum concentrator. The remaining pellet was dissolved in 200 µL of methanol (LC/MS grade) for thin layer chromatography (TLC) and high performance liquid chromatography (HPLC) analysis described below.

Native-PAGE

To further demonstrate enzymatic activity of purified condensing syntahse, native-polyacrylamide gel electrophoresis (Native-PAGE) was carried out. Native-PAGE (10.0 %) was freshly prepared prior to electrophoresis. A separation gels were prepared using 2.33 mL of 30% acrylamide/bisacrylamide solvent, 1.75 mL of 4X Tris (pH 8.8), 2.85 mL of dH_2O, 70 uL of 10% (w/v) ammonium persulphate (APS), and 5 uL of tetramethylethylenediamine (TEMED). Stacking gel was prepared using 500 uL of 30% acrylamide/bisacrylamide solvent, 375 uL of 4X Tris (pH 6.8), 2.1 mL of dH2O, 30 uL of 10% APS and 4.0 uL of TEMED. The size of comb created 40 µL volume wells for sample loading. Native-PAGE was prepared using a caster (10 x 8 cm). Native-PAGE was then installed in a Bio-Rad Mini Protean® Tetra Cell Electrophoresis apparatus (Bio-Rad, USA). Ten ug of protein sample was mixed with 10 uL of protein loading buffer, which was composed of 50% glycerol, 0.5 M Tris-Cl (pH:7.0), 0.15 uM bromophenol blue (Bio-Rad), and dH_2O.

The resulting mixture was gently mixed then loaded onto a Native-PAGE. The polyacrylamide gel and 1 L of 1 X Tris-Glycine-running buffer including 3.03 g of Tris and 14 g of Glycine were placed in an electrophoresis chamber. In addition, 10 µg of Bio-Rad Precision Plus Protein™ ladder was loaded a molecular weight standard. The electrodes of the electrophoresis apparatus were wired to a power source. The electrophoresis apparatus was placed in a container and surrounded with ice to avoid any protein degradation due to heating. The voltage of electrophoresis was set at 70 Volt for 30 min and then increased to 120 Volt for 90 min. After the completion of electrophoresis, the gel was rinsed using dH_2O and 0.02 M Tris-Cl buffer (pH:7.0) and then placed into in a glass tank for incubation with substrate. The gel was suspended in 0.02 M Tris-Cl buffer pH 7.0 containing 1 mg/mL (+)-catechin or (-)-epicatechin.

The incubation was achieved by shaking the gel smoothly. Color changes on the gel were recorded at 0, 30 and 60 minutes after incubation started.

TLC assay

TLC was performed to check products from the incubations of substrates and purified condensing synthase with PPO activity. Samples (10 µL) were spotted on aluminum-backed silica Kieselgel 60 F_{254} TLC sheets (0.2 mm layer thickness; EM Sciences, Busking Ridge, NJ, USA),which was placed in in a developing buffer consisting of water;formic acid;ethyl acetate (1:1:18), v/v). After buffer reached to the edge of plates, plates were dried in air and then sprayed with 0.1% (w/v) dimethylaminocinnamaldehyde (DMACA), which was freshly prepared in 6 M HCl:ethanol (1:1,v/v). DMACA immediately react substrates and enzymatic products to produce bluish coloration on plants. The results visualized flavan-3-ols and PA compounds.

The protein extracts from P3 (unboiled) and 6R (boiled and unboiled) suspension cells immediately gave yellowish blue color (Figure 10). Procyanidin B1 and monomeric flavan-3-ols were used as standards. TLC analysis showed that proteins from Wt and transgenic suspension cells (6R) catalyze the conversion of (+)-catechin and (-)epicatechin to yellowish compounds.

HPLC analysis

HPLC was performed to further examine enzymatic products from the incubations. Based on our protocol, HPLC analysis was carried out on a Shimadzu LCMS-2010 EV instrument. In brief, metabolites in samples were separated on an Eclipse XDB-C18 analytical

column (250 mm × 4.6 mm, 5.0 µm, Agilent, Santa Clara, CA, USA). The mobile phase solvents used for metabolite elution included 1% acetic acid in water (solvent A, HPLC-grade acetic acid, LC/MS-grade water) and 100% acetonitrile (solvent B, LC/MS-grade). A gradient solvent system, which was developed to separate products, was composed of ratios of solvent A to B: 80:20 (0–5 min), 80:20 to 70:30 (5–10 min), 70:30 to 65:35 (10–20 min), 65:35 to 60:40 (20–30 min), 60:40 to 55:45 (30–40 min), 55:45 to 50:50 (40–45 min), 50:50 to 48:52 (45–50 min), 48:52 to 45:55 (50–55 min), 45:55 to 40:60 (55–58 min) and 40:60 to 10:90 (58–58.5 min). After each elution, the column was washed for 11.5 min with a mixture of elution buffer consisting of 20% of solvent B and 80% solvent A. The flow rate was 0.4 ml/min and the injection volume was 10.0 uL. Chromatograms were recorded at 280 nm. Two substrates, (-)-epicatechin and (+)-catechin, were used as positive control.

PRELIMINARY RESULTS

Condensing synthase purification

As we previously showed, protein extracts from both red 6R and wild-type P3 cells expressed multiple boiling-tolerant proteins (Figure 4). After pigment removal described in Chapter 4, the use of DEAE-Sephadex (Ion-exchange chromatography) and Sephadex (Size-exclusion chromatography) columns resulted in proteins with a good quality of purification (Figure 5). This result showed the effectiveness of our protocol developed in this research (Figure 3). In addition, peptide sequence analysis of a purified protein band numbered as ‘1” showed 31% similarity with a peroxidase-like protein (Gene #: LOC107814252) in *Nicotiana*

tabacum (Figure 6). The function of this peroxidase-like protein was not identified and not reported yet. Therefore, it may suggest that the condensing synthase purified from 6R protein extract in our study would be either a peroxidase with a putative PPO function or a PPO enzyme.

Condensing synthase catalysis

Our lab's previous enzyme assays have shown that crude protein had PPO activity to catalyze both (+)-catechin and (-)-epicatechin to dimeric PA-like metabolites. In this study, enzymatic activity of condensing synthase digested by proteinase K was inhibited (Figure 9). However, when two substrates were incubated with purified condensing synthase with a putative PPO activity, new compounds with yellowish color were formed, but this reaction did not occur in all controls (Figure 8 and 9). This result demonstrated an enzymatic activity of a condensing synthase with a putative PPO activity from P3 and 6R protein extratcs for catalysis of condensation of the substrates.

TLC and DMACA were used to analyze PA and PA-like compounds (Xie, Sharma et al. 2006). In this study, TLC and DMACA staining showed that the incubations of totally purified condensing synthase with a putative PPO function and two substrates produced PA-like compounds (Figure 10). Although their Rf values (the ratio of the distance moved by the solute) are less than those of the two substrates, but due to being close to substrates, new compounds are likely dimeric PA-like compounds. In addition, purified condensing synthase from 6R was boiled 1 min to test its temperature stability. The enzyme assay showed that boiling one min did not inhibit its activity, indicating that this enzyme was tolerant to boiling (Figure 8).

HPLC was performed to further show enzymatic products from the incubations. The chromatograms recorded at 280 nm showed that in addition to (+)-catechin detected at 21.33 min, four different major peaks were detected at 19.21, 22.83, 35.75, and 42.46 min (Figure 11). However, these three peaks were not detected from control incubations. Although they did not elute at the same retention times of two procyanidin standards, based on their UV-spectra features, these four peaks were PA-like compounds.

Native gel was performed to demonstrate enzymatic reactions. After electrophoresis, gel was suspended in (+)-catechin and (-)-epicatechin. After one-hour incubation, a strong brownish-yellowish band appeared from the lane with condensing synthase in the gel. However, this color did not appear from BSA control lane and other lanes. This *in situ* reaction demonstrated the putative PPO activity observed from *in vitro* assay showed in Figures 7, 8, and 9.

All these results demonstrate our previous unpublished results that red cells express a condensing synthase with a putative PPO activity, which catalyzes the formation of oligomers from (-)-epicatechin and (+)-catechin.

Overall conclusion

I extracted crude proteins from P3 (wild) and 6R (transgenic) tobacco callus and suspension cell cultures, and removed pigments from crude protein extracts, and then purified a putative condensing synthase from the protein extracts. Native gel staining using (+)-catechin and (-)-epicatechin substrates demonstrated that putative condensing enzyme(s), which were hypothesized to be either a peroxidase with a putative PPO activity or a PPO, catalyzed the

substrates to new compounds. Further preliminary *in vitro* enzyme assay coupled with thin-layer chromatography (TLC) and high-performance liquid chromatography (HPLC) showed that the candidate PPO catalyzed (+)-catechin and (-)-epicatechin substrates to new dimeric compounds. These preliminary data demonstrate that transgenic tobacco red cells express a condensing synthase with a putative PPO activity, which catalyzes condensation of flavan-3-ols to PA-like oligomers.

Current and future work

Other graduate students are working on sequence, condensation kinetics of condensing enzyme with a putative PPO activity, gene cloning from cells and plants, and identification of those oligomers using nuclear magnetic resonance (NMR). Our future work will use our new condensing enzyme(s) with a putative PPO activity for metabolic engineering of PAs in plants.

REFERENCES

Borevitz, J. O., Y. J. Xia, et al. (2000). "Activation tagging identifies a conserved MYB regulator of phenylpropanoid biosynthesis." Plant Cell 12(12): 2383-2393.

Dixon, R. A., D. Y. Xie, et al. (2005). "Proanthocyanidins - a final frontier in flavonoid research?" New Phytologist 165(1): 9-28.

Mathews, H., S. K. Clendennen, et al. (2003). "Activation tagging in tomato identifies a transcriptional regulator of anthocyanin biosynthesis, modification, and transport." Plant Cell 15(8): 1689-1703.

Tohge, T., Y. Nishiyama, et al. (2005). "Functional genomics by integrated analysis of metabolome and transcriptome of Arabidopsis plants over-expressing an MYB transcription factor." Plant Journal 42(2): 218-235.

Weigel, D., J. H. Ahn, et al. (2000). "Activation tagging in Arabidopsis." Plant Physiology 122(4): 1003-1013.

Xie, D. Y. and R. A. Dixon (2005). "Proanthocyanidin biosynthesis - still more questions than answers?" Phytochemistry 66(18): 2127-2144.

Xie, D. Y., S. B. Sharma, et al. (2006). "Metabolic engineering of proanthocyanidins through co-expression of anthocyanidin reductase and the PAP1 MYB transcription factor." Plant Journal 45(6): 895-907.

Zhou, L. L., H. N. Zeng, et al. (2008). "Development of tobacco callus cultures over expressing Arabidopsis PAP1/MYB75 transcription factor and characterization of anthocyanin biosynthesis." Planta 229(1): 37-51.

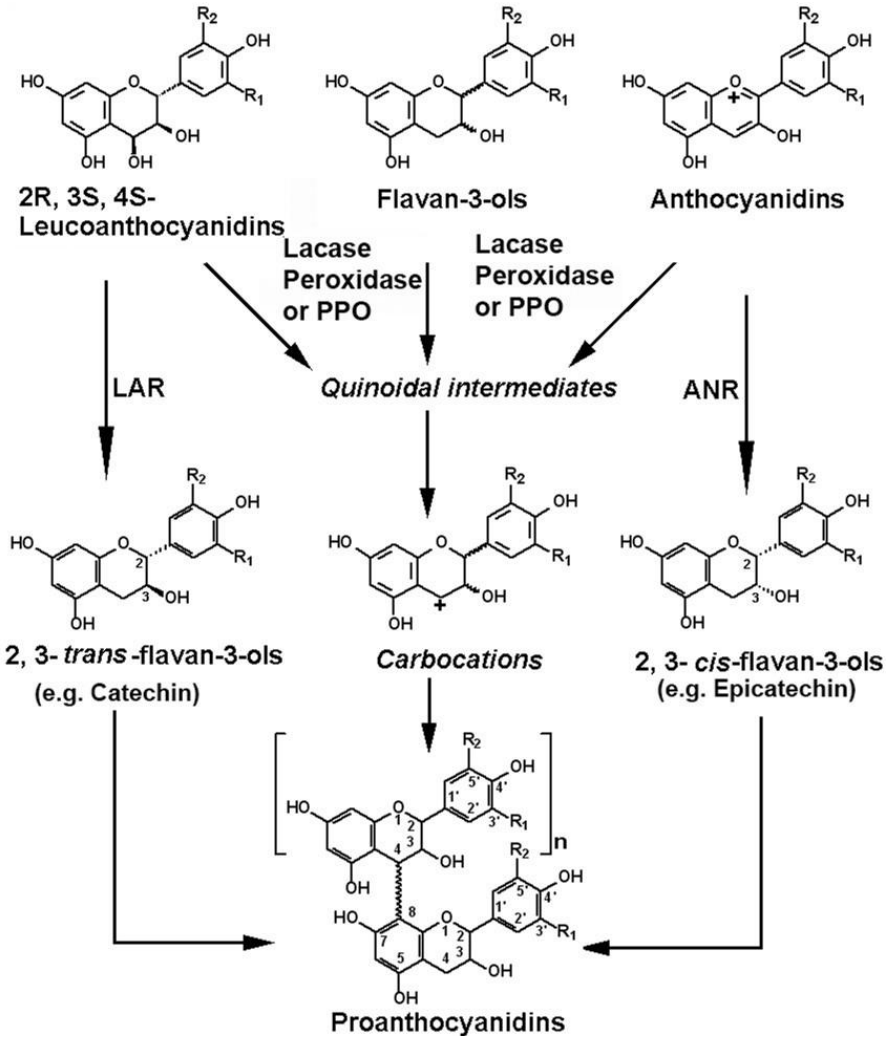

Figure 5.1: **Speculative diagram for the origin of extension units for PA biosynthesis.** ANR, anthocyanidin reductase; LAR, leucoanthocyanidin reductase; PPO, polyphenol oxidase Modified from (Xie and Dixon 2005).

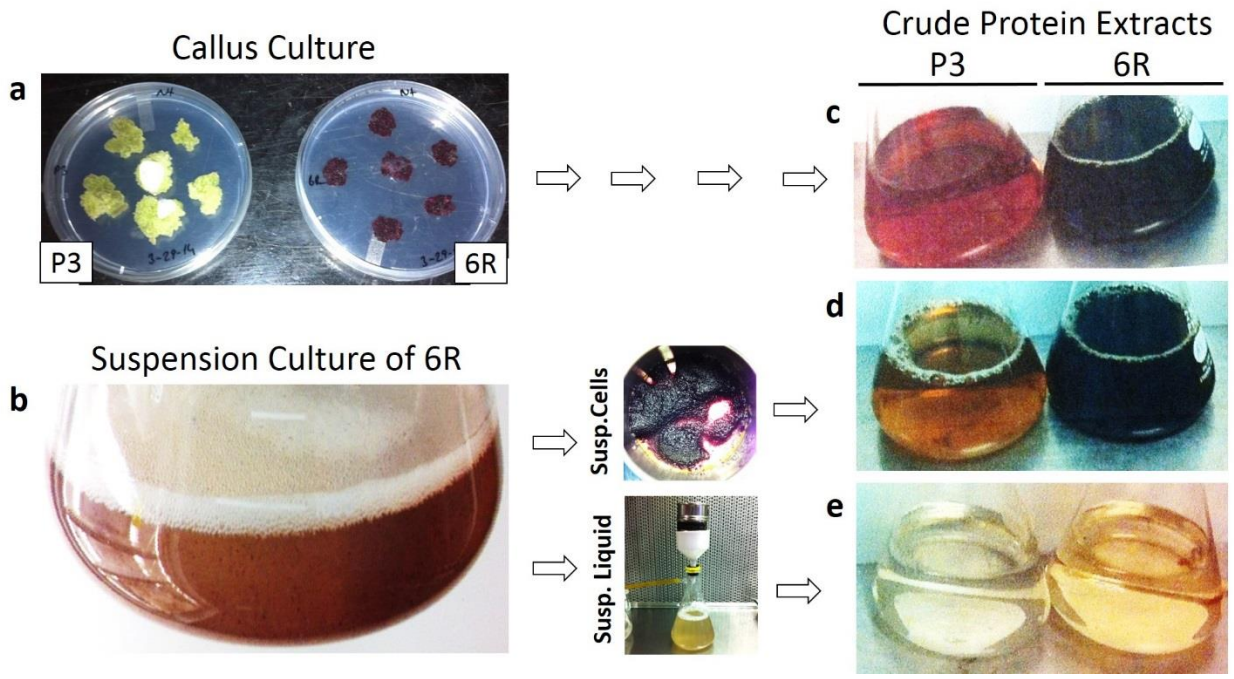

Figure 5.2: Callus and suspension culture of red and wild-type cells. a; callus culture of wild type tobacco (P3) and PAP1 transgenic (6R) tobacco cells grown on subculture media, **b**; suspension culture of 6R tobacco cells growing in liquid medium, **c-e**; crude protein extracts harvested from both 6R and P3 callus cells (**c**), 6R and P3 suspension cells (**d**), and 6R and P3 suspension liquid mediums (**e**).

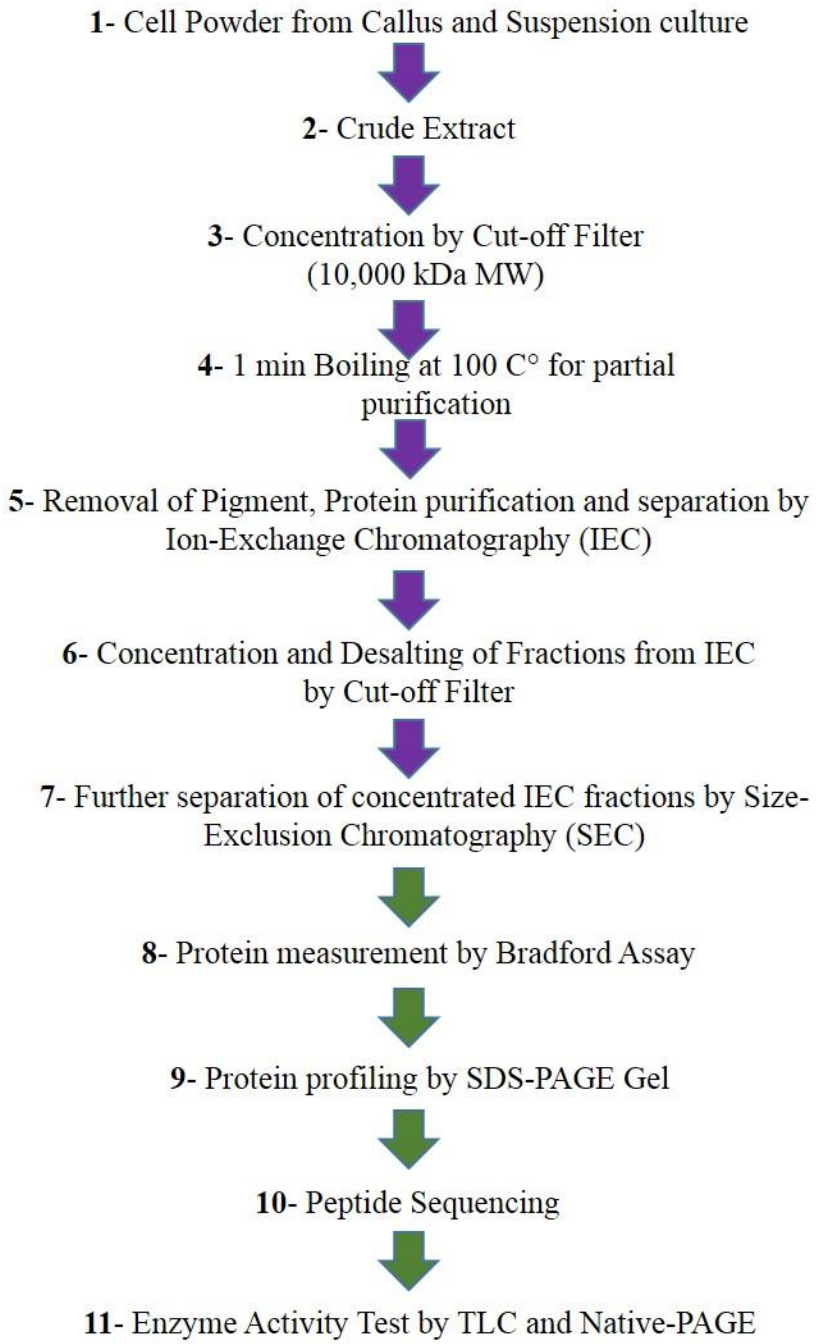

Figure 5.3: Overview steps of protein extraction and purification from callus and suspension cells. The steps highlighted with purple arrows from one to seven show the extraction (#1-3) and purification steps (#4-7). The rest of the steps highlighted with green arrows display protein analysis.

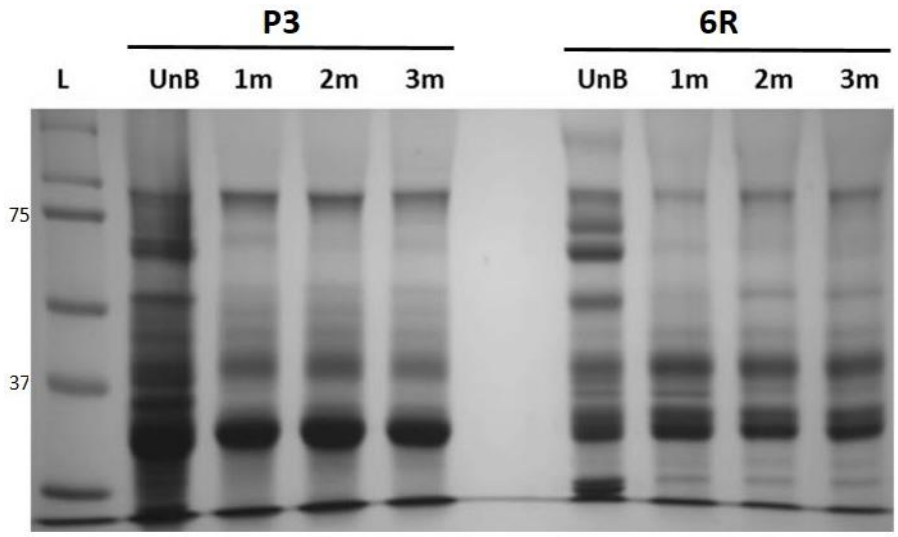

Figure 5.4: SDS-PAGE image shows different profiles of proteins among un-boiled and boiled extracts from liquid parts of P3 (wild type) and 6R (PAP1 transgenic) cell suspension cultures. L, protein ladder (kDa), UnB; unboiled total protein extract, 1-3m; partially purified extracts boiled for 1 , 2 and 3 minutes at 100 °C. 10% SDS-PAGE.

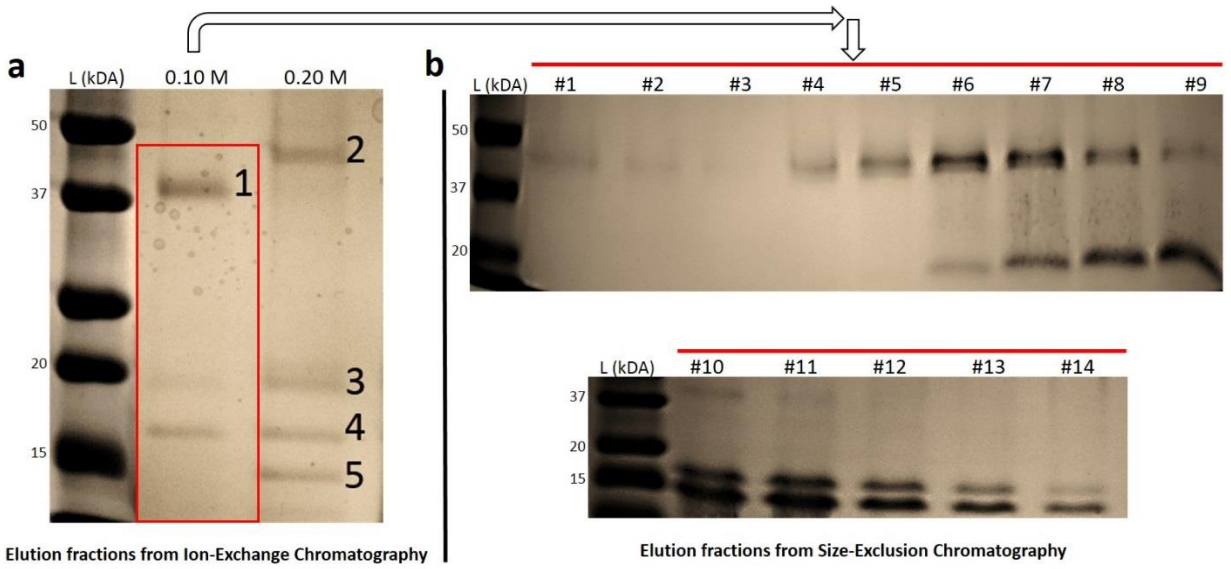

Figure 5.5: SDS-PAGE images show consecutive elution fractions for 6R crude protein extract. a; 0.10 and 0.20 M NaCl elution fractions from ion-exchange chromatography (IEC), **b**; fractions (#1-14) from further purification of 0.10 M of IEC elution fraction by size-exclusion column chromatography (SEC). There were 5 different protein bands (1-5) detected after IEC purification. 3 different protein bands shown in red box were further separated and purified by SEC to get single protein band. L, protein ladder (kDa). 12.5% SDS-PAGE.

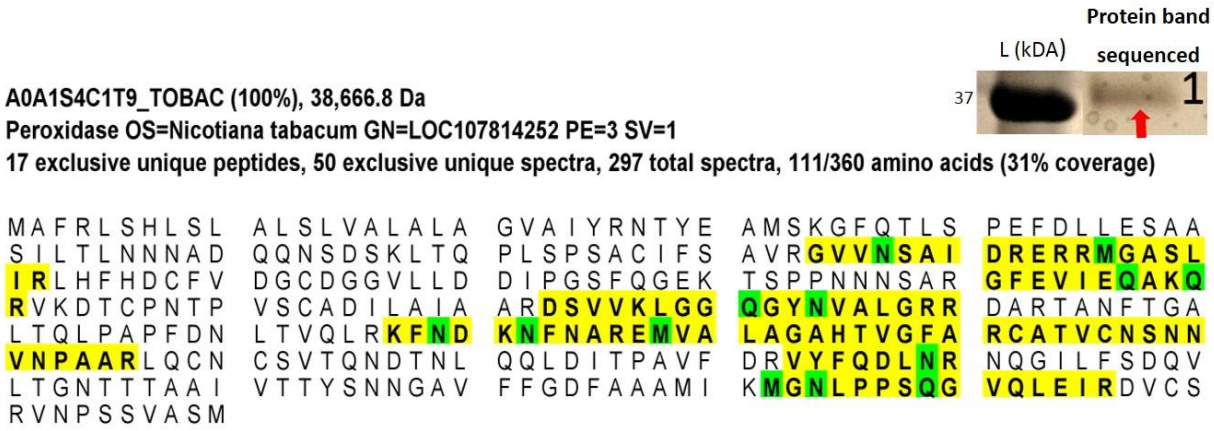

Figure 5.6: Peptide sequence result shows similarity of a putative condensing protein with a peroxidase-like enzyme in *Nicotiana tabacum*. Protein band numbered as '1' (from Figure 5.5) pointed with red arrow displayed 31% coverage with a peroxidase –like protein. Aminoacids highlighted with green and yellow colors represent ≥95% and ≥85-95% possibility for matching.

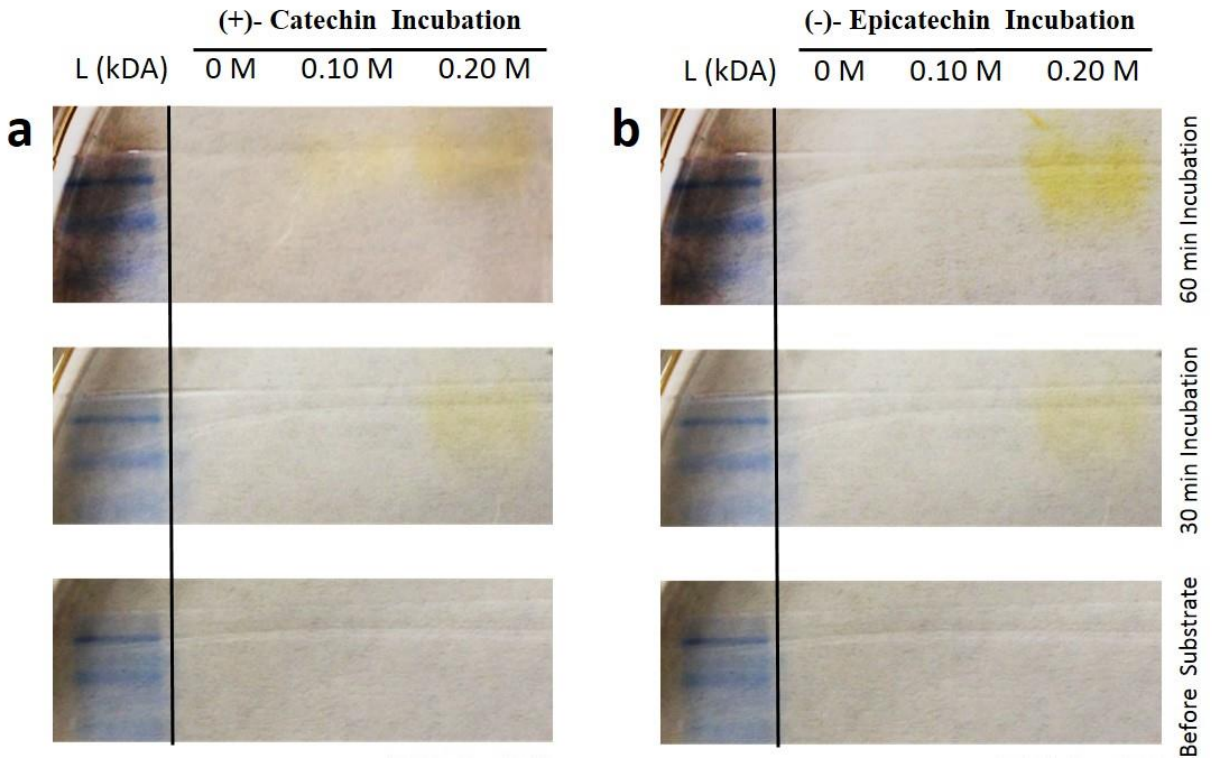

Figure 5.7: Native-PAGE images show condensation products from *in vitro* incubations. a; condensation product of incubation between (+)-catechin and elution fractions of IEC, **b**; condensation product of (-)-epicatechin incubations with protein fractions eluted through IEC. L; protein ladder (kDa). 10% Native-PAGE.

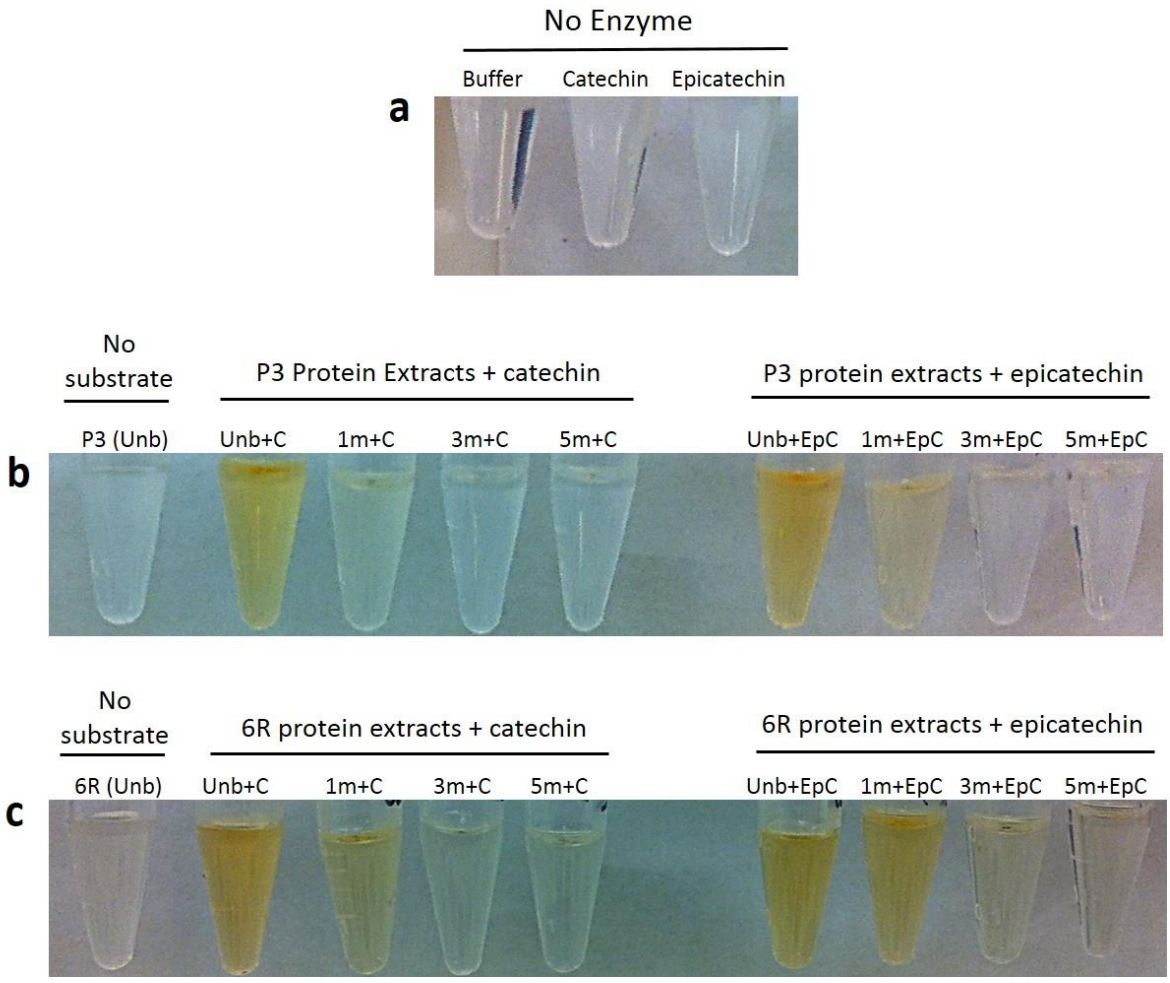

Figure 5.8: Incubation of crude proteins with substrates produce new compounds. Proteins used here include un-boiled and boiled (1, 3, and 5 min, labeled as 1m, 3m, and 5m). **a**; colors of buffer and two substrates, **b**; color changes from the incubation of P3 proteins (un-boiled and boiled) and substrates, **c**; color changes from the incubation of P3 proteins (un-boiled and boiled) and substrates. Unb; unboiled protein extract, C; catechin, EpC; Epicatechin.

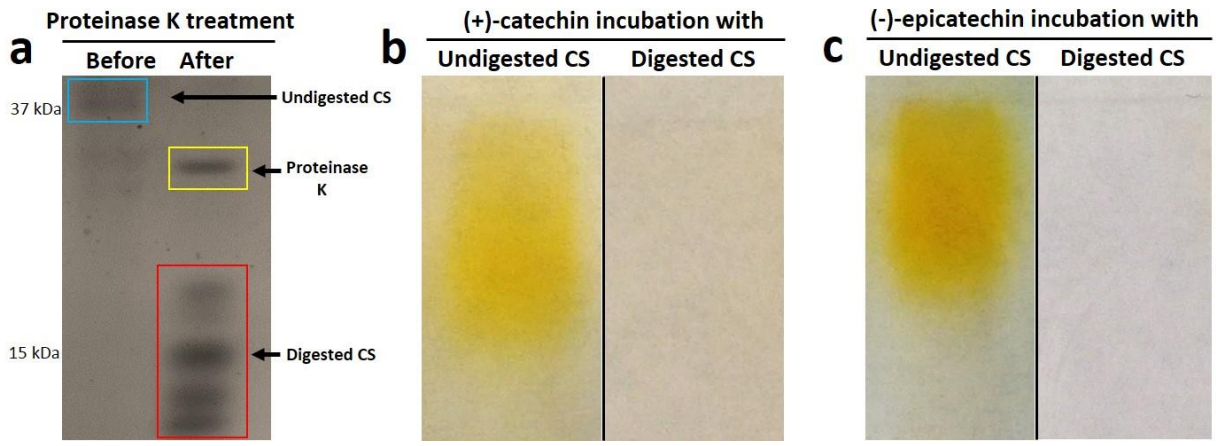

Figure 5.9: Protein digestion by proteinase K treatment on SDS-PAGE gel, and *in vitro* incubations of digested and undigested condensing synthase with a putative PPO function incubated with substrates on Native-PAGE gels. a; SDS-PAGE gel image shows proteinase K (in yellow box, ~30 kDa) digestion product of condensing synthase with a putative PPO function (in red box) from 6R, and protein band of undigested condensing synthase with a putative PPO function (in blue box, ~40 kDa), **b**; products of one hour of incubations between (+)-catechin substrate and condensing synthase with a putative PPO function before and after the digestion by proteinase K, **c**; products of one hour of incubations between (-)-epicatechin substrate and condensing synthase with a putative PPO function before and after digestion by proteinase K. 12.5% SDS-PAGE gel, 10% Native-PAGE gels, CS;condensing synthase.

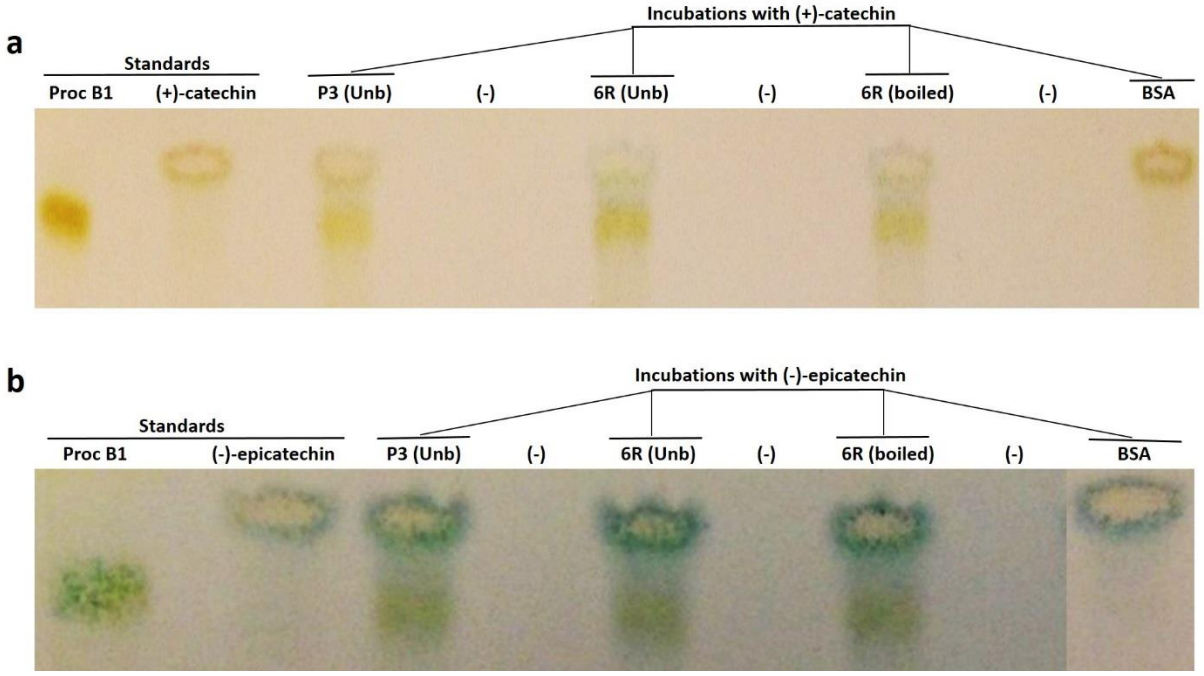

Figure 5.10: TLC and DMACA staining analyses show PA-like oligomers from *in vitro* incubations. a; purified PPO from P3 and 6R cells were incubated with (+)-catechin, **b**; purified PPO from P3 and 6R cells were incubated with (-)-epicatechin. PPO from 6R was boiled for 1 min and tested for activity assay. BSA was used as protein control. In addition, negative (without substrate) was performed. Controls (BSA), and standards (Proc B1, (+)-catechin and (-)-epicatechin). Proc B1;procyanidin B1, Unb; unboiled, BSA; bovine serum albumin.

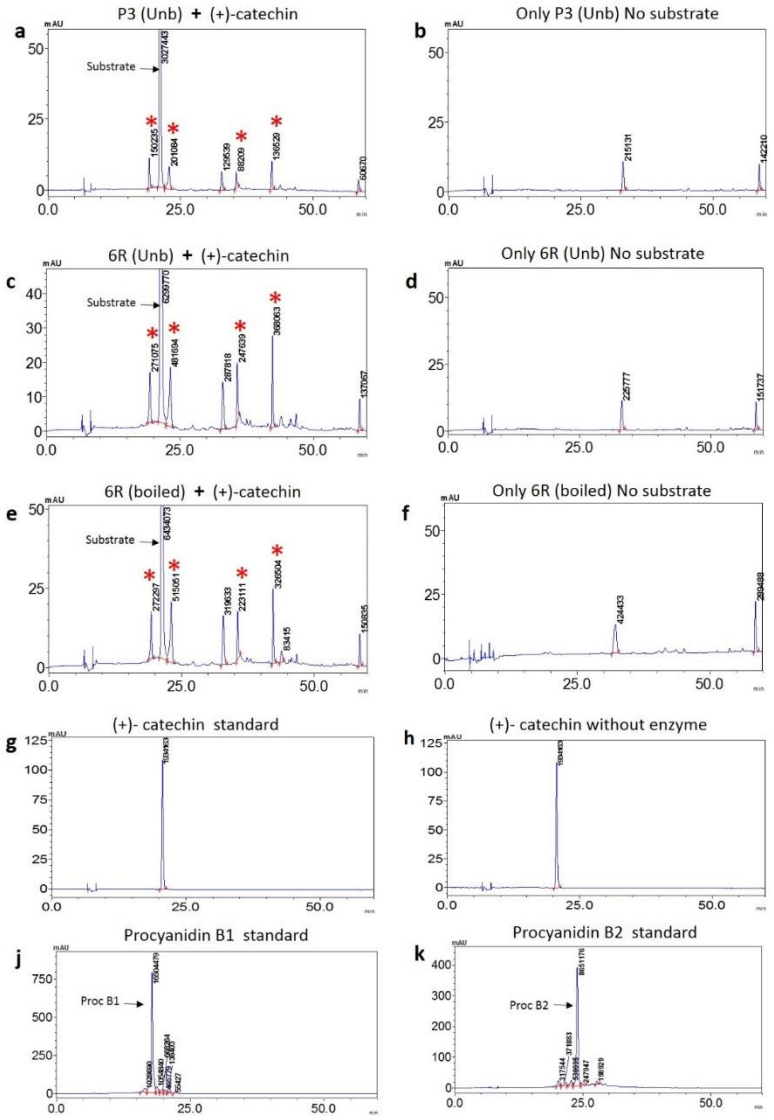

Figure 5.11: HPLC profiles showing products from incubations of (+)- catechin and protein extracts from P3 and 6R suspension cell culture. Catechol (substrate, S) and pigment-free crude protein extract (PE) alone were used as controls, respectively. Absorbance values and chromatographs were recorded at 280 nm. 4 new products (labeled with star) are formed from (+)-catechin catalyzed by condensing synthase. **a**; unboiled P3 protein extract incubated with (+)-catechin, **b**; unboiled P3 protein extract incubated without substrate, **c**; unboiled 6R protein extract incubated with (+)-catechin, **d**; unboiled 6R protein extract incubated without substrate, **e**; boiled 6R protein extract incubated with (+)-catechin, **f**; boiled 6R protein extract incubated without substrate, **g**; (+)-catechin standard, **h**; only (+)-catechin substrate extracted, **j-k**; procyanidin B1and B2 standards.